TESIS DOCTORAL

CONTRIBUTION TO THE STUDY OF COMBUSTION NOISE OF AUTOMOTIVE DIESEL ENGINES

presentada por

LUCA MONELLETTA

en el

DEPARTAMENTO DE MÁQUINAS Y MOTORES TÉRMICOS DE LA UNIVERSIDAD POLITÉCNICA DE VALENCIA

Para la obtención del grado de

DOCTOR

Valencia, 2010

TESIS DOCTORAL

CONTRIBUTION TO THE STUDY OF COMBUSTION NOISE OF AUTOMOTIVE DIESEL ENGINES

Realizada por: D. Luca Monelletta
Dirigida por: Dr. D. Alberto Broatch Jacobi

TRIBUNAL CALIFICADOR:

Presidente: Dr. D. Francisco Payri González
Secretario: Dr. D. Antonio José Torregrosa Huguet
Vocales titulares: Dr. D. Juan Jesús García Bonito
Dr. D. Jordi Romeu Garbí
Dr. D. Octavio Armas Vergel

Vocales suplentes:

Dr. D. Pedro Acisclo Rodríguez Aumente
Dr. D. Andrés Melgar Bachiller

Valencia, 2010

ABSTRACT

Despite their important advantages in terms of fuel consumption in comparison with gasoline engines, for a long time the characteristic impulsive combustion noise has been one of the main causes why customers are reluctant to buy cars equipped with Diesel engines. This is the main reason for the efforts devoted by car manufacturers to mitigate Diesel engine noise while improving performance and driveability. In spite of all technical improvements, vehicles equipped with High Speed Direct Injection (HSDI) engines still offer a comfort level inferior to gasoline engine vehicles.

Noise represents one of the most important aspects in the definition of comfort, and especially combustion noise plays an essential role in the acoustic of a vehicle as, in the case of DI engines, it represents one of the most important noise sources. Thus, the great potential of diesel engines for environment preservation –due to their lower CO_2 emissions– could be missed. This situation worsens with the current design trends (engine downsizing) and the emerging new diesel combustion concepts (Homogeneous Charge Compression Ignition-HCCI, Premixed Charge Compression Ignition-PCCI, etc.) conceived to further reduce NO_x and particulate matter to comply with forthcoming legislation, which are intrinsically noisy.

Therefore, combustion noise must be considered as an additional essential factor in engine development, together with performance, emissions and driveability. Thus, suitable evaluation procedures that can be integrated into the global engine development process in a timely and cost-effective manner are imperative, both for noise level and sound quality. In this thesis, a procedure, based on the consideration of suitable indicators extracted from in-cylinder pressure, is proposed and validated. Such indicators are obtained from an innovative procedure to decompose in-cylinder pressure signal, so that features associated with combustion and with resonance excitation may be properly identified. Indicators obtained were correlated with a mark characteristic of the quality as well as with the overall noise level. In the first case, a direct physical explanation of subjective issues is not forthcoming but significant correlations were obtained and it was possible to obtain guidelines for the design of engines with a higher sound quality. In the second case, a prediction of the radiated noise level more accurate than that obtained from the classical block attenuation approach was achieved, while combustion process features related with the resulting noise level can be identified and thus corrective actions could be proposed.

In a complex issue, such as the noise radiated by a Diesel engine for a wide range of operation conditions, the classical analysis techniques are mainly useful for the evaluation of final products but not in early stages of engine development. The novelty of the approach proposed in this Thesis lies in the fact that the signature of the in-cylinder noise source is determined and characterized by reliable combustion indicators that are well correlated with both the sound pressure level and the subjective judgements for the whole operation range of interest. Since in-cylinder pressure traces are available at early stages of engine development, the proposed procedure becomes an attractive tool, that allows the integration of noise issues into the global development process, avoiding the need to resort to long and expensive noise tests.

RESUMEN

A pesar de sus importantes ventajas en términos de consumo de combustible en comparación con los motores de gasolina, por mucho tiempo, el característico ruido impulsivo de la combustión Diesel ha sido una de las principales causas por las cuales, los clientes han sido reacios a comprar automóviles equipados con este tipo de motores. Por esta razón los fabricantes de vehículos han dedicado esfuerzos para mitigar el ruido del motor Diesel, y mejorar al mismo tiempo el rendimiento y la facilidad de conducción. A pesar de todas las mejoras técnicas, los vehículos equipados con motores Diesel rápidos de inyección directa (HSDI), aun no ofrecen el nivel de confort de los vehículos con motores de gasolina.

El ruido constituye uno de los aspectos más importantes en la definición de confort, y especialmente el ruido de combustión desempeña un papel esencial en la acústica de un vehículo debido a que, como en el caso de los motores de inyección directa (DI), este representa una de las fuentes de ruido más importantes. Así, el gran potencial de los motores Diesel para la preservación del medio ambiente –debido a sus bajas emisiones de CO_2– podría perderse. Esta situación empeora con las tendencias de diseño actuales para la reducción del tamaño del motor, y con los nuevos conceptos de combustión Diesel (Carga Homogénea -HCCI, Carga Premezclada -PCCI, etc), los cuales han sido concebidos para reducir aún más las emisiones de NO_x y de partículas para cumplir con las futuras legislaciones, que son demasiado ruidosos.

Por lo tanto, el ruido de combustión debe ser considerado como un factor esencial en el desarrollo de los motores, junto con el rendimiento, las emisiones y la facilidad de conducción. Por esta razón, son imprescindibles nuevos procedimientos de evaluación, tanto del nivel de ruido como de la calidad sonora, que puedan ser integrados en el proceso global de desarrollo de un motor de manera oportuna y rentable. En esta tesis se propone y valida un procedimiento basado en indicadores de la combustión obtenidos de la señal de presión en cada uno de los cilindros. Estos indicadores son obtenidos por medio de un innovador procedimiento de descomposición de dicha señal, con lo que las características asociadas con la combustión y la resonancia de la cámara de combustión se han identificadas correctamente. Los indicadores obtenidos se correlacionaron con una nota representativa de la calidad sonora, así como con el nivel global de ruido emitido. En el primer caso, no se encontró una explicación física de los aspectos subjetivos, pero se obtuvieron correlaciones significativas que aportaron guías para el diseño de motores con mejor calidad

de sonido. En el segundo caso, se logró una predicción más precisa del nivel de emisión de ruido, que la que se puede obtener utilizando el procedimiento tradicional a través de la determinación de la curva de atenuación del bloque, debido a que con el método desarrollado es posible tener en cuenta las características del proceso de combustión con mayor contribución al nivel de ruido emitido.

En una cuestión tan compleja como lo es el ruido emitido por motores Diesel en un amplio rango de condiciones de operación, las técnicas de análisis clásicas son útiles principalmente para la evaluación del producto final, pero no en las etapas iniciales del desarrollo de los motores. La novedad del procedimiento propuesto en esta tesis, reside en el hecho de que permite identificar las características más relevantes de la fuente de ruido (consecuencia de la combustión) y cuantificarlas mediante indicadores robustos y fiables que están bien correlacionados, tanto con el nivel global del ruido como con la calidad sonora dentro del rango de operaciones de interés. Dado que la señal de presión de los cilindros está disponible desde las etapas iniciales del desarrollo del motor, el procedimiento propuesto resulta una atractiva herramienta que permite la integración del ruido en el proceso global del desarrollo, evitando así la necesidad de depender de pruebas de escucha costosas y de larga duración.

RESUM

A pesar de les seues importants avantatges en termes de consum de combustible en comparació amb els motors de gasolina, per molt temps, el característic soroll impulsiu de la combustió Dièsel ha sigut una de les principals causes per les quals, els clients han estat poc inclinats a comprar automòbils equipats amb aquest tipus de motors. Per aquesta raó els fabricants de vehicles han dedicat esforços per a mitigar el soroll del motor Dièsel, i millorar al mateix temps el rendiment i la facilitat de conducció. A pesar de totes les millores tècniques, els vehicles equipats amb motors Dièsel ràpids d'injecció directa (HSDI), encara no ofereixen el nivell de confort dels vehicles amb motors de gasolina.

El soroll constitueix un dels aspectes més importants en la definició de confort, i especialment el soroll de combustió ocupa un paper essencial en l'acústica d'un vehicle degut al fet que, com en el cas dels motors d'injecció directa (DI), aquest representa una de les fonts de soroll més importants. Així, el gran potencial dels motors Dièsel per la preservació del medi ambient –a causa de les seues baixes emissions de CO_2– podria perdre's. Aquesta situació empitjora amb les tendències de disseny actuals per la reducció de la grandària del motor, i amb els nous conceptes de combustió Dièsel (Càrrega Homogènia -HCCI, Carrega Premezclada -PCCI, etc), els quals han estat concebuts per reduir encara més les emissions de NO_x i de partícules per complir amb les futures legislacions, que són massa sorollosos.

Per tant, el soroll de combustió ha de ser considerat com un factor essencial en el desenvolupament dels motors, juntament amb el rendiment, les emissions i la facilitat de conducció. Per aquesta raó, són imprescindibles nous procediments d'avaluació, tant del nivell de soroll com de la qualitat sonora, que puguin ser integrats en el procés global de desenvolupament d'un motor de manera oportuna i rendible. En aquesta tesi es proposa i valida un procediment basat en indicadors de la combustió obtinguts del senyal de pressió en cadascun dels cilindres. Aquests indicadors són obtinguts per mitjà d'un innovador procediment de descomposició d'aquest senyal, amb el que les característiques associades amb la combustió i la ressonància de la càmera de combustió s'han identificat correctament. Els indicadors obtinguts es van correlacionar amb una nota representativa de la qualitat sonora, així com amb el nivell global de soroll emès. En el primer cas, no es va trobar una explicació física dels aspectes subjectius, però es van obtenir correlacions significatives que van aportar guies

per al disseny de motors amb millor qualitat de so. En el segon cas, es va assolir una predicció més precisa del nivell d'emissió de soroll, que la que es pot obtenir utilitzant el procediment tradicional a través de la determinació de la corba d'atenuació del bloc, degut al fet que amb el mètode desenvolupat és possible tenir en compte les característiques del procés de combustió amb major contribució al nivell de soroll emès.

En una qüestió tan complexa com ho és el soroll emès per motors Dièsel en un ampli rang de condicions d'operació, les tècniques d'anàlisis clàssiques són útils principalment per a l'avaluació del producte final, però no en les etapes inicials del desenvolupament dels motors. La novetat del procediment proposat en aquesta tesi, resideix en el fet que permet identificar les característiques més rellevants de la font de soroll (conseqüència de la combustió) i quantificar-les mitjançant indicadors robusts i fiables que estan bé correlacionats, tant amb el nivell global del soroll com amb la qualitat sonora dintre del rang d'operacions d'interès. Atès que el senyal de pressió dels cilindres està disponible des de les etapes inicials del desenvolupament del motor, el procediment proposat resulta una atractiva eina que permet la integració del soroll en el procés global del desenvolupament, evitant així la necessitat de dependre de proves d'escolta costoses i de llarga durada.

A Ebru a me e alla tigna.

AGRADECIMIENTOS

En primer lugar, quisiera agradecer a Alberto Broatch, el director de esta tesis, por el criterio con el que dirigió mis trabajos y en particular por el apoyo y la paciencia que me ha demostrado en la corrección de esta tesis Doctoral. Del mismo modo, quiero expresar mi agradecimiento a toda la línea de ruido y en particular a Antonio Torregrosa, por sus sabios consejos y a Bernardo Planells, por sus medidas siempre fiables. Además un gracias particular va a la línea de CFD en las personas de Xandra Margot, Antonio Gil y Cristian Donayre.

También quiero agradecer a CMT - Motores Térmicos y a PSA Peugeot - Citroën por haberme permitido realizar esta Tesis y particular, a la dirección del departamento, Francisco Payri y José María Desantes así como a todos sus profesores, técnicos, proyectandos, administrativos y personal en general.

Un gracias especial a Vincent Marant, Sjoerd Hermens, David Moreno y todos los doctorandos de la CMT que han compartido conmigo alegrías y dolores en estos años inolvidables.

Finalmente quisiera agradecer a Valencia y su gente, una ciudad y un pueblo que nunca me han hecho sentir extranjero y que siempre me llevaré conmigo.

Un grazie speciale alla mia famiglia e a Ebru per la pazienza, l'appoggio e la fiducia che in questi anni non mi hanno mai fatto mancare.

General Index

List of Notation

Latin

A	Area bounding reaction region or Open loop Gain or Interior noise quality index
A, B	Original and modified piston bowl shape, respectively
B	Cylinder bore diameter or Cavity diameter
c	Speed of sound
c_p	Specific heat at constant pressure
(c_i, c_3, c_4)	Coefficients of the combustion noise quality assessment model
(C_c, C_r, C_t)	Capacities of transducer, cable and capacitor
(C_{1mn}, C_{2mn})	Modal Coefficient
D	Burner diameter
Da	Damkohler number
E	Energy
E_c	Kinetic energy
E_0	Excitation level in the acoustic modal theory
f	Frequency
f_R	Resonant frequency
F	Fuel mass fraction or Piston side force
H	Fuel heating value
i, j, k	Cartesian directions
$\mathbf{i}, \mathbf{j}, \mathbf{k}$	Cartesian vectors
i	$\sqrt{-1}$
I	Sound intensity
I_i	Combustion indicators
k	Wave number
$(k_i, k_0, k_n, k_3, k_4)$	Coefficients of the combustion noise level assessment model
K	Stiffness
J	Bessel function
l	Conrod length
L	Cavity axial length
$\dot{m}_f$	Fuel mass flow rate
(m, n, p)	Integers denoting the circumferential, radial and axial mode
M	Mass
M	Mach number

n	Crankshaft speed
n_z	Axial mode in the acoustic modal theory
N	Combustion Index
p	Pressure
P	Acoustic power or Piston vertical force
P_0	Pressure level in the acoustic modal theory
q	Charge generated by the transducer
Q	Injected fuel mass
$\dot{Q}$	Volumetric heat release rate
r	Crankthrow length or Radial position
$\mathbf{r}$	Position vector
R	Universal gas constant
$\mathbf{R}$	Correlation coefficient
R_i	Resistance of input circuit
R_t	Resistance of amplifier
Re	Reynolds number
s	Entropy
S	Radiating surface area
S_L	Laminar flame speed
S_{trav}	microphone transverse area
St	Strouhal number
t	Time
t_0, t_n, t_t	Coefficients of noise level assessment model in transient operation
T	Temperature
U	Mass weighted average axial velocity
v	velovity
v_i	Speed vector in ith direction
V	Volume enclosing reaction
V_o	Output voltage
W	Power
W_{rad}	Radiated acoustic power
x, y, z	Cartesian coordinates
Z_c	Mechanical cross impedance

Greek

α	Thermal diffusivity
$\alpha_{m,n}$	Coefficient of circumferential and radial mode or Bessel coefficients
$\alpha, \beta, \gamma, \delta$	Weighting coefficients
γ	Ratio of specific heats
δ	Clearance
ε	Error
η_{ta}	Thermoacoustic efficiency
θ	Angle defining the position of a vector

ν	Velocity
ρ	Density of the medium
σ	Standard deviation or Radiation efficiency
τ	Time delay
ω	Angular frequency

Subscripts and Superscripts

x_0	Reference or initial value
x_A	Relative to piston bowl (A)
x_B	Relative to piston bowl (B)
x_{comb}	Relative to the combustion sub-signal
x_i	Cartesian coordinate in ith direction
x_{idle}	Relative to idle condition
x_{max}	Maximal value
x_{mean}	Mean value
x_{min}	Minimal value
x_{ps-mot}	Relative to the pseudo-motored sub-signal
x_{res}	Relative to the resonance sub-signal
x_{tot}	Relative to the total pressure signal
x^{main}	Relative to the main injection
x^{pil}	Relative to the pilot injection (conventional injection)
x^{pil1}	Relative to the second pilot injection (multiple injection)
x^{pil2}	Relative to the first pilot injection (multiple injection)

Abbreviations

A/D	Analogic/Digital
AI	Annoyance Index
ARI	Annoyance Response Index
BDC	Bottom Death Cylinder/Center
BEM	Boundary Element Method
BMEP	Brake Mean Effective Pressure
cc	Per cylinder per cycle
C_{ASO}	Overall structural and acoustical response of the engine
CN	Cetane Number
CFD	Computational Fluid Dynamics
Lp	Charge percentage
CRP	Composite Rating of Preference
DFT	Discrete Fourier Transform
DI	Direct Injection
DWT	Discrete Wavelet Transform
ECU	Electronic Control Unit

EGR	Exhaust Gas Recirculation
EXP	Experimental
FEM	Finite Element Method
FFT	Fast Fourier Transform
FIE	Fuel Injection Equipment
HF	High Frequency
HR	Heat Release or Harmonic Ratio
HSDI	High Speed Direct Injection
IDI	Indirect Injection
NCI	Noise Combustion Index
NVH	Noise Vibration Harshness
OASPL	Overall Sound Pressure Level
OH	Mean power of odd harmonics
PC	Personal Computer
$PrePer$	Preferred Periodicity
rpm	revolution per minute
RN	Rumble Noise
RNQ	Rattle Noise Quality
RoHR	Rate of Heat Release
SB	Spectrum Balance
SEA	Statistical Energy Analysis
SI	Spark Ignition
SIL	Speech Interference Level
SML	Sum of Modulation Levels
SOI	Start Of Injection
SPL	Sound Pressure Level
SQM	Sound Quality Metric
STFT	Short Time Fourier Transform
TC	Time Constant
TDC	Top Death Cylinder/Center
TOH	Mean power of third order harmonics
WD	Wigner Distribution

Mathematical notation

$\mathbf{x}$	Vector
x'	Fluctuation about a mean value
x^*	Conjugate transpose
$\dot{x}$	Time derivative of x
$\ddot{x}$	Second order time derivative of x
Δx	Variation
$\overline{x}$	Mean Value
d	Differential
$d2$ or d^2	Second order differential

D	Total differential
∂	Partial differential
∇	Nabla operator$\nabla = \frac{\partial}{\partial \mathrm{x}}\mathbf{i} + \frac{\partial}{\partial \mathrm{y}}\mathbf{j} + \frac{\partial}{\partial \mathrm{z}}\mathbf{k}$

Chapter 1

Introduction

Index

1.1. Justification

In 2004 Jaguar Cars, a historical luxury cars manufacturer, launched in the market its first S-type model powered by a Diesel engine. A new twinturbo 2.7 l common rail V6 engine, product of an agreement between PSA Peugeot Citroën and Ford Motor Company was developed. This engine supplied 435 Nm of maximal torque, more than the 4.2-litre V8 Jaguar S-type petrol engine, and improved its consumption by a massive 47 %. Furthermore, what Jaguar really concentrated on was offering the comfort –in terms of driveability, noise, vibration and harshness– that buyers of petrol powered luxury cars have traditionally demanded.

In June 2006 the Audi R10, a sport car powered by a 5.5L TDI (Turbocharged Direct Injection) Diesel engine won the 24 hours of Le Mans, probably the most famous endurance racing event in the world. This marked the first significant victory for a diesel-powered car in a major racing event, and possibly an important turning point in the perception that diesels are noisy, stinky, and slow: the Audis were the quietest, cleanest, and fastest cars in the race. Furthermore, they were also the most fuel efficient.

These are just two examples of the technological revolution happened in last decades at least in Europe, which has seen the Diesel engine gaining increasing automotive market shares also in those vehicle segments that have traditionally been considered gasoline engine strongholds, such as the luxury and sports vehicle segments. European market share of Diesel engines has been continuously increasing, from a more or less constant 14 % between 1987 and 1991 to 33 % in 2000 and then to around 45 % in 2003. In 2007, according to the European Union Economic Report by ACEA (European Automobile Manufacturers Association), more than half (53.3 %) of new passenger cars registered in the European Union are powered by Diesel engines.

The continuous rise in demand for Diesel cars is explained to a large extent by the significant increase of fuel prices with consequent greater requirement of fuel efficient engines. Furthermore, recognition of the importance of the global warming has increased the pressure on automobile manufacturers to decrease emissions of CO_2 from vehicles. According to the last European regulations the fleet average to be achieved by all cars registered in the EU is 130(g/km), this means that automotive manufacturers will be forced to shift their production to engines with less CO_2 emissions.

Diesel engines have a greater thermodynamic efficiency and hence a lower fuel consumption and lower CO_2 emissions than gasoline engines. A transition from gasoline to diesel powered vehicles offers a possible approach for reducing CO_2 emissions from vehicles. Based on European Diesel and gasoline certification data of 2004, a study of Sullivan et al. [249] quantifies such CO_2 reduction opportunities for cars and light duty trucks in approximately 24-33 %.

The improved Diesel engine technology has permitted a significan advance of this type of engines in terms of performance and driveability. Exhaust gas recirculation (EGR), variable geometry turbocharging and Common Rail direct injection (CRDI) are just some examples of the sophisticated technologies that have been in-

troduced in the last decades by the engine manufacturers in the development of the CI (compression ignition) engines.

In spite of these technical improvements, the conventional combustion process in Diesel engines may still be considered as the most important source of noise, thus, the great potential of Diesel engines for environment preservation –due to their lower CO_2 emissions– could be missed. Moreover, the advanced combustion concepts –e.g. the HCCI (Homogeneous Charge Compression Ignition) and the PCCI (Premixed Charge Compression Ignition)– conceived to comply with forthcoming emissions legislation without affecting the efficiency of current engines, are expected to be noisier because they are characterized by a higher amount of premixed combustion. For these reasons many efforts have been and are going to be dedicated by car manufactures to reduce the overall level and improve the sound quality of Diesel engines. Consequently, evaluation procedures are required, both for noise levels and sound quality, that may be integrated in the global engine development process in a timely and cost-effective manner.

The noise generation process in a DI Diesel engine is a complex phenomenon, it originates from the self-ignition of the air-fuel mixture, which produces an important sudden pressure increase giving rise to the well-known Diesel knock. The combustion process is mainly responsible for block vibration through two excitation sources: the pressure and mechanical forces. Pressure forces act directly on the surface of combustion chamber walls and strongly depend on the combustion concept, which is controlled by the injection strategy, compression ratio, bowl geometry, etc. Mechanical forces are induced by the pressure forces through the mechanical systems and are due to piston slap, clearances, deformation, friction, etc. This process is characterized by non-linearity and non-stationarity that make the use of a rigorous mathematical approach impossible. These facts justify the original approach, which is at the basis of this Thesis, to find direct correlations between indicators characteristic of the in-cylinder pressure signal evolution and the noise radiated by the engine, considering the noise from a quantitative point of view (noise pressure level), as well as qualitative (a mark describing the concept of quality).

This work claims to be a contribution in response to current requirements of suitable tools for combustion noise analysis in state-of-the-art Diesel engines. The approach proposed in this Thesis appears to be a reliable and attractive tool for early stages of engine development, not only for estimation of the engine noise features but also for the establishment of guidelines for optimal injection settings regarding combustion noise issues.

1.2. Objectives and development of the work

The main objective of this Thesis is to develop a complete methodology to allow the estimation of noise radiated by the engine starting from the in-cylinder pressure measurement. The engine noise will be tackled by a double point of view: subjective (through a mark given by a jury of listeners) and objective (overall noise level).

The attention will be focused on the analysis of the in-cylinder pressure evolution, as the main source of Diesel engine noise [8]. Consequently, the effect of passive systems for noise attenuation, such as engine encapsulation and cabin acoustic insulation, as well as the optimization of engine structure and materials will not be treated in this work.

The final goal is to elaborate a tool that permits an assessment of the engine noise characteristics by analyzing the in-cylinder pressure traces. Accordingly, a direct correlation between the combustion indicators and the quantity and quality of noise –expressed by the sound pressure level in decibels and by a mark, respectively– has to be researched.

The development of a new approach for the evaluation of the combustion noise characteristics requires a preliminary exhaustive analysis of the problems related to its generation and of the techniques already existing. Accordingly, the first step of this research has been an exposition of the state of the art, this will give a general overview of the problems related to the combustion noise generation and will permit to understand the novel approach developed in this Thesis. The theory and classic techniques for the study of the combustion noise will be thoroughly analyzed. Furthermore, the concept of quality applied to the noise will be introduced and the basic guidelines to give a subjective evaluation as well as the intents to get an objective quantification of this concept will be presented.

Subsequently it is necessary to define a general methodology in order to accomplish the objectives proposed in this Thesis. First of all, an adequate experimental methodology was defined, the main requirement of the experimental set-up is to be able to record simultaneously the pressure evolution inside every cylinder and the noise radiated by the engine. The in-cylinder pressure signal acquisition has to be done with constant time increment and high sampling frequency, the noise measures have to be performed in free field conditions to avoid any reverberation effect, an anechoic room is used for this scope. Moreover, a robust methodology for the evaluation of the combustion noise quality was developed in order to qualify every noise with a mark in a reliable and repeatable manner.

Once the experimental methodology was defined, the data recorded were processed, the purpose of this phase is to get possibly all the information related to the combustion noise generation process. The approach proposed is based on a novel procedure for the decomposition of the in-cylinder pressure signal in three sub-signals: pseudo-motored, combustion and resonance. From this sub-signals, by means of advanced statistical techniques, indicators characteristic of the combustion process were obtained. Finally predicting models –as direct correlation between the selected indicators and the noise– were defined, considering both the noise quality (quantified by the jury mark), and objective noise (overall noise level measured in decibels).

The problematic of the noise quality was structured in three phases:

- Definition of a model for the assessment of the noise quality of engines operating with single and conventional (pilot + main) injection.

- Definition of a model for the assessment of the noise quality of engines operating with multiple injection strategies.

- Analysis of the influence of the resonance phenomena in the combustion chamber on the combustion noise quality. For this part CFD calculations will be also analyzed in order to get a deeper comprehension of the resonance phenomena occurring in the cylinder during combustion.

The task of defining a predictive model for the assessment of the noise level will be approached in two main tasks:

- Definition of a model for the assessment of the combustion noise level with the engine operating in stationary conditions. For this issue a preliminary study will be performed considering a classical approach based on the attenuation curve, this will be done in order to have a point of reference allowing an evaluation of the potentiality of the novel approach.

- The second phase of the study on the noise level assessment has been conducted on an engine operating in transitory conditions. Also in this case the proposed approach has been compared with the results obtained with the attenuation curve methodology.

Finally the main conclusions obtained by this research will be remarked and the potential future works that could be done will be shortly introduced.

Chapter 2

State of the art of combustion noise

Index

2.1. Introduction

The objective of this chapter is to provide a general overview of the most important concepts related to the combustion noise generation problem. This is done by presenting and analyzing the main methodologies and results of the engine acoustic investigations described in the scientific literature. A review of the state of the art of the combustion noise is a first, essential step in order to frame the problem, furthermore it contributes to explain and justify the hypothesis at the basis of the methodology developed in this Thesis.

After this first short introduction, the second section of this chapter will present a physical interpretation of the combustion noise generation. The main theories that try to explain, in a rigorous physical way, the noise generation from combustion will be shortly described. The simple case of a premixed turbulent flame will be analyzed presenting the results obtained with both experimental and theoretical approaches. The main factors affecting combustion noise generation as well as the limitations due to the complexity of a physical approach will be reported.

The third section will focus on the engine noise components and sources. Considering the total radiated noise as the sum of combustion and mechanical noises, definitions of the engine noise components will be given. The mechanism characteristic of the noise generation, from the excitation sources to the radiation of noise by vibration of the engine surface will be described. The main analysis techniques for the identification of the engine noise sources will be shortly presented.

The following section is dedicated to give a highlight to the concept of combustion, as the main noise source in Diesel engines. A description of the combustion features in compression-ignition engines will be given, identifying the basic ways to control the combustion evolution. In-cylinder pressure analysis is widely described, as it represents the most reliable method for characterizing the combustion, and some studies based on this type of analysis will be presented.

In the fifth section the most widely used techniques for the analysis of combustion noise will be described. The block attenuation curve analysis, empirical formulae, as well as time-frequency and numerical methods will be considered and some examples of their application will be given, focusing on the potential and the limits of these methods for the assessment of combustion noise.

In the sixth section the concept of sound quality as feature of the engine noise will be introduced. The basic guidelines to give a subjective evaluation to the noise quality will be reported. To conclude the chapter, some intents of getting an objective noise quality evaluation will be presented.

Finally, the main conclusions of this bibliographic review will be summarized evidencing the problems and complexity characteristic of the combustion noise generation. This will explain and justify the ideas that form the basis of the novel approach introduced in this Thesis.

2.2. Physical interpretation of combustion noise generation

The main problem related to the study of combustion generated noise is that it represents quantitatively only a minimal part of the energy involved in the phenomenon. Te noise sound power radiated by a well behaved combustor device is about 5 - 6 orders of magnitudes smaller than its thermal input. Nevertheless, combustion noise has been clearly identified as an important noise source in industrial furnaces and heaters, aircraft turbopropulsion system, gas turbine units and, of course, Diesel engines. However, the fundamentals of the problem are the same in all systems [239].

From a physical point of view, combustion noise is the result of the interaction of turbulence and combustion. On the one hand, turbulence dominates the transport mechanisms from the molecular level to the macroscopic level increasing the rapidity of transport processes. On the other hand combustion still requires interactions at the molecular level, the fact that combustion takes place in a turbulent field alters the noise production mechanism as compared with non-reacting turbulent fields. Acoustic waves are produced in turbulent flames by local temporal fluctuations of volume change. Hence, alterations are caused by chemical reactions and convective transport of turbulence into the flame front.

In literature [239] on combustion noise generation, from a specific physical point of view, combustion noise is conventionally distinguished in two forms, direct and indirect:

- Direct combustion noise - this noise is generated in and radiated from a region undergoing turbulent combustion and is related to the unsteady combustion process itself. This is caused by a temporal fluctuation in the aggregate heat release of the reacting region. This overall fluctuation, while small, exists and generates pressure waves.

- Indirect combustion noise - This is generated downstream of the combustion region where the fluid presents nonuniform entropy, for this reason it is also called entropy noise. In turbulent fields, all streamlines are not equally heated by combustion, hot and cold spots are generated in the flow. These regions cause noise when interact with downstream components of the combustor device.

This distinction must not be confused with that relative to the engine direct combustion noise and the engine indirect combustion noise. Definition introduced by several authors for the classification of the engine noise generation sources [2, 214], that will be presented in Section 2.3.1.

Depending on the device, either direct or indirect noise may be dominant. Anyway, the issue of indirect combustion noise only exists in systems which terminate the combustor after a short running length with an extreme pressure gradient. Consequently only jet and rocket engines are affected by this phenomenon, while in the case of Diesel engines most of problems arise from direct noise. A Diesel engine is a particular type of combustor as it operates as a nearly constant volume, intermittent

device. Nevertheless, the gases in the combustion chamber are in turbulent motion during combustion and from cycle to cycle it is imposible to reproduce in space and time exactly the same event. As a result, there will be the presence of random fluctuations due to the turbulence superimposed upon an almost periodic pressure-time trace. Strahle and Handley [243], and more recently Schuller *et al.* [226], observed that in Diesel engines noise is caused by combustion randomness, to a large degree. Using spectral and time-frequency analysis, they showed that stochastic fluctuations, representative of direct combustion noise, dominate the periodic part of the pressure-time trace in a range of frequencies above 1500 Hz. In some cases about one half of the total overall sound pressure level is due to direct combustion noise.

In the next sections some experiments and theories developed for the study of the combustion noise generation will be shortly described. The intention is to give some information about the physics of the phenomenon showing the difficulties related to a mathematical approach of the problem and evidencing the limits of the physical models.

2.2.1. Combustion noise theory

The first explicit analysis and modelling of the source of combustion noise has been performed in early sixties by Bragg [39], who treated the flame front as a distribution of monopoles. More rigorous analysis were subsequently performed by Strahle [242], Hassan [89], Chiu and Summerfield [59], Doak [73] and others that developed approximate wave equations describing the sound generation by unsteady heat-release processes. Most of these analysis were primarily interested in developing theoretical predictions or rational empirical correlations for the total sound power radiated by the flame. Several different approaches have been considered and several different results have been obtained. The main reason for such divergence is the inaccuracy of the mathematical formalisms used, seeing that many approximations are hardly required for analytical tractability.

Most of combustion noise theories are based on two aeroacoustics theories, one based upon Lighthill's acoustic analogy and one on Phillip's analogy. Here, a theory introduced by Strahle in 1971 [242] and improved in 1978 [239] will be described. As in the classical aeroacoustic analogies, also the Strahle's theory starts from the conservation equations of mass, momentum and energy, applied to the air-fuel mixture, considered as an inviscid, non-heating conducting fluid:

$$\frac{\partial \rho}{\partial t} + \frac{\partial}{\partial t}(\rho v_i) = 0, \tag{2.1}$$

$$\rho \frac{\partial v_i}{\partial t} + \rho v_j \frac{\partial v_i}{\partial x_j} = -\frac{\partial p}{\partial x_i} = \rho \frac{D v_i}{D t}, \tag{2.2}$$

$$\frac{Ds}{Dt} = \frac{\dot{Q}}{\rho T}, \tag{2.3}$$

where ρ is the fluid density, v_i the velocity vector i, x_i the cartesian coordinate in ith direction, p the pressure, s the entropy, $\dot{Q}$ the volumetric heat release rate and T the temperature. The combustion effect is introduced through the heat source in Equation (2.3). In the three conservation equations no molecular transport phenomena are included since they are considered unimportant to noise generation problem. Large scale motions of the turbulence are responsible for noise while molecular transport phenomena are slow on the scale of the periods characteristics of the noise generation.

Another hypothesis, normally assumed in most of these theories, is that the fluid is a perfect gas, consequently:

$$p = \rho RT, \quad c^2 = \frac{\gamma p}{\rho}, \quad \frac{s}{c_p} = \frac{1}{\gamma}\ln p - \ln \rho \tag{2.4}$$

where R is the universal gas constat, c the speed of sound, c_p specific heat at constant pressure and γ the ratio of specific heats.

From equations (2.1) and (2.4) a more useful form of the energy equation is obtained:

$$\frac{D\ln p}{Dt} + \gamma\frac{\partial v_i}{\partial x_i} = (\gamma - 1)\frac{\dot{Q}}{p}. \tag{2.5}$$

The Strahle's approach is based in constructing a Lighthill equation by time differentiating Equation (2.1), taking the divergence of Equation (2.2), subtracting the two and subtracting $\partial[\overline{c}^2\partial\rho/\partial x_i]/\partial x_i$ from both sides of the resulting equation. The result is a sound wave operator for a stationary medium, that takes into account variable speed of sound and inhomogeneity:

$$\frac{\partial^2\rho}{\partial t^2} - \frac{\partial}{\partial x_i}(\overline{c}^2\frac{\partial\rho}{\partial x_i}) = -\frac{\partial^2}{\partial x_i\partial x_j}(\rho v_i v_j) + \frac{\partial}{\partial x_i}(\frac{\partial p}{\partial x_i} - \overline{c}^2\frac{\partial\rho}{\partial x_i}), \tag{2.6}$$

On the other hand, the approach of Chiu and Summerfield [59] is based in formulating a Phillips equation by using the variable $\eta = \ln p$, taking the time derivative of Equation (2.5), the divergence of Equation (2.2) and subtracting the two. The resulting equation would be:

$$\frac{D^2\eta}{Dt^2} - \frac{\partial}{\partial x_i}(c^2\frac{\partial\eta}{\partial x_i}) = (\gamma - 1)\frac{D}{Dt}(\frac{\dot{Q}}{p}) + \gamma\frac{\partial v_j}{\partial x_i}\frac{\partial v_i}{\partial x_j}. \tag{2.7}$$

This leads to another convective sound wave operator that also takes into account variable speed of sound and inhomogeneity.

The terms $\frac{\partial}{\partial x_i}(\frac{\partial p}{\partial x_i} - \overline{c}^2\frac{\partial\rho}{\partial x_i})$ of Equation (2.6) and $(\gamma - 1)\frac{D}{Dt}(\frac{\dot{Q}}{p})$ of Equation (2.7) are selected as the responsible in combustion noise generation. As these terms are presumed known, the question reduces to solve an inhomogeneous wave equation. In effect, both approaches are inexact and incorrect. The main problem is that the

velocity terms on the right side of both Equations (2.6) and (2.7) contain fluid dilation terms, but $\dot{Q}$ and $\frac{\partial v_i}{\partial x_i}$ are actually linked by Equation (2.5). To throw away these terms is to throw out parts of the problem which may be important.

Considering the simple case of a free flame radiating to a uniform free field as is presented in Figure 2.1 (A), the solution obtained with Equation (2.6) is:

$$p' \propto \frac{1}{\mid \mathbf{r} \mid} \int_V \frac{1}{\overline{c}^2} \frac{\partial \dot{Q}}{\partial t}]_{\mathbf{r_0}, \mathbf{t}-(|\mathbf{r}|/\mathbf{c_0})} dV(\mathbf{r_0}) \tag{2.8}$$

and with Equation (2.7) is:

$$p' \propto \frac{1}{\mid \mathbf{r} \mid} \int_V \frac{1}{\overline{c}^2} [\frac{\partial \dot{Q}'}{\partial t} + \overline{v}_i \frac{\partial \dot{Q}'}{\partial x_i} + (v_i' - \frac{T'}{\overline{T}} \overline{v}_1) \frac{\partial \overline{\dot{Q}}}{\partial x_i}]_{\mathbf{r_0}, \mathbf{t}-(|\mathbf{r}|/\mathbf{c_0})} dV(\mathbf{r_0}) \tag{2.9}$$

where p' is the pressure fluctuation, $\mathbf{r}$ the position vector, V the volume enclosing reaction. According to Strahle, thanks to its simplicity, Equation (2.8) represents the best tool for modeling simple flames, on the other hand, other authors prefer Equation (2.9) assuming that its additional terms have an extremely strong contribution to combustion noise.

As commented before, direct and indirect noise have their origin in heat release fluctuations. The terms of Equations (2.8) and (2.9), relative to the fluctuation in heat release rate, represent the source of direct combustion noise. Indirect noise is explained by (2.3), the heat release determines the entropy, if this fluid interacts with a boundary which is sensitive to entropy fluctuations, noise may be generated.

An important obstacle to the use of Equations like (2.3), (2.8) or (2.9) for the calculation of the sound output and spectra, is that the turbulence details must be known and this is complicated by the presence of combustion. A flame is characterized by oscillations and instability, furthermore, a feedback interaction between the flame and the acoustic fields is also present. Actually, there is a lack of detailed turbulence theory for the combustion process and experimental information on the statistics of the problem. This is also due to the fact that in many situations the flame pattern is not directly observable.

Summarizing, on the one hand, the significant results of these studies have been a general understanding of the physics of the problems related to combustion noise generation and the important role of heat-release rate as well as fuel heating value and flame speed on the acoustic emission. On the other hand, it appears clear that with these approaches it is still imposible to make a precise prediction of noise emission and spectral content because of the lack of knowledge of turbulence details in a turbulent flame.

2.2.2. Simple premixed turbulent flame model

One of the cases most commonly analyzed for the study of the combustion noise generation, is that of a simple turbulent jet flame of premixed gases burning in

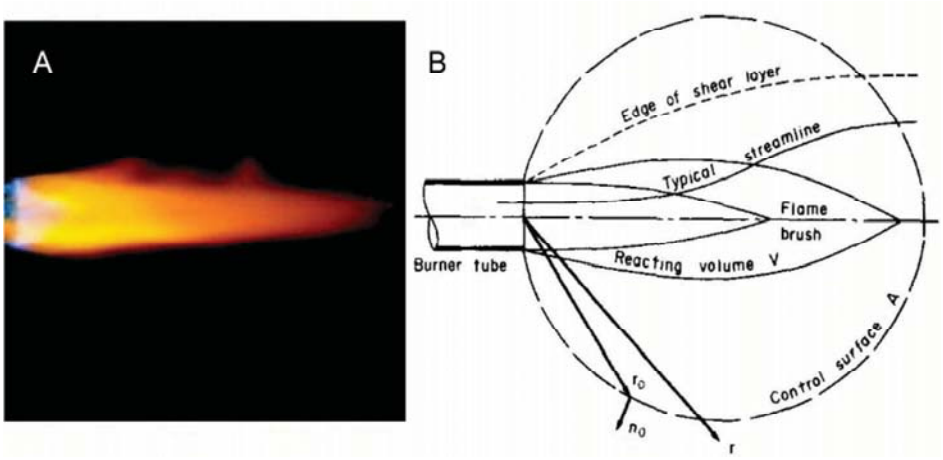

Figure 2.1: Picture (A) and scheme (B) [239] of a turbulent premixed open jet flame

a free field, or, in other words, the flame of a Bunsen burner. A picture of this type of flame is presented in Figure 2.1 (A). In this section a deeper analysis of this simple case will be presented, comparing the results obtained with both experimental and theoretical approaches. The factors affecting combustion noise generation will be also described highlighting the limitations of these physical models.

2.2.2.1. Experimental

Through experimental measurements a common practice [231, 240, 244] is to attempt a dimensional analysis, searching a correlation of some interesting quantity, such as sound power P, made dimensionless by the thermal input rate $\dot{m}_f H$, with dimensionless variables which characterize the phenomenon. Since the details of the individual reactions are not known, it is common to replace the aggregate of reactions with a single global reaction characterized by an effective Damkohler number defined as:

$$Da = S_L^2 D/\alpha U \tag{2.10}$$

where S_L is the laminar flame speed, D the burner diameter, α the thermal diffusivity and U the mass weighted average axial fluid velocity. From the experiments it was found that the thermoacoustic efficiency η_{ta} can be estimated by:

$$\frac{P}{\dot{m}_f H} = \eta_{ta} \propto \mathrm{M}^{2,68}\mathrm{Re}^{-0,09}\mathrm{Da}^{0,92}F^{-1,26}, \tag{2.11}$$

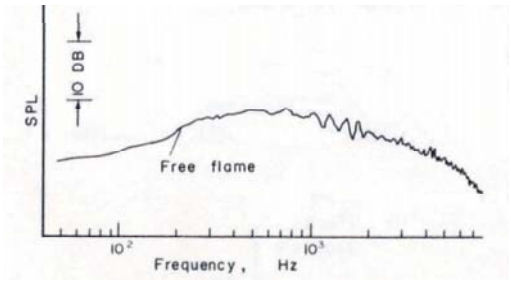

Figure 2.2: Typical spectral shape of combustion noise for a premixed free jet flame in free field [239]

where M is the Mach number, Re the Reynolds number and F the fuel mass fraction. From the Equation (2.11) it can be observed the absence of a strong dependence on Reynolds number, indicating that transport processes play very little role in the noise generation process and that this is dominated by the large scale eddies.

An example of the frequency spectrum of a Bunsen burner flame is presented in Figure 2.2. It can be observed that noise from open premixed flames is a typical broad band noise with a single spectral maximum in correspondence of $f_p \simeq 800Hz$. Searching another correlation for the estimation of the Strouhal number – a dimensionless number describing oscillating flow mechanisms defined as $St = f_p D/U$ – one may obtain:

$$\mathrm{St} \propto \mathrm{M}^{-0,40}\mathrm{Re}^{0,02}\mathrm{Da}^{0,39}F^{-1,1}, \tag{2.12}$$

It can be observed again the absence of a strong dependence on Reynolds number. From Equations (2.11) and (2.12) the chemistry, through Da, and the flame temperature, through F, result having a strong role in the combustion noise generation.

2.2.2.2. Theory

The purpose of this section is to present the theoretical approach [244] for the study of combustion noise from free field premixed flames capable of explaining the results of Equations (2.11) and (2.12). Figure 2.1 (B) represents a scheme of the analyzed flame. This simplified theory considers the limit situation that the flame size decreases to zero with the control surface "A" remaining fixed, so that the problem is reduced to the study of a puntual monopole noise radiator. Under this hypothesis, the wavelengths emitted by the flame can be considered long compared with the maximum dimension of the reacting volume V surrounded by A. Furthermore, nearly complete mixing of the post flame gases with the ambient air took place, so that the speed of sound outside of A can be considered constant and the flow speed approximate to zero. Consequently, outside of A, a simple Helmholtz wave equation can be formulated:

$$\nabla^2 p_\omega + k^2 p_\omega = 0. \tag{2.13}$$

whose solution under the hypothesis of free field, compactness of the flame and absence of mean flow can be expressed by:

$$p_w = \frac{e^{-ik|\mathbf{r}|}}{4\pi \mid \mathbf{r} \mid} \bar{\rho} \int_A \Big(\frac{\partial \nu'_{n_0}}{\partial t} \Big)_\omega dA \tag{2.14}$$

This equation, that depends only on the vector position $\mathbf{r}$, represents a spherically symmetric monopole radiation. Furthermore, it results that the noise is generated in the flame by a fluctuating normal component of velocity ν'_{n_0} on the surface A. From Equation (2.14) the acoustic power can be expressed by:

$$P = \overline{p'^2} \frac{4\pi \mid \overline{r} \mid^2}{\bar{\rho}\bar{c}}. \tag{2.15}$$

Summarizing, in the case of this simple flame, combustion noise can be considered as a monopole noise field caused by dilation of the volume enclosing the flame. From Equations (2.14) and (2.15) it results that direct combustion noise is a consequence of the dilation of the flow, volumetric expansion and contractions. This dilation, in turn, is caused by a heat release rate fluctuation in the flame. Furthermore, using these two equations the thermoacoustic efficiency η_{ta} can be expressed by:

$$\eta_{ta} = \frac{P}{\dot{m}_f H} = \frac{\bar{\rho}}{4\pi\bar{c}} \Big(\int_A (\frac{\partial \nu'_{n_0}}{\partial t})_\omega dA \Big)^2 \frac{1}{\dot{m}_f H} \tag{2.16}$$

Taking into account the experimental absence of the Reynolds effect on sound, it can be assumed that $\nu'_{n_0} \propto S_T T_f / \overline{T}$, which is equivalent to saying that the normal component of velocity ν'_{n_0} is proportional to velocity downstream of an isobaric adiabatic one dimensional flame propagating at the turbulent flame speed S_T. Furthermore, assuming that only large scale turbulence is involved in the noise generation process, taking A proportional to the observed flame area, using Equation (2.12) and other necessary relations, it results that:

$$\frac{P}{\dot{m}_f H} = \eta_{ta} \propto \mathrm{M}^{2,2} \mathrm{Re}^{0,04} \mathrm{Da}^{0,78} F^{-1,2} \Big(\frac{H}{c_p \overline{T}} \Big). \tag{2.17}$$

This recovers closely Equation (2.11). Theory and experiments appear to be consistent for the relative simple case of free field premixed turbulent flames.

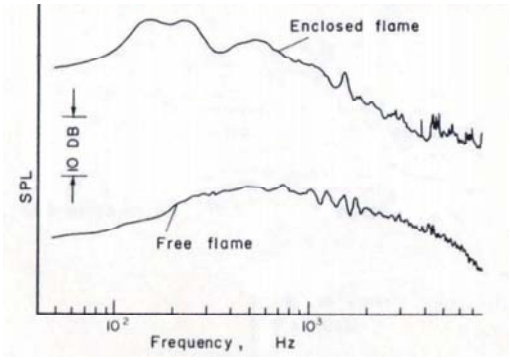

Figure 2.3: Spectral comparison of the sound pressure inside a tube and in anechoic surroundings [239]

2.2.3. Factors affecting combustion noise generation

Unfortunately the models and equations presented above are well suited only for small, gaseous, premixed flames radiating in free filed, but do not hold for all flame types. The size of the flame affects the combustion: the radiated sound pattern is influenced by the ratios of the wavelength to flame size and to burner size, respectively. Furthermore the size affects the turbulence structure and frequency content of noise.

The fact that the flame is premixed or diffusive influences the flame aerodynamics, shape and turbulent structure. Moreover, depending on the primary forces controlling the flow, the flame can be affected by the gravitational field and distinctions could also be made if swirl is induced in the flow. Fuel type also affects the flame noise, since there are different mechanisms for noise generation in liquid fueled burners correlated with vaporizing phenomena.

Another essential aspect to consider in combustion noise generation process is the fact that most of practical situations do not take place in free field conditions. The sound radiation characteristics of an acoustic source enclosed in a limited space change in comparison with free field condition. Enclosing a noise source causes phenomena like the excitation of resonant modes and possible feedback between reflected waves and source. Figure 2.3 shows a spectral comparison of the sound pressure from a flame inside a tube and in free field condition. Form the figure it can be easily observed how the presence of a duct amplifies the sound pressure level. In the spectrum of the enclosed flame it is also evident the appearance of the first two longitudinal modes.

2.2.4. Physical interpretation limitations

From the previous sections follows that the physics of the combustion noise generation process are well enough understood. Since combustion noise is recognized

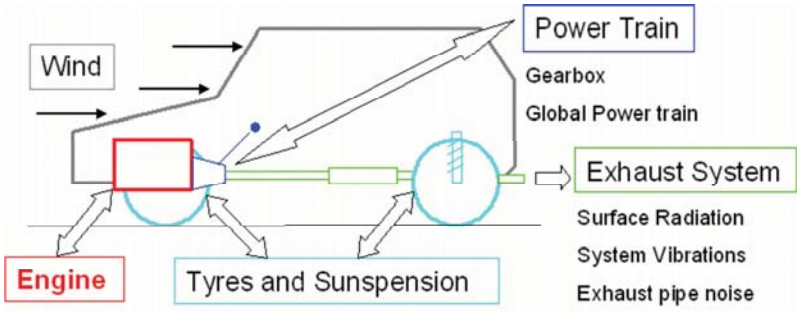

Figure 2.4: Identification of the noise sources in a vehicle

as the result of dilation fluctuation of the flow caused by heat release rate variation in the flame, it is also possible to predict the effects of various design parameters on the noise output.

On the other hand, this type of approach does not seem sufficiently reliable to get an accurate quantitative prediction of the noise characteristics and its spectral content. Mathematical approaches are characterized by an enormous complexity and need inevitable approximations. Depending on the case, they can bring to incorrect answers due to the incorrect mathematical formalisms used and to the lack of knowledge of the phenomena linked to the interaction between turbulence and combustion.

Interesting results can be obtained from the study of simple situations, such as a small premixed turbulent flame in free field conditions. In any case, in practical situations, such as the combustion in Diesel engines, innumerable factors play an important role in the noise combustion generation process. All this strongly limits the use of a rigorous physical or mathematical approach for the study of combustion noise in Diesel engines.

Consequently, other approaches have been developed to study the combustion noise from Diesel engines. The goal of the next sections is to introduce the classification of the various components that contribute to noise radiation in Diesel engines, focusing on the noise from combustion, and to present the numerous techniques developed for its analysis.

2.3. Engine noise components and sources

Noise control on commercial vehicles deserves increasing interest from vehicles manufacturers due to the increasingly stringent legislation [40] and to the fact that acoustical comfort plays an essential role in customer purchasing decision [52, 212]. Therefore, it is important to understand and separate different contributions to vehicle noise focusing on the main source of noise which is the engine. There are several

possibilities to differentiate the noise sources in a vehicle [3, 16]. Figure 2.4 presents five main sources responsible for noise generation:

- Wind - noise due to the interaction of the vehicle with the air, it depends on the speed and streamlining of the vehicle

- Tyres and Suspensions - noise effects by wheel road contact, it depends on the speed, on the characteristics of tyres and suspensions as well as of the road surface

- Power Train - noise radiated by the gearbox surface and by the others gears and axels of transmission

- Exhaust system - vibration and noise radiation of the system as well as the exhaust pipe noise due to orifice effect

- Engine - noise radiated by engine block and accessories, it can be distinguished into combustion noise and mechanical noise

At lower speed (under 30 Km/h for passenger cars, under 50Km/h for trucks) the engine, especially a direct injection Diesel engine, represents the main noise source of a vehicle, tyre noise dominates above that, and aerodynamic noise becomes louder as these increase with vehicle speed. According to Russell and Haworth [207] the engine as a whole contributes between one quarter and a half of the total sound of a vehicle. Consequently, it results essential to identify the different components of the noise radiated by an engine in order to analyze separately every cause trying to limit its effect.

In the next sections the engine noise component will be presented separately and a short review of the classical techniques for the separation of the various components will be given.

2.3.1. Combustion noise

According to Russell and Haworth [207], in many high speed direct injection engines, in practical situations such as during the tests specified in vehicle noise legislations, combustion noise dominates not only the engine noise but also the noise from the complete vehicle . Consequently, it appears clear that many researches on the engine combustion noise have been done in order to get a better understanding on this phenomenon, also this Thesis will focus on it and will leave out the other sources of noise in a vehicle.

Combustion noise in internal combustion engines is the result of the forces generated by the gases that expand during combustion. In Diesel engines combustion produces an abrupt pressure rise, this is the main cause for the typical impulsive noise, also known as "knock" [186, 207], that characterize these engines.

On the one hand, the pressure forces are transformed into noise and radiated directly to the environment by the cylinder head and the upper part of the cylinder

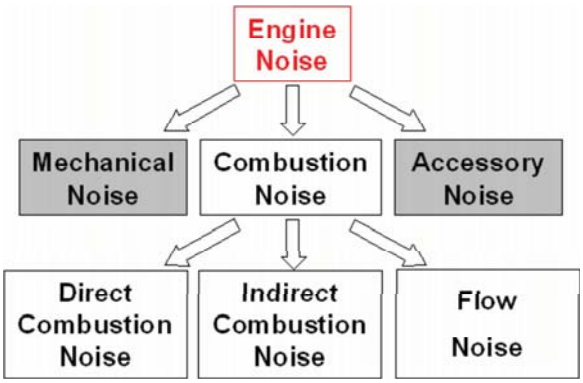

Figure 2.5: Identification of the noise sources in a vehicle

block. On the other hand, these forces, acting on the piston, are transformed into mechanical forces and transmitted, even more intensively, internally, through the crank train components, mean bearing and crank case [15, 214, 272].

Alt [2, 3] gave a complete and clear classification of the engine noise shares. Figure 2.5 shows how the engine noise can be divided into mechanical noise, combustion noise and accessory noise. With the term mechanical noise is indicated the noise that comes from the movement of all mechanical devices of the engine: valves, drive shaft, axels, gears, etc. The accessory noise is noise caused by the auxiliar elements such as the injection system, the turbo-compressor group, etc.

Combustion noise, in turn, can be considered as the sum of direct and indirect combustion noise as well as flow noise. This classification must not be confused with the definition of direct and indirect combustion noise introduced in Section 2.2 for the physical interpretation of combustion noise generation process.

According to this engine noise classification, the acting forces generated by the combustion fall into two categories depending on their characteristic time. The first group of forces, also indicated as pressure forces or gas forces, follows the cylinder pressure curve, and the resulting noise radiated by the structure is defined as direct combustion noise. Ideally this noise would be the result of the pressure forces directly acting on the structure assuming that no clearances are involved.

The second group follows the rotary force curve which causes the indirect combustion noise forcing the engine components to move through their clearances resulting in impacts. The momentum load of the crankshaft and piston side force generate the crankshaft rumble and piston slap, respectively. Following Alt's definition, the flow noise, radiated by the intake and exhaust system components, is also ascribed to the combustion noise, as both are load related noises. In any case, flow noise share assume a certain importance only in the case of gasoline direct injection engines, due to the high volumetric flow during stratified operation [2].

Other authors [6,202] consider the engine noise as simply composed by combustion induced noise and mechanical induced noise. Figure 2.6 shows a schematization

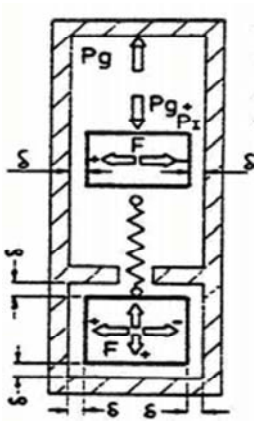

Figure 2.6: Engine structure scheme [6]

of the engine structure and of the exciting forces from combustion. In this case the exciting forces are divided into unidirectional forces and reversible forces. Unidirectional exciting forces are the gas forces P_g and the inertia forces P_I acting mainly around the TDC (top death center) on the compression stroke, produced from compression and combustion, and responsible for combustion induced noise. Reversible forces F change direction due to the engine crank mechanism and associated inertia forces, they are the cause of the mechanical induced noise. The forces accelerate the various elements of the internal carrying structure across the clearances δ causing impacts and inducing the engine structure vibration. According to this classification, piston slap and crankshaft rumble are considered as mechanical noise, instead of indirect combustion noise (as resulted from the Alt's nomenclature).

2.3.2. Mechanical Noise

The slight divergences in the definition of the various combustion noise shares are due to the fact that, in the practice, it is almost imposible to separate completely combustion noise and mechanical noise. Consequently, even though the intention of this Thesis is to focuss on combustion noise, the main characteristics of the indirect combustion noise and mechanical noise will be also described.

2.3.2.1. Piston slap noise

One of the main sources of noise and vibration in internal combustion engines is the impact between piston and cylinder wall, also known as piston slap. Figure 2.7 shows a scheme of the forces acting on the piston during the phases of compression (Fig. 2.7a) and expansion (Fig. 2.7b), P represents gas plus inertia forces acting on the piston, vertically. These forces are reacted by the connecting rod which changes its direction during the engine working cycle. The crank-slider mechanism presents a small clearance δ between piston and cylinder liner wall, the connecting rod induces a sideways component F that changes its direction depending on the position. As a result the piston bounces from one side of the cylinder wall to the other, the impacts excite the engine block that, in turn, vibrates and radiates noise.

Many experimental and theoretical studies can be found in scientific literature trying to understand, quantify and reduce this phenomenon. Whose importance is

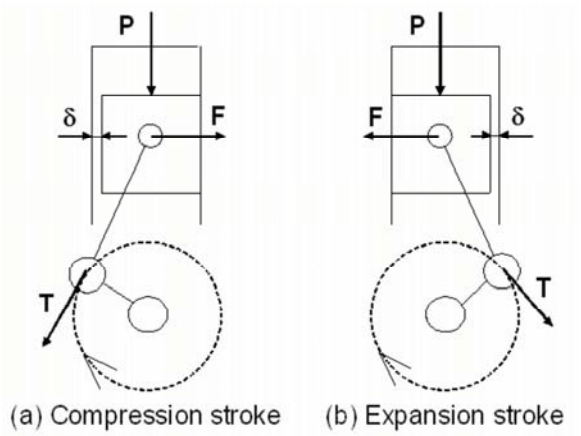

Figure 2.7: Generation of reversible forces in a crank mechanism

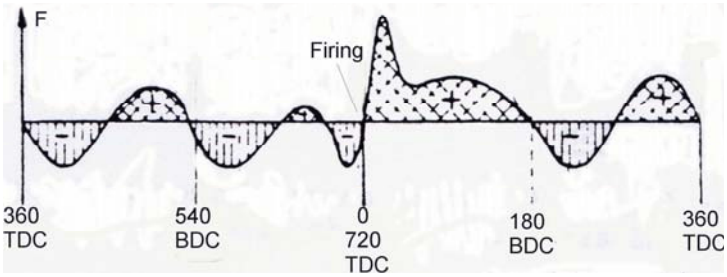

Figure 2.8: Example of side force history over a working cycle in a four-stroke Diesel engine

due to the fact that it represents one of the major sources of noise and vibration, but also a possible cause of deterioration of the engine performance [112,194,196,237,269].

Figure 2.8 shows a typical time history of the side force F over a working cycle of a four-stroke Diesel engine. The figure shows that the force side reverses eight times during a working cycle, in the proximity of the top death center (TDC) and of the bottom death center (BDC), when the piston inverts its vertical direction. Anyway, the rate of this side force change is too slow to produce any significant high frequency harmonics. From the figure it can be also observed that the dF/dt is greatest around the TDC at the beginning of the working stroke due to the high pressure gradient from combustion. As a result, the most severe piston impact usually occurs at this point.

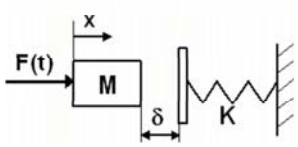

Figure 2.9: Simple schematization of the piston slap

The simplest way to schematize the piston slap generation phenomenon is presented in Figure 2.9. It considers the piston, gudgeon pin and reciprocating part of the connecting rod as a point mass M thrown through the clearance δ against the cylinder wall, whose stiffness K is considered as a massless linear spring [14, 126]. This model is not adequate for predicting the time history of the impact force but it can be used to understand the basic principles of the phenomenon and to estimate the energy transfer related to it. According to this approach, the time taken for the piston to transverse the clearance can be considered relatively short and the rate of change of the side force is approximately constant over this period. The basic equation describing the scheme of Figure 2.9 can be expressed as:

$$Md^3x/dt^3 = dF(t)/dt = constant = \sigma_0, \tag{2.18}$$

Integrating this equation three times, neglecting the damping effect of the oil film and supposing that the kinetic energy is completely absorbed by the spring deflection x_0, the force amplitude imposed on the cylinder liner due to a single piston impact can be expressed by:

$$\mid F_0 \mid = Kx_0 = (\frac{81}{4}\sigma_0^2\delta^4 MK^3)^{1/6}, \tag{2.19}$$

With reference to Figure 2.7, the piston side force F can be related to the vertical force P by the equation:

$$F = \frac{(r/l)Psin\theta}{\sqrt{1-(r^2/l^2)sin^2\theta}}; \tag{2.20}$$

where r is the crankthrow length and l the conrod length. Differentiating this equation with respect to θ, the constant σ_0 can be expressed by:

$$\sigma_0 = \frac{r}{l}P_0 n\frac{\pi}{30}; \tag{2.21}$$

where n is the crackshaft speed (rev/min) and P_0 is the result of gas forces and inertia forces at TDC. According to some authors [14,126] the kinetic energy achieved during slapping is a good indicator of the intensity of the impact, simplifying, it can be expressed by:

$$Ec = \frac{1}{2}Kx_0^2 = [\frac{81}{32}\sigma_0^2 M\delta^4]^{\frac{1}{3}}, \tag{2.22}$$

From Equations (2.19), (2.21) and (2.22) it can be deduced which parameters must be taken into account to reduce the impact force as well as the kinetic energy. To do this, it is therefore necessary to reduce clearance, reciprocating mass, rotational speed, r/l ratio and pressure forces. Another conclusion is that an important parameter is also the injection timing, as it has a significant effect on the pressure at TDC, advancing the injection will increase P_o and the lateral force. This simplified mass-spring model can not take total account of the complex behavior of the piston during slapping. To have a more precise approach to such a phenomenon two dimensional models have been developed [60, 155, 197] considering other important influential parameters, such as piston profile, oil film, pressure distribution, position of the gravity centre and of the axis of the piston, mass and inertia of the piston.

Reduction of the piston slap may be achieved in a variety of ways, used singly or in combination [196, 200, 216, 266]:

- Reducing running clearances between piston and bore - use of pistons with steel struts that control the thermal expansion of the skirt, use of light alloy cylinders [196]. The running clearances reduction, even though is theoretically an effective approach, in practice, gives limited possibilities for optimization. Excessive clearance reductions lead to mechanical problems such as seizure but also to increase fuel consumption through higher frictional losses.

- Guiding piston separately from piston crown - use of cross head design and articulated pistons (pistons formed by more pieces with different thermal expansion characteristics) [196].

- Holding piston to one wall - through elliptical piston rings, sprung shoe incorporated in skirt, hydrostatic pressure.

- Altering timings of piston slap to reduce impact severity - crankshaft and gravity center offset,piston pin offset. This last method involves moving the piston pin axis off-centre from piston axis by a relatively small amount changing the timing of the piston slap which no longer take place shortly afer TDC, under the sudden burst of the combustion, but rather already before the TDC under compression pressure which builds up relatively slowly.

- Cushioning impact of piston on cylinder wall - through the use of resilient skirts, oil cushion or lamina of different materials pasted to the skirts [196].

- Designing cylinder liner - in order to isolate the high frequency components of the piston slap impacts from the rest of the engine structure.

From these brief considerations on piston slap it appears clear the complexity of this phenomenon and its strong correlations with combustion. In fact, one of the main difficulties is the separation between combustion noise and piston slap, as both phenomena are mainly generated around the firing TDC. The main obstacle to have a clear identification of the two noise sources comes from the fact that combustion

has a direct influence on the side forces generation. Furthermore, the thermal conditions affect the piston motion pattern through the piston dilation and consequent modification of clearances.

Recent studies have developed analytical techniques with this intention [23, 227], anyway, there is no reliable method to determine both combustion and slap noise within a reasonable time and cost. According to Priede and Grover [187], combustion noise or piston slap can represent the predominant noise depending on the noise size: combustion knock is dominant in Diesel vehicle engines and piston slap in marine engines, respectively. Kanda *el al.* [113] confirmed in their experiments on a small direct injection Diesel engine that combustion noise share is slightly superior to that from piston slap and that the sum of both contributions represents more than 80 % of the total noise.

2.3.2.2. Crankshaft rumble noise

As commented before, the pressure forces generated by combustion, acting on the piston are transformed into mechanical forces and transmitted internally, through the crank train components, mean bearing and crank case. As can be observed in Figure 2.7, during a working cycle, the crankshaft system is submitted to forces that change in direction and intensity, this, together with the inevitable presence of clearances, generates crankshaft bearing impacts that induce bending-torsion vibrations of the system and noise generation.

This phenomenon is also known as rumble noise or engine harshness, this is a noise of low frequency character. It is more evident on petrol engines with relatively high performances and compression ratio and usually occurs at high engine speed or accelerating [22, 126, 133]. Many studies have been conducted to evaluate the effects of the dynamic properties of the crankshaft and of the radial clearances on rumble intensity as well as quality. The psychoacoustic concept of roughness has been applied to the measured noise and vibration data to quantify the overall sensation of rumble more accurately [22, 133, 153]. According to Maetani *et al.* [137] the crankshaft vibration can be reduced by improving the stiffness with respect to both bending and axial vibrations. Nehl *et al.* [153] found an optimal combination of radial clearance ranges for conrod and main bearing in order to improve the rumble noise quality. However, the precise theory of how crank noise rumble is generated is still uncertain.

If the engine is equipped with timing gear drives , as a result of the crankshaft torsional vibration and of the fluctuating torque, impacts occur between timing gear teeth, this noise is known as timing gear rattle. According to Russell [200], there are many ways to reduce this noise at source:

- Very close control of the teeth form, gear dimensions and distance between gear centres, to minimize backlash in the gear drive.

- Reduction of torsional vibrations in crankshaft, locating gears at torsional vibration node near the flywheel.

- Reduction of torque fluctuations in driven shafts, through coupling auxiliaries which require steady drive torques (oil, water pumps) rigidly to camshaft and fuel injection pump drives.

- Fitting backlash eliminators to timing gears, and use of resilient idler gears.

- Replacement of gear drives by quieter alternatives. A Dixon's work [70] is focused on the mechanisms to synchronously drive the valve gear as noise sources. Gears, chain-sprockets and toothed belt and pulleys systems have been compared with respect to noise emissions. Tooth belts resulted as the quietest of the drive systems [205].

Another important device to take into account is the crank pulley, as it can represent one of the main radiating sources. In fact, because of its many resonant modes and cone shape, it can work as an amplifier of the crankshaft resonant vibrations [34, 131, 137, 271]. For this reason particular attention should be payed to the study of this component by the engine manufacturers.

2.3.2.3. Auxiliar elements noise

As commented before, according to Alt's classification [2, 3], piston slap and crankshaft rumble are considered as indirect combustion noises also if their origin is due to the movement trough clearances and impact of these mechanical components. With the term mechanical noise is intended the noise that comes from the movement of all the others mechanical devices of the engine: valves, drive shaft, axels, gears, etc. The accessory noise is noise caused by the auxiliar elements such as the injection system, the turbo-compressor group, etc.

Some studies have been conducted on the valve train system considered as a noise source [34, 248]. Valve train produces noise according to two mechanisms: the dynamic interaction force between rotating cam and tappet movement and the impact from valves seating. Dixon [71] has presented a study of the contribution of other components to the total engine noise. In particular the injection system (fuel injection pump, pipes and injectors) [118, 200], the alternator as well as cooling fans have been treated as noise sources. In addition, noise from turbo-compressor group [95, 98, 141, 146] as well as gear train noise [84, 141] have been taken under consideration in several works.

Anyway, in several studies [113], it has been demonstrated that the accessory noise represents a minimal share of the total noise radiated by an automotive Diesel engine.

2.3.3. Noise from engine vibration

In the case of internal combustion engines, especially Diesel engines, combustion can be considered as a sort of controlled explosion, the control is in the form of an iron or aluminium structure which does not allow the explosion to propagate

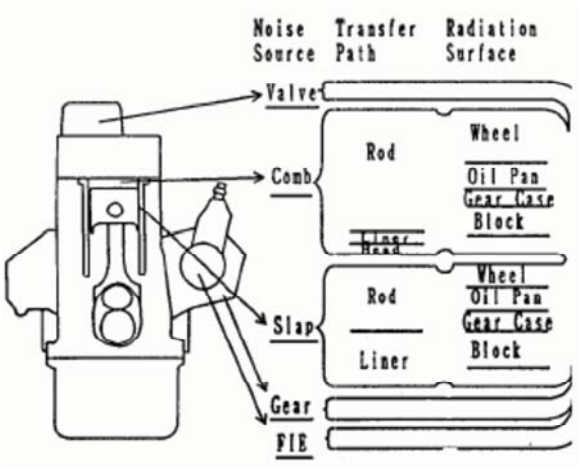

Figure 2.10: Noise flow from source to radiation surfaces [113]

directly through the open air until the pressure is reduced to a few atmospheres by an expansion and heat loss process. During the explosive combustion, the containing structure is forced to expand end deflect slightly, causing a pressure wave many times less powerful than that of an open explosion and the pressure wave is perceived as noise rather than a destructive pressure blase. The characteristics of this noise depend on the features of the combustion, the containing structure deformation and its ability to radiate noise [8].

Furthermore, combustion generates the movement of mechanical parts, the mechanical and inertia forces are applied to the engine structure (internal moving parts, crankcase, cylinder block, etc.). The components of the engine structure have to be stiff enough to prevent excessive deflections, they transmit vibrations from the sources to the external surfaces of the engine. This vibrations, in turn, excite resonances in the surface structures, particularly the thin section areas of the engine surface, inducing the radiation of noise of considerable intensity. According to Russell [204], the dynamic magnification factors of the resonances in conventional engine structures are usually in a range of 5 to 40, so the normal modes of the cast panels and covers control the noise radiated by the engine surface. It appears evident that each normal mode has a radiation efficiency and directional radiation, depending on material, dimension and position of the structure components.

In an interesting work, Kanda *et al.* made a detailed study of the entire noise generation process, combining the noise sources, transfer paths and radiation surfaces analysis [113]. Figure 2.10 shows the noise flow scheme relative to the small HSDI 3 cylinder engine used in this work. According to this figure, the predominant noise sources are combustion and slap while the noises from the valve train, the gear box and the fuel injection equipment represent a minimal share of the total. From the

transfer path analysis they observed that most of the forces are transferred through the connecting rod to the crankshaft mechanism, the rest pass through the cylinder liner and only a small share of the forces are transmitted through the cylinder head. With respect to the radiation surfaces, the engine block, flywheel, oil pan and gear case have the largest contributions, the sum of the radiated noise from these four surfaces account for more than 80 % of the total noise.

Most of internal combustion engines employ similar materials and constructions in the design of crankcase panels, sump and valve gear covers, and the load carrying parts of the structure tend to be designed following similar criteria. Actually, in-line engines can be considered as a box divided into compartments, the cylinders. The top of this box is closed by the cylinder head, which is comparatively stiff, and the bottom is closed by a relatively flexible oil sump. Also at the top and about halfway down are horizontal decks that support the cylinders. Although these decks are quite thick, their stiffness is reduced by the cylinder bores. Since the oil sump is not enough rigid, such a structure is flexible in torsion about an axis parallel to the crankshaft [131,211]. Considered as a beam, the engine is much stiffer in bending in the vertical plane than in the horizontal plane [123]. It is the horizontal stiffness which most affects the noise, this is because bending in the horizontal plane produces vibration normal to the engine sides, which constitute the major noise reacting area. It is only the vibration normal to the outer engine surface which radiates noise [123].

As a consequence, it is not surprising that inline engines of similar size have similar structure response characteristics [204, 205]:

- At low frequency, the engine response is stiffness controlled, the radiation efficiency of the oil sump the thin covers panels that constitute engine surface tend to be low [203].

- Between 200 Hz and 1 kHz, approximately, most of inline engines present flexural resonances of the crankcase and cylinder block. Fortunately the in-cylinder pressure excitation are not particularly well coupled to these modes of vibration [204].

- Above 1 kHz, and below 5 kHz the cast panels and the valve gear covers present strong resonances and the first crankcase panel mode is closely coupled to the cylinder pressure excitation via the connecting rod and crankshaft vibration. Between 1 kHz and 4 kHz, approximately, there is also a longitudinal mode of the piston, conrod and crankshaft which increases the engine structure response in this frequency range [120, 203, 279].

- Above 5 kHz, the cast aluminium covers and small thin-section cast iron areas as well as intake manifold surfaces radiate quite efficiently sound. However the cylinder head route for transmitting vibration is very much stiffer than the piston connecting-rod route, so the engine structure response falls off [203].

This general tendencies of the vibration characteristics of in-line engine structures will be confirmed from the study of the attenuation curves that will be thoroughly discussed in the Section 2.5.1.

2.3.3.1. Vibration measurement techniques

As commented before the radiated noise is the direct consequence of the engine surface vibration, consequently, many studies have taken into consideration the vibrational characteristic of the engines for assessing engine noise. The simplest way to measure vibration is using accelerometers, a simple vibration sensor attached to the surface of the vibrating body. This is a widely used experimental device [20,65,113,116,127,189], its success is mainly due to its relatively low cost and to the fact that it can be easily mounted on an engine surface. This experimental devices have showed good results in studies for the reconstruction of the cylinder pressure from vibration measurement [288, 289] giving the advantage of avoiding the use of expensive in-cylinder pressure transducers. Furthermore these are widely used for the detection of knock and misfire in gasoline engines [58, 144].

On the other hand, an accelerometer is normally a single degree of freedom system, giving information only in the direction of its axis and in well defined frequency ranges. Furthermore, it has been experimented that the signal obtained with an accelerometer is strongly dependent on its position [286]. As a result, this measurement technique it is not able to detect the vibrational characteristics of a global surface and it is inadequate in the case that the objective of the study is the radiated noise of the whole engine.

Another interesting technique introduced for studying the vibrational characteristics of an engine is the holographic analysis [105, 136, 151]. This is an optical technique that can make a three-dimensional image of an object surface through the use of laser waves. This method is widely used in automotive development process for example to analyze the knocking behavior of modern engines and for correct positioning of knocking sensors [25]. The main problems of this technique stays in the high cost of the laser measurement equipments.

2.3.4. Noise sources identification techniques

In their first works Austen and Priede [18] observed that, for the engines they studied, combustion noise was most prominent in the frequency range between 800 Hz and 2 kHz, but, at retarded injection timings, mechanical noise could become dominant even in this frequency range. Also Anderton in some works [8] refers to engines "combustion noise controlled" and "mechanical noise controlled" as an important factor for an engine manufacturer seeking to control the noise of his product. Many studies have been conducted and numerous techniques have been developed to identify the sources of noise and to limit their effects. Unfortunately there is not a unique technique that permits to recognize and isolate the noise sources completely out of uncertainty, but various analysis [7, 170] can be conducted to estimate the different contributions of the engine noise:

- Motoring Tests - The entire engine or a single component is driven by an electric motor and the noise radiation measured [214]. Motoring is very suitable

for the assessment of auxiliary components which are solely driven [98,109,113]. The main limits of this technique stay in the fact that it does not take into account the influence of the clearances variation due to the thermal dilation of the piston and engine block. Furthermore, a separation of the noise sources can be achieved by this method only if the combustion noise is predominant [170].

- Disconnection Tests - The effects of a component is evaluated by removing from the engine, or substituting it with a quieter component (close tolerance pistons, stiffer fuel pump drives, etc.) [113,185]. This technique is limited since it can only assess noise contributions which are very srong compared to the rest of the sources [98].

- Critical Noise Measurement - This technique is based in the establishment of combustion excitation levels in an IC engine which produce a combustion noise magnitude that equals the mechanical noise. The combustion excitation is reduced (usually acting on injection timing) and the corresponding changes of the engine overall noise are observed [170]. When reducing combustion excitation no further overall noise reduction is observed then it is assumed that mechanical noise is predominant and the relative cylinder pressure level – indicated as critical pressure – can be used as a design guide for combustion development [16, 180]. The weakness of this technique is that it is not always possible to reduce combustion excitation to the required low levels and that it is assumed that mechanical noise does not change with combustion variations. Particularly, this last hypothesis is incorrect for sources such as piston slap and bearing impact noise.

- Test Rig Simulation - This type of procedure is used to test a particular mechanism. The aim is to develop a special experimental apparatus where the only noise produced is via the mechanism under study. For example, to study piston slap an hydraulic shaker can be used to shake the piston in a non-running engine [113,196,237], an explosion ("Banger Rig") inside a non-running engine can be produced to simulate combustion excitation [117,159,255].

- Correlation Techniques - With this term is indicated a wide variety of Signal Processing Techniques. This type of analysis is very useful when dealing with signals of a random nature where time domain studies cannot be considered [23,170,227,253].

- Coherence Techniques - This is based on the study of an ordinary coherence function between an input signal (normally combustion characterized by the in-cylinder pressure signal) and an output signal (normally the engine noise or the block vibration) [64,94,113]. One of the main difficulties stays in the fact that it is almost imposible to measure any other primary input for mechanical sources, furthermore, the signals are fundamentally periodic and precisely phased in the engine cycle, so they are naturally coherent with any other at least up to 2kHz [8,207,232,243].

- Analytical Studies - These can be helpful where it is possible to model a particular noise source accurately. Unlike coherence technique this method can

often be used to identify excitation such as piston slap [60,155]. On the contrary, bearing impacts can be hardly analyzed because not enough is known about the behavior of bearings and oil films.

- Reciprocity Technique - This is based on a principle characteristic of the linear systems, in accordance with this principle a single source at A produces the same vibration at B as would have been produced at A wether the source had been located at B. Parts of a structure are excited and the response of an accessible point on the structure can be measured and a transfer function calculated. This transfer function can be then used to estimate the force input using the vibration measure at the accessible part of the structure. Some results can only be achieved by making several measures over an area and taking average results [11].

Actually, it can be concluded that noise source identification in internal combustion engines is one of the most difficult tasks for the noise control engineers. Many techniques have been developed, all of which give acceptable results under ideal well defined conditions. However, till now no truly satisfactory solution in terms of costs and reliability has been found.

2.4. Combustion as noise source

Over the past decades, many efforts have been dedicated to the reduction of Diesel engine noise, anyway these have not led to the definition of a single successful design concept, nor an overall mathematical has been found to tackle this task. According to Dixon [72], from all the studies which attempted to approach this problem, three simple "rules of thumbs" can be derived to produce low noise engines:

- Attention to engine geometry and operating parameters.
- Control of exciting forces, both pressure and mechanical.
- Control of the response of the outer structure

During the design stage all these aspects can be considered to achieve low noise engine. The mass, stiffness and damping properties of the engine components can be appropriately chosen to reduce vibration [254]. All the engine characteristics (speed, bore stroke, number of cylinders, BMEP, etc.), components (alternator, fuel pump, oil pump, etc.) as well as the mechanical layout (belts, chains, gears, crankshaft, flywheel, etc.) and injection system can be properly chosen [251,283].

Another important aspect that can be considered in the design stage is the control of the vibration response of the engine block [49, 183, 200, 203]. Using very stiff structures, shaping, and attaching appropriately softer components, there is the possibility to reduce the vibration of the engine walls and to shift the modes of the attached assemblies out of the range of maximum excitation of the structure [45,63].

Russell showed that through the development of a conventional engine structure, the radiated noise could be reduced of 5 dB [204].

On the contrary, on a fully developed engine the opportunities to control the noise emissions are limited. Only small variations in operating variables and slight casting changes to the block are permitted as well as the re-design of manifolds and covers [72]. In this case, the development of the existing injection system is the main form to control the exciting forces. This task is made easier by the new generation Diesel injection systems. These systems are electronically controlled and permit a variation of the injection parameters independent from the engine working conditions.

Another possible approach to reduce noise emissions is the use of sound reducing shells, flexible panels mounted at a certain distance from the engine surfaces, and of sound reducing enclosures covering the whole engine [154, 254, 273]. On the one hand, these can represent very effective solutions, on the other hand, in some cases, this approach is too expansive on commercial vehicles and can lead to problems of engine accessibility, weight and over heating [1, 254].

In this work all experiments have been carried out on a fully developed engine, consequently the main efforts have been focused on the control of the source of excitation: the combustion. The easiest way to characterize combustion evolution is through the analysis of the in-cylinder pressure signals. In the next sections this approach to the noise generation problem starting from the excitation control will be detailed, and more information of the in-cylinder pressure analysis will be given describing some of the most important characteristics of the combustion in Diesel engines.

2.4.1. Control of combustion in Diesel engines

Combustion in Diesel engines occurs spontaneously after a complex series of events has occurred in the cylinder. First of all the air charge has to be brought to a temperature which is sufficient to ignite the fuel. The air charge is heated during intake, by the manifold and in the passages in cylinder head, then, it is drawn into the cylinder.

In four strokes engines, during the intake and compression strokes, some pressure energy is converted into kinetic energy in the form of swirl, squish turbulence and in some cases more complex flow patterns. Furthermore, during these phases significant heat transfer affects the temperature and pressure reached in the combustion chamber at the end of the compression stroke.

The fuel injection nozzle is designed to help mixing between air charge and fuel, in the periphery of the fuel spray, fuel is heated, evaporated and heated further. During the "ignition delay", the period between the start of injection and ignition, a number of relatively slow chemical reactions take place until a sufficient quantity of fuel meets certain fuel/air concentration as well as pressure and temperature conditions, in close consequence of which very rapid chemical reactions take place and fuel ignites. The ignition delay period is affected by both the air motion and fuel spray characteristics, it diminishes if the air charge is hotter.

The portion of the injected fuel which is evaporated and mixed with the air charge during the ignition delay burns very rapidly after ignition, causing large and sudden release of heat with a consequent rapid rise in combustion chamber pressure. This phase of combustion is also known as premixed combustion. Successively the combustion of Diesel is dominated by diffusion processes of the liquid part of the spray. Most of the drops, especially in the nucleus of the spray, do not have time to evaporate completely, as a result in this phase the combustion speed depends on all the factors (turbulence, spray characteristic, heat release, etc.) which regulate the evaporation and the diffusion of the injected fuel [75].

The characteristic rise in cylinder pressure, induced by the premixed combustion, is more abrupt and larger in naturally aspired direct injections engines, because the ignition delay is longer than in turbocharged or indirect injection engines. This rapid pressure growth acts like a hammer blow on the piston crown and cylinder head, causing the engine structure to vibrate. This is one of the origins of the "knock" characteristic of most Diesel engines [200].

On the other hand, the diffusive combustion shows little influence on the noise. The amount of heat release of the diffusive combustion portion and its duration have a pronounced influence on the engine performance but they do not affect significantly the engine noise [149].

It is well-known that a noise reduction is the result of a smoother cylinder pressure diagram, with a less abrupt rise in cylinder pressure. Optimization of combustion, through the control of the in-cylinder pressure evolution, has been widely tackled [2, 171]. According to Russell [200], on a fully developed engine, there are three basic ways to control the combustion evolution, in which noise may be reduced:

1) - Decreasing ignition delay period

   - Retarding the start of injection
   - Increasing the compression ratio
   - Increasing the intake pressure by turbo-charging
   - Heating intake air
   - Increasing cetane number of the fuel

2) - Reducing fuel injected during the ignition delay period

   - Control of initial rate of injection through injection split (pilot and multiple injection)

3) - Restrict air/fuel mixing during the ignition delay period

   - Injection into pre-chamber
   - Mixture control by evaporation from in-cylinder air field characteristics (piston bowl shape and temperature, swirl [51])
   - Mixture control by evaporation from spray characteristics (rail pressure, number and dimension of nozzles)

- Increasing EGR (Exhaust gas recirculation)

The optimization of fuel injection characteristics and EGR flow rate are widely known as means of reducing the rising rate of cylinder pressure and noise [34,205,267]. In the last generation direct injection Diesel engines, the use of one or more pilot injections resulted to be one of the most effective ways to reduce noise, as pilot injection can reduce the ignition delay [206,280]. In fact, it is generally believed that an increase in the ignition delay would result in an increase in the combustion noise level, however, a lack of O_2, as a consequence of exhaust gas recirculation can increase the delay period without adversely affecting the noise [38,191,230]. The optimization of the combustion characteristics focused on a noise reduction is a particularly complex task, since any changes to the combustion system to reduce noise will affect other aspects of the engine performance such as fuel consumption and pollutant emissions.

2.4.2. In-cylinder pressure analysis

The analysis of the cylinder pressure evolution has been widely used as one of the most reliable methods for combustion noise assessment. From the first studies on engine acoustics it was observed a clear relationship between combustion noise and in-cylinder pressure evolution. Anderton, as well as Priede, observed that when combustion was abrupt, the rate of pressure rise and initial peak rate of heat release were large and the level of the high frequency (above 500Hz) cylinder pressure spectrum components were also high [9, 186]. Tung and Crocker [265] suggested that the frequency content of the cylinder pressure up to about 300 Hz is related to the maximum cylinder pressure. Between 300 Hz and 2 kHz it is related to the maximum rate of cylinder pressure rise and above 2 kHz it is related to both the magnitude and the duration of the second derivative of the cylinder pressure.

Many experiments [217] have been conducted in order to estimate the combustion noise starting from the measurement of in-cylinder pressure, taking into account:

- rate of pressure rise
- rate of heat release curve
- spectral contents

In the next sections the main results of some studies on the effect of heat release on combustion noise will be presented. Furthermore, a short description of the cycle-to-cycle variations characteristic of the Diesel combustion will be given.

2.4.2.1. Effect of Rate of Heat Release on combustion noise

Different researches [149, 205, 207] showed the existence of an overall relationship between peak Rate of Heat Release (RoHR) and combustion noise. A computer analysis program was created by Russell so that simple, triangular shaped RoHR diagrams could be entered as input data instead of experimental data. These diagrams

were combined with different compression ratio combustion systems (ranging from 16:1 to 21:1) and, assuming no heat transference during combustion, a series of cylinder pressure diagrams was computed. Combustion noise which would be generated by such pressure excitations was calculated using a standard structure attenuation curve, the SA1-7 curve calculated by the Russell by meaning the response of eight different engine families [207]. This methodology, also known as "block attenuation curve technique" permits to estimate the radiated noise from the in-cylinder pressure trace. This procedure is widely used in combustion noise studies and will be presented in Section 2.5.1.

A first study was performed to investigate the influence of the timing, initial slope and the peak of the RoHR. The three independent variables were each varied one at a time, and the resulting combustion noise was calculated. Figure 2.11 shows that higher slopes of RoHR give rise to higher combustion noise levels at all ignition timings. The high slope of RoHR causes cylinder pressure to rise rapidly giving a spectrum rich in high frequency components. In this case, combustion noise levels are high and insensitive to ignition timing. On the other hand, when RoHR with more gradual initial slope are considered, combustion noise becomes more timing dependent and 5 degrees before TDC was chosen as the best position for ignition timing in order to diminish the noise [207]. It was also evidenced that as the peak of RoHR is reduced, the noise level reduces too. However no unique relationship has been found which covers the three parameters examined, they can be used as a guide to reduce combustion noise but they can not be used as predictors by themselves [205].

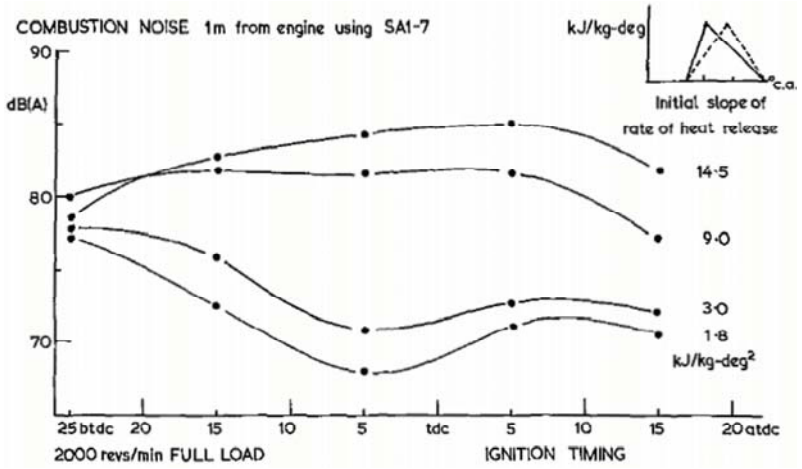

Figure 2.11: Effect of ignition timing on combustion noise for RoHR diagramas with different initial slope [207]

From experimental researches [134,207] it resulted a sort of "trade-off" between combustion noise and efficiency. Usually, in fact, the most efficient combustion is

associated with high combustion noise levels. This is explained by the high RoHR near top dead centre required to maintain a high peak cylinder pressure, which gives rise to high frequency components in the combustion noise. On the one hand, if too much heat is released before TDC, then the peak cylinder temperature and pressure are excessive with the risk of exceeding the safe working loads within the engine structure and the limits of the nitrogen oxides emissions. On the other hand, if the peak of RoHR is excessively retarded, peak cylinder pressure will be too low for an efficient cycle and excessive smoke will be present at the exhaust.

Figure 2.12 shows how, with the software developed by Russell, it was possible to shape the RoHR curve such that a 10 dB reduction of combustion noise could be theoretically achieved without increasing peak cylinder pressure and indicated specific fuel consumption. To reduce combustion noise it is necessary to reduce the cylinder pressure spectral content, at least at all frequencies above 200 Hz. It was observed that a RoHR with a gradual initial slope reduces high frequency generation, while components in the range between 200 and 1000 Hz are controlled by a combination of the overall shape and peak value of the cylinder pressure. For a given peak pressure, a broader cylinder pressure shape has lower spectral content in this frequency range. To achieve a broader shape a retarded heat release is required. However, experiments suggested that excessive smoke will be produced if the rate of heat release diagram is not terminated before 50 degrees after TDC. Furthermore, the RoHR can not be terminated suddenly, because in the last phases of combustion the remaining fuel takes progressively longer to find oxygen for burning.

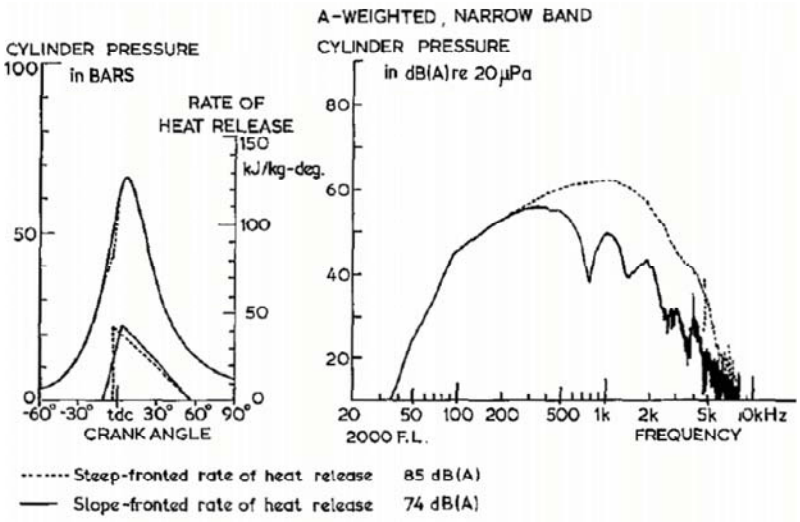

Figure 2.12: Influence of the shape of RoHR diagram on the spectrum of combustion noise [207]

From the simulations obtained with this software and the experience from previous experiments, it was possible to define an optimal triangular shape which would permit a strong reduction of combustion noise, without deteriorating the engine performance. From successive experiments resulted that, in practice, such a theoretical RoHR shape could best be approximated by turbocharged engines with pilot injection systems. Indeed, this technical solution permits to reduce considerably the premixed combustion and the increase of the rate of heat release diagram. A variety of injection systems were applied to different DI engines in the attempt to achieve quiet RoHR diagrams, however the reduction of noise level was inferior to the theoretical value. This was due to the fact that with the injection system used in the experiments the fuel quantity of the pilot injection was relatively high and hardly to regulate. As a result the combustion of the pilot injection was itself a high peak in the RoHR diagram, since the necessity to develop electronically operated injectors was evidenced in order to the get minimum pilot injection quantities together with more flexibility and precision [205, 206, 210, 247, 281].

2.4.2.2. Influence of cycle-to-cycle combustion variations

Combustion noise of Diesel engine is characterized by short, loud peak values of the sound pressure. Furthermore, combustion in Diesel engines is characterized by cyclic fluctuation. This, in turn, generates cycle-to-cycle noise variation which is one reason for the annoying character of Diesel engine noise [107, 274].

Even though, Diesel engine combustion can be considered as being regular and stable, the magnitude of the impulses characterizing the noise can vary from engine to engine, from cylinder to cylinder, and also from cycle to cycle. Variations from engine to engine are known to be caused by different combustion systems [180], cylinder-to-cylinder variation can be attributed to several causes, for instance rates of injection and compression ratios variations due to production tolerances. Various research works [180, 222, 274] evidenced the presence of another type of variation, a cycle-to-cycle variation of the combustion process which can be observed in the cylinder pressure trace and that, in turn, is responsible of the cycle-to-cycle variation occurring in the engine noise. Some studies [226, 243] evidenced this variation is intrinsic to combustion, as the high frequency components (> 1500 Hz) are characterized by stochastic fluctuations.

According to Schmillen *et al.* [222] the plausible causes for this cyclic variation in Diesel engines can be distinguished between those of macroscopic and microscopic nature. Those parameters concerning the injection system are of macroscopic nature, whereas the processes of spray and mixture formation are regarded as microscopic. Variations within the injection system, as start of injection, injected quantity/rate, needle lift and injection line pressure, have been taken into account. According to this study's results, fluctuations of the injection system do not explain the large variations in combustion excitation, consequently, also variations of microscopic nature have to be considered.

Through optical measurements it has been possible to obtain a more detailed

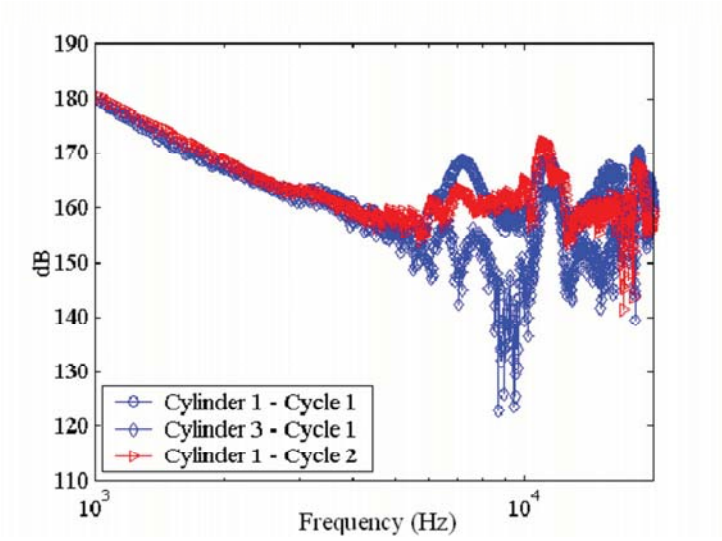

Figure 2.13: Experimental detection of the cycle-to-cycle and cylinder-to-cylinder variation with respect to the combustion chamber resonance phenomenon, for 3500 rpm and 28 % load

knowledge of the combustion excitation and its characteristic variation of microscopic nature. The measurements revealed that the point of ignition as well as the flame propagation are subject to significant variations from cycle to cycle. No clear relationships with noise were evidenced, although different ignition patterns could be observed, confirming that the ignition of sprays by neighbouring sprays rather than by auto-ignition lead to low noise combustion cycles.

Also Torregrosa *et al.* [262, 263] evidenced a strong cyclic variation in Diesel engines, particularly at high frequency range, this can be clearly observed in Figure 2.13. The high level exhibited by the harmonics in that range can be explained through the resonant character of the oscillation of the gas inside the combustion chamber. The level difference observed between different cycles in the same cylinder or different cylinders seems to be related to both the random character of the combustion process and the position of the pressure transducer relative to the combustion ignition zones. In effect, the ignition zone can be changing randomly cycle to cycle and cylinder to cylinder, and the pressure transducer location is fixed in the combustion chamber.

In the next section the phenomenon of combustion chamber resonance will be highlighted and some of the basic methodologies developed to approach its study will be presented.

2.4.3. Combustion chamber resonance

Noise emission from Diesel engines is significantly influenced by combustion chamber resonances, especially in the annoying high frequency range [221]. Already in the sixties, Priede and Grover [187], observing the spectrum of the noise of large stationary Diesel engines for industrial application, observed the presence of peaks in relatively high frequency range (> 1000 Hz). With gas sources adequately silenced, also the spectrum of the noise of the big engines for commercial vehicles presented pronounced peaks at high frequencies. From this work, it resulted that one of the most significant sources of noise, which becomes more pronounced with increasing engine size, is due to pressure oscillation in the engine cylinder, phenomenon also known as in-cylinder resonance.

Even though with Diesel engines for passenger cars the contribution of this resonance to the noise seems to be less dominant with respect to trucks and industrial engines, this phenomenon has been widely investigated. Many works have been conducted to study the influence of the resonant frequency on the control of knock in Diesel engines [97,193], as well as to estimate the bulk temperatures in the gas within the combustion chamber through the analysis of the resonance [96].

In Diesel engines, immediately after the auto-ignition of the air-fuel mixture, the combustion chamber acts as an acoustical cavity and high frequency pressure oscillations occur in the cylinder pressure. These pressure oscillations are acoustical in nature, because their amplitude is small compared to the average pressure in the cylinder at the time the oscillations occur. The presence of the resonance frequency can be easily detected observing the in-cylinder pressure spectrum of a Diesel engine. An example is showed in the Figure 2.13 where the spectra of different in-cylinder pressure evolution, relative to different cylinders and working cycles, are plotted.

Hickling [97] was one of the firsts who centered his work on this particular aspect of Diesel combustion. From in-cylinder pressure-time records, using high-pass filters with cutoff frequencies from 200 to 1500 Hz (depending on the size of the tested engine) and Fourier analysis, it was possible to show clearly the presence of numerous high frequency peaks. Comparing different cases, it was observed that increasing the engine load shifts the spectral peaks upwards in frequency, this is because higher loads increase the temperature of the gas in the combustion chamber and correspondingly increase the speed of sound. Furthermore, it was confirmed that the frequency of the spectral peaks varies inversely with bore. The peaks for larger engines occur at lower frequencies than in smaller engines.

These experimental observations can be easily explained using the theory of the resonances of a homogeneous gas in a rigid-wall cylindrical cavity with plane ends. The various possible resonant frequencies f_R in the cavity of diameter B and axial length L, are given by the equation:

$$f_R = c\left[\left(\frac{\alpha_{mn}}{B}\right)^2 + \left(\frac{p}{2L}\right)^2\right]^{1/2} \tag{2.23}$$

where, c is the speed of sound, m, n and p are integers denoting the circumferential,

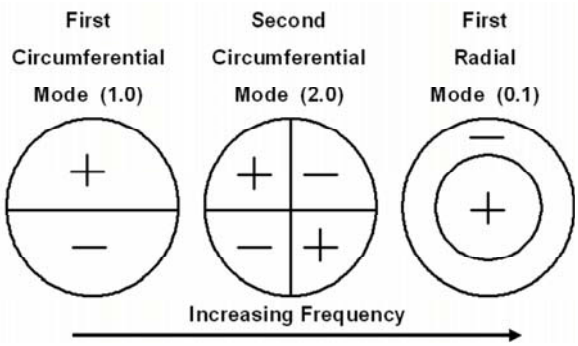

Figure 2.14: Cross-sectional view of acoustic cavity modes in combustion chamber

radial and axial mode numbers (these can be equal to 0,1,2,3,etc.). The coefficient α_{mn} corresponding to the different circumferential and radial numbers are determined from theory.

Figure 2.14 is a schematic representation of the first three modes in the circular cross section of the cylinder. In the case of Diesel engines only the lowest resonant modes have to be taken into account because higher modes are generally negligible and outside the audible frequency range. Moreover, in automotive engines, the peak clearly visible in the in-cylinder pressure spectrum normally corresponds to the resonance frequency of the first circumferential mode, while the other modes are hardly detectable.

Furthermore, since resonance phenomena only happen during a portion of the engine cycle (near TDC) where the axial length of the combustion chamber is many times smaller than the bore, the contribution of the axial modes can be neglected. As a result, Equation (2.23) becomes:

$$f_R = \frac{c}{B}\alpha_{mn}, \tag{2.24}$$

the resonance frequencies are proportional to the average speed of sound in the gas and inversely proportional to the bore, as it was observed experimentally.

The resonance phenomenon has been widely studied in the last years at CMT Motores Térmicos. In the next sections two methodologies used to approach the problem, as well as some results of these investigations will be summarized [262, 263].

2.4.3.1. Acoustic modal approach

One of the first approaches developed at CMT for the study of the combustion chamber resonance is based on the acoustic modal theory. This theory is based on the

resolution of general three-dimensional wave equation inside the combustion chamber volume taking into account the boundary conditions associated with the problem. Calculations allow to get a representation of the pressure in the bowl at certain fixed times and eventually to obtain the time evolution, and so the spectrum, in determined points. To simplify the problem, a cylindrical combustion chamber has been considered. A virtual, single excitation has been used with a level set to unity, moreover, the velocity of sound has been supposed to be constant in spite of the real temperature changes and no damping effects have been taken into account.

Thus, this simplified analytical model is based on the computation of the natural frequencies associated with the cylindrical dimensions of the bowl studied. In the most general case, each natural frequency corresponds to circumferential, radial or axial vibration mode. Total pressure p in the geometric point (r, θ, z) of the cylinder, due to a single excitation and at the instant t can then be expressed as an infinite sum of modes:

$$p(r,\theta,z,t) = \sum_{m=0}^{\infty}\sum_{n=0}^{\infty} J_m(k_{rmn}r)e^{jm\theta}e^{j\omega t}(C_{1mn}e^{-jk_{zmn}z} + C_{2mn}e^{-jk_{zmn}z}), \quad (2.25)$$

where (m, n) are the modal circumferential and radial numbers and n_z is the modal axial number, J_m are the Bessel functions, k_0 , $k_{rmn} = \alpha_{mn}/B$ and $k_{mnz} = \sqrt{{k_0}^2 + {k_{rmn}}^2} = 2\pi n_z/L$ the wave numbers, total and associated with circumferential, radial and axial directions respectively; here, α_{mn} are the Bessel coefficients, B and L the diameter and height of the cylinder respectively and C_{1mn} and C_{2mn} are modal coefficients defined by boundary conditions, cylinder dimensions and k_{zmn}.

However, as it was commented in the previous section, longitudinal evolutions can be neglected and it is sufficient to add together the first three modes: first and second circumferential modes and first radial mode, schematized in Figure 2.14. If, in a first step, a single excitation point (r_0, θ_0, t_0) is considered, the pressure in a transverse plane can be expressed as:

$$\begin{aligned} p(r,\theta,t) = {} & C_{10}J_{10}(k_{10}r)cos(\theta-\theta_0)cos(2\pi f_{10}(t-t_0)) \\ & + C_{20}J_{20}(k_{20}r)cos(2(\theta-\theta_0))cos(2\pi f_{20}(t-t_0)) \\ & + C_{01}J_{01}(k_{01}r)cos(2\pi f_{01}(t-t_0)), \end{aligned} \quad (2.26)$$

where

$$C_{mn} \propto \frac{E_0 P_0}{J_{mn}(\alpha_{mn})} . \frac{(J_{mn}(k_{mn}r_0)}{[J_{mn}(k_{mn}r)]_{max}}$$

are coefficients that depend on the z position of the plane considered, the proportionality coefficient being null at the bottom and top walls in all cases.

The factor $J_{mn}(k_{mn}r_0)/[J_{mn}(k_{mn}r)]_{max}$ modulates the excitation according to the radial position, P_0 and E_0 are the reference pressure and the excitation level respectively and $f_{mn} = c_0 k_{mn}/(2\pi) = \alpha_{mn}c_0/(\pi B)$ is the natural frequency of the mode (m, n). Finally, c_0 is the approximate speed of sound assumed to be constant

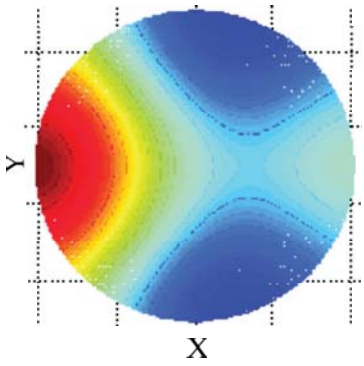

Figure 2.15: Oscillation pattern from modal theory: cylindrical bowl, single ignition site.

and determined from $c_0 \approx \sqrt{\gamma RT}$ for air as a perfect gas with the adiabatic coefficient $\gamma \approx 1{,}4$ and gas constant $R \approx 287 J/kgK$. Assuming a temperature at the start of combustion $T \approx 1100K$ (chosen for consistency with the CFD approach, described in the next section and determined with a combustion diagnosis model [130]) gives $c_0 \approx 665 m/s$.

In Figure 2.15, the pattern of the whole evolution obtained from modal theory for the simple configuration studied is shown. The figure was obtained with an excitation located in $(r_0 = B/2, \theta_0 = \pi)$, and corresponds to the pressure distribution in a transverse plane when the total maximum, both in space and time, is reached. It should be noted that the term $J_{mn}(k_{mn}r_0)/[J_{mn}(k_{mn}r)]_{max}$ in Equation (2.26) is also maximum and equal to unity. At this time, one maximum and two minima appear clearly, next to the cylinder wall. According to Equation (2.26), this maximum is reached in the direction $\theta = \theta_0$ of the excitation. Then, in the general case, the radial location of the excitation modulates the amplitude of the maximum (and that of all points in its field), although a mode can totally disappear if the ignition point takes place in an oscillation node of this mode. Then the time evolution of this figure would be periodic, with a global frequency depending on the natural frequencies of the three modes considered, and symmetric with respect to the axis $\theta = \theta_0$ because of the symmetry of the three modes. For instance, after a time equal to a semi-period, the maximum would become a minimum and the minima, maxima.

2.4.3.2. CFD approach

The acoustic modal approach provides a first assessment of the phenomenon as well as validation criteria for another approach, the numerical computational fluid dynamic (CFD). In order to validate the CFD approach and have a better understanding of the influence of the ignition site with respect to the measurement point

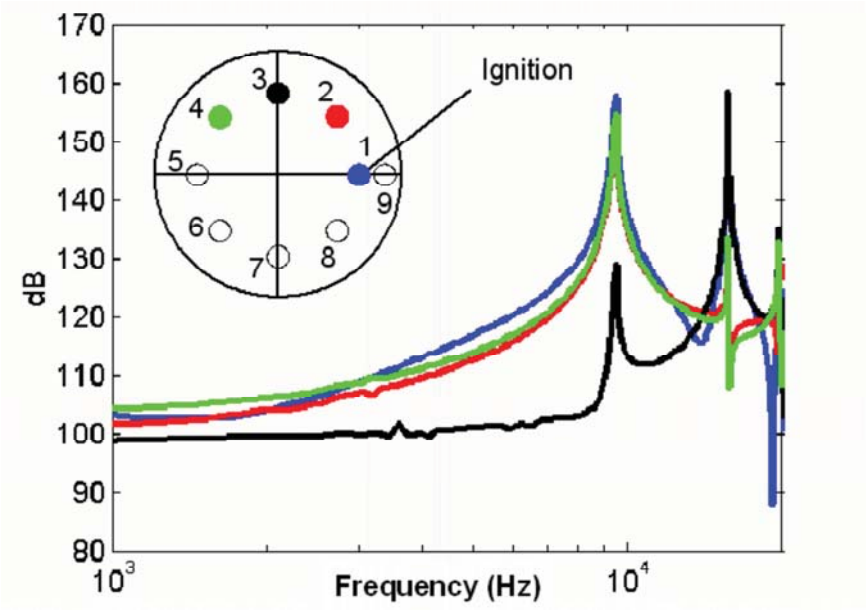

Figure 2.16: Location of source and virtual measurement points for the CFD approach, spectra resulting from the calculations

a simple cylindrical bowl geometry is considered firstly. In this case a simplified configuration based on the real experimental situation at 3500 rpm and 28 % load single injection is chosen, whose spectrum is represented in Figure 2.13 for two cycles and two cylinders. A small localized area was meshed in the point 1 of a transversal plane located at half height of the chamber, as indicated in Figure 2.16, where temperature and pressure are higher at the beginning of the computation, corresponding to the pressure rate of change due to the combustion. This is equivalent to the simplified case of a single injection spray, giving rise to a single ignition point.

The side size of the cubic cells was chosen equal to 0,6 mm, and the time step was set to about $2{,}5 \times 10^{-7}$ s in order to account for high frequency issues while keeping the computation time reasonably low. The fluid was considered to be air, assumed to be a perfect gas. Other computation parameters were the usual ones for this type of resolution, such as the $\kappa - \varepsilon$ turbulence model, for instance. By means of this simulation, different measurement points representing eventual pressure transducers, as indicated in Figure 2.16, can be analyzed. So, the whole time evolution of the pressure in any point of the combustion chamber can be obtained.

In the nine points simulating eventual transducers, and for instance the four ones presented in the spectra of Figure 2.16, three resonance peaks can be observed in the human hearing range. Their frequencies are equal to about 10, 16 and 20 kHz

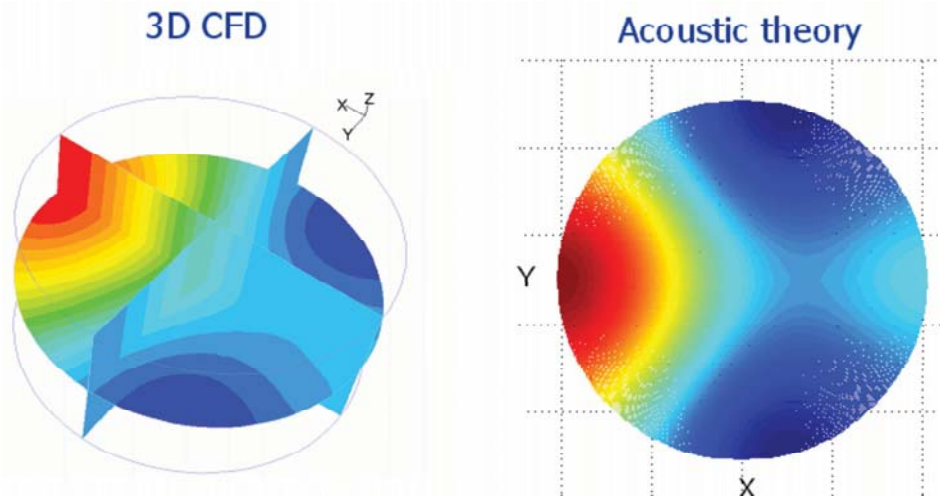

Figure 2.17: Oscillation patterns obtained with the CFD approach and modal theory for a cylindrical bowl and single ignition site

respectively, which is quite consistent with experimental measurements. Among the points of Figure 2.16, the peak levels are different because of the location of the points relatively to the excitation, and to the direction of the influencing modes. For example, signals from points 2 and 4 are hardly equal because of their symmetric positions and the symmetry of the modes. This confirms experimental dispersions, and shows as in the simplified case of a single injection spray giving rise to a single injection point the measured signal of a single combustion cycle would depend strongly on the location of the transducer in the chamber, because of the relatively random location of the ignition point.

2.4.3.3. Comparison of the approaches

In Figure 2.17, comparison between the oscillation patterns obtained from the CFD approach and from modal theory in the simple configuration studied is presented. The patterns are very similar and thus modal theory may provide a basis for the analysis of the results from the CFD approach. The maximum and minima locations are the same, as well as the overall trends. The amplitudes are different because of differences in the strength of the excitation, since the latter was not quantified in the modal computation. However, differences in excitation strength would only modulate the level of the calculated modes at all points in the plane; they would not alter the pattern. The speed of sound used in modal theory was fixed in order to predict the correct frequencies for the spikes, and it is remarkable that all of the three values match perfectly. The consistency of the results issued from the CFD and modal the-

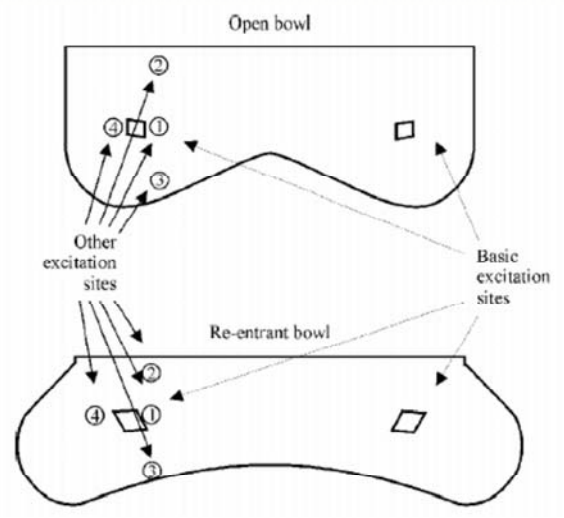

Figure 2.18: Bowl geometries and excitation sites

ory computations indicates that the CFD approach gives a reasonable description of the resonance phenomena. This was considered adequate to allow study of combustion chamber resonances with more complex, realistic geometries, as described in the following.

2.4.3.4. Influence of bowl geometry

Two bowl configurations, schematized in Figure 2.18 with open and re-entrant chambers of equal volume, were meshed and computed. All calculation parameters were as for the first case, with the cylindrical bowl. In order to achieve a closer description of the real situation, the excitation considered in this case consisted of two non-symmetric out-of-phase sources of the same excitation level; this gave a good compromise between computation time, technical difficulties and description of the actual excitation. The time lag between the excitation sources was taken to be small enough to avoid any influence of the first excitation affecting development of the other. In addition, the sources were located in what were considered realistic and similar places, taking into account size differences. In this way, the main overall effects of change in bowl geometry could be assessed.

In Figure 2.19 the pressure resonance spectra calculated at a point 5 mm above one of the two basic excitation points, for the three bowls considered in this study (cylindrical, open and re-entrant), are presented. Because of the non-symmetry of the first mode and the symmetry of the second and third ones (and the symmetry of the ignition points), if all sources were in phase or symmetric, the first spike could disap-

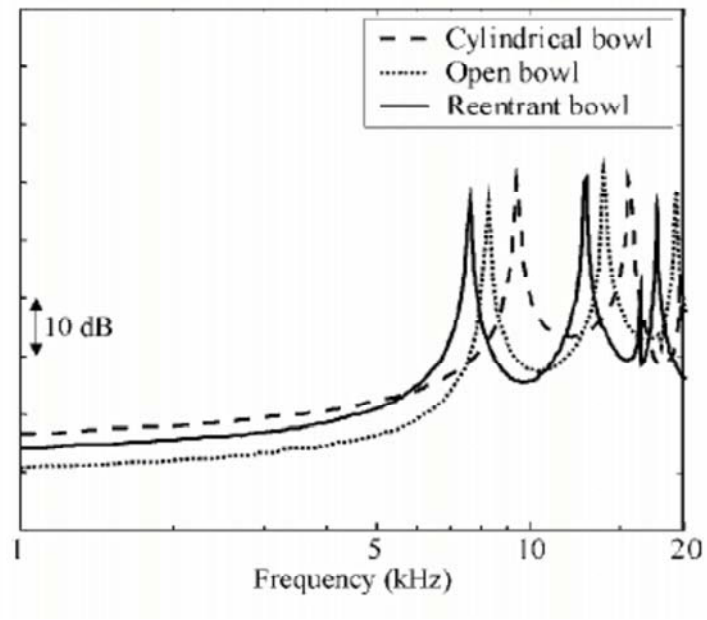

Figure 2.19: CFD simulations with two symmetric out-of-phase sources different bowl geometries

pear while the second and third ones could be duplicated at all points. Consequently, the pressure pattern during the time evolution could always remain symmetric, from the initial excitation up to the achievement of the stationary regime. However, out-of-phase and non-symmetric configurations can break or invert symmetries of maxima, minima, nodes or pressure records at virtual transducers, especially in the direction of the sources.

Furthermore, as it has been observed with the modal theory, also with CFD it was verified that the frequencies of the three spikes decrease with the increasing of the characteristic bowl diameter. However, this case remains quite far from the real one. The main differences are related to the inexact bowl geometries, the unreal type of excitation and neglect of piston movement. That is why low- and medium-frequency components are not estimated, spikes are so narrow and frequencies are not exactly the same as the real ones. To overcome this, it would be necessary to consider as many realistic excitation points as injectors and a moving piston in order to verify the effects of any changes in the combustion process and, also, to consider the effects of transmission through the block.

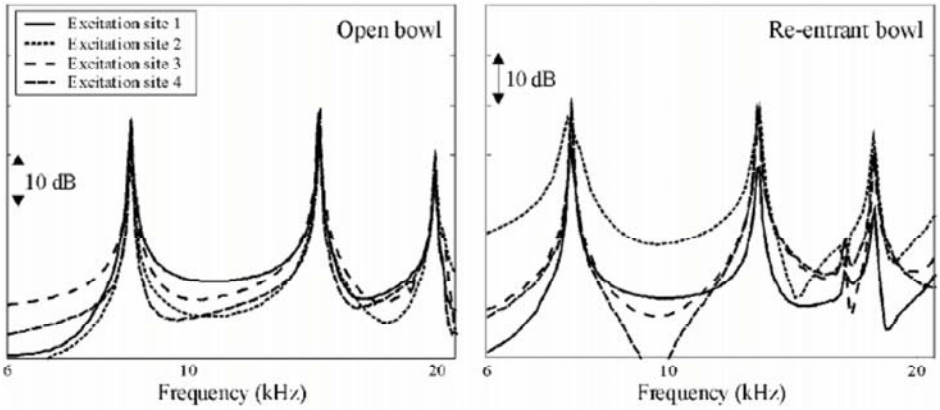

Figure 2.20: CFD simulations in the case of different ignition locations for open and re-entrant combustion chambers

2.4.3.5. Influence of ignition site

Since open and re-entrant geometries are irregular, the ignition site in the simulation might be the determinant for the results. In particular, for these geometries, diameters vary with the height of the ignition point in the chamber and this position could affect the frequencies obtained for the modes. Moreover, the bottoms of these bowls are highly irregular; this could also modify amplitude and frequency results.

In order to discount this possibility and to prove that the previous conclusions are not dependent upon the chosen ignition location, four supplementary cases were processed. Here, both radius and height of a single ignition point were changed for both open and re-entrant bowls. These new ignition points are indicated as "other excitation sites" in Figure 2.18. The results of the computations are shown in Figure 2.20; here, the registered signal always corresponds to a monitor situated at the same location as excitation site 1.

From Figure 2.20, it can be concluded that the excitation area location does not affect the peak frequencies obtained. In fact, these frequencies are not modified because they should depend only on temperature and on the overall bowl geometry, not on the diameter of the plane where the excitation takes place. For both chamber geometries considered, these parameters were fixed. However, the peak amplitudes can vary slightly, depending on whether the excitation point is located near or far from a node or from a response maximum of any of the three influencing modes.

2.5. Classic techniques for combustion noise analysis

The permissible level of exterior vehicle noise is being continuously reduced by governmental legislation. Furthermore, the standards for noise quality set by the individual customer and by competitive vehicle manufacturers are increasing too [211, 212]. The new generation of Direct injection systems offer the possibility to limit engine noise through the use of pilot and multiple injections. These systems are very flexible and permit a number of injection parameters combination almost infinite [195,247], therefore one of the main tasks for the engineers is to find, for every working condition, the injection settings that permit an optimal balance of noise, performance and exhaust emissions [19, 36, 138].

Consequently, there is an increasing demand for the development of analysis tools that permit understanding the engine noise generation problem as well as to assess the acoustic features of the engine. In this section, four of the most widely used techniques for the analysis of the combustion noise will be described. Particularly, the attention will be focused on the potential and the limits of these techniques for the estimation of the radiated noise level.

2.5.1. Block attenuation curve technique

One of the most commonly used techniques to study the combustion noise emitted by an engine is based on the "block attenuation" curve, also known as "structure attenuation" curve, introduced by Austen and Priede in 1958 [18]. This methodology considers the block attenuation as a transfer function between the excitation (in-cylinder pressure) and the effect (radiated noise). Accordingly, the curve is calculated as the difference between the spectra of in-cylinder pressure and the radiated noise (measured at 1 meter from the engine block).

The basic hypothesis of this theory is to assume a linear response of the engine structure, as a result its characteristic attenuation curve can be used to estimate the sound pressure level relative to the combustion noise emitted by the engine. Subtracting the attenuation curve from the in-cylinder pressure spectrum an estimation of the radiated noise spectrum can be assessed. With an integral sum of the harmonics of this spectrum the noise level can be easily calculated.

The measurement of noise outside the engine may be used for combustion noise measurement only if the combustion contribution to the noise is predominant. This can be achieved by operating the engine with very advanced injection timing, or with low cetane fuel [203, 207]. At any rate, in modern direct injection Diesel engines this condition is almost always respected [113].

The original technique for measuring structure attenuation has been refined and it's now a standard technique in many laboratories. As a general rule, to get better results from such an analysis, it is advisable to measure the structure attenuation at

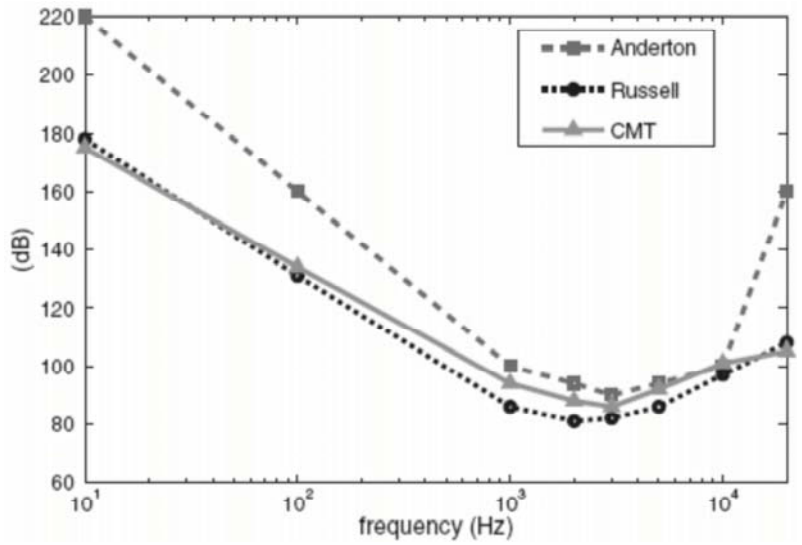

Figure 2.21: Examples of attenuation curves

different speeds and loads, and to use at least 20 engine cycles to calculate a mean in-cylinder pressure spectrum [159,207]. Furthermore, the spectra of in-cylinder pressure and acoustic pressure are both calculated in 1/3-octave band and the level amplitude is scaled and divided by the reference pressure ($2*10^{-5}$ Pa) and expressed in decibels.

Several structure attenuation curves can be found in the literature. Figure 2.21 shows three standard attenuation curves, 1/3-octave band: a classical curve proposed by Anderton [8], the curve introduced by Russell [200, 207] and the curve obtained from former studies at CMT Motores Térmicos [66]. This figure evidences for all these curves an abrupt reduction of the attenuation level at low frequencies and a "pass-band hole" in the range between 1 and 6 kHz, after which the attenuation increases. Important differences between Anderton's curve and the other two are also observed in the very low and very high frequency ranges while those differences are reduced in the range of minimum attenuation. These discrepancies should be related to differences in the type, size and the design concept of the engines studied to obtain each attenuation curve [264]. The global common shape of these curves is a confirmation of the fact that inline engines of similar size have similar structure response characteristics, as it has been highlighted in Section 2.3.3.

From the first studies on several automotive Diesel engines, the structure attenuation curves had been measured and were found to be so similar that many efforts have been done to propose a single average attenuation curve, a sort of "universal curve" which could allow easy comparisons of different combustion systems, fuels and fuel injection equipment for automotive engines [1, 45, 209]. Furthermore,

based on these average attenuation curves, several experimental tools have been developed: one of the first devices was the Combustion Noise Meter developed at Lucas Industries Noise Centre [192, 207, 209]. Another widely used experimental tool for combustion noise level estimation is the AVL 450 Noise Meter, produced by AVL List GmbH [19, 36, 61, 101].

As a matter of fact, this methodology is one of the most used for the assessing of combustion noise in Diesel engines. The main reason for its wide application is its simplicity and the fact that the acquisition of in-cylinder pressure signals is a normal procedure in engine development. Consequently, it results easier and cheaper to get an estimation of the radiated noise level instead of directly measure it. Engine acoustics measurements, in fact, require specific and expensive experimental tools.

On the other hand, this methodology leads to quite high estimation errors, in this work it will be evidenced that the use of standard attenuation curves to estimate the radiated noise can bring to excessive differences with the measured levels. This is mainly due to the basic assumption that the engine structure behaves as a linear system, while many studies evidenced that this is a quite rough hypothesis [66, 170, 264]. Consequently, this methodology seems to be a suitable tool only for comparative studies, where no particular estimation precision is required.

A deeper description of the attenuation curve methodology will be given in the Chapter 5, where this methodology has been used for a first analysis of the experiments conducted in this work.

2.5.2. Noise prediction through empirical formulae

In this section, the results of a wide study carried out at the Institute of Sound and Vibration Research (ISVR) of Southampton University and Ricardo on the overall noise at full load of 44 different IC engines [8] will be summarized. The engines tested include two-stroke Diesels, naturally aspirated and turbocharged four-stroke Diesels, indirect injection (swirl chamber) Diesel and petrol engines. However, it has to be reminded, that this study was carried our between the seventies and the nineties, consequently new generation direct injection Diesel engines were not taken into account and it can be expected that results could differ with this engine type.

Figure 2.22 shows the overall noise of these 44 IC engines as function of engine speed. For all engines considered at rated speed the variation in noise measured 1 m from the engine block is from 95 to 110 dBA. The importance of engine speed in controlling engine noise is clear from the figure, but even at a constant engine speed of 2000 rpm, for instance, there is a 35 dBA spread in overall noise level according to engine type. Also, from Figure 2.22 it can be observed that in naturally aspired direct injection Diesel engines at 2000 rpm the average noise is about 100 dBA, while for petrol engine the lowest noise level measured is around 75 dBA. It is therefore clear that very large differences in combustion excitation level should be measured in the various IC engine combustion systems.

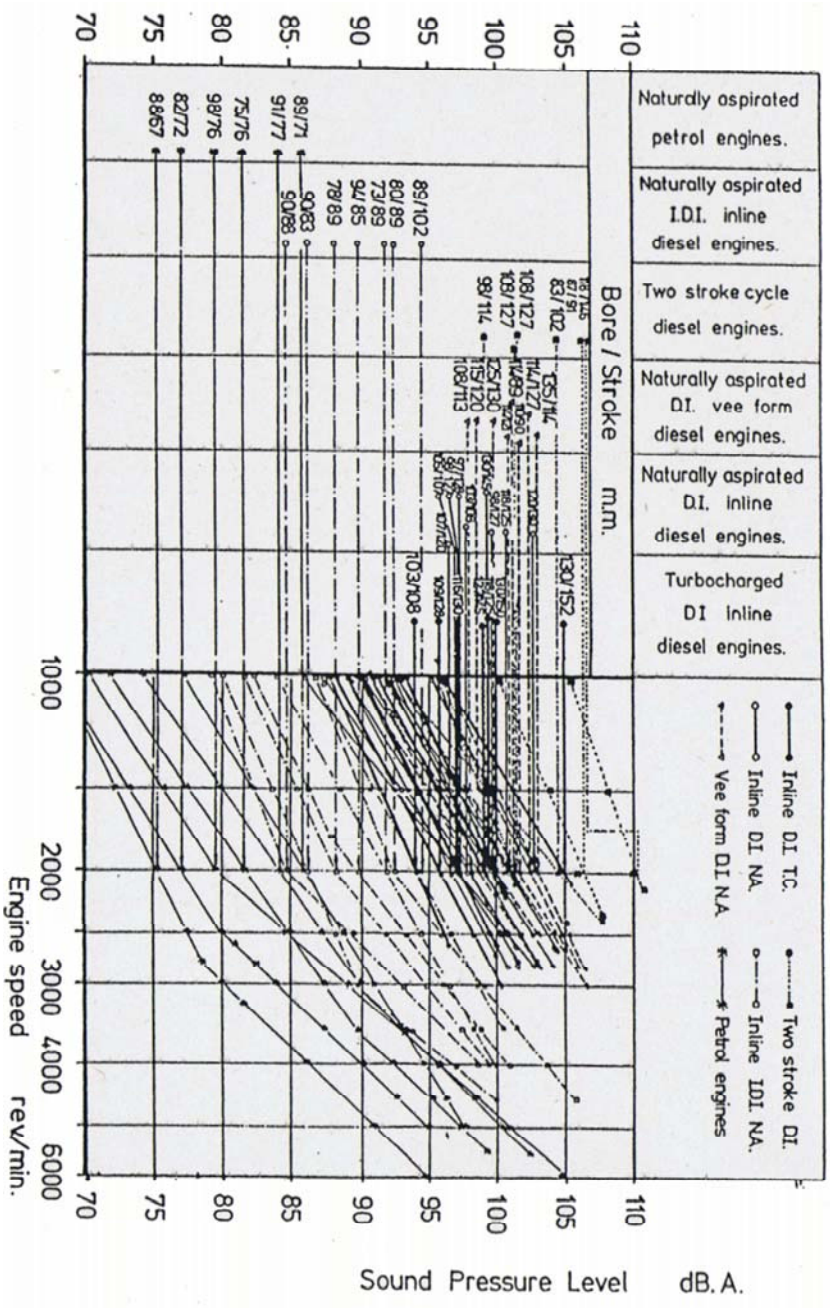

Figure 2.22: Noise versus speed at full load for different engine types

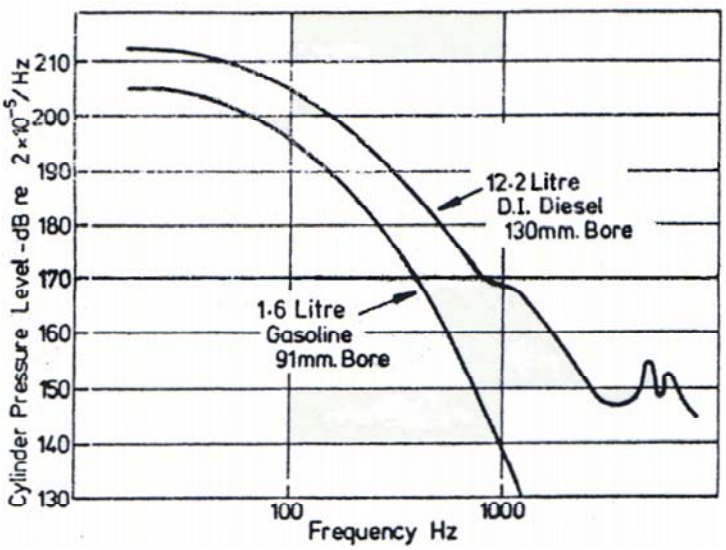

Figure 2.23: Cylinder pressure spectra for DI Diesel and gasoline engine [8]

This can be easily confirmed observing Figure 2.23 which compares the in-cylinder pressure spectra of a normally aspired Diesel engine of 12.2 l, 130 mm of bore, and that of a 1.6 l gasoline engine, 91 mm of bore. From the analysis of this spectra, at 1000 Hz, generally a frequency of maximum engine noise level, a difference of some 26 dB was observed. Starting from these observations, Anderton [8] developed a simple, linear combustion noise model in order to classify engines into various groups according to their combustion system.

This combustion model assumes an engine as a linear system and that the major force path is via the connection rod. It introduces the concept of cross impedance, at every frequency f, between the force applied to the top of the piston, $P(f)$, and the area averaged mean square velocity of the outer surface of the engine, $v(f)$. The equation defining this mechanical cross impedance is:

$$Z_c(f) = \frac{\sqrt{< v^2(f) >}}{P(f)}, \tag{2.27}$$

calculating the force as the product of the in-cylinder pressure p_c and the piston surface, the area average velocity of surface becomes:

$$< v(f) >= \frac{p_c(f)\pi B^2}{4Z_c(f)}, \tag{2.28}$$

where B is the cylinder bore. The radiated acoustic power of a surface can be expressed by:

$$W_{rad}(f) = \rho c S < v(f) > \sigma(f), \tag{2.29}$$

where ρ is the density of the medium, c the speed of sound in the medium, S the total radiating surface area and σ is the radiation efficiency. When measured with a microphone, the radiated acoustic power can be also expressed by:

$$W_{rad}(f) = \frac{p_s^2(f)}{\rho c} S_{trav}, \tag{2.30}$$

where p_s is is the sound pressure and S_{trav} is the microphone transverse area. Joining Equations (2.28), (2.29) and (2.30), the intensity of noise radiated $I(f)$, proportional to overall SPL in dBA, can be calculated as:

$$I(f) = \rho c \frac{S}{S_{trav}} \sigma(f) \frac{p_c(f) \pi B^2}{4 Z_c(f)} \tag{2.31}$$

In order to eliminate the dependence on the engine speed, Anderton plotted the in-cylinder pressure spectra of engines with different combustion systems, with the amplitude expressed in dB and the frequency normalized for engine speed and on a logarithmic scale. It was observed that, in the frequency range between 800 and 3000 Hz (considered as the predominant range of engine structure resonances), the in-cylinder pressure spectra could be approximated to a straight line. The slope of this line, in dB/decade, was defined as the combustion index N. A comparison of these simplified and normalized cylinder pressure spectra also provided a method of rating the combustion systems as a noise source, associating a characteristic combustion index to each combustion system. According to this simplified model, the cylinder pressure at every frequency could be expressed with the proportion:

$$p_c^2(f) \propto (\frac{n}{f})^N Alog_{10}(3N) \tag{2.32}$$

where n is the engine speed, N is the combustion index for the given combustion system, and $Alog$ indicates the antilogarithm. From Equations (2.31) and (2.32) it results:

$$I(f) \propto \rho c \frac{S}{S_{trav}} \sigma(f) \left[\frac{\pi B^2 (\frac{n}{f})^N Alog_{10}(3N)}{4 Z_c(f)} \right] \tag{2.33}$$

$$I(f) \propto \frac{S}{S_{trav}} \sigma(f) (\frac{n}{f})^N \frac{B^4}{Z_c^2(f)} \tag{2.34}$$

Since the noise is harmonic in nature, the intensity of the overall noise, I_O, proportional to overall SPL in dBA, is given by summing the contribution of each harmonic over the audio frequency range. This gives:

$$I_O \propto \frac{S}{S_{trav}} n^N B^4 \left[\frac{\sigma(f)}{f^N Z_c^2(f)} \right]_{f_1}^{f_2} \propto \frac{S}{S_{trav}} n^N B^4 C_{ASO} \tag{2.35}$$

where C_{ASO} is called the overall structural and acoustical response of the engine, this was observed not to vary greatly within conventional engine design constraints and

approximately proportional to $1/B$, while S for multicylinder engines was found to be proportional to B^2. Concluding, the overall noise level level resulted:

$$SPL \propto 10log_{10}I_O \propto 10log_{10}\left[\frac{n^N B^5 C_{ASO}}{S_{trav}}\right] \tag{2.36}$$

Using this model a series of empirical formulae for the prediction of the engine noise were developed already in the seventies [8]. In the last years many innovations have been introduced to redesign engine structures for lower noise, consequently also the formulae have been updated [7]. The empirical noise prediction formulae actually used at ISVR are:

- Naturally Aspired Direct Injection Diesel Engine -

$$SPL = 30log_{10}n + 50log_{10}B - 106{,}0 \tag{2.37}$$

- Turbocharged Direct Injection Diesel Engine -

$$SPL = 40log_{10}n + 50log_{10}B - 135{,}8 \tag{2.38}$$

- High Speed Indirect Injection Diesel Engine -

$$SPL = 43log_{10}n + 60log_{10}B - 176{,}0 \tag{2.39}$$

- Petrol Engine -

$$SPL = 50log_{10}n + 60log_{10}B - 203{,}4 \tag{2.40}$$

where SPL is the predicted noise level at 1 meter from the engine expressed in dBA, n is the engine speed in rpm and B is the bore size in mm. These formulae have the advantage to be really simple, the noise level at full load can be estimated simply knowing combustion type, engine speed and engine bore.

Another formula was introduced in a study of the CIMAC International Council on Combustion engines [160], in order to estimate the noise of an engine at a given regime and maximal power W:

$$SPL = 10log_{10}n + 5{,}5log_{10}W + 55 \tag{2.41}$$

Also Padoan [160] proposed two empirical equations for the assessment of the noise level of direct injection Diesel engines, the first, for naturally aspired engines, was:

$$SPL = 28{,}8log_{10}(n/1000) + 1{,}5W_{1/4} + 0{,}86V, \tag{2.42}$$

the second, for turbocharged engines, was

$$SPL = 21{,}2log_{10}(n/1000) + 1{,}2W_{1/4}. \tag{2.43}$$

where, $W_{1/4}$ is the engine charge expressed in "1/4" of the charge (it could a positive number between 0 a 4), and V is the total engine displacement in liters.

Even though the presented equations have been calculated for an estimation of the noise under different working conditions, it is interesting to note as in all empirical formulae the engine regime appears in a logarithmic tendency. These empirical formulae have the advantage to be simple and to permit an immediate estimation of the noise level, starting from parameters of the engine that are always available. However, it appears clear that these formulae give only a rough estimation, they can be useful for the comparison of engines of different families but their use doesn't make any sense when an accurate assessment of the noise level is required.

2.5.3. Time-frequency methods

Wide-band signals are frequently encountered in Noise Vibration Harshness (NVH) applications and, in general, the statistical properties of such signals have a strong dependence on the time interval of the analysis [161]. In these non-stationary signals the time-evolution of the spectrum is an integral part of the whole information and time-frequency representations must be employed [156].

The global noise level has been traditionally used to quantify the combustion noise in Diesel engines. As commented before, this can be estimated calculating the engine block attenuation curve through the Discrete Fourier Transform (DFT). The basic equation describing the DFT of a function of time $f(t)$ on a finite interval $[0, T]$ is:

$$DFT\{f(t)\} = F(\omega) = \int_0^T f(t)e^{-i\omega t}dt, \tag{2.44}$$

it yields information about cosine amplitude/phase and frequency ω, the main limit of this technique is that it requires a signal to be periodic and stationary, conditions that can not be achieved in the case of an engine [67]. However, the in-cylinder pressure signals of an engine running at constant speed can be considered, in a first approximation, as periodic. For this reason the DFT is widely applied also in engine studies.

Figure 2.24 represents a spectrum analysis carried out by means of DFT, it compares the in-cylinder pressure spectra with and without (motored) combustion, showing the energy distribution among frequency harmonics associated with the temporal evolution of the pressure. As expected, this plot shows an apparent difference between the energy level related to in-cylinder pressure at the two conditions considered. In low frequency range ($<$ 1 kHz), in both operating conditions, the energy is distributed among the characteristic harmonics of the fundamental frequency of the process, correlated to the engine speed. However, for higher frequencies a very low energy distribution can be noted in the motored-condition pressure spectrum. Furthermore, in the spectrum with combustion, a clear peak at about 10 kHz can be appreciated. This high energy harmonic is related to the resonant frequency of the combustion chamber associated with the first circumferential mode of the bowl

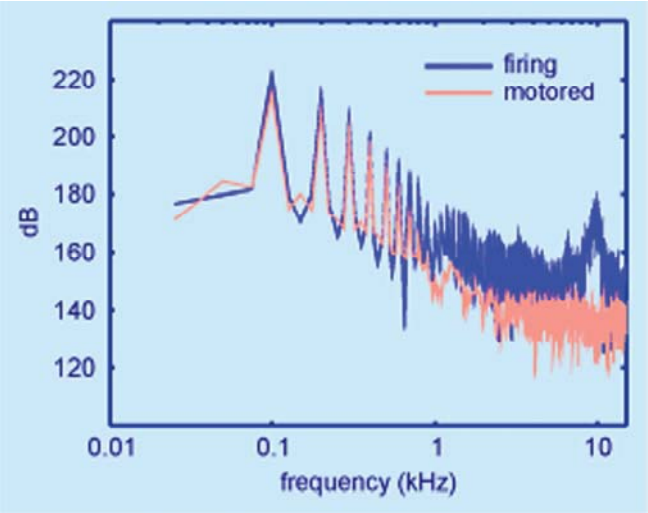

Figure 2.24: In-cylinder pressure spectrum of a 2.2 l Diesel engine at 3000 rpm: 70 % charge and motored

cavity. This has been demonstrated to be mainly determined by the gas temperature and the combustion chamber geometry [96]. As the gas temperature as well as the combustion chamber volume vary considerably when combustion takes place, the resonant frequency are non-stationary. Consequently, for a deeper analysis of this phenomenon a simple DFT analysis is inadequate and time-frequency techniques are essential tools [53, 193, 235]. In previous studies at CMT [47, 163–165, 262–264], the in-cylinder resonance generated during combustion has demonstrated to have some influence on the characteristics of the noise, this aspect will be widely explained in the next chapters.

In the continuous-time case, as an extension of the Fourier analysis to the non-stationary problems, the function to be transformed is multiplied by a window function which is non-zero for only a short period of time. The Fourier transform (a one-dimensional function) of the resulting signal is taken as the window is slid along the time axis, resulting in a two-dimensional representation of the signal. This is known as Short Time Fourier Transform (STFT). Mathematically, this is written as:

$$STFT\{f(t)\} \equiv F(\tau,\omega) = \int_{-\infty}^{+\infty} f(t)w(t-\tau)e^{-i\omega t}dt, \tag{2.45}$$

where $w(t-\tau)$ is the window function, commonly a Hann or Gaussian window. Unfortunately, in the case of noise from engines, the spectrogram obtained by means of the STFT is not efficient enough due to the high non-stationarity effects present in the signals affected by the combustion process [235]. These signals should be analyzed

by means of other time-frequency techniques, as the Wigner Distribution (WD) or the Discrete Wavelet Transform (DWT).

The WD, also known as Wigner-Ville distribution, is a transformation that may be used to give a representation of a signal in the time-frequency domain, in continuous time and frequency, it is defined as:

$$WD\{f(t)\} \equiv W(t,\omega) = \int_{-\infty}^{+\infty} f(t+\tau/2)f^*(t-\tau/2)e^{-i\omega t}d\tau. \tag{2.46}$$

In engine applications, to eliminate the problem of the cross terms in the Wigner distribution, an averaging of theoretically infinite combustion cycles is required [235], thus increasing the capability requirements of the acquisition system, mainly if broad-band analysis is necessary [66].

On the contrary the wavelet transform does not present any restriction on the signal duration. Moreover it is a reliable method for the analysis of physical systems where the characteristics signals contain time discontinuities and/or sharp spikes, as in the case of in-cylinder pressure signals and radiated sound of Diesel engines [66]. A Wavelet function can be represented by the equation:

$$DWT\{f(t)\} \equiv [W_\psi f]_{(a,b)} = \int_0^T f(t)\psi_{(a,b)}dt, \tag{2.47}$$

where $\psi_{(a,b)}$ is the shifted and dilated version of the original wavelet ψ given by:

$$\psi_{(a,b)} = \frac{1}{\sqrt{a}}\psi(\frac{t-b}{a}). \tag{2.48}$$

For integers values of a and b, a is the dilation (level) coefficient and b is the shift coefficient. The power of the DWT lies in its time dependence, particularly in its shift component that can assume a wide variety of forms.

Comparing STFT and DWT as time-frequency analysis tools it can be observed that both techniques are based on windowed functions. On the one hand, the STFT is essentially a constant width for all shifts and dilations, once the size of the window is selected the low- and high-frequency spectral components are analyzed with the same resolution. On the other hand, the DWT window is a function of time, as the function is shifted and dilated, the window is shifted and dilated too resulting in a more efficient time-frequency representation [67, 156].

Both WD and DWT techniques have been widely used in automotive applications and demonstrated to be particularly adequate for the detection of misfire and knock in spark ignition engines [37, 58, 87, 119, 132, 144, 225, 282]. Good results have been also obtained for the characterization of the noise and vibration in Diesel engines through the analysis of: the in-cylinder pressure signal [66,141,161,277], the vibration response on the engine block [228, 285, 287] and the radiated noise [66, 253, 284].

Recently a study has been carried out to develop a combustion noise meter based on the wavelet transform. Christen *et al.* [61] modified of the classical AVL's

Combustion Noise Meter substituting the original filtering system (basically the transfer function representing the block attenuation), with shift-invariant wavelet transforms. According to the authors, this software implementation would be more flexible and cheaper, while no improvements have been obtained in noise level assessment respect to the original experimental tool. This represents one of the few intents to use the wavelet transform for quantitative analysis of noise. The use of these time-frequency methods, in fact, is normally limited to qualitative considerations.

In the next section an example of the application of the time-frequency analysis techniques will be presented. The wavelet transform will be used to describe qualitatively the influence of the pilot injection on the in-cylinder pressure and on the noise radiated by the signal.

2.5.3.1. Analysis of the pilot injection influence

In this section, some results of a previos study performed at CMT [66] on the application of Wavelet transform to combustion noise analysis will be presented. In this work, measurements of the in-cylinder pressure traces and radiated noise from a 2.2 l high speed direct injection Diesel engine have been considered. The DWT has been used as a time-frequency technique, in order to analyze qualitatively the noise radiated by a Diesel engine during its combustion process. Furthermore, an analysis of the influence of the pilot injection on the in-cylinder pressure and on the radiated noise has been performed.

In order to have a more clear assessment, the spectrograms have been computed (from 0.8 to 12 kHz) for two consecutive cycles of the engine, consequently, a sequence of eight combustion can be observed. Furthermore the gray scale has been reduced to the 10 % of the maximum scale obtained in the case without pilot injection in order to highlight the energy distribution in the low frequency range and to permit a direct comparison of the spectrograms.

Since the acoustic power radiated by the engine is proportional to the block vibration velocity [127], the velocity of the in-cylinder pressure variation has been considered as the characteristic source of combustion noise. Figure 2.25(a) shows an example of spectrogram corresponding to in-cylinder pressure derivative without pilot injection. In this figure, the periodicity of the in-cylinder pressure fluctuation can be noticed and the resonant frequencies of the combustion chambers are appreciated in the frequency range between 5 and 10 kHz. In the band from 1 to 5 kHz an almost constant distribution of the energy among the frequencies is observed in every cylinder. Below 1 kHz the amplitude of in-cylinder pressure is higher during a longer interval.

In Figure 2.25(b) the spectrogram of the derivative of in-cylinder pressure with pre-injection is shown. In this plot a different energy distribution along time and frequency can be distinguished. Particularly in the band from 1.5 to 4 kHz the amplitude decreases noticeably, while below 1 kHz the energy is distributed in a band wider than in the condition above. This characteristic causes differences also between the noise radiated by the engine.

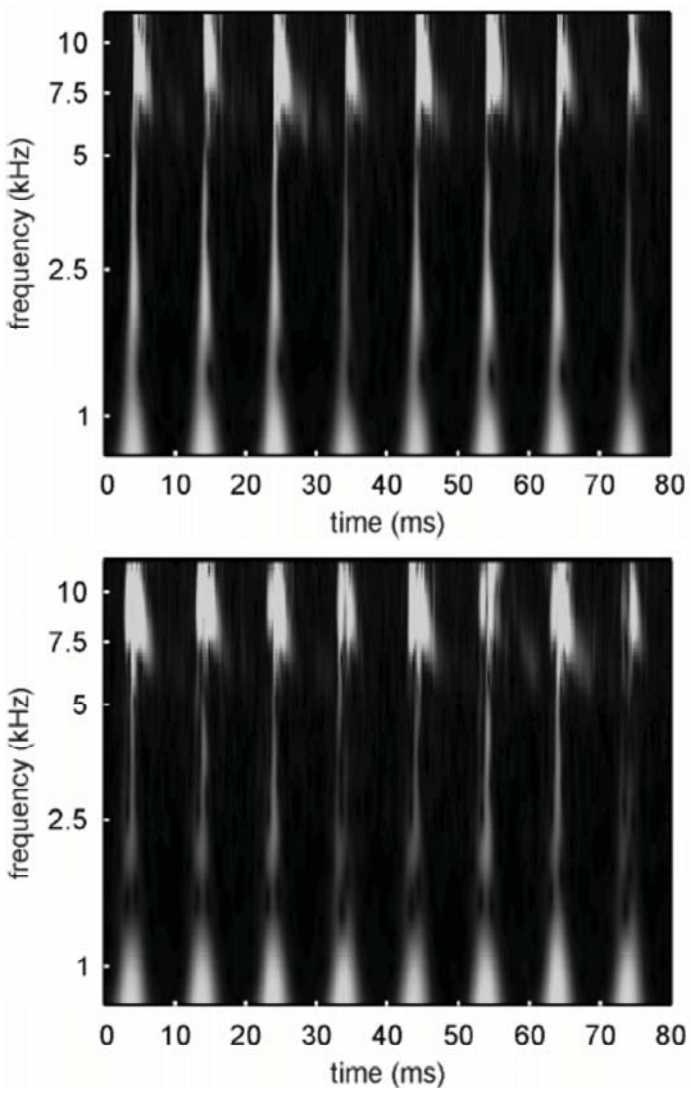

Figure 2.25: In-cylinder pressure derivative spectrogram: 3000rpm, 10 % charge: without pilot injection (a), with pilot injection (b)

Figure 2.26(a) shows the spectrogram of the sound pressure level measured at 1 meter from the block of the engine working without pilot injection. On the one hand, in this figure it can be observed that the radiated sound energy is concentrated in a relatively narrow band between 0.8 and 5 kHz. This seems to be coherent with the fact that the minimum of the block attenuation is observed for the same frequency band. On the other hand at frequencies lower than 4 kHz, the periodicity observed in Figure 2.25(a) has been lost, while a similar power distribution along time can be guessed in the 5-6 kHz band. This confirms the fact that assuming the engine block as a linear and invariant system is an assumption rather imprecise. Furthermore, the spectrogram obtained does not exhibit any noticeable sound power in the frequency associated with the resonance of the combustion chamber (between 5 and 10 kHz). This is probably due to the high attenuation level of the engine block in this frequency range.

Figure 2.26(b) shows the spectrogram of the engine noise when pilot injection is used. Globally, these results present a power level lower than without pre-injection, but concentrated in a lower frequency band, as was obtained in the in-cylinder pressure derivative. Furthermore, observing the spectrograms, it seems clear that for this operating condition the combustion noise arises predominantly through the mechanical forces, as 0.8 and 2.5 kHz is the frequency band characteristic of the mechanical noise [66, 266]. Moreover pilot injection strategy seems to reduce mainly the contribution of this source, causing a more uniform energy distribution among frequencies.

This is coherent to the fact that combustion noise level is considerably reduced when pilot injection is used. This was evidenced in another study conducted by Yajima and Nakashima [277] applying the wavelet analysis to in-cylinder pressure signals. It was determined that with a single injection strategy two combustion excitations with high frequency contents occur at ignition timings of both premixed and diffusion combustion and that both of them are noise sources. When using a pilot injection the ignition delay period of the main injection is shortened by the firing of this small quantity of combustible. As a result, premixed combustion excitation is mitigated and, even though the diffusive combustion excitation does not change, combustion noise can be reduced.

2.5.4. Numerical Methods

Due to the evolution of suitable analysis techniques together with the increase in computational capacity of affordable computers, in recent years, the Finite Element Method (FEM) and the Boundary Element Method (BEM) have become widely accepted as extremely valuable analysis tools also with acoustic problems [124]. FEM and BEM are the two most commonly used numerical methods and each one has its advantages and disadvantages depending on the problem to be solved. In applying the boundary element method, only a mesh of the surfaces is required, making it easier to use and often more efficient that the more common finite element method. Contrarily, the computational advantage of the FEM increases with high ratio of boundary area to volume. According to Saad [214], for steady state harmonic response, the BEM is

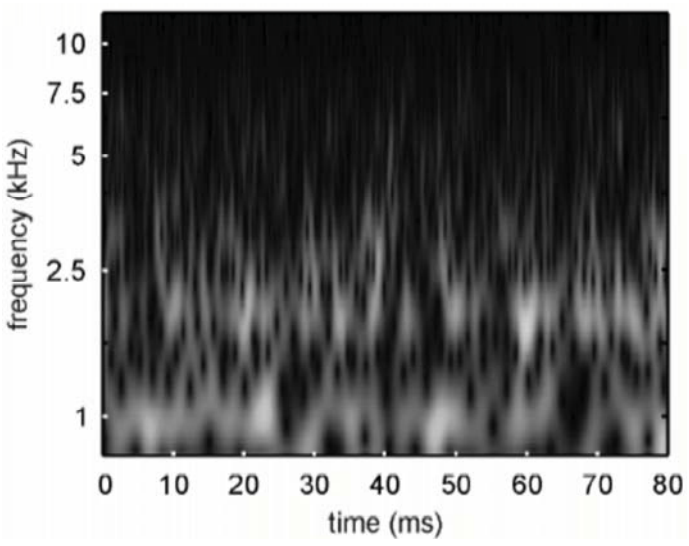

(a)

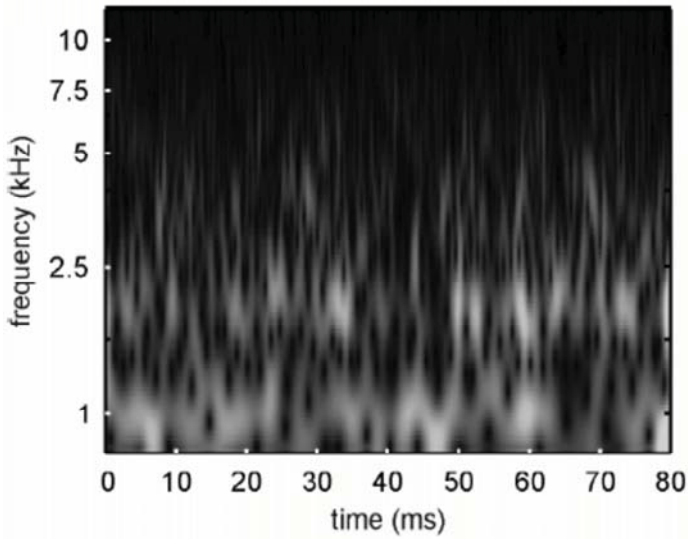

(b)

Figure 2.26: Engine noise spectrogram: 3000rpm, 10 % charge: without pilot injection (a), with pilot injection (b)

preferable for exterior problems, while for interior problems, either technique can be used. One of the main advantage of these simulation methods is that no hardware is required and a lot of modifications can be analyzed through simulations [223]. On the other hand, the main disadvantage is that the FEM and BEM methods do not give satisfactory results in a frequency range between 500 and 1500 Hz, being this gap particularly important in the analysis of combustion noise [104].

2.5.4.1. Application of FEM for vibration analysis

A typical application of the FEM technique is the prediction of the vibrational behavior of engine components [2, 125, 173, 175]. Even though the computer simulations can be performed with a model of the entire powertrain, in the early design phase, not all design data are available. Therefore, only simplified models of individual components can be built. This can help designers to have a rough estimation of the acoustical behavior of the engine. The engine block, for instance, is the main component of the powertrain and it is the part where the combustion excitation is induced to the structure; Figure 2.27 represent an example of FE engine block model. Experimental investigations revealed that the engine block and the auxiliares attached to the block often emit between 50 and 70 % of the total engine noise. Acoustical optimization by structural modifications often can be conducted on the bare engine block as mainly local mode shapes are responsible for noise which are generally not influenced by the assembly of other components [49, 100, 136, 223]. According to the

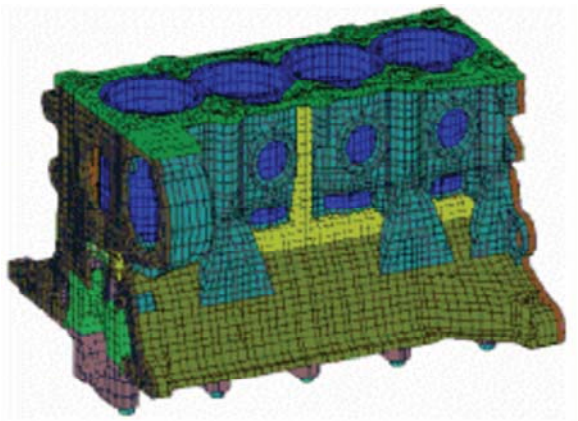

Figure 2.27: Example of engine block finite element mesh

design progress, the present models are further detailed and other components, such as the oil sump, cylinder head, auxiliaries etc. are enclosed. These models offer the possibility to perform forced response calculations in order to estimate the structural

transfer behavior. The FE structure is excited by means of spectra derived from cylinder pressure curves and the structural response is calculated as structure-borne noise velocity on the radiating surface. This permits an estimation of the sensitivity to combustion excitation of the respective structure facilitating its acoustic evaluation. Furthermore with this procedure the effect of structure modifications can be predicted and also structural weaknesses can be identified [79].

This type of analysis carried out with a model of the complete powertrain is also used to estimate the structure-noise induction into the vehicle body. In fact, the combustion excitation is transmitted as structure-borne noise and, on the one hand, it is radiated as airborne noise which enters the passenger compartment at a muffled level, on the other hand, it is induced into the vehicle body via the powertrain supports and then further transmitted to the interior of the vehicle [2]. Noise in the passenger compartment between 200 and 500 Hz is mainly structure-borne noise transmitted through engine supports [267].

2.5.4.2. Prediction of noise through numerical methods

When the vibration characteristics of an engine have been estimated, the prediction of radiated noise can take several approaches, most of them are based on the acoustic theories of vibrating solids. Even though the radiation of mechanical systems exhibit complex frequency dependent on spatial distributions of amplitude and phase, a simple approach can be made comparing radiation from actual structures with an infinite flat surface. The sound power radiated from a vibrating structure can be defined as:

$$W_{rad} = \rho c S \langle \overline{v^2} \rangle \sigma, \tag{2.49}$$

where ρ is the density of the medium, c the speed of sound in the medium, S is the total surface area,$\langle \overline{v^2} \rangle$ is the surface averaged mean square normal velocity and σ is called the radiation efficiency. To a first approximation, the structure can be considered radiating as efficiently as the infinite flat surface, a simple unity radiation efficiency value can be assumed, but it represents a rough approximation if a quantitative estimation of the radiated noise is researched [105]. Consequently, two alternatives methods, based on the Rayleigh's piston theory and on the Helmholtz integral equation, have been widely investigated [49, 54, 62, 80, 250].

Rayleigh method assumes that the surface of the structure is covered with a finite number of pistons, which move perpendicular to the surface with a radial frequency ω. The sound pressure p at a point j, whose position from the structure can be defined with the distance r and the angle θ, can be calculate using equation:

$$p_j = -iA\frac{\omega}{2\pi}\rho\frac{u}{r}e^{ikr}2\frac{J(ka\sin\theta)}{ka\sin\theta}, \tag{2.50}$$

where $i = \sqrt{-1}$, A is the cross section of the piston, a is the equivalent piston radius, u is the piston velocity, ρ is the density of the medium, c the speed of sound in the medium, $k = \frac{\omega}{c}$ the wave number and J the Bessel function. The overall sound

pressure results from the complex sum of all individual piston pressures:

$$SPL = \sum_{j=1}^{N} p_j, \tag{2.51}$$

where N is the total number of the pistons that compose the radiating structure. Equation (2.50) is only valid, if the wave length of the radiated noise caused by the piston is small compared to the dimensions of the radiating surface. For an engine block this is only true for high frequencies [49].

The Rayleigh method is a good tool to predict the acoustic effect of design modifications [54], but if the intention is to estimate absolute values of the radiated noise, the Helmholtz integral equation applied to BE methods represent a more adequate solution. This method consists is a numerical implementation of Helmholtz integral equation that, in case of points of the volume exterior to the radiating surface, defines the pressure distribution p as:

$$p(\overline{x_0}) = \int_S [p(\overline{b})q^*(\overline{x_0}, \overline{b}) - q(\overline{b})p^*(\overline{x_0}, \overline{b})]dS, \tag{2.52}$$

where $\overline{x_0}$ is the vector defining the position of the field point outside of the boundary surface S radiating the noise, q is defined as:

$$q = \frac{\partial p}{\partial n} = -ik\rho cu, \tag{2.53}$$

where p^* comes from Green's function and is defined as:

$$p^* = \frac{e^{-ikr}}{a\pi r}, \tag{2.54}$$

where $r = \mid \overline{x_0} - \overline{b} \mid$ with $\overline{x_0}$ and $\overline{b}$ the locations of field and boundary points, and:

$$q^* = \frac{\partial p^*}{\partial n} = \overline{n}\nabla p^* \tag{2.55}$$

Through the discretization of the problem boundary into elements and approximating the acoustic pressure and its derivative to interpolating functions on each element, Equation (2.52) can be expressed in matrix form as:

$$[A]\{p\} = [B]\{q\} \tag{2.56}$$

where $\{p\}$ and $\{q\}$ are the pressure and its derivative at each boundary point. Matrices $[A]$ and $[B]$ are found by integrating over the boundary and are functions only of the geometry of the boundary and of the wave number k. Vector $\{q\}$ is the surface vibration velocity and it is normally calculated with FEM simulations permitting an estimation of the pressure acoustic pressure field [250]. In other cases the inverse technique has been used, taking advantage of the pressure information from holographic measures, the intensity field can be projected back to the surface of the source, predicting the vibration velocity of the surfaces [80].

Sung *et al.* [250], using both FEM and BEM techniques, developed an engine system model in order to predict structural vibration and radiated noise of a running engine. The engine system model was developed by synthesizing modal modes of the major bolted-together substructures (engine block, cylinder head, oil sump, etc.), which are obtained by solving the substructure FE models for their normal modes. Non-structural mass models of the remaining engine components were added to represent the overall inertial properties of the engine. Operating loads (combustion pressure loads, piston side thrust loads and main-bearing loads) were applied to the engine system model and the engine surface vibration was calculated. The engine radiated noise was evaluated from the engine surface by using an acoustic BE model of the surface, based on the Helmholtz integral equation. According to the results of this study, this model adequately predicted the engine surface vibration up to 800 Hz octave band but the overall radiated noise resulted excessively underestimated. The authors considered as the main cause for these bad results, the necessity of including other mechanical noise sources (crankshaft loads, chain impact load, etc.) into the model. Another plausible explanation is related to the difficulty of modeling oil films and bearing dynamics and incorporating these effects within the FE model.

Furthermore, recent works [121, 259] have evidenced that, nowadays, all the numerical methods for the assessment of the wave propagation permit to obtain valid solutions only in enclosed frequency ranges. In case of car engine studies, FEM demonstrated to give fiable results only up to 500 Hz approximately, for higher frequency ranges more approximate methods are actually investigated, such as the Statistical Energy Analysis SEA [49, 69, 126, 236], in which a system is modeled as a collection of subsystems, each of which is assigned a single response variable corresponding to the vibrational energy [121].

Nevertheless, as commented above, actually none of these techniques permits satisfactory results in the medium and high frequency ranges (above 500Hz) [104]. Furthermore, due to its high complexity and computational costs, its application is reduced only to the phase of the structural design of the engine block. Consequently, when numerical methods are the only viable techniques, the aim should be to identify trends which will reduce radiation noise, rather than precisely predict absolute levels [62].

2.6. Engine noise quality

The main objectives of the last decades studies on vehicle noise have been mainly focused on the reduction of the associated noise level, but, lately, sound quality have been gaining an increasing importance. Car manufacturers have been shifting their efforts towards improving quality of vehicles noise through a complete vehicle noise-vibration-harshness (NVH) optimization [93, 212]. The task of these researches has been not only to meet certain noise levels, but most importantly to achieve a high quality subjective noise character, both inside and out of the vehicle [224].

One of the most important issues, which is today widely accepted, is that noise

contains information. In many cases, instead of trying to eliminate completely a noise, it is better to modify it in order to emphasize quality information and to reduce annoying components. A vehicle engine noise must satisfy the customer expectations giving information about engine operational condition and comfort. In the case of Diesel engines, this task is complicated by the impulsive characteristic of Diesel combustion which amplifies other noise sources such as piston slap [208]. For a long time, the well-known "knock" of Diesel engine remained one of the main obstacles to a wide application of this type of engines to passenger cars. Actually, despite the important advantages in terms of fuel consumption in comparison with gasoline engines, vehicles customers still consider Diesel knock as a potential negative aspect on their purchasing decision [188].

Sound quality problems represent a really complex challenge for sound engineers. The main difficulty resides in the fact that it is practically impossible to give a scientific definition to the concept of "quality", which is for its own nature a subjective perception. From a qualitative point of view the concept of sound does not refer simply to a physical event like a sound wave. The term "sound" in this context can be considered as the result of an auditory perception process. A listener can judge the concept of quality with reference to desired features which are apparent to him, according to the particular cognitive, actional and emotional situation at the time of judgement [32, 114], as well as to its cultural background [102, 229].

Furthermore, in many listening experiments it has been demonstrated that also differences in the age of the juries bring to disagreement during sounds evaluation. This is due to the natural loss in hearing sensitivity especially at high frequencies resulting from the physiological changes that occur with age [76].

In the next sections some details on the definition of sound quality in the automotive field will be given, and the main methods used to evaluate the noise quality will be presented. The last section of this chapter will describe several approaches found in the scientific literature, which try to give an objective, quantitative evaluation of the abstract concept of noise quality.

2.6.1. Automotive sound quality definition

In the study of automotive sound quality, the first task is to identify which aspects of a sound define its quality. According to many authors [29, 215] the concept of sound quality in a vehicle is mainly related to two aspects: pleasantness and power. Consequently, it results really hard to find a sound which combines a high amount of pleasantness with an equal amount of power, as these two concepts are contrasting on a certain degree. If a sound of a car is designed to be as pleasant as possible the impression of power might be strongly affected and vice versa. Takao *et al.* [252] conducted a study for determining the major factors which affect the sound quality of car interior noise. Three factors: pleasantness, powerful-ness and boomingness were recognized as the more representative, and finally, among these, the pleasantness was selected as the most important factor on the definition of quality.

With respect to a Diesel engine noise, usually, the abstract idea of quality is correlated to the sensations of annoyance [26, 103, 111]. This concept is not linked to the overall noise level that can be expressed on well-established, reliable measurement scales (dB, dBA, etc.). It frequently happens that sources whose noise level measured in decibels are acceptable are still rather annoying, and it is also possible that engines, which by virtue of their noise level would quantify as noisy, leave subjectively a more pleasant impression than quieter ones [219].

2.6.2. Noise quality subjective evaluation

Even though subjective testing and analysis represent a long, bothering and expensive job, they are widely recognized as an essential tool in automotive sound quality investigations [32, 50, 86, 141, 157]. Actually, to date, no instruments or analysis techniques have been able to quantify the concept of quality without the aid of subjective testing of some kind [158].

Otto *et al.* summarized in a paper [158] the general guidelines for jury evaluations of automotive sound quality tests. In this work, the authors provide guidance for the making up of the listening environment as well as for the selection of the jury members. Furthermore, advises are given with respect to the samples preparation, from the adequate recording practices, level setting, equalization and calibration, to the samples editing and presentation. Finally, also several, classical jury evaluation methods are presented:

- Rank order - Subjects are asked to order sounds from the first to the last according to an evaluation criterium (preference, annoyance, magnitude, etc.) [158]. The sounds are presented sequentially and the subjects have the option of listening to a sound as many times as they want. The complexity of the ordering task grows with the number of sounds, accordingly the number of samples to be evaluated is usually kept low. Another disadvantage of this method is that it does not give scaling information. So, it can be used only to obtain a quick idea of how the sounds compare, and is not suitable for correlation with objective properties of the sounds.

- Response scales - With these terms are intended all the methods in which subject's responses are represented on a scale [30, 43, 44, 86]. A widely used rating scale is the numbered response scale from 1 to 10, normally familiar to most people. Subjects are asked to assign to each sound a number of the scale. The sound are presented sequentially with, generally no options to replay. This method is quick and scaling information is directly provided. However, rating scales can be quite difficult for inexperienced, untrained jury members. In fact, a numbered response scale do not allow the subjects to express their impressions in an easy and natural way. Different subjects could use the scales differently, some could use small rating range while others may use most of the scale. Moreover, the extremes of the scales are generally not used.

- Paired comparison - These are the methods in which sounds are presented in pairs and subjects asked to make relative judgements on the sound of the pair, based on some evaluation criterion [26,57,103,110,246]. If all the samples are unpleasant, like in case of engine noises, the criterion of annoyance is often used. The pair judgment process is repeated until all possible pairs have been evaluated. This method of evaluation is quite natural and easy for untrained subjects. A disadvantage of this method is that the number of pairs to listen can be quite large and the evaluation procedure can result tedious. Furthermore, also this method does not give scaling information [219].

- Semantic differential - This technique allows evaluation of multiple sound attributes. Subjects evaluate sounds on a number of descriptive response scales, using bipolar adjective pairs (adjective and antonym) [57,86,88,147,215]. The adjectives lay at the extremes of a scale with several gradations labeled with appropriate adverbs that allow the subject to rate the magnitude of their impressions (for instance: extremely, very, somewhat, neither, etc.)

- Magnitude estimation - This is a method where subjects assign a number to some attribute of the sound. Magnitude estimation is basically a scaling task without a bounded scale [86]. On the one hand, with respect to bounded response scale, this method offers the advantage that the subject's evaluations never run out of the scale. On the other hand, there could be the problem that different subjects may give extremely different magnitude estimates, consequently, this method requires expert and trained subjects.

Each one of these jury evaluation methods has its strengths and weaknesses and no one works best in every applications. In this work an original procedure, combination of these classical evaluation methods, has been developed. This has been obtained by adapting to the case of combustion noise quality a procedure usually used at PSA Peugeot Citroën for the evaluation of the concept of quality in general. More details will be given in Section 3.6.

2.6.3. Approaches to an objective noise quality evaluation

In the last years many efforts have been made by the automotive industry to develop a systematic approach to relate the sound quality to physical characteristics of noise, or, in other words, to express the abstract, subjective concept of noise quality as an objective, measurable quantity. Many authors [77, 81, 83, 103, 110, 219] have tried to tackle this problem using the psychoacoustics, which is the science that deals with the relationship between parameters of acoustic waves and the subjective human perception of sounds. Hearing, in fact, is not a purely mechanical phenomenon of wave propagation, but is also a sensory and perceptual event.

This evolution is presently observed throughout the whole of the car industry, as the possibility to consider noise quality as an integrated parameter in a car design may represent a huge advantage on the competitive market [83,208,268]. As a result, it is thus not surprising that there is a strong demand for instrumentation tools for

sound quality evaluation, consequently, many studies have been conducted and some instruments have been developed with this purpose [33].

Most of sound quality evaluation methods are based on the determination of two types of indices [33]:

- Psychoacoustic and statistic indices -

- Combined indices - normally consisting of the combination of psychoacoustic indices and standard signal analysis indices as well as spectral and statistic parameters.

Furthermore, softwares and experimental tools have been developed and introduced into the market, most of them are based on the computation of the above mentioned indices. More details and some examples will be given in the next two sections.

2.6.3.1. Psychoacoustic and statistic indices

The psychoacoustic indices are methods to predict psychoacoustic quantities, which are descriptive parameters of the sound. A variety of psychoacoustic indices can be calculated and some of them are even international standards [74, 90, 290]:

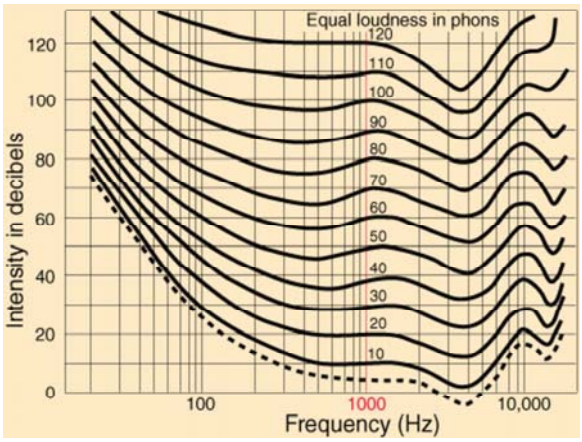

Figure 2.28: Equal-loudness contours for pure tones in a free sound field

- *Loudness* -

It belongs to the category of intensity sensations. Loudness level of a sound is the sound pressure of a 1 kHz tone in a plane wave and frontal incident that is

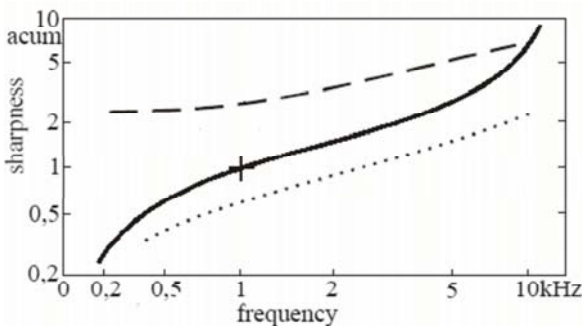

Figure 2.29: Sharpness of narrow-band noise (solid), high-pass noise (dashed), and low-pass noise (dotted)

perceived by the human hears as loud as the sound. Its unit is *phon* but sometimes it is also expressed in *sone*. Lines which connect points of equal loudness in the hearing area are called as equal-loudness contours. Figure 2.28 shows equal-loudness contours for pure tones; according of its definition all curves have to go through the sound pressure level at 1 kHz that has the same value in dB as the parameter of the curve in phon. Threshold of audibility, where the limit of loudness sensation is reached, is the equal-loudness dashed contour. These curves indicate that the human hearing system is most sensitive for frequencies around 4 Hz. There are various procedures for physical loudness measurements, the Zwicker's one [290] is the more general and has been standardized.

- *Sharpness* -

It represents a measure of the proportion of loudness within critical frequency bands. For example, two different types of noise may have equal loudness, but the one with greater sharpness will have louder frequency components within frequency bands to which the human ear is particularly sensitive (in the world of music, the "timbre" of a sound is related to its sharpness). Figure 2.29 shows the dependence of sharpness on frequency. The solid line represents the result for narrow-band noise, with increasing centre frequency of the narrow-band noise, the perceived sharpness increases. The dashed curve represents the result for high-pass noise of different cut-off frequencies while the dotted curve shows the data for low-pass noise. A 60 dB narrow-band noise at 1 kHz has a sharpness of 1 *acum*. For higher values of sharpness significant spectral components at high frequencies are required. According to its definition, the sharpness of a sound can be lowered either by decreasing high frequency components or by adding low frequency components. Even though this last modification increases the loudness of the sound, in many cases a reducing of sharpness make preferible the resulting sound [74, 219]. When a sound contains only high frequency components it provokes sharp and metallic impression, the sharpness is an es-

timation of this sensation. Subjective sound sharpness impression also depends on its duration, the shorter duration of sound the sharper the sound estimate.

- *Fluctuation Strength and Roughness* -

Temporal variations of sound can lead to two different perceptions. Fluctuation strengths at low frequencies of variation, and roughness at higher frequencies. A frequency tone of 1 kHz and 60 dB level, which is amplitude modulated by a frequency of 4 Hz with degree of modulation $m = 1$, represents the reference sound for fluctuation strengths of 1 *vacil*. Roughness is a parameter that has been introduced to approach the sensation that occurs in the case of modulated sound with frequencies higher than 20 Hz. Its unit is the *asper*, a roughness of a 1 asper corresponds to a tone of 1 kHz and 60 dB level which is amplitude modulated by 70 Hz frequency with degree of modulation $m = 1$. It is experimentally established that roughness increases proportionally to the second power of the degree of modulation and increases slightly with noise level. This parameter is particularly important for sound quality improvement [99, 169]. For example, a sport car engine must have a sound with a certain roughness, while this sensation has to be avoided in the sound quality inside a luxury car.

- *Impulsiveness* -

This is an example of a statistic parameter, also known as Kurtosis, it represents the impulsiveness of the sound pressure distribution. It is a measure of the amplitude and frequency of occurrence of pulse peaks versus the background part of the signal and its unit is *Kurt*. It is of particular significance during the idling of an engine [208, 219].

When using psychoacoustic indices for sound quality evaluation tasks it has to be considered that these indices can not be applied to any kind of signal. Many of these have been developed on the basis of stationary signals. Furthermore, all of them are only defined as monaural indices, in contrast to the fact that auditory system combines signals of both ears. The psychoacoustic indices have become rather popular in the last years and several sound analysis tools can calculate them without difficulties, with sufficient accuracy for a wide range of application. In spite of all, it appears clear that the use of a single psychoacoustic index permits the description of a sound attribute but can not suffice for the description of the global concept of quality in Diesel engine noise.

2.6.3.2. Combined indices

In order to render a global description of the noise quality, some indices, obtained from the combination of psychoacoustic parameters and standard signal analysis indices, have been proposed. Some examples are presented here:

- *Speech Transmission Index* -

This represents one of the first intents, developed by Brüel & Kjær [150] to quantify the subjective interior noise character of a vehicle. The basic idea

was to use indices developed for an objective rating of speech intelligibility, introduced in studies for the acoustics of rooms. A simplified version of the speech transmission index is the RASTI method (RApid Speech Transmission Index), which was also used by Rust *et al.* for some preliminary studies of interior noise quality of vehicles [212].

- *Annoyance Index* -

Developed by AVL List GmbH in the early nineties [103, 219], this index was introduced to obtain by measurement an objective parameter capable to define the annoyance of an engine. More than 150 engines and 40 vehicle noises were judged using a pair comparison method and statistically evaluated by the application of multidimensional scaling techniques. The resulting order of noise was compared with many subjective criteria in the time and frequency domains in order to identify those parameters which best described the presented stimuli. Finally multiple regression technique was used to combine the parameters of different auditory tests into one common index representing the subjective annoyance. This index, AI was found to be composed by four terms: loudness, periodicity, sharpness and impulsiveness; it is defined as:

$$AI = [\alpha.f(Sone) - C] + [\beta.f(PrePer)] + [\gamma.f(Bark)] + [\delta.f(Kurt)] \quad (2.57)$$

where $\alpha, \beta, \gamma, \delta$ are weighting coefficients, f means function of (), PrePer (preferred periodicity) is a parameter characteristic of the repetition frequency of a periodic sound and Bark is a scale from 1 to 24, corresponding to the first 24 critical bands of hearing. The final measure of annoyance is calibrated via the constant value C, included in the first term because it resulted as the most significant.

Typical applications of this method are the comparative analysis of the noise quality of different engine families or the engine optimization with respect to low idle noise quality by means of the application of different injection systems or oil sump damping materials [219, 246]. In other studies, this method was used in a global optimization procedure for the development and refinement of new engine families [26, 52] and of complete vehicles [42].

- *Annoyance Response Index* -

This index was developed by Shafiquzzaman [110] for estimating the annoyance sensation for heavy-duty Diesel engine. From the analysis of three heavy duty truck engines, through a multivariate analysis, an index named ARI, similar to that proposed by AVL, was obtained:

$$ARI = C + \alpha.Sone + \beta.Acum + \gamma.HR \quad (2.58)$$

where C is the constant of proportionality, α, β, γ are the regression coefficients and HR is the harmonic ratio expressed in dB (average level of harmonic ratio of the first 60 harmonics). The other two parameters are characteristic of the loudness and sharpness like in Equation (2.57).

- *Composite Rating of Preference-*

Introduced by Callow and Hedges [50] and considered also by other authors [77,199,258], this is a noise rating scheme presenting a good subjective/objective correlation, it is defined as:

$$CRP = ((dBA)^2 - 1{,}5(HF)^2 + 0{,}5(SB)^2)^{0,5} \tag{2.59}$$

where dBA is the overall sound level in dBA, HF stands for high frequency and is calculated as the overall noise leven minus SIL (speech interference level, arithmetic mean of unweighted levels in the octave bands centered in 1,2 and 4 kHz), and SB is the spectrum balance (arithmetic mean of unweighted levels in the octave bands below firing frequency minus SIL). This index is based on amplitude averaging of frequency band levels, consequently, its use is not indicated for the study of sound quality in Diesel engines, characterized by strong time domain variations [106].

- *Sound Quality Metric-*

Developed by Ingham *et al.* at Ford Motor Company [106], this index was introduced for the estimation of the sound quality of different commercial vans equipped with Diesel engines. Two different equations have been obtained:

$$SQM = C - a * N50 - b * R50 \tag{2.60}$$

in case of idling conditions, where C is the constant of proportionality, a and b are the regression coefficients, $N50$ is the median loudness value in sones and $R50$ is the median roughness value in asper. And:

$$SQM = C - a * N10 - b * S10 \tag{2.61}$$

in case of full load conditions, where C , a and b are different constant of proportionality and regression coefficients, $N10$ and $S10$ are ten percentile values of loudness (in sones) and sharpness (in acum), respectively.

- *Rattle Noise Quality Index-*

Created by Weisch *et al.* [270] at AVL LIST Gmbh, this index is intended to be used for the analysis of the rattle noise produced in the vehicle interior noise due to broadband excitation by road irregularities. Through a methodology similar to that used for the development of the Annoyance Index, this quality index was found to consist of the following parameters:

$$RNQ = f(Loudness, SML, PrePer, Sharpness) \tag{2.62}$$

where SML stands for Sum of Modulation Levels (modulation calculated for each octave band with weightings according to human sensitivity) and $PrePer$ is the preferred periodicity as defined for the Annoyance Index AI, Equation (2.57).

2.6.3.3. Softwares and experimental tools

In this section some softwares and experimental tools for the assessment of the noise quality are described, these represent only an extract of the numerous examples found in the literature, however it can be expected that several other indices have been developed by researchers, but are not published and kept confidential. This indicates the huge interest that the concept of noise quality has gained also in the automotive industry.

- *Noise Quality Map* -

This is a software developed at AVL as an evolution of the Annoyance Index for a real time assessment of vehicle interior noise quality [43]. According to this model a interior noise quality index A is defined depending on the vehicle operating condition:

Idle Condition

$$A = f(loudness, low\, frequency\, content) \tag{2.63}$$

Stationary Operating Conditions

$$A = f(loudness, low\, frequency\, content, sharpness, tonality) \tag{2.64}$$

Acceleration Conditions

$$A = f(loudness, low\, frequency\, content, roughness, sharpness) \tag{2.65}$$

Cost Down Conditions

$$A = f(loudness, low\, frequency\, content, roughness, articulation\, index) \tag{2.66}$$

where the *articulatio index* is a measure of speech intelligibility in continuous noise, it determines a ratio between the received speech signal and the level of interfering noise.

- *Engine Noise Evaluation Meter* -

This is an experimental tool developed at Yamaha Motor [135], that provides an index for the noisiness of motorcycle engines at idle condition. Auditory sensations of engine noises have been analyzed using multidimensional scaling techniques. As a result, the total evaluation level index L_E, expression of the subjective rating, has been found as a linear combination of loudness, impulsiveness and frequency characteristics of noise.

- *CombustioMetré* -

Developed by GIE MOTUS (CRMT + METRAVIB R.D.S.) for PSA [20, 21], this is another experimental tool to objectively quantify the subjective quality of combustion noise of an engine. This is based on an estimation of the noise quality (expressed by a mark in an evaluation scale from 0 to 10), starting from the vibrational characteristic of the engine, measured with accelerometers fitted onto the engine. The main difficulty of this tool is the necessity of a long and complicated "training phase" for the calibration of the model with every engine analyzed.

- *Ride Quality Meter* -

Developed at NASA [275], this experimental tool was conceived to have a comprehensive model for estimating passenger comfort response to combined interior noise and vibration environment typical of transportation vehicles, such as helicopters, trains, trucks and automobiles. In the case of cars it gave acceptable results in the estimation of an index of discomfort evaluated for different ride conditions (different speeds and road surfaces).

- *QUALIdB* -

Developed by Lamotte and Beguet at MICROdB [128,129], this software presents between its various applications a procedure for the quantification of the acoustic quality. The information about the sound quality is obtained from signals through the computation of different parameters that have to be properly selected according to the sound quality problem examined. In case of piston slap two parameters: "roughness" and "shock balance" have been considered. From these metrics, a notation system similar to a neural network gives a single mark.

- *Noise Combustion Index* -

This index is the result of a collaboration between the CMT Motores Térmicos and the DCOM (Departamento de Comunicaciones) of the Polytechnic University of Valencia [139]. The target of this study was to define a quality index for HSDI engines in order to substitute the listening tests with a simple post-processing of the acoustic data recorded.

Measures have been performed on a 2.2 l DI Diesel engine, eight different engine speed have been considered (between 900 and 4000 rpm) and three different load conditions: low (under than 20 %), middle (between 20 and 60 %) and high (higher than 60 %).

The recorded noises have been evaluated with a mark by a jury of listeners, furthermore for the analysis of the noise signals a total of 42 parameters have been taken into account, divided into:

- Psychoacoustic parameters
- Spectral parameters
- Statistical parameters

The basic idea was to select the best parameters P_i that give in a multiple linear regression $Mark = a_0 + \sum a_i.P_i + \varepsilon$ the minimum error ε. The Noise Combustion Index (NCI) is expressed by the same multiple regression model: $NCI = a_0 + \sum a_i.P_i$.

The results of this exhaustive study are summarized in the Tables 2.1 and 2.2. Table 2.1 presents the equations of the NCI obtained depending on the engine speed considered, together with the statistical results:

From the table it can be observed that for the noises recorder at 3000 rpm it was not possible to select parameters sufficiently correlated with the mark given by the jury. In other words no one of the 42 parameters used in this

SPEED	NCI=	R^2	E_{med}	E_{max}
900 rpm	22+OH-32.SharpZ	99,7 %	0,05	0,08
1500 rpm	39-0,8.TOH-1,8.Rough70	95,5 %	0,21	0,64
2000 rpm	139-1,3.TOH-12.SharpA	99,9 %	0,06	0,08
2500 rpm	-83+5,9.Rough70+3,5.SharpA-3,3.SLoud	88,2 %	0,31	0,76
3000 rpm	No correlation found	-	-	-
3250 rpm	-43-8,2.Sk-3,6.Rough70+12.SharpA-2,5.SLoud	94,9 %	0,22	0,40
$\geq$3500 rpm	-52-5,6.Rough70-16.Sk+42.SharpZ	90,9 %	0,31	0,82

Table 2.1: NCI obtained for the engines speed considered, where OH is the mean power of the odd harmonics, SharpZ the mean Sharpness calculated according to the Zwicker definition, SharpA the mean Sharpness calculated according to the Aures definition, TOH the mean power of the third order harmonics, Rough70 the mean Roughness for a modulation frequency of 70 Hz, SLoud the stationary Loudness and Sk the Skewness.

investigation could describe the acoustic sensation caused by the engine at this specific engine speed.

Table 2.2 presents the results of the NCI obtained considering different load conditions, together with the statistical results of the correlations:

LOAD	NCI=	R^2	E_{med}	E_{max}
Low	27-3,7.SLoud+3,2.ILoud-5,4.RN-1,8.Rough70	71,7 %	0,48	1,69
Medium	20-0,33.SLoud-2,2.Rough70	53,2 %	0,42	0,85
High	9+11.SharpZ-4,7.Rough70-0,33.SLoud	89,0 %	0,22	0,54

Table 2.2: NCI equations obtained depending on the engine load and statistical results, where ILoud is the mean instantaneous Loudness, RN the Rumble Noise (ratio between middle order harmonics)

From a first analysis of this table it results that also in this case a particularly unlucky condition has been detected. The regression equation obtained at medium load presents an extremely low correlation coefficient (53,2 %).

Apart from the really poor correlations obtained in particular engine operating conditions, all parameters considered resulted to be dependent on the engine speed and torque. From this study it resulted evident that this Noise Combustion Index is unable to give a reliable estimation of the noise quality.

Summarizing it can be concluded that, in the case of noise from Diesel engines, the concept of quality can be estimated joining psychoacoustic and statistical parameters. In many analysis, combinations of loudness, roughness, sharpness, impulsiveness,

periodicity, etc. have shown a certain degree of correlation with the engine noise quality. Nevertheless, it becomes obvious that this types of indices can only render reliable results for rather limited and well-defined tasks.

This is confirmed by the results obtained with the Noise Combustion Index described above, this study is particularly interesting as it has been conducted on an single engine of the same family of those considered in this Thesis. Noise variations have been obtained by changing the engine operating conditions (speed and torque) and the injection settings. Also in this simplified case it was not possible to define a unique index that could give an acceptable estimation of the combustion noise quality.

These observations justify the necessity to perform listening tests of the recorded noises, although it represent a quite expensive and unpleasant task. The noise quality evaluation procedure developed in this Thesis will be described in Section 3.6.

2.7. Basic idea of the proposed approach

To conclude this chapter, before introducing the methodology developed for this work, it is important to emphasize again the complexity of the combustion noise generation mechanism evidenced in this bibliographic review of the state of the art of combustion noise. This is essential in order to explain and justify the hypothesis at the basis of the novel approach introduced in this Thesis.

Figure 2.30 summarizes the problems, mainly due to the non-stationary and non-linear behavior of the various phases of the examined process, already highlighted in the this chapter:

- As commented in Section 2.3.1, the main excitation source in a Diesel engine is the in-cylinder pressure that generates both pressure and mechanical forces. Pressure forces act directly on the surface of combustion chamber walls and strongly depend on the combustion concept, which is controlled by the injection strategy, compression ratio, bowl geometry, etc. Mechanical forces are induced by the pressure forces through the mechanical systems in the cylinder and are due to piston slap, clearances, deformation, friction, etc. Therefore, these two contributions are characterized by the in-cylinder pressure evolution.

- At the start of combustion, an abrupt pressure rise that provokes an important oscillation of the gas inside the combustion chamber is produced. This gas oscillation causes the vibration of the engine block and thus noise is radiated. Moreover, as introduced in Section 2.4.3 a resonant oscillation of the gas inside the combustion chamber is also produced by the pressure gradient induced by combustion. This oscillation is controlled mostly by the bowl geometry and the gas temperature. Therefore, the combustion chamber resonance is a non-stationary process because both the bowl position and the gas temperature change during the combustion process.

- Excitation is transmitted from the combustion chamber to the block, since it acts as an attenuator of in-cylinder sound pressure, its design is also critical for

engine noise control. As it has been already commented in Section 2.5.1, and it will be evidenced successively in this work from the study of the engine attenuation curves, the weakness of the traditional approaches is related precisely to the basic hypothesis that a linear response of the block is expected independently of the engine operating conditions. Indeed, as evidenced in Section 2.5.3 the engine block response is highly nonlinear and time variant. In-cylinder excitation propagates through multiple and extremely complex paths, either directly through the action of the forces exerted by the gases on the cylinder walls or through the different elements forming the mechanical system of the engine. Indeed, since the mechanical loads applied to the moving elements in the cylinder depend not only on the engine operating conditions but also on the relative position of the piston inside the cylinder, the deformation of such elements and hence that of the block is also load dependent and non stationary.

- Furthermore, despite the fact that noise emission due to the block vibration is mostly a linear phenomenon, non linearities become relevant again when sound quality of noise is assessed. Indeed, as evidenced in the last Section 2.6.3, it is practically impossible to give an objective definition to the concept of quality.

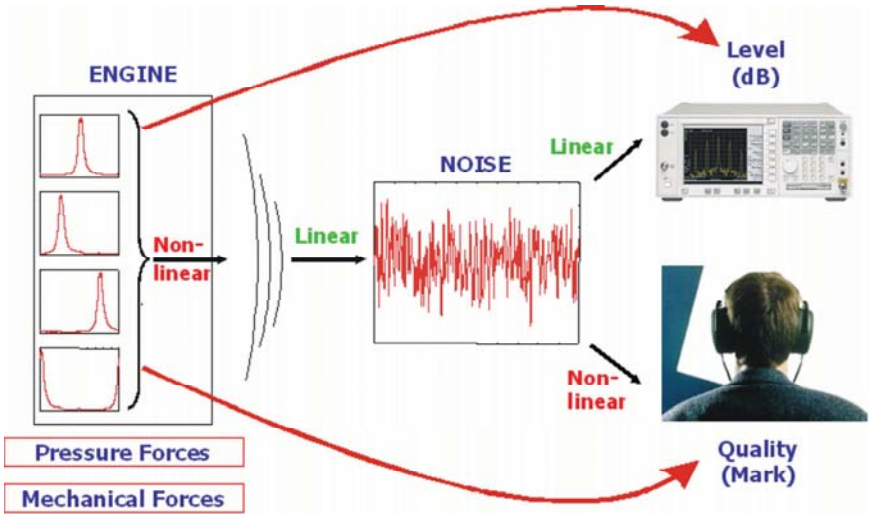

Figure 2.30: Problems correlated to combustion noise generation

According to these observations classical approaches, such as block acceleration analysis or the use of the block attenuation as a transfer function between the excitation (in-cylinder pressure) and the effect (radiated noise) do not seem to be feasible in practice for the analysis of combustion noise in state-of-the-art engines. This situation induces us to attempt the combustion noise study from the analysis of intuitive physical mechanisms in the noise source, directly extracted from in-cylinder

pressure measurements during engine operation. Difficulties associated with block vibration issues may thus be surpassed by establishing direct correlations between those mechanisms and the overall noise level.

In other words, instead of developing an extremely complex modelization of the phenomenon or of trying to solve mathematically non-linear problems, the basic idea of this work is to find direct correlations between indicators characteristic of the in-cylinder excitation source and noise. As schematized in Figure 2.30, this noise radiated from the engine block is taken into account from a double point of view, both quantitative (sound pressure level, measured in decibels) and qualitative (noise quality, expressed with a mark given by a jury of experts).

Chapter 3

Methodology

Index

3.1. Introduction

As introduced in the previous chapter, the work presented in this Thesis has been based on the study of the sound source, and in relation to this the different factors leading to the emission of combustion noise have been studied, so that the origin of the characteristics observed in the noise can be traced back to the characteristics defined for the source, thus permitting the necessary feed-back allowing for the design of acceptably silent engines.

In this context of ideas, it is indispensable to use in a systematic way a theoretical-experimental methodology, in which not only the experimentation provides the relevant information for the study, but the theoretical work provides in turn a guide for the critical evaluation of the experimental results, given that these are going to yield information with a highly empirical content.

The methodology developed in this Thesis is basically experimental, different engine families and sizes were considered, measurements of in-cylinder pressure signals and noise radiated by the engines were analyzed and post-processed with time-frequency and statistical methods. Besides, three-dimensional CFD calculations have been also used for a better understanding of the resonance phenomena taking place in the cylinder during combustion.

With the purpose of finding direct correlation between in-cylinder pressure and noise characteristics, a reliable experimental set-up and test procedure have been defined in order to record simultaneously the pressure evolution inside every cylinder and the noise radiated at 1 meter from engine block. For this study, a passenger car engine has been considered: a 1.6 l , 4-cylinder, turbo-charged Diesel engine equipped with common rail injection system. The results will be compared with those obtained from former studies on two different engine families: a 2.2 l and a 1.4 l.

In order to get reliable acoustic measurements free from reflection and reverberation effects, the noise measures have been performed in an anechoic chamber capable of simulating free-field conditions avoiding any external disturbance to the measurement. Figure 3.1 shows the engine assembled inside the anechoic chamber, on the righthand side of the picture the torso head of the binaural recording system can be also observed.

In the next section the general methodology developed in this Thesis will be synthesized and the relations between the different activities followed in this work will be schematized. Then, a section will be dedicated to the statement of the problem. The approach followed and the main tasks of this study will be shortly described.

In the fourth section the set-up used for the experiments will be introduced. More details of the experimental devices: anechoic chamber, in-cylinder pressure measurement system, binaural measurement system as well as ECU control system and engine test bench are given in the Appendix A.1.

In section five some information on the test procedure and a description of the methodology introduced for the signals postprocessing are given. The in-cylinder pressure signal analysis based on the decomposition technique developed by Payri *et*

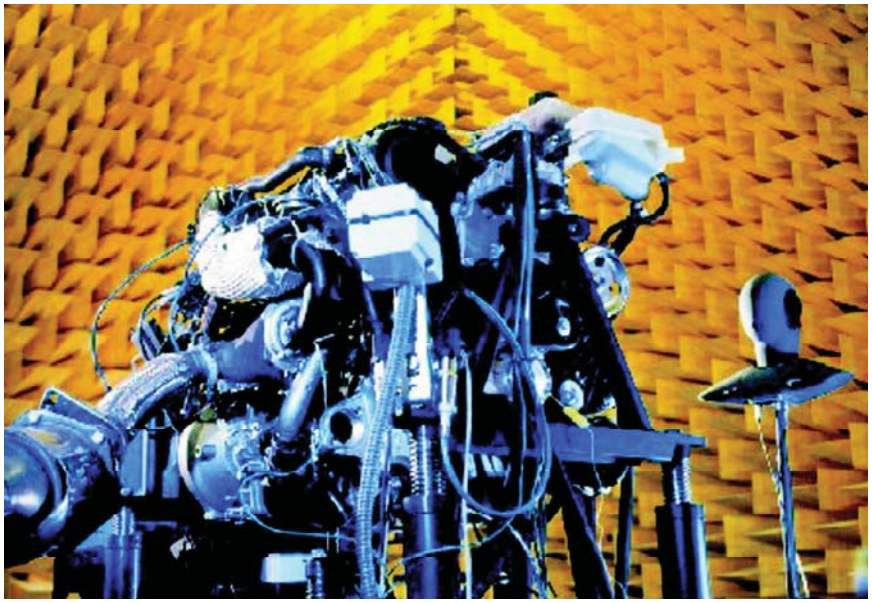

Figure 3.1: Picture of the engine inside the anechoic chamber

al. [163] is briefly explained. Then, the methodology for the definition of the indicators characteristic of the excitation sources is described. To conclude this section, a short explanation of the CFD calculation is given.

In the last section of this chapter the procedure for the combustion noise quality evaluation is detailed.

3.2. General methodology

Figure 3.2 synthesizes the relations between the different activities that have been performed in the various phases of the methodology developed in this Thesis. A methodological structure with a fundamentally empirical base has been proposed, as it is inevitable given the complexity of the phenomenon under study, but with an important theoretical and experimental support in order to ensure the self-consistency of the results obtained.

The **experimental phase** was planned at two qualitatively different levels and successive in time:

- The performance of objective measurements of the source characteristics (in-cylinder pressure) as well as of the resulting outside acoustic field (combustion

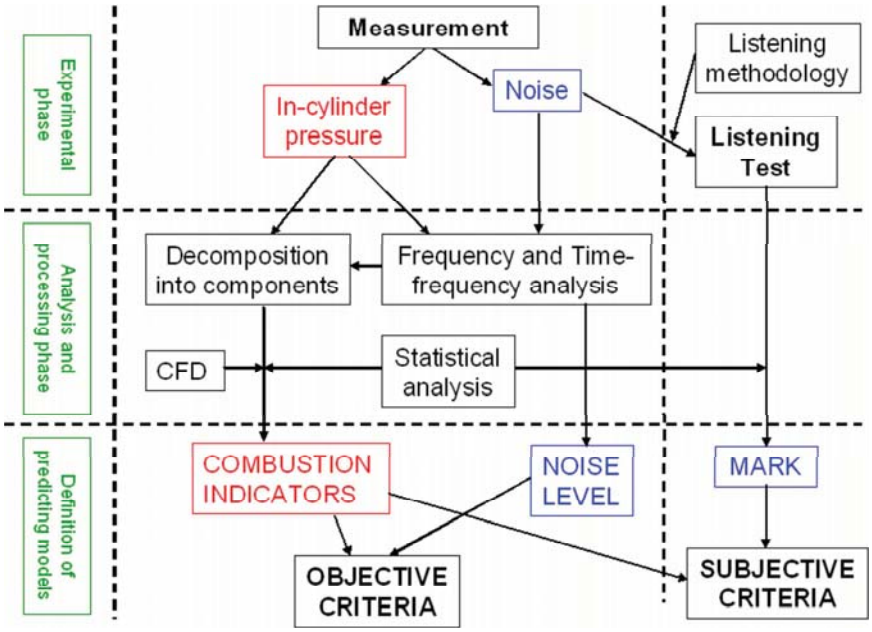

Figure 3.2: Scheme of the general methodology

noise). As commented before, the achievement of reliable measurements in this context implies the installation of the engine in an anechoic room and the binaural recording of the noise, in order to permitting its subjective evaluation.

- The performance of listening tests by a jury of experts, that provide the subjective evaluation of the noise. The achievement of reliable and repeatable evaluations implies the definition of a robust listing methodology, which is indispensable given the intrinsic subjective character of the evaluation process and the multitude of factors that can influence the evaluation obtained.

Given the essential differences between both types of experimentation, also the procedures of **analysis and processing phase** were different:

- In the case of the objective measurements (in-cylinder pressure as well as combustion noise), the tools used have been multiple:

  - The analysis of the signals in time domain have been performed to establish the relation between the control strategies used to govern the combustion process and the characteristics found in the in-cylinder pressure that can be related to noise emission.

- The analysis in frequency domain necessary to quantify the acoustic effects, and the time-frequency processing techniques that may permit to identify the eventual non-stationary character of the phenomena.
- From the integration of time domain and frequency domain analyses arises another phase of the data processing corresponding to a procedure for the decomposition of the pressure inside the cylinder into physically significant components, related to the physical processes that take place in the combustion chamber.
- In this phase of the methodology CFD calculations have been also performed as theoretical support, in which the geometry of the combustion chamber, and consequently the three-dimensional character of the flow, is taken into account. This has permitted to get a better understanding of the resonance phenomenon in the combustion chamber and of its effect on the indicators selected.
- From the decomposition of the in-cylinder pressure, by mean of a statistical analysis, indicators relevant from the point of view of noise have been defined, that provide the conceptual framework for the definition of criteria in the subsequent phase of definition of predictive models.
- In the case of the exterior acoustic field, frequency analyses have performed to define objective magnitude of the radiated noise (as for example the sound pressure level). Furthermore these analyses are at the basis of other classical approaches for the study of the combustion noise, such as the bloque attenuation technique that has been used as a comparison for the new approach proposed in this Thesis.

- In the case of the listening tests, the most important aspect lies in the prior analysis of the results, for this reason a statistical analysis has been performed in order to evaluate the consistency of the jury members and the degree of reliability of their appreciations. This is a fundamental point in this phase of the methodology, since the final results (the evaluation in terms of a mark) do not admit any type of subsequent processing.

The methodology culminates with the **definition of predictive models**, obtained from the search of cause-effect relations quantified through the correlation between the indicators selected in the previous phase and the characteristic parameters of the acoustic field, for both the levels (objective criteria) and the sound quality (subjective criteria), this last quantified by means of the mark.

3.3. Statement of the problem

As for the general methodology, the work has been approached by dividing the issue in two main tasks:

- Combustion noise quality assessment (subjective criteria)

- Combustion noise level assessment (objective criteria)

The problematic of the **noise quality** has been approached by structuring the research in three main tasks:

- Definition of a model for the assessment of the noise quality of engines operating with single and conventional (pilot + main) injection. In this phase a model has been introduced from the measurements obtained with two different engines families (1.4 l and 2.2 l engines). Furthermore the model has been validated with an engine of different size (1.6 l).

- Definition of a model for the assessment of the noise quality of engines operating with multiple injection strategies. This task has been implemented analyzing the experimental measures from the 1.6 l engine.

- Analysis of the influence of the resonance phenomena in the combustion chamber on the combustion noise quality and on the predictive models. For this part of the work an experimental analysis considering different piston bowl geometries has been performed using the 1.6 l engine. Furthermore CFD calculations have been also performed in order to get a deeper comprehension of the resonance phenomena occurring in the cylinder during combustion.

The task of defining a predictive model for the assessment of the **noise level** has been approached by structuring the research in two main tasks:

- Definition of a model for the assessment of the combustion noise level with the engine operating in stationary conditions. For this issue a preliminary study has been performed considering a classical approach based on the attenuation curve, this has been done in order to have a point of reference allowing an evaluation of the potentiality of the novel approach. The new model has been developed taking into account the experiments performed on the 1.6 l and 2.2 l engines.

- The second phase of the study on the noise level assessment has been conducted on the 1.6 l engine operating in transient conditions. Also in this case the proposed approach has been compared with the results obtained with the attenuation curve methodology.

The results obtained with this approach are presented in the following chapters of the Thesis: Chapter 4 is dedicated to the analysis of the qualitative aspect of combustion noise and Chapter 5 describes the research done for the assessment of the noise level. These chapters have been structured according to the approach presented in this section.

In the next sections more details of the experimental set-up and of the main activities described in the general methodology will be highlighted.

3.4. Experimental set-up

The measurements of in-cylinder pressure and noise emitted provide the basis for all the subsequent developments and they constitute, in this sense, the task which depends the success of the complete research, being therefore indispensable a rigorous control of the tests and their adequate definition in function of the subsequent processing.

In order to study the main features and the causes of combustion noise in Diesel engines a test set-up that permits the simultaneous recording of noise and in-cylinder pressure has been defined. The main properties required from a system for the study of combustion noise in Diesel engines are that:

- The measurement system should allow a synchronized acquisition of the signals.

- The system must permit recording of data relative to a large number of consecutive cycles. For this reason a quite big physic memory together with a high speed of data transfer are required.

- The recorded signals should be digitally stored in order to be processed and analyzed afterwards.

- The recorded data must be easily accessible.

Furthermore, in order to get fiable acoustic measures, the tests must be performed in free-field conditions. The scheme of the acquisition system used in this work is shown in Figure 3.3. The engine, equipped with four in-cylinder pressure transducers and an optical encoder, was located inside an anechoic room. The torso head for the noise recording was placed near to the engine, at exactly 1 meter of distance from the engine block, to avoid near field effects, and in front of the fourth cylinder opposite to the side where the turbo-group and the exhaust system are located.

The in-cylinder pressure acquisition system was formed by:

- piezoelectric pressure transducers installed on glow plug adapters allowing a direct access in the combustion chamber
- charge amplifiers to yield an electric signal with an adequate level of voltage and impedance
- a digital multichannel oscilloscope where the signals are A/D converted and digitally stored in buffer memories
- a personal computer where the data are transferred and stored

The signals from the in-cylinder pressure transducers and the optical encoder signals (1 pulse per revolution (1xV) and n pulses per revolution (nxV)) were recorded and digitally converted by a Yokogawa DL708 oscillographic multi-channel data acquisition system and successively transferred and stored in a personal computer.

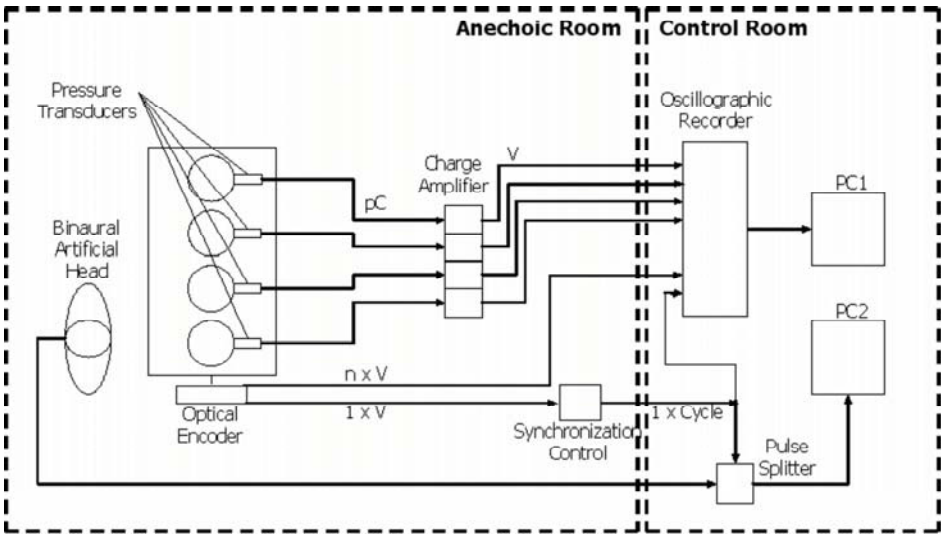

Figure 3.3: Scheme of the acquisition system

All measures on the engine, included the in-cylinder pressure signal, are performed at constant-time increment instead of the more conventional constant-angular increment. This choice is accounted for by the acoustical goal of this study; noise is in fact a time-related phenomenon and in the experiments it is essential to conserve its temporal component. Furthermore, a constant-time sampling permits specific signal analysis, such as spectral analysis, that ease the correlation of in-cylinder pressure with sound pressure.

The sampling frequency has been chosen taking into account that the human hearing range covers a frequency range from 20 Hz to 20 kHz. According to the Nyquist-Shannon sampling theorem, the sampling frequency must be greater than twice the signal bandwidth to avoid aliasing effects, for this reason the sampling frequency of 50 kHz has been selected in the set of frequencies available in the digital oscillographic recorder. Also the length of every measure has to be limited, in every test not more than 50 consecutive engine cycles have been recorded, depending on the buffer memory capacity of the multichannel oscilloscope.

Simultaneously with the in-cylinder pressure record, the engine noise is binaurally recorded with a torso head measurement system, connected through a high resolution sound card to a personal computer, where the measures are stored. This PC also controls the play-back system, formed by an equalizer, an amplifier and two high-dynamic-range electrostatic headphones (substituted by powered monitor speakers during the listening tests). For the same reasons explained above, the noise emitted by the engine is sampled with a frequency of 48 kHz. Furthermore, the length of every record is set on 10 seconds in order to have a noise duration that can allow a correct

evaluation.

The two acquisition systems are synchronized by using a pulse splitter box. As can be observed in Figure 3.3, the one pulse per revolution signal (1xV) from the optical encoder is converted by an electronic device into a one pulse per engine working cycle signal (1xCycle). This signal is the input of a pulse splitter box, and permits the synchronization of the different signal acquisition systems. The measure begins when the pulse splitter box is activated by a trigger, the signals from the optical encoder and in-cylinder pressure transducers are recorded in the multichannel digital oscilloscope and successively transferred to a personal computer (PC1). Simultaneously the sound pressure signals from the artificial head microphones are stored directly into an other personal computer (PC2).

In addition, two personal computers (not shown in Figure 3.3 for simplicity) were also required for the experiments:

- One PC commands the electronic control unit (ECU) of the engine allowing the setting of the injection system and of other engine parameters (EGR valve position, boost pressure, etc.)
- Another PC is used for controlling the engine bench operation, that is monitoring the engine speed, the breaking torque and the principal temperatures

The main characteristics of the anechoic chamber and of the various components of the measurement system are detailed in the Appendix A.1.

3.5. Measurement and post processing

Due to the complexity of the measurement system, as well as to the necessity of respecting security measures, different experimental routines have been defined in order to control the phases of start, data recording and stop of the experimental set-up. In this section only a short description of the experimental phase will be given.

In a first moment, in order to cover a wide range of engine working conditions, several speeds and torques are chosen. These working conditions have been chosen in agreement with the engine manufacturer as they represent critical zones of the engine map from the point of view of the combustion noise. Table 3.1 shows the running conditions considered in this study for the 1.6 l engine. Figure 3.4 shows the distribution of these conditions on the engine map, it can be noted that most of the points points have been chosen at low and medium load covering a wide range of engine speeds. Furthermore the engine idling condition (750 rpm) has been also included in the study, together with a point at relatively high load (2400 rpm, 168 Nm) characterized by the EGR valve completely closed.

For each condition considered an experimental plan was defined using different injection schemes and parameters, the intention was to obtain variations of the noise radiated by the engine keeping the engine speed and torque as constant as possible. The variation ranges of the injection parameters are not unlimited but their choice

Speed (rpm)	Torque (Nm)
750	0
1350	12
1500	37
1500	75
1900	124
2250	12
2280	102
2400	168
2850	87

Table 3.1: Running conditions tested on the 1.6 l engine

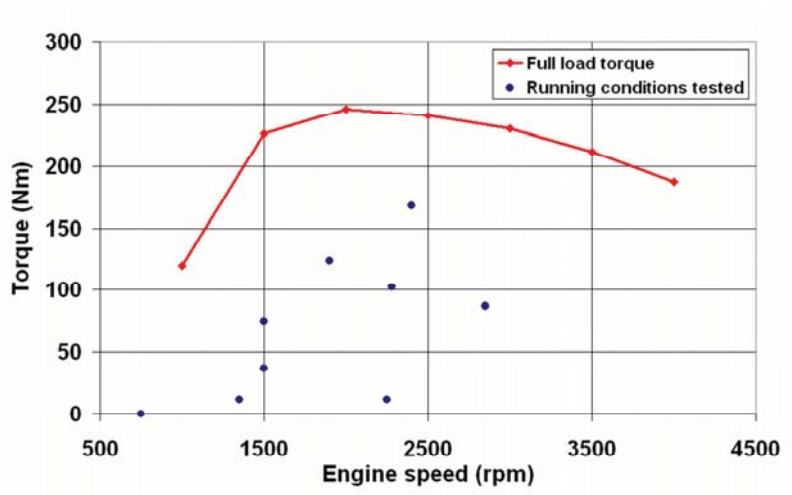

Figure 3.4: Distribution of the running conditions tested on the engine map

comes from the best balance between two opposite requirements: on the one hand, as wider as possible noise variation is required, on the other hand, the engine should be stable and the torque as constant as possible. A deeper description of the experimental plans defined for this research will be given in the next chapters.

Once the engine is preheated and the whole system has reached stationary temperatures the data recording can be started. Activating on the dyno control and on the accelerator pedal actuator, the engine is led to a working condition under analysis. Through the personal computer controlling the ECU, the injection parameters are progressively varied till getting the injection settings defined in the experimental plan.

The simultaneous recording of the in-cylinder pressure and cranking signals and noise are performed manually triggering the pulse splitter box. Before changing the injection settings, the data are transferred and saved in the personal computers. Then, the "pseudo-motored"signal, which is the in-cylinder pressure evolution caused by the piston movement when the intake pressure is boosted by the turbo compressor, is recorded.

The pseudo-motored signal is measured by switching off fuel injection in one of the cylinders during one cycle, this action is automatically repeated every twelve combustion through the recording of more than 100 consecutive cycles allowing the engine speed to remain quite stable and permitting the estimation of an average pseudo-motored pressure. To do this, a specific electronic system, synchronized with the ECU, has been developed to allow independent control of injector operation.

3.5.1. In-cylinder pressure decomposition technique

The approach proposed for the in-cylinder pressure signal analysis takes advantage of the decomposition technique developed by Payri *et al.* [163]. The main idea of this technique is to decompose the in-cylinder pressure evolution according to three governing phenomena taking place during Diesel engine operation: compression-expansion, combustion, and resonance excitation. These contributions may directly affect the characteristics of the noise radiated by the engine. The compression-expansion signal does not represent any tendency related with combustion and thus it is considered just as a reference signal. The combustion signal characterizes the combustion process and its associated pressure evolution is strongly influenced by the rate of heat release, which is defined by the injection strategy for any operating condition.

At constant engine speed the in-cylinder pressure traces can be considered approximately periodic [222]. Taking advantage of the crankshaft turn signal it is possible to split the pressure signal of each cylinder and to extract and examine separately the pressure evolution of each cycle. This permits to use the in-cylinder pressure decomposition technique with each one of the recorded cycles acquiring precise information about the combustion phenomenon at a given operating condition.

The first step of this decomposition technique is the separation between pseudo-motored (or compression-expansion signal), depending only on piston movement and boost pressure supplied by the turbo compressor, and the "excess pressure" related to the heat-release signal associated with the combustion process. This distinction is quite usual in the literature [9,34,66]. The pseudo-motored signal simply corresponds to the rise and fall of in-cylinder pressure due to the volume variation experimented as a consequence of piston motion, the signal itself does not contribute to the combustion process and, as indicated before, its use in this methodology is justified merely as a reference signal. Figure 3.5 represents the pseudo-motored and the excess pressure sub-signals together with the total pressure, in both the time and the frequency domains. The pressure spectra show that the low frequency content of the total pressure ($<$ 200 Hz) is clearly dominated by the pseudo-motored sub-signal.

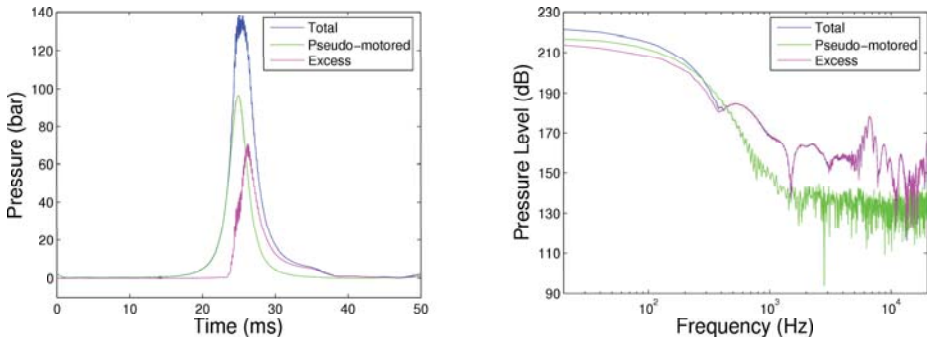

Figure 3.5: Total pressure, pseudo-motored pressure and excess pressure signals: time domain (left) - frequency domain (right)

Subtracting the compression-expansion sub-signal from the total pressure recorded, the "excess pressure" can be estimated. Furthermore, the resulting signal contains contributions of both combustion and resonant pressure fluctuations inside the combustion chamber. This last contribution is clearly identifiable by the presence of high amplitude peaks in the in-cylinder pressure spectrum, located at high frequencies. This fact suggests estimating the pressure fluctuation related to the resonance by high-pass filtering of the "excess pressure" signal. The cut-off frequency of the filter is an empiric function:

$$f_c = \frac{1}{D}.(132{,}2 + 9{,}2.\frac{n}{n_{idle}} + 0{,}41Lp) \tag{3.1}$$

depending on the load percentage Lp in %, engine speed n in rpm (normalized by the same parameter at idle condition) [163] and bowl diameter D [47]. Then, the combustion pressure is estimated by subtracting the resonance from the "excess pressure".

Figure 3.6 shows an example of in-cylinder pressure decomposition for one of the engine conditions tested. The total in-cylinder pressure signal is plotted together with the pseudo-motored, combustion and resonance pressure sub-signals, in both the time and the frequency domains. The pressure spectra show that the low frequency content of the total pressure is clearly dominated by the pseudo-motored sub-signal, whereas the combustion signal is predominant in the intermediate frequencies, and the high frequency peaks are consequence of the resonance related to the combustion chamber. In the novel approach proposed in this Thesis, these in-cylinder pressure decomposition technique will be used to define suitable indicators characteristic of the combustion that may be correlated with the engine noise level and quality.

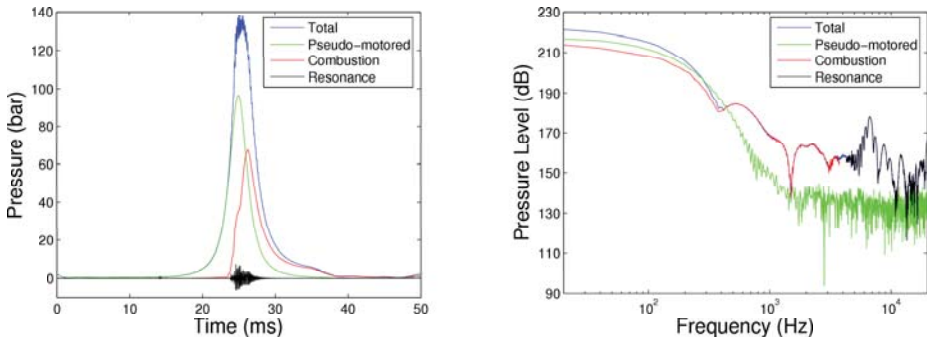

Figure 3.6: Example of in-cylinder pressure decomposition: time domain (left) - frequency domain (right)

3.5.2. Indicators definition methodology

As commented above, in this study direct correlation between the characteristics of combustion inside the cylinders and the noise radiated by the engine will be explored. The combustion noise will be considered from a quantitative point of view, analyzing the sound pressure level, as well as qualitatively, through a subjective evaluation. In this section, the methodology followed for the definition of indicators relative to the engine working conditions, containing information of the excitation sources, will be described. In a first phase direct correlations of the noise features with the engine operation parameters are searched, and then other parameters capable of characterizing the excitation sources, pressure and mechanical forces, are explored.

Figure 3.7 shows a block diagram representing the possible relation between noise and parameters that define the engine operation. Automotive Diesel engines are required to provide good performance and driveability, limiting consumption and emissions. In order to achieve these objectives, the engine control system acts on the injection settings and on the thermal and intake air management systems. Consequently, inside the engine, variations of the combustion process are produced. When the engine internal geometry is known, combustion can be properly characterized by the in-cylinder pressure evolution. As a result, a series of physical parameters that meet the initial requirements, i.e.torque, fuel consumption and emissions, characterize engine operation at a certain speed. Noise, together with pollutant substances in the exhaust gases, is considered as a form of engine emission.

In this work, indicators correlated with the excitation sources have been selected from the control, performance and combustion parameters according to the following methodology:

- Redundant parameters detection. In order to predetermine the parameters that contain the same information, the correlation coefficient between all parameters

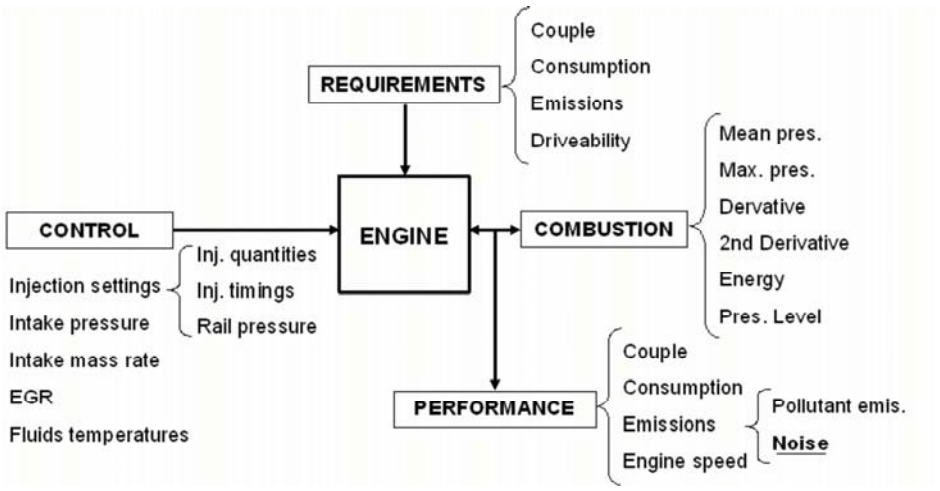

Figure 3.7: Relations between engine operation parameters and noise

of the same group is calculated. If the correlation coefficient of two parameters is greater than 90 %, are considered redundant and belonging to a same sub-group.

- Selection of the most representative parameters of each sub-group. Once the sub-groups have been formed, the parameter having the best physical sense in relation with the noise source is selected.

- Ranking of the selected parameters. For every parameter selected, the correlation coefficient with the noise characteristics examined (mark and overall noise) is calculated and ordered in ranking.

- Mathematic formulation of the indicators. Using the parameters best correlated with noise, a mathematical expression that defines the indicators related to the excitation sources is obtained.

- Definition of a correlation function. The indicators related to the excitation sources are used as independent variables in multiple regression equations for the estimation of the noise characteristics (mark and overall noise).

As was commented previously, both quantitative and qualitative aspects of combustion noise will be addressed in this work. Consequently, this methodology was applied for the definition of indicators correlated with noise quality, expressed with a mark given by a jury of experts, as well as with the overall noise, measured in decibels. More details of the results obtained with this methodology will be given in the following chapters.

3.5.3. Resonance analysis with CFD calculation

In this work the influence of the resonance in the combustion chamber on the combustion noise quality will be investigated. Experiments will be performed on an engine taking into account different geometries of the piston bowls. In order to have a deeper understanding of the resonance phenomenon, a preliminary study with a tree-dimensional CFD code (Fluent 2001) has been performed as a theoretical support to estimate the influence of the combustion chamber shape on the resonance phenomenon.

The engine manufactured furnished two types of piston with different combustion chamber shapes here referred as: "standard piston" (A) and "new piston" (B). The finite volume commercial program, with the standard $k-\varepsilon$ turbulence model has been used for the three-dimensional calculations of both bowl geometries. The turbulence model has been chosen because it is the most efficient and widely used in reciprocating internal combustion engines calculations. Figure 3.8 shows the three-dimensional mesh of the combustion chamber of both standard and new pistons.

A mesh independence study has been initially performed to ensure the numerical accuracy of the solution. The temporal discretization is explicit, with a variable time step depending on the flow conditions and on the cell size, in order to keep a Courant number of approximately 1. In any case, the time-step is of the order $2e-7s$, which is sufficient to capture the relevant frequencies.

Taking advantage of the symmetry with respect to a longitudinal plane that would go through the combustion chamber axis and through the middle of the excitation zone, the computational domain could be reduced to half the geometry. Furthermore the movement of the piston has not been simulated, this simplification is motivated by the fact that the phenomenon of resonance is normally detected immediately after the ignition and for a short part of the working cycle, in which the piston remains near the TDC. These assumptions simplify the model and allow lower computational costs.

Both bowl geometries have been calculated with the same operation and initial conditions. The initialization values for pressure and temperature in the combustion chamber were obtained from experimental tests, with both variables considered as homogeneous in the whole domain. The perfect gas assumption has been made for the working fluid. The temperature on the walls has been set using a correlation, which depends on the mean piston speed of the engine, following a model proposed by Woschni [276].

In order to simulate the auto-ignition occurring in the combustion chamber, a small zone within the bowl (indicated in red in Figure 3.8), corresponding to a single excitation source, has been defined as a patch where a pressure and temperature gradients are imposed at the start of the calculations. The latter correspond to the gradients caused by the start of combustion and they are determined experimentally with the combustion diagnosis programme CALMEC [140]. The duration of the pressure pulse imposed corresponds to one time-step and its intensity is defined according

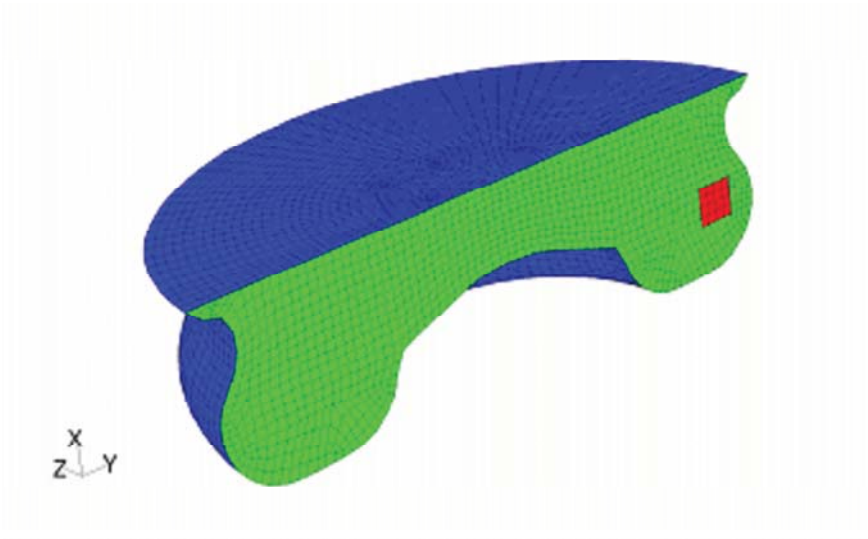

(A)

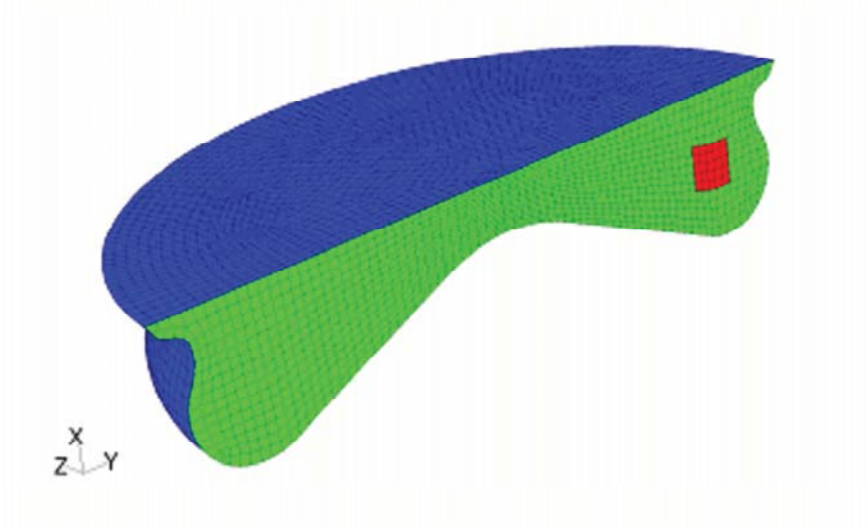

(B)

Figure 3.8: Three dimensional meshes of the combustion chambers: standard piston (A), new piston (B)

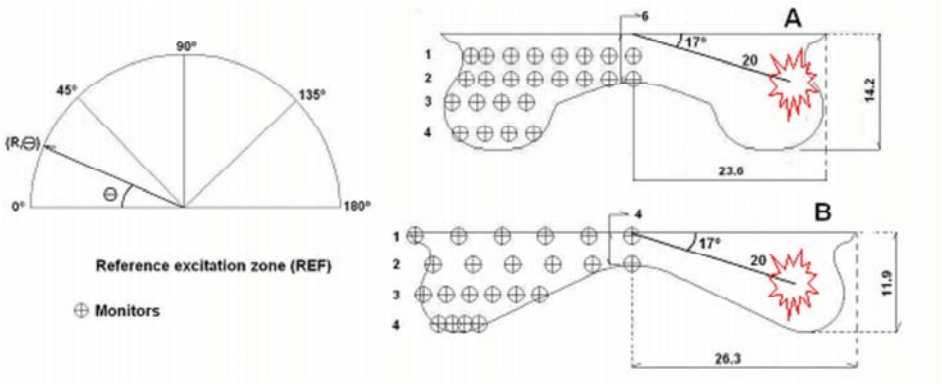

Figure 3.9: Geometry of the combustion chambers and distribution of monitors in plane 0^o with indication of the excitation sources

to the quantity of energy liberated during the premixing combustion phase, calculated from the combustion diagnosis programme.

The location of the excitation is identical for both combustion chambers, as indicated in Figure 3.9. By placing various monitors in the engine bowl, it is possible to obtain the pressure and temperature temporal evolution in different points of the combustion chamber and study the effects of the oscillating pressure waves within the human hearing frequency range (20 Hz to 20 kHz). In both piston bowls, in order to cover the whole chamber volumes, the pressure monitors have been distributed along longitudinal planes every 45^o and at various depths.

The results of this CFD calculation and their comparison with the experimental data will be presented in the Section 4.5.1.

3.6. Noise quality evaluation procedure

As commented in Section 2.6.3, the idea of giving an objective evaluation to the noise quality is a task that has been widely investigated. However, in a case as complex as the combustion noise generation, the classical methodologies based on psychoacoustic parameters don't bring to sufficiently trustworthy results. Consequently, in this study listening tests with a jury of experts have been performed, although they represent an expansive, lengthy and unpleasant task. In accordance with the procedure usually used at PSA Peugeot Citroën, the methodology adopted in this study is based on a listening phase of all the recorded noises, grouped for engine speed and torque.

A jury of listeners, adequately selected, attributes to every noise a mark representative of the subjective noise quality. The selection of the jury members, as a general rule, is based on listening experience, product experience and demographics:

- Listening experience - In general, it is desired that the listening experience level of the jury members is appropriate to the task considered as well as representative of target customer. Anyway, this type of test, as well as most automotive sound quality studies, do not require such a high level of expertise. Since, experts often pick up details that are not particularly important from the point of view of a normal customer.

- Product experience - The product experience of the subjects must be matched to the task under consideration. Listener's judgements of sound are influenced by the experience they have with the products. For this study, members of the department, familiarized with Diesel engines and passenger cars, have been considered as jury members.

- Demographics - Subject demographics doesn't present a strong influence on automotive sound quality application. Nevertheless, the subject population has been formed with a demographic mix (with respect to age, gender and economic status) representing the customer base for the product.

Auditory sensation	Mark	Customer satisfaction	Interpretation
Painful noise	1	The customer refuses to use the vehicle	Unbearable situation
Unbearable noise	2		
Hardly bearable noise	3	The customer requires an immediate correction	Necessity of an important correction
Very annoying noise	4		
Annoying noise	5	Strong dissatisfaction	Necessity of an Improvement
Unpleasant noise	6	Dissatisfaction	
Acceptable noise	7	Acceptation	Limit situation
Comfortable noise	8	Satisfaction	Favourable Situation
Pleasant noise	9	Strong Satisfaction	
Very pleasant noise	10	Total Satisfaction	

Figure 3.10: Mark table used for the noise quality evaluation

Figure 3.10 shows the table used for the evaluation of the noise quality, the first two columns of the table refer to the auditory sensation produced by the noise on the listener and the relative mark, a number in a rating scale between 1 and 10. Furthermore the third and fourth columns describe the meaning of the mark

with respect to the customer satisfaction and to the interpretation for the engine manufacturer, respectively. A mark of 1, for instance, corresponds to an extreme situation, a noise that causes pain to the listener's ears, in this case a potential customer would refuse to use the vehicle and this would represent an unbearable situation for the engine manufacturer. On the other extreme, a noise of 10 refers to a very pleasant noise, with total satisfaction of the customer and, consequently, also of the manufacturer. A particular case is a grade of 7, which is considered as the limit situation, the customer accepts the condition but he does not feel entirely satisfied.

The jury is formed by a minimum of eight subjects, five fixed and three variables. Prior to evaluation a short training is given to the jury members in order to familiarize the subjects with both the noises and the evaluation task. All the listening tests have been carried out in the anechoic chamber, the sounds have been played back through a pair of powered monitor speakers. The number of samples included in each test is usually inferior to 20 in order to limit the maximum test length to 30 minutes. Too long tests would induce fatigue in the jury producing, in turn, less discriminating results.

As commented before, the noises included in each listening test are at constant engine operating condition (speed and torque), the various steps of evaluation procedure are as follows:

- At first, the samples are presented randomly to the jury in order to permit the subjects to familiarize with the noises. Furthermore, the playback volume is set at a level that permits a clear perception of the acoustic stimuli avoiding to annoy the members of the jury.

- A rank ordering is then performed. Every subject is asked to order the noises according to its subjective preference criteria. If the number of samples is higher than 10 a first division into two groups is preferred. The noises are played sequentially and the jury members are required to divide the set of noises into "good noises" and "bad noises". They are also allowed to repeat any sound stimulus if they have difficulty making a judgement, till to get a ranking from the best to the worst noise.

- Through a paired comparison listening method at every noise is assigned a mark between 1 and 10 with a confidence degree of 0,5, in this phase the jury members are also allowed to repeat any sound stimulus if they have difficulty making a judgement. With the aim to be consistent with the quotation at the previous works three different noises, corresponding to a similar engine working at comparable conditions (speed and torque), are selected from the data base of the noises recorded and evaluated with different injection strategies or with different engine families, and used as reference. These noises have well-known marks and are selected in order to possibly cover a wide range of the evaluation scale (for example noises with marks 4, 7 and 8). In this way, it is expected that all noises are qualified as far as possible with the same metrics, so that one can be confident that a given mark represents the same sensation of quality at any engine running condition or operation strategy.

The following step deals with the quantification of each noise with a single mark. With this purpose, the marks given by all members of the jury are arithmetically averaged. Before the assignment of the mark, the consistency of each member of the jury is checked. The intention is to assure that the final mark is representative of the quality sensation of the majority of the jury members, and that it is not excessively influenced by natural divergence in the evaluation. Discrepancy between marks is also due to the presence of variable subjects in the composition of the jury.

Figure 3.11 represents the results of a study conducted on the listening tests performed on the 1.4 l engine. In this example two evaluation tests obtained with the engine running at high and low speed are compared, on the upper part of the figure the mean values of marks given by each one of the ten jury members and the confidence interval are shown, on the lower part of the figure a Box-and-Whisker analysis of the marks considering ten and eight members is plotted.

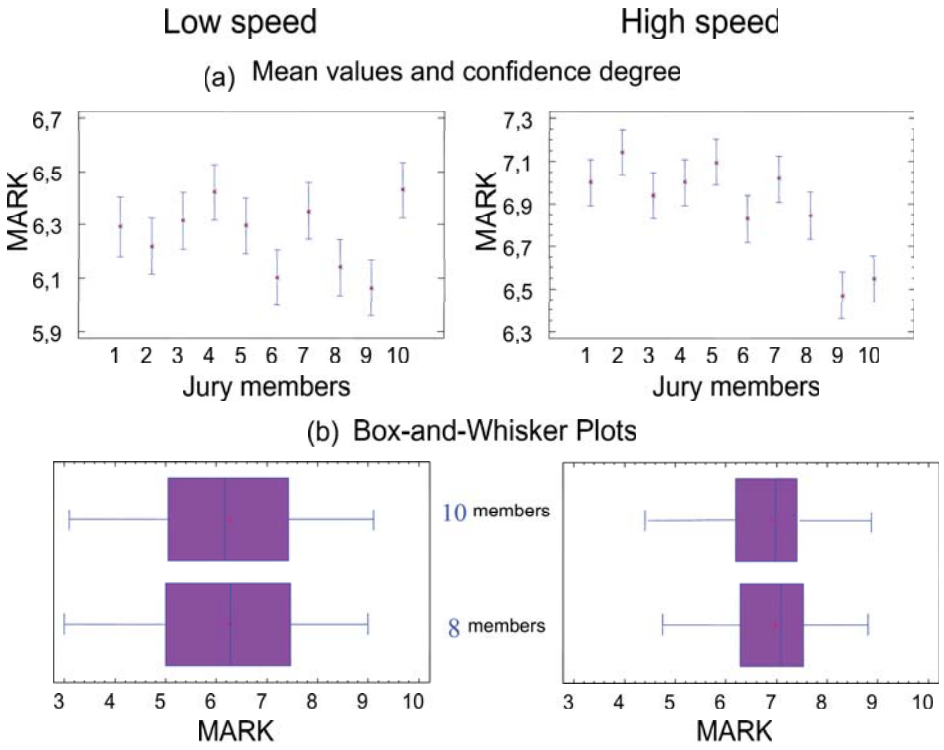

Figure 3.11: Analysis of the consistency of the jury

In Figure 3.11(a) it is shown that in the tests performed at low speed the mean mark assigned by each jury member varies between 6 and 6,4 and the confidence interval relative to the mean value of whichever member overlaps at least with the

confidence interval of the other members. This represents an excellent consistency, confirmed by the Box-and-Whisker analysis of Figure 3.11(b): al low speed if the jury members 9 and 10 are excluded (due to the fact that their mean values represent the limits of the set) quartiles, median (represented as a vertical line inside the box) and mean (plotted as a point) of the marks obtained considering only 8 members are quite similar to the values obtained considering all the jury members.

At high speed Figure 3.11(a) shows that the jury members 9 and 10 are again assigning out-of-trend marks, furthermore in this case their mean values and confidence interval are not overlapping the values given by the other members. In this case it could be supposed to exclude the two members from the marks analysis, nevertheless the Box-and-Whisker of Figure 3.11(b) indicates that this discrepancy is not significative, because also in this case the results obtained with 8 and 10 jury members are similar.

From this study it has been deducted that, as a general rule, is not necessary to exclude systematically a jury member. However, when in a single evaluation test (for a given engine speed and torque), a mark with deviations from mean value greater than 1 is detected the member is excluded from the analysis and the average mark is re-calculated. That is, for a specific speed and torque engine condition, the mark representative of the noise quality is obtained as the mean value of the marks assigned by the non-rejected jury members.

Chapter 4

Combustion noise quality assessment

Index

4.1. Introduction

This chapter is dedicated to the description of the main results that have been obtained in the study of the combustion noise quality. In the last years, models for the estimation of the combustion noise quality by means of in-cylinder pressure signal analysis have been researched and developed at CMT Motores Térmicos [139, 162, 165, 166]. As commented before, the basic idea of the models developed to approach the combustion noise generation problem is to find direct correlations between source and effect: in-cylinder pressure evolution and characteristics of radiated noise.

The next section will present the various phases that brought to the definition of the predicting model for noise quality assessment of engines operating with single and conventional injection strategies. The development of this predicting model has been achieved by analyzing the data base of measures performed on two different engine families, 1.4 l and 2.2 l engines. Successively, experiments have been done taking into account another engine size 1.6 l (of the same family of the 1.4 l engine). The equations characteristic of the model were calculated for this specific engine and the results have been compared with those obtained with the other engines. The goal of this study is to analyze the sensibility of the model to the size of the engine and the structural features of the block.

In the third section of the chapter the suitability of the model for engine noise assessment with multiple injection strategies will be explored. Firstly, the results of a preliminary study of the influence of the post injection on the noise quality will be presented. Finally the original model for single and conventional injection strategies will be updated, the purpose of this study is to allow the use of this model either with conventional or multiple injection strategies. Taking advantage of the suitable experimental plans defined for the study of multiple injection, in the fourth section, the noise quality sensitivity to some injection parameters and EGR will be analyzed.

The last section is devoted to the analysis conducted in order to examine the influence of the bowl geometry on the in-cylinder resonance and on the noise quality. To do this a different shape of the piston bowl has been taken into account in order to obtain variations of the resonance characteristics. The results of a preliminary CFD analysis of the piston bowl modification, taking into account its effect on the resonance generation and on the estimated noise quality, will be presented. Measurements were done on the 1.6 l engine equipped with the modified piston bowl, the experiments will be analyzed and compared with the outcomes of the CFD simulations. This study permit a better comprehension of the sensitivity of the noise quality prediction model to the resonance phenomenon and to the bowl geometry.

4.2. Model for single and conventional injection strategies

In this section the various steps of the development of a model for the prediction of noise quality will be described. As commented in the introduction, this study has

been conducted analyzing the data base of experimental measures performed on two different engine families: a 1.4 l and a 2.2 l HSDI Diesel engines. Part of the results presented in this section were already the object of a previous PhD thesis [139] written at the CMT Motores Térmicos.

4.2.1. Indicators selection

A first approach for the analysis of the noise quality using the decomposition technique was already presented by Payri *et al.* [163]. In order to go into the qualitative study of the Diesel noise in depth, the in-cylinder pressure decomposition technique exposed in Chapter 3 has been used to establish suitable parameters from the three sub-signals obtained with this procedure –pseudo-motored ($p_{\mathrm{ps-mot}}$), combustion (p_{comb}) and resonance (p_{res})– to assess the sound quality of combustion noise.

For this study the measurements performed on two different engine families were used:

- a 1.4 l engine, operating with split injection (pilot + main)
- a 2.2 l engine, operating with single and split injection

these two engines were intensively studied at CMT-Motores Térmicos, and hence a great data base was available. Initially several control and performance parameters have been considered. These parameters are those indirectly related to the combustion process, such as engine speed, torque, intake air mass, boost pressure, fuel consumption (total and split), energizing time, injection timing, injection pressure, EGR rate and fluid temperatures (air, coolant, oil and fuel).

All these parameters have been considered first, since these are normally monitored by the ECU in a commercial Diesel engine whose injection system is controlled electronically. If these parameters were enough to assess the noise quality, no further specific experimental devices (such as in-cylinder pressure transducers) would be necessary. This would represent a strong advantage with a clear reduction of time and costs during the engine development phase.

Unfortunately, through this analysis it was concluded that, individually, any of these parameters was weakly correlated with the noise quality mark given by the jury. Consequently, with the purpose of defining parameters that characterize the in-cylinder source (caused by combustion), several combustion components were determined using the three sub-signals obtained from the in-cylinder pressure decomposition. Some of the parameters considered were: the maximum pressure (p_{max}) and maximum first ($\mathrm{d}p_{\mathrm{max}}/\mathrm{d}t$), and second order pressure derivative ($\mathrm{d}^2p_{\mathrm{max}}/\mathrm{d}t^2$). Other components evaluated were the mean pressure (p_{mean}), signal energy (E) and sound pressure levels (L).

As was shown in Figure 3.6, the time-domain resonance sub-signal appears as a pressure oscillation characterized by sharp peaks, which makes it impossible to

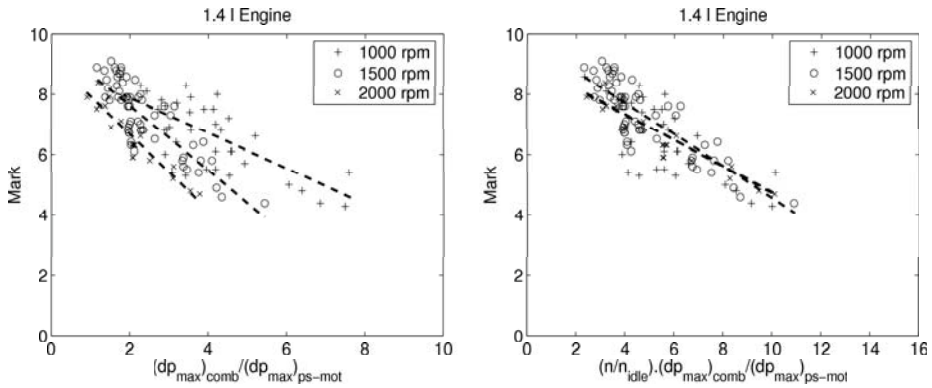

Figure 4.1: Correlation between noise mark and the dimension-less component relative to the maximum first order combustion pressure derivative in 1.4 l engine: with temporal information lose (left) and recovering temporal information multiplying by the engine speed non-dimensioned (right).

consider the corresponding derivative parameters in the study. Hence, the contribution of the resonance sub-signal to combustion noise was only evaluated through energy and pressure level components. The characteristic value of each component was quantified by the average of the values estimated for all the cycles recorded in the four cylinders.

Since the pseudo-motored sub-signal does not contain any information relative to combustion, it has been used to obtain non-dimensional components. This procedure, that allows reducing the number of analyzed factors, also permits more consistency when a relation with a mark –also non-dimensional– is established. To do this, each parameter relative to the combustion and resonance sub-signals was divided by the value of the same parameter associated with the pseudo-motored signal. In Figure 4.1 the maximum first-order pressure derivative of the combustion sub-signal non-dimensioned with the pseudo-motored sub-signal is presented. Figure 4.1(left) shows that the correlation trends between this component and the jury mark are highly dependent on the engine speed, which indicates that the temporal information has been lost in this component, as a consequence of non-dimensioning. To recover this information, however, the component may be further multiplied by the dimensionless engine speed n/n_{idle}, which effectively eliminates the speed dependency , as illustrated in Figure 4.1(right). The idle engine speed n_{idle} was set at the constant value of 750 rpm for all engines considered in this study. Indeed, Figure 4.1(right) shows now a better collapse of the samples along the same slope. Before starting with the components selection, the same procedure has been applied to recover the temporal information of the components that required it.

These components were then grouped into families of redundant parameters. This was done by computing the correlation of each of the dimensionless combustion components with the rest. If the correlation coefficient between two components was

Sub-group	Non-dimensional Component
(i)	E_{res}
(ii)	$(p_{\mathrm{mean}})_{\mathrm{comb}}$, $(p_{\mathrm{max}})_{\mathrm{comb}}$, E_{comb}
(iii)	$(\mathrm{d}p_{\mathrm{max}})_{\mathrm{comb}}$
(iv)	$\left(\mathrm{d}^2 p_{\mathrm{max}}\right)_{\mathrm{comb}}$
(v)	L_{comb}
(vi)	L_{res}

Table 4.1: Sub-groups of non-dimensional combustion components

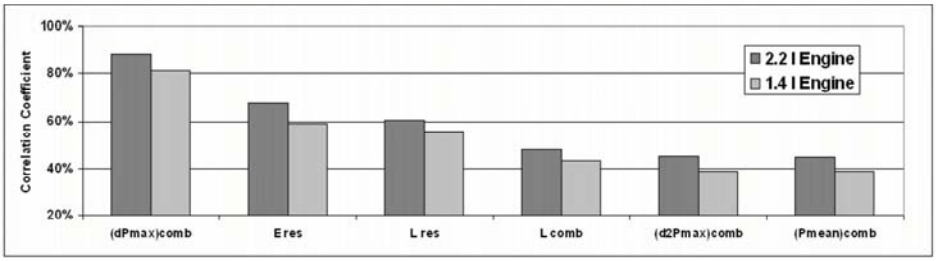

Figure 4.2: Ranking of the correlation coefficients of the combustion components with the noise mark.

higher than 90 %, they were considered as redundant and belonging to the same sub-group. This procedure led to the formation of the six sub-groups detailed in Table 4.1.

The calculation of the correlation coefficient of every selected parameter with the noise quality marks given by the jury led to the conclusion that the components of sub-groups (i) and (iii) were the best correlated with the noise quality. Figure 4.2 shows the ranking of the combustion components most representative of each sub-group obtained for the 2.2 l and 1.4 l engines . This bar plot shows that the first order maximum pressure derivative of the combustion sub-signal is clearly the most relevant combustion parameter that affects engine noise quality, and that the contribution of the resonance sub-signal seems to be important too. Finally, two combustion indicators have been initially defined, based on the correlation degree with the engine noise mark of these two components.

The first combustion indicator I_1, which is related to the initial high fuel burning velocity, is defined by the following equation:

$$I_1 = \frac{n}{n_{\mathrm{idle}}} \left[\frac{(\mathrm{d}p_{\mathrm{max}}/\mathrm{d}t)_{\mathrm{comb}}}{(\mathrm{d}p_{\mathrm{max}}/\mathrm{d}t)_{\mathrm{ps-mot}}} \right], \tag{4.1}$$

where:

- $(\mathrm{d}p_{\max}/\mathrm{d}t)_{\mathrm{comb}}$ and $(\mathrm{d}p_{\max}/\mathrm{d}t)_{\mathrm{ps-mot}}$ are the peak values of the pressure derivatives corresponding to the combustion and pseudo-motored sub-signals, respectively.

The second indicator I_2 contains the signal energy relative to the combustion chamber resonance sub-signal and is estimated by

$$I_2 = \frac{E_{\mathrm{res}}}{E_{\mathrm{ps-mot}}}; \tag{4.2}$$

where:

- E_{res} is the signal energy of the resonance, defined as $\int p_{\mathrm{res}}^2 \mathrm{d}t$, evaluated between the start of combustion and the instant of the exhaust valve opening

- $E_{\mathrm{ps-mot}}$ is the signal energy of the pseudo motored component, defined as $\int p_{\mathrm{ps-mot}}^2 \mathrm{d}t$, evaluated for the whole closed cycle

To obtain the regression functions between noise quality and the combustion indicators, only the four or five combustion processes which provoked the widest range of noise quality variation were considered for every engine operating condition. Thus the rest of tested conditions have been used for checking the suitability of the final model for sound quality assessment at any other engine operation.

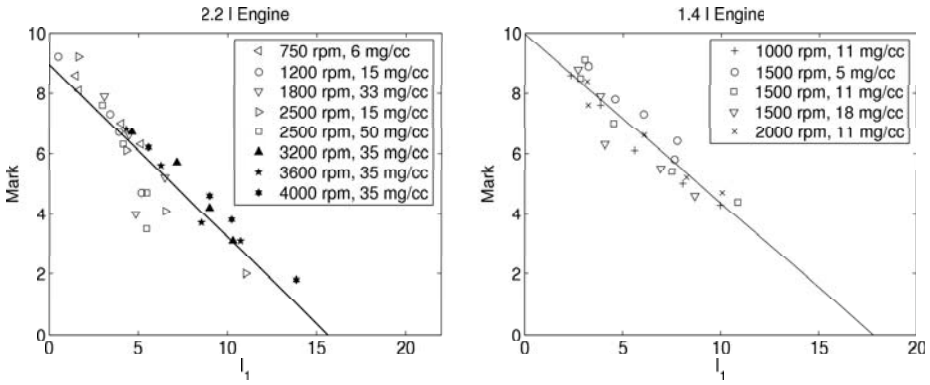

Figure 4.3: Relation between the noise mark and the combustion indicator I_1: 2.2 l engine (left) and 1.4 l engine (right).

Figure 4.3 shows the correlation degree between the I_1 indicator and the noise marks assigned by the jury in the two engines studied. These plots show that under all operating conditions, the I_1 indicator is linearly correlated with the noise marks, evidencing a high correlation level in both engines. However, the dispersion with

respect to the trend line is nonetheless high, as is confirmed by the standard deviation levels (σ) indicated in Table 4.2. In addition, Figure 4.3 (left) relative to the 2.2 l engine shows that the dispersion obtained for engine speeds higher than 3000 rpm (symbols filled in black), in which single injection is used, is lower than for the rest of the conditions (symbols without filling), in which split injection is employed. Figure 4.3 (right) also presents high dispersion in the 1.4 l engine, for which split injection was used in all the operating conditions tested.

Table 4.2: Statistical parameters of estimated noise mark with the defined indicators.

	Large engine			Small engine		
Indicator	$\epsilon_{\max}$	σ	R(%)	$\epsilon_{\max}$	σ	R(%)
I_1	2.34	0.84	91	1.38	0.56	97
I_3	0.90	0.38	99	0.53	0.30	99
I_4	2.50	0.94	95	1.40	0.70	94

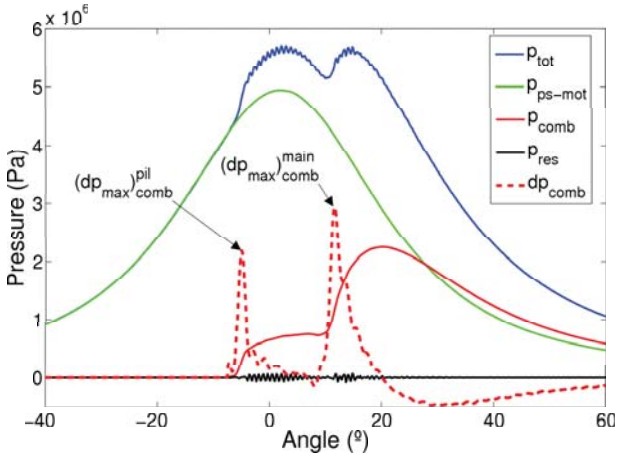

Figure 4.4: In-cylinder pressure decomposition in the 2.2 l engine with split injection at 1200 rpm, 15 mg/cc.

These observations evidence the weakness of the I_1 indicator to assess the engine noise quality when split injection is used. Figure 4.4 shows an example of in-cylinder pressure decomposition in one of the engine operating conditions included in Figure 4.3 (left), in which double injection (pilot and main) strategy was employed. In this figure, the pressure derivative curve of the combustion sub-signal is also included.

This curve presents two peaks, which are associated with the burning velocity of the fuel injected during the pilot and main injections. The amplitude of both peaks are of the same order of magnitude, so that it is not absolutely clear if just one of them contributes to the engine noise or both contributions should be considered in the indicator to improve its suitability. To clarify this, the dimension-less peak pressure derivative of the pilot and main injections, and the I_1 indicator were plotted against the noise mark individually for each operating condition with split injection used in both engines. Figure 4.5 shows the results obtained in the 2.2 l engine at 2500 rpm and 15 mg/cc and in the 1.4 l engine at 1000 rpm an2d 11 mg/cc. These plots evidence that, even though the three parameters are correlated with the mark, there is significant dispersion with respect to a virtual trend line in the three cases. However, graphically, it seems clear that the mean values of the pilot and main pressure derivatives –their correspondence is indicated by the horizontal lines– preserve the good correlation observed previously, but with a considerable reduction of the dispersion, as can be intuitively checked along the dashed trend lines included in both plots.

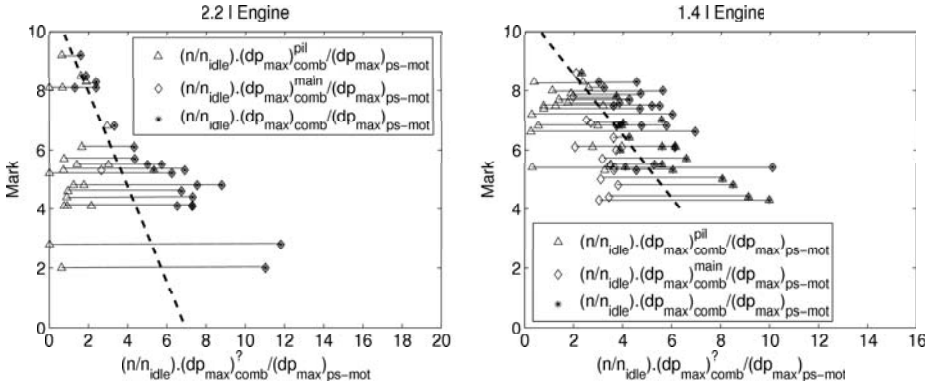

Figure 4.5: Relation between the noise mark and the pilot and main peak pressure rate-of-change and I_1: in 2.2 l engine at 2500 rpm, 15 mg/cc (left) and in 1.4 l engine at 1000 rpm, 11 mg/cc (right).

These results indicate that in Diesel combustion with split injection strategies, the engine noise can be accurately assessed by considering the contribution of the pressure rate-of-change due to the heat release of the fuel in both pilot and main injections. Following this observation, the I_1 indicator was modified to yield a new indicator I_3 calculated with the following equation:

$$I_3 = \frac{n}{n_{\text{idle}}} \left[\frac{(\mathrm{d}p_{\max}/\mathrm{d}t)^{\text{pil}}_{\text{comb}} + (\mathrm{d}p_{\max}/\mathrm{d}t)^{\text{main}}_{\text{comb}}}{(\mathrm{d}p_{\max}/\mathrm{d}t)_{\text{ps-mot}}} \right], \tag{4.3}$$

where:

- $(\mathrm{d}p_{\max}/\mathrm{d}t)^{\text{pil}}_{\text{comb}}$ and $(\mathrm{d}p_{\max}/\mathrm{d}t)^{\text{main}}_{\text{comb}}$ are now the pressure derivative peak dur-

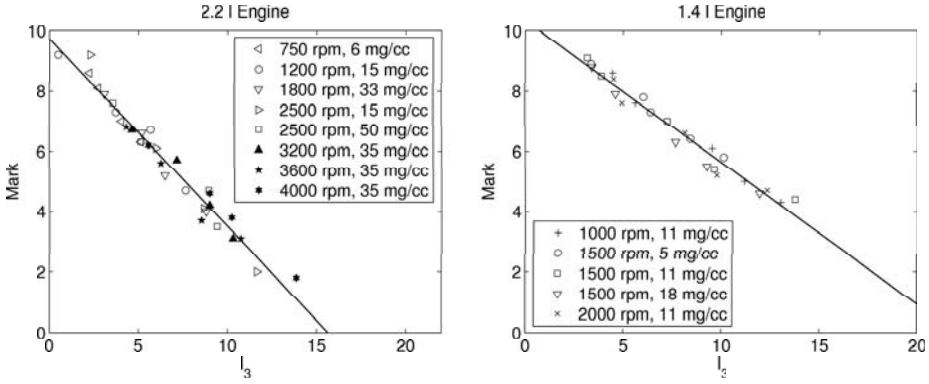

Figure 4.6: Relation between the noise mark and the combustion indicator I_3: 2,2 l engine (left) and 1.4 l engine (right).

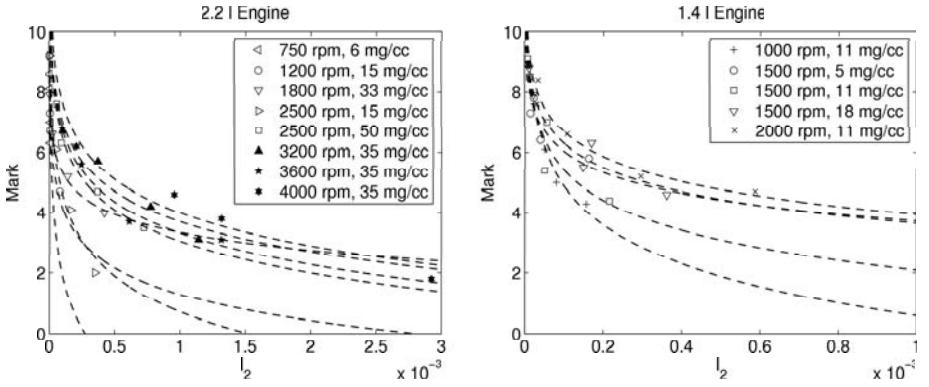

Figure 4.7: Relation between the noise mark and the combustion indicator I_2: 2.2 l engine (left) and 1.4 l engine (right).

ing the combustion of the fuel injected in the pilot and main injections, respectively.

Figure 4.6 shows the correlation plot between the new indicator I_3 and the noise marks in the two engines studied. The new I_3 indicator has brought about a significant improvement in engine noise prediction, which is quantified by the notable increase of the correlation coefficient (R) and reduction of the dispersion and of the maximal absolute error ($\epsilon_{\max}$) in both engines, as shown in Table 4.2.

Regarding the indicator associated with the resonance of the combustion chamber, in Figure 4.7 the relation between the I_2 indicator and the noise marks is graphically represented for the two engines. This indicator, unlike the previous one, shows

a non-linear correlation with the jury marks that can be represented by a logarithmic functional dependence. Following this observation, the I_2 indicator has been redefined with the logarithm function, so that the relation linking this new indicator with the noise mark can also be described by a linear correlation. Furthermore, in order to maintain an ideal mark of 10 when there is no resonance in the combustion chamber, the new indicator is conveniently scaled by the factor $E_0 = 10^6$. Hence, with this procedure another combustion indicator I_4 carrying the resonance contribution was defined as:

$$I_4 = \log\left(E_0 \frac{E_{\text{res}}}{E_{\text{ps-mot}}}\right). \tag{4.4}$$

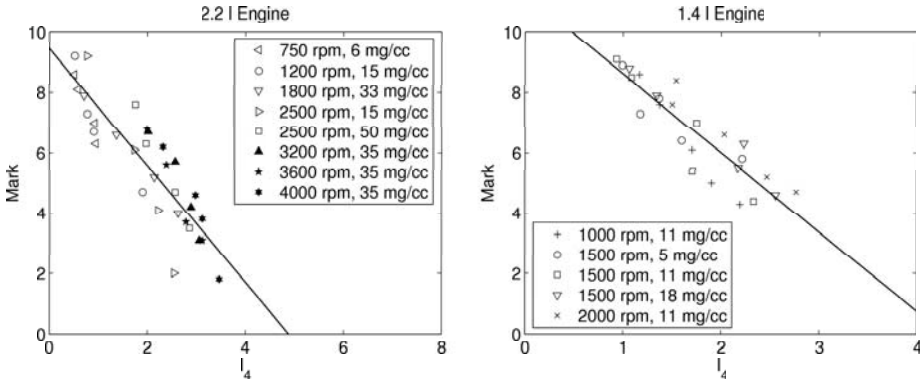

Figure 4.8: Relation between the noise mark and the combustion indicator I_4: 2.2 l engine (left) and 1.4 l engine (right).

Figure 4.8 presents the relation between the new combustion indicator I_4 and the noise marks obtained in both engines tested. As expected, these results show an acceptable correlation I_4-mark but with high dispersion in comparison with the results obtained with the I_3 indicator. Table 4.2 shows the main statistical parameters that qualify this regression. However, the inclusion of this indicator should be interpreted in the sense that the defined indicators contain complementary information, so that it seems necessary to consider both together and not individually.

4.2.2. Evaluation of indicators contribution

As commented before, these two combustion indicators were selected as the more appropriate to determine suitable relations with engine noise quality. In addition, the analysis also evidenced that the I_3 indicator –relative to the peak velocity of fuel burning– should be the most significative parameter in any possible multiple component correlation for noise quality evaluation. I_4 seemed to be as a complementary variable that supply the lack of information in I_3.

2.2 l engine				1.4 l engine			
ϵ_{mean}	ϵ_{max}	σ	R(%)	ϵ_{mean}	ϵ_{max}	σ	R(%)
0.38	2.12	0.50	95	0.48	2.16	0.59	91

Table 4.3: Statistical parameters of estimated noise mark with single component correlations.

With the purpose to check this observation, a single component regression in which I_3 indicator has only been included was evaluated first. That is:

$$Mark = 10 - c_3 I_3, \tag{4.5}$$

where the coefficient c_3 was optimized to maximize the correlation coefficient of the regression. Figure 4.9 presents the comparison between the noise marks estimated with this single component equation and the marks given by the jury for the two considered engines. A quite good agreement can be observed in these results with both 2.2 l engine (left) and 1.4 l engine (right). This observation is statistically corroborated by the absolute mean (ϵ_{mean}) and maximal (ϵ_{max}) errors, the standard deviation (σ) and the correlation coefficient (R), whose values are summarized in Table 4.3. Moreover, in the 2.2 l engine, 72.4 % and 94.6 % of the samples have absolute errors lesser than 0.5 and 1, respectively. While, in the 1.4 l engine, this percentages are 59.1 % and 91.4 %, respectively. In both engines, the correlation coefficients were higher than 90 % and the mean absolute errors lesser than 0.5, which is of the same order of magnitude than the uncertainties of jury noise evaluation procedure. Despite these parameters should indicate that single component regression would permit enough accuracy for noise mark estimation, the high ϵ_{max} levels obtained seemed to confirm the necessity of additional information that may be provided by the I_4 indicator.

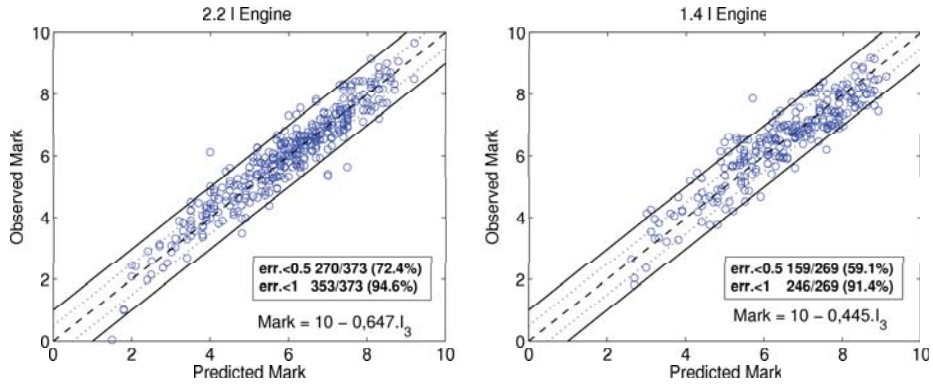

Figure 4.9: Mark noise estimation with single component regression: 2.2 l engine (left) and 1.4 l engine (right).

Finally, with the aim to improve the reliability of the single component correla-

2.2 l engine				1.4 l engine			
ϵ_{mean}	ϵ_{max}	σ	R(%)	ϵ_{mean}	ϵ_{max}	σ	R(%)
0.37	1.89	0.48	95	0.41	1.52	0.51	94

Table 4.4: Statistical parameters of estimated noise mark with two-component correlations.

tion, a multiple regression with the two defined indicators (I_3 and I_4) was considered for the noise mark estimation as:

$$Mark = 10 - c_3 I_3 - c_4 I_4, \tag{4.6}$$

where coefficients c_i were optimized to maximize the correlation coefficient of the regression. From a physical point of view, this equation may indicate that the sudden in-cylinder pressure rise as well as the chamber resonance deteriorate the ideal mark of 10.

The results obtained with two-component correlation are evaluated through the statistical parameters shown in Table 4.4. A significant contribution of the I_4 indicator to improve the statistics has been observed mainly in the 1.4 l engine, for which an apparent rise of the correlation coefficient and a reduction of standard deviation, mean and maximal absolute errors is obtained in comparison with single component regression. Furthermore, the inclusion of I_4 has permitted also to reduce the maximal absolute error in the 2.2 l engine.

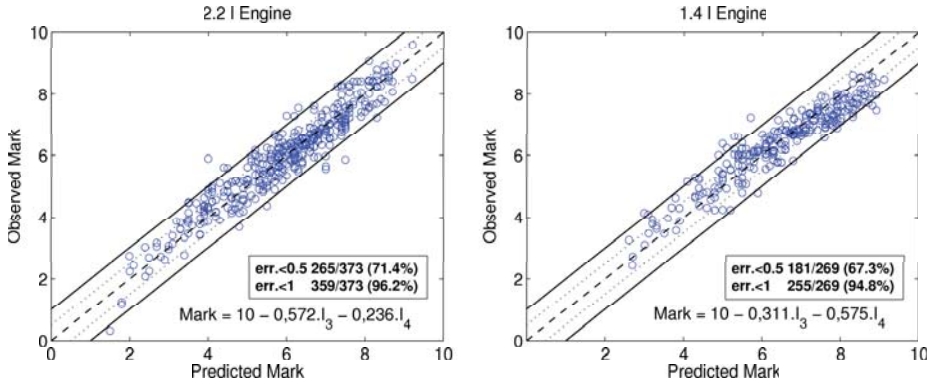

Figure 4.10: Mark noise estimation with the proposed approach: 2.2 l engine (left) and 1.4 l engine (right).

Figure 4.10 shows the comparison between the noise marks estimated with the two-components approach based on Equation (4.6) and the noise marks assigned by the jury. The agreement may be regarded as very good. The fact that, at each operating condition, the noise variation was induced varying the injection parameters

may indicate the suitability of the proposed approach not only for noise quality estimation but also for the prediction of the effect of a given injection strategy on engine noise, which is useful for the optimization of injection settings aiming a noise quality improvement.

From these first studies it seems clear that the size of the engine and the structural features of the block emerge through the regression coefficients c_i. Nevertheless, a deeper analysis of this dependence is necessary. Accordingly, the next phase of this research has been the validation of this predicting model for single and conventional injection strategies on a different engine. For this further study an engine with a displacement of 1.6 l has been used. The engine size has been chosen between 1.4 and 2.2 liter, considered in the previous analysis, and the block structural features are similar those of the 1.4 l engine. Moreover, this new generation engine offered the possibility to operate with multiple injection strategies, this arose the opportunity to further develop the predicting model in order to permit its use also with multiple injection.

4.2.3. Model suitability evaluation

In order to evaluate the suitability of the existing model for the assessment of the noise quality from the in-cylinder pressure signal analysis and to estimate the sensitivity of the model coefficients c_i to the engine size and structural characteristics, a 1.6 l engine, direct injection, Diesel engine has been taken under consideration. Using an adequate ECU configuration, the engine was induced to operate with conventional injection strategy (pilot + main). For every working condition listed in Table 3.1, an experimental plan with injection-combustion settings variations has been defined. For each plan, those factors that in previous studies have been detected as the most significant for engine noise variation were modified. These parameters are :

- Mass of pilot injection
- Start of injection (SOI) of the pilot injection
- Start of injection (SOI) of the main injection
- Rail pressure
- EGR rate

For every factor, three levels of variation were considered for designing the experiments at each running condition. An orthogonal plan, based on a Taguchi model, was used to combine the factor variations in order to get clear noise variations. The outcome of this statistical analysis was a matrix of 27 tests per each running condition. However, the previous experiences indicate that the jury can hardly evaluate more than 18 noises at the same time. For this reason, from the 27 tests, only 21 have been chosen, being 18 used for the calculation of the coefficients c_i of the model, and 3 for the further phase of validation.

The criteria used to choose the 21 tests has been based on maintaining the engine torque as constant as possible with the wider range of noise variation. A tolerance of $\pm 20\,\%$ from the nominal torque value has been considered acceptable, so that just tests with the minimal torque variations were considered. Using the in-cylinder pressure decomposition and evaluating the noise records with the methodologies described in Sections 3.5.1 and 3.6, through multiple regressions, the coefficients c_i of Equations (4.5) and (4.6) were calculated with the 18 measures chosen from each one of the nine experimental plans (162 points in total). The accuracy of the model for the prediction of the noise quality has been validated later with the 3 additional measures from each experimental plan (27 validation points in total).

Figure 4.11 (a) shows the comparison between the noise marks assigned by the jury and the noise marks estimated with a single component regression (based on Equation (4.5)). Figure 4.11 (b) presents the same analysis performed with two-components approach (based on Equation (4.6)). Both plots show a quite good correlation between the marks predicted and estimated, even when just one combustion indicator is used. However, as it was remarked in the previous section, the correlation can be enhanced when the two defined components are included. Furthermore, the plots show that both models permit a good estimation of the noise quality at the 27 validation points, which have not been used to calculate the c_i coefficients. Particularly the two components model (Figure 4.11(b)) has been capable to predict the mark representative of the noise quality of the validation points with high accuracy keeping the maximal error inferior to the unity. This demonstrates the suitability of this methodology and confirms that this approach represents a reliable and attractive tool for engine noise quality estimation, but also for the establishment of guide lines for optimal injection settings regarding combustion noise quality issues.

Engine	c_3	ϵ_{mean}	ϵ_{max}	σ	**R(%)**
1.4 l	0.445	0.48	2.16	0.59	91
2.2 l	0.647	0.38	2.12	0.50	95
1.6 l	**0.515**	**0.62**	**2.03**	**0.76**	**90**

Table 4.5: Statistical parameters of estimated noise mark with one component correlation.

Engine	c_3	c_4	ϵ_{mean}	ϵ_{max}	σ	**R(%)**
1.4 l	0.311	0.575	0.41	1.52	0.51	94
2.2 l	0.572	0.236	0.37	1.89	0.48	95
1.6 l	**0.303**	**0.821**	**0.43**	**1.37**	**0.54**	**95**

Table 4.6: Statistical parameters of estimated noise mark with two-component correlations.

Tables 4.5 and 4.6 show a comparison of the coefficient values c_i and statistical parameters of the correlation found for the different engines tested, with both

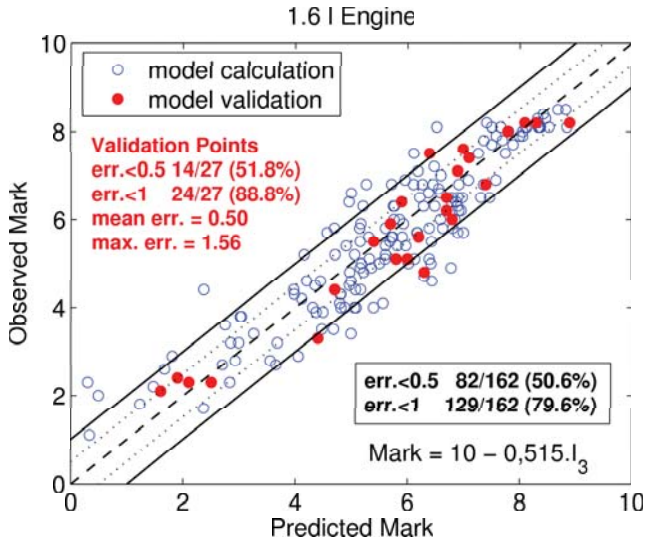

(a)

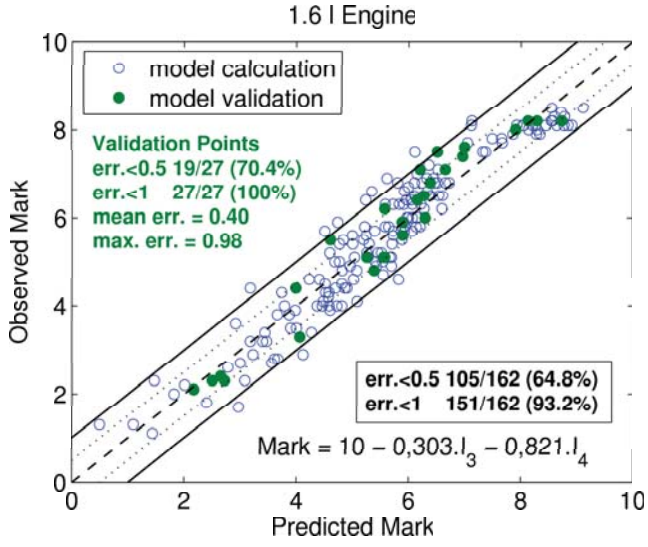

(b)

Figure 4.11: Mark noise estimation with 1.6 l engine: single component regression (a) and two components regression (b).

single component and two-components regressions, respectively. Coefficients c_3 and c_4 obtained for the 1.6 l engine are consistent (same order of magnitude) with those determined in the previous researches. Furthermore, the current results seem to confirm that the coefficients are dependent on the engine family. From the Table 4.5 it turns out that the coefficient of the single component regression seems to have a direct

correlation with the engine size (c_3 increases as the engine size increases). When the second combustion indicator I_4 is included in the model, further conclusions can be observed, from Table 4.6 it results that values of c_3 relative to the 1.4 l and 1.6 l engines are almost the same, this can be explained by the fact that these two engines belong to the same family, with quite similar structural features of the block. Furthermore the resonance phenomenon seems to be be less influent on the 2.2 l engine and more significant with the other engine family.

However, no clear tendencies can be observed of the contribution of the resonance. This is more weighty in the case of the 1.6 l engine –c_4 has the highest value– but its contribution seems to be dependent on the combustion chamber geometry. In order to have a better understanding further researches on the contribution of the resonance energy have been conducted on this engine. With this purpose an experimental analysis of the influence of the combustion chamber shape on the coefficients of the model, and more in general on the noise quality, has been conducted. The results of this study will be presented and commented in Section 4.5.

4.3. Model for multiple injection strategies

In the lately years, the development of the first generation common-rail systems, has permitted the introduction of more complex injection strategies. In the new generation systems, the maximal injection pressure has been increased up to 1800 *bar* and the injection can be split in a multiple sequence of up to five times per working cycle. This allows more degrees of freedom to decide the timing and quantity of the split injections, which can be used to obtain significant reductions in engine noise and emissions [19].

As commented before, the aim of the previous works was the estimation of the quality of the noise radiated by the engine block by means of the in-cylinder pressure analysis. In these studies, only two different injection strategies have been used:

- single injection
- double injection (pilot + main)

In these conditions, as showed in the previous section, a model based on two combustion components, capable to accurately predict the combustion noise quality has been developed. Unfortunately, the selected combustion indicator I_3 (Equation (4.3)) considers the pressure derivative peak during the combustion of the fuel injected in the pilot and in the main injection, then its definition is suitable only for single and double injection strategies.

For these reasons, an experimental study has been performed in order to update the model for assessing the combustion noise quality of engines operating with multiple injections. The experiments have been performed on the 1.6 l engine that has been equipped with an ECU allowing different injection strategies:

- three injections (2 pilots +1 main)

- four injections (2 pilots + 1 main+ 1 post)

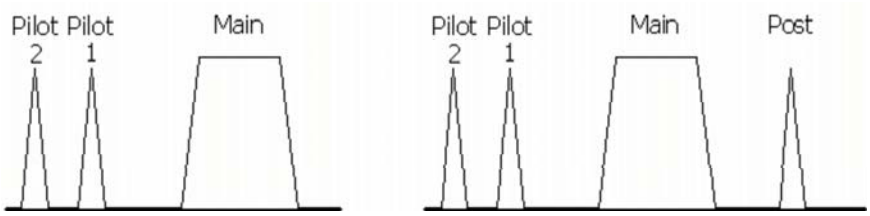

Figure 4.12: Nomenclature used for the study of three and four injection schemes

Figure 4.12 shows injection rate schemes with the nomenclature used in this study. The fourth injection is also called post injection and is used with a double intention:

- to sustain the combustion due to the main injection for burning off soot, and thus bringing down pollutant emissions before exhaust gases have left the combustion chamber

- to regenerate the particulate filter by keeping high exhaust temperatures

Despite the purpose of the post injection deals only with the control of pollutant emissions, before approaching the problem of assessing the noise quality in case of multiple injection, a brief study to check the sensitivity of combustion noise quality to post injection strategy has been preliminarily performed in this phase of the work.

4.3.1. Sensitivity study of noise quality to post injection

Three different base points with four-injections strategies have been considered in order to cover a wide range of engine speeds and loads:

- 2850 rpm, 87 Nm

- 1500 rpm, 75 Nm

- 1900 rpm, 124 Nm

To investigate the influence of the post injection on the combustion noise, three experimental plans have been designed. In these plans, the start of injection (SOI_{post}) and the injected quantity (Q_{post}) relative to the post injection have been varied, keeping the rest of the parameters constant as in the baseline, except for the quantity of fuel in the main injection, that has been set in order to keep the torque as constant as

Q pilot 2 (mg/str)	Q pilot 1 (mg/str)	Q main (mg/str)	Q post (mg/str)	SOI pilot 2 (° - TDC)	SOI pilot 1 (° - TDC)	SOI main (° - TDC)	SOI post (° - TDC)	Pression Rail (bar)	EGR (%)	Torque (Nm)
1,76	1,76	4,58	2,00	27	5	-4	-9	1035	48	75
1,76	1,76	6,44	2,00	27	5	-4	-13	1035	48	75,1
1,76	1,76	9,62	2,00	27	5	-4	-17	1035	48	74,9
1,76	1,76	2,44	4,60	27	5	-4	-9	1035	48	75
1,76	1,76	4,60	4,60	27	5	-4	-13	1035	48	75,4
1,76	1,76	8,43	4,60	27	5	-4	-17	1035	48	74,4
1,76	1,76	2,08	7,20	27	5	-4	-9	1035	48	76,2
1,76	1,76	2,13	7,20	27	5	-4	-13	1035	48	74,7
1,76	1,76	6,59	7,20	27	5	-4	-17	1035	48	74,7
								σ Torque		0,517

Figure 4.13: Example of experimental plan for the study of the post injection, 1500 rpm 75 Nm

possible. Figure 4.13 shows an example of test matrix defined for this brief study, where the standard deviation of the nominal torque is also included. In all cases, a torque variation less than 1 % from the nominal value has been obtained.

As shown in Figure 4.13, Q_{post} (expressed in milligrams per stroke) and SOI_{post} (expressed in degrees before TDC,"-" means after TDC) have been varied according to three levels and in every experimental plan, all the possible combinations have been tried. The variation range of the SOI_{post} is quite narrow, since on one hand earlier post injection could cause the overlapping with the main injection and on the other hand, an excessive delay could keep the injected fuel unburned. Fortunately, the injected quantity can be strongly varied without particular inconveniences. So the Q_{post}, that normally represents only a small percentage of the total mass, has been varied until it was 60 % of the total injected fuel. However, despite of these variations, during the listening phase of each experimental plan the jury was not able to appreciate apparent noise variations, since all noises at the same engine operation point resulted quite similar.

In order to have a better understanding of the phenomenon in the combustion chamber, in-cylinder pressure signals have been decomposed. In the previous studies a strong correlation between the noise quality and the pressure derivative peaks of the combustion curve has been evidenced. For this reason, the following analysis has been mainly based on the evaluation of the pressure derivative of the combustion curve. Figure 4.14 shows an example of in-cylinder pressure decomposition, the plot also includes the derivative curves of the total pressure, compression and combustion sub-signals together with the "injection signal", obtained from a clamp meter that measures the electric current governing the injector solenoid (black line). From the injection signal it can be clearly observed the presence of four positive peaks and four negative peaks, these correspond to the moments when the ECU commands the opening and the closing of the injector, respectively.

In this figure the pressure derivative of the combustion sub-signal (blue line) shows that the peak relative to the post injection is the smaller if compared to the peaks relative to the pilots and main injection. This was confirmed at all tested conditions. For each experimental plan, also in the worst conditions where the highest pressure derivative peaks due to post combustion are expected –maximal Q_{post} and SOI_{post} are used– the same outcomes have been obtained. This behavior is explained by the fact that the post injection produces a too delayed combustion, fuel burning takes place when the expansion stroke is already advanced, so that an abrupt pressure rise which could contribute to the radiated noise should not occur.

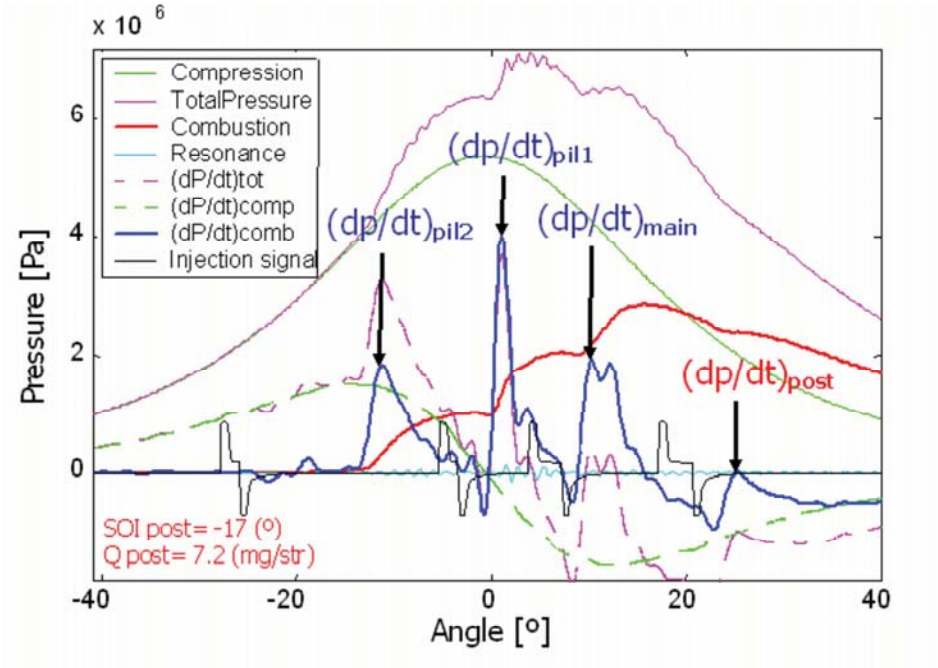

Figure 4.14: Example of in-cylinder pressure decomposition in case of a 4 injections multiple strategy, 1500 rpm 75 Nm

Table 4.7 shows the range of variation of the combustion sub-signal pressure derivative peaks due to the injection at each experimental plan. It is evident that the maximal values relative to the post injection combustion are lower than the peaks caused by the rest of injections. Therefore, since pressure derivative peaks are dominant on combustion noise, it is confirmed that negligible influence of post injection on the engine noise should be expected.

Working Condition	$(dp/dt)_{pil2}$ (kPa/ms)	$(dp/dt)_{pil1}$ (kPa/ms)	$(dp/dt)_{main}$ (kPa/ms)	$(dp/dt)_{post}$ (kPa/ms)
2850 rpm - 87Nm	2548 ↔ 3676	2326 ↔ 2907	1915 ↔ 3694	**94 ↔ 1561**
1500 rpm - 75Nm	1728 ↔ 2322	3429 ↔ 3798	1845 ↔ 2718	**-162 ↔ 1224**
1900 rpm - 124Nm	3853 ↔ 4765	2132 ↔ 2633	3716 ↔ 4560	**-278 ↔ 1480**

Table 4.7: Variation ranges of the pressure derivative peaks of combustion sub-signal

This conclusion has permitted the simplification of the further studies. The experimental confirmation that the post injection does not have any influence on the engine noise quality reduces the study of multiple injection to the definition of experiments with just three injection strategies. The post injection can be eliminated taking into account that this work concentrates only on the radiated noise without considering the engine emissions.

4.3.2. Adaptation of the model

In Section (4.2) a predicting model for the assessment of the noise quality has been developed. Studying different engine families under several operating conditions in terms of speed, load and combustion parameters, a good correlation between the components I_3 and I_4 and the noise quality quantified by a jury has been evidenced. In particular, the indicator I_3 associated with the burning velocity demonstrated to be the most relevant contributor of the predicting model. However, it was defined for conventional injection strategies (pilot + main), which in current developments have been replaced by multiple injection strategies. For this reason the model was adapted in order to respond to multiple injection features. With this purpose three injection strategies have been considered, since it has been previously observed that the post injection doesn't have any relevant effect on combustion noise.

Figure 4.15 shows the results of the in-cylinder pressure decomposition in one cylinder and one cycle at 1900 rpm and 124 Nm. In this figure, all parameters that are relevant to estimate the indicators of the model are shown together with the injector signal (plotted in black line). The blue line, which corresponds to the pressure derivative of the combustion sub-signal (red line), evidences three peaks that are associated with the three injections (pilot 2, pilot 1 and main) used in the tested condition. These results differ from those a priori expected if conventional injection strategies (pilot + main) are used and therefore, some refinements of I_3 to adapt the model to multiple injections should be performed. Unlike this, the I_4 indicator – relative to the resonance of the combustion chamber – seems to be independent of the injection strategy employed as can be seen in the cyan line of Figure 4.15.

According to these observations, the natural way to adapt the I_3 component to multiple injection strategies seems to be through the contribution of the three

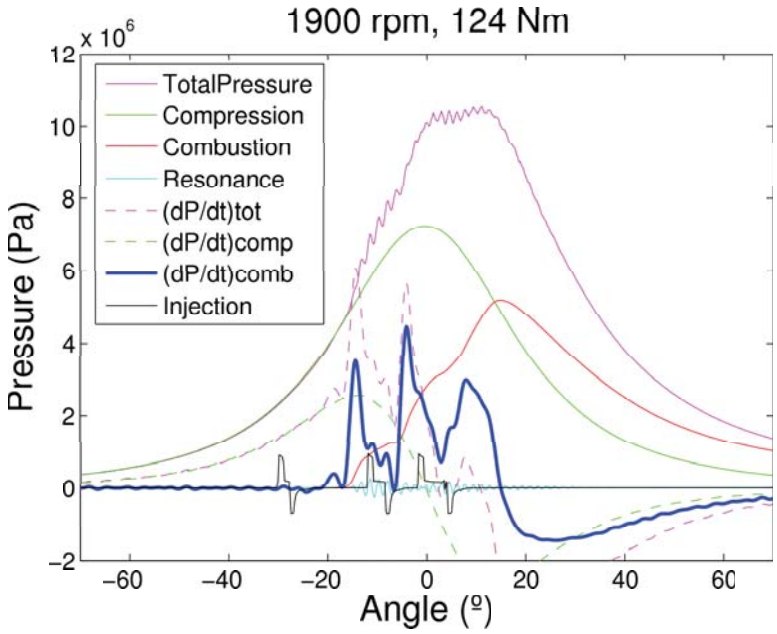

Figure 4.15: Example of the decomposition of in-cylinder pressure with multiple injection strategy

expected pressure derivative peaks, so that a new component can be defined as:

$$I_{3sum} = \frac{n}{n_{\text{idle}}} \left[\frac{(\mathrm{d}p_{\max}/\mathrm{d}t)^{\text{pil2}}_{\text{comb}} + (\mathrm{d}p_{\max}/\mathrm{d}t)^{\text{pil1}}_{\text{comb}} + (\mathrm{d}p_{\max}/\mathrm{d}t)^{\text{main}}_{\text{comb}}}{(\mathrm{d}p_{\max}/\mathrm{d}t)_{\text{ps-mot}}} \right], \qquad (4.7)$$

where:

- $(\mathrm{d}p_{\max}/\mathrm{d}t)^{\text{pil2}}_{\text{comb}}$, $(\mathrm{d}p_{\max}/\mathrm{d}t)^{\text{pil1}}_{\text{comb}}$ and $(\mathrm{d}p_{\max}/\mathrm{d}t)^{\text{main}}_{\text{comb}}$ are the pressure derivative peaks corresponding to the combustion of the two pilots and main injections. These parameters are quantified by the average of the values estimated for the whole recorded cycles and cylinders.

However, the weakness of such a definition is clear in situations where the combustion of the fuel injected in pilot 2 overlaps with that of the fuel injected in pilot 1, as shown in Figure 4.16. In these cases, due to the simultaneous burning of the two pilot injections only two pressure derivative peaks have been produced, as it would be expected with single pilot injection. This situation should be highly probable in two concrete cases: when too advanced pilot injections are used (Figure 4.16 (left)),

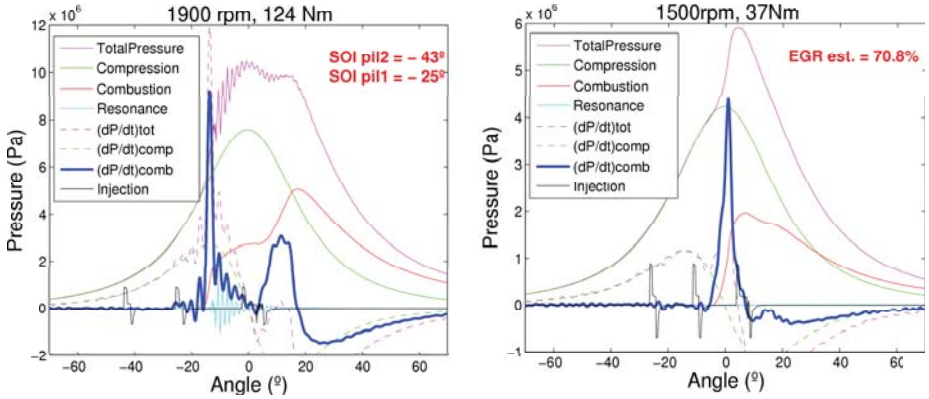

Figure 4.16: Examples of cases where the pilot injections burn at the same time: advanced pilots (left); high EGR rate (rigth)

and with high EGR rate (Figure 4.16 (right)). In both circumstances, a long ignition delay of the fuel injected in Pilot 2 is expected and therefore a premixed combustion, just after Pilot 1 takes place, is provoked.

When this type of combustion occurs, the term $(\mathrm{d}p_{\max}/\mathrm{d}t)^{\mathrm{pil2}}_{\mathrm{comb}}$ in Equation (4.7) can not be determined and the indicator relative to the burning velocity should be calculated as for conventional injection strategies by means of Equation (4.3). Through this procedure, two different trends of correlation between the I_3 component and jury mark are obtained as is shown in Figure 4.17. In this figure, the blue line fits the prediction for multiple injection while the red line shows the trend obtained for pilots combustion overlapped. These results confirm that the pressure derivative component is still adequate to asses the sound quality of combustion noise. Moreover, it has been also verified that the differences between both correlations are not due to differences in the component I_4 associated with the resonance of the combustion chamber. Apart of this, a prediction model with one correlation for each injection strategy seems to be weakly attractive for industrial applications. For this reason, this first approach has been rejected and an alternative adaptation of the pressure derivative component has been searched.

In this way and from the results of the preceding approach, it seems clear that the indicator relative to the burning velocity should be defined by two terms relative to the combustion due to pilot/s and main injections, so that it would be reliable for any conventional or multiple injection strategies. On the other hand, the previous studies with conventional injection strategies have shown that the peak values of the pressure derivative are strongly correlated with the sound quality of combustion noise.

Therefore, a new combustion indicator can be redefined making use of the

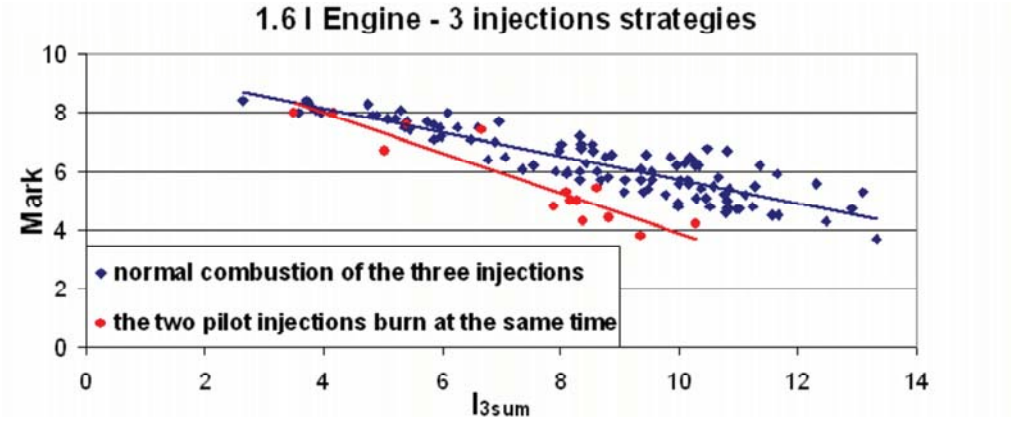

Figure 4.17: Correlation between I_{3sum} and the mark given by the jury

maximum peaks of the pressure derivative of the combustion curve as:

$$I_{3max} = \frac{n}{n_{\text{idle}}} \left[\frac{(\mathrm{d}p_{\max}/\mathrm{d}t)^{\max 1}_{\text{comb}} + (\mathrm{d}p_{\max}/\mathrm{d}t)^{\max 2}_{\text{comb}}}{(\mathrm{d}p_{\max}/\mathrm{d}t)_{\text{ps-mot}}} \right], \tag{4.8}$$

where:

- $(\mathrm{d}p_{\max}/\mathrm{d}t)^{\max 1}_{\text{comb}}$ and $(\mathrm{d}p_{\max}/\mathrm{d}t)^{\max 2}_{\text{comb}}$ are the two maximal pressure derivative peaks of combustion sub-signal. These parameters are quantified by the average of the values estimated for the whole recorded cycles and cylinders.

The structure of the new I_{3max} component is similar to that of I_3, but its numerator contents now the information relative to the maximal peak values of the pressure derivative of combustion curve without taking into account if these are caused by the pilot/s or main injection. In Figure 4.18, the correlation between the new definition of the pressure derivative component I_{3max} (Equation (4.8)) and the sound quality of the combustion noise is shown. This plot evidences a valuable improvement in comparison with the correlation obtained by means of the preceding definition I_{3sum} (Equation (4.7)). Even though an apparent dispersion is observed, the indicator I_{3max} with the two cases of combustion –represented by the blue and red symbols in the graph– seems to have now similar trends.

Furthermore, it has been verified that, taking into account only the points characterized by a "normal" combustion –i.e. when the two pilot injections burn separately– better results are obtained with I_{3max} instead of I_{3sum}. Using the prediction model with a single indicator correlation, the correlation coefficients improved from 88.7 % to 91 % and the mean and maximal errors decreased from 0.42 to 0.38 and from 1.34 to 0.98, respectively. In addition, considering in the model also the

second indicator I_4, better correlation coefficients (from 91.3 % to 92.9 %) as well as lower mean (from 0.38 to 0.34) and maximal errors (from 1.13 to 0.91) were obtained with I_{3max}.

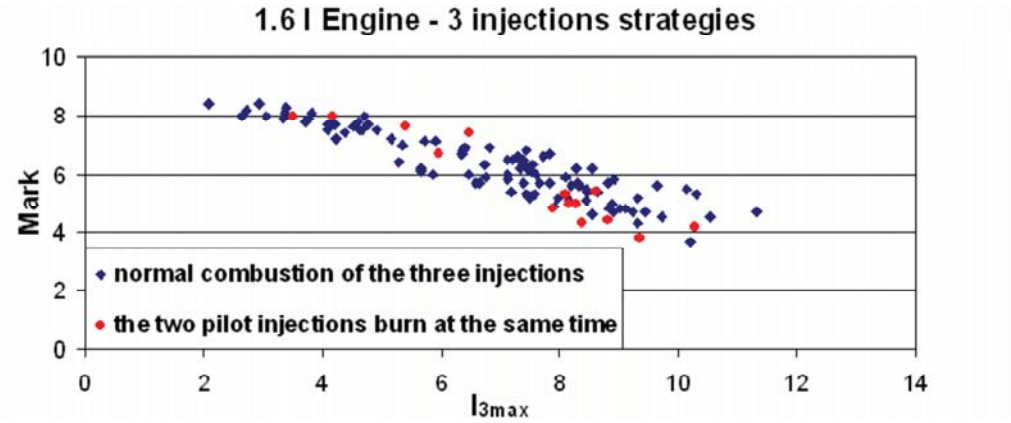

Figure 4.18: Correlation between I_{3max} and the mark given by the jury

4.3.2.1. Results

In the first place of this study only the cases with three injections strategies have been analyzed. Making use of the standard regression analysis, a first model with a single indicator for multiple injection has been obtained.

$$Mark = 10 - c_3 I_{3max} \tag{4.9}$$

Figure 4.19 (left) shows the observed-predicted plot obtained by means of the model in Equation (4.9). A quite good correlation coefficient of 91 % has been obtained with this model, being the mean error lower than 0,5 and the peak error just slightly higher than 1. Moreover, considering the 116 evaluated tests, 66 % of them have an error lower than 0,5 and the error is lower than 1 in the 97 % of cases.

Although such encouraging results have been obtained with this model, taking advantage of the outcomes of previous studies, the contribution of the I_4 component associated with the resonance of the combustion chamber has been also evaluated. With this purpose, a further regression equation including also the I_4 indicator has been considered:

$$Mark = 10 - c_3 I_{3max} - c_4 I_4, \tag{4.10}$$

The observed-predicted plot obtained with this model is shown in Figure 4.19 (right). As expected, this graph shows a better collapse of the measurements on the fit line with respect to the single component model as in Equation (4.9). Effectively, the

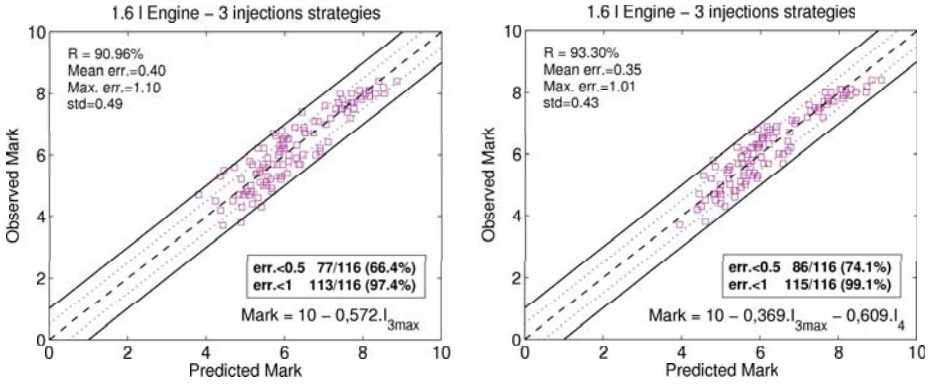

Figure 4.19: Mark noise estimation with the proposed approach 1.6 l Engine: single component (left) and two components (right) correlations.

correlation coefficient has been improved now up to 93 %, being the mean and peak errors, as well as the standard deviation, reduced. The rate of tests where the error has been lower than 0,5 was substantially increased up to 74 % and now almost all tests have an error lower than 1.

These results can be regarded as very good, however it has to be kept in mind that these have been obtained only for the case of three injections sets. In this case the noise variations have been obtained only by varying the injection parameters one by one, consequently, the variation range of the marks assigned by the jury is smaller than those obtained in the former studies where all injection settings were varied at once. Therefore, in this case a limited dispersion of the results was to be expected.

Since in the proposed model, the pressure derivative component I_{3max} does not take care anymore of which injection causes the peak values of the derivative of the combustion curve, it appears now interesting to evaluate also its feasibility on conventional injection strategies. The main goal of this task is to dispose of a unique simpler model that responds to any type of combustion, so that it would be more practical and suitable for industrial application.

Due to the different definitions of the components I_3 and I_{3max}, with conventional injection strategies, there are particular conditions in which these indicators have different values. These particular conditions are characterized by combustion processes similar to that analyzed in Figure 4.20. In this figure, the two highest peaks of the pressure derivative of the combustion sub-signal (solid red line) are caused by the main injection, being smaller the peak value relative to the pilot injection. In this case, since I_{3max} is calculated with the two highest peaks of the whole combustion curve while I_3 is estimated with the peak relative to the pilot and the highest peak associated with the main injection, I_{3max} is bigger than I_3. These results have been checked through the estimation of the heat release (HR) and the rate of heat release (RoHR) in the combustion process performed by the software CALMEC. The plots

of the estimated HR and RoHR are also shown in Figure 4.20 by the dashed green and solid green lines, respectively.

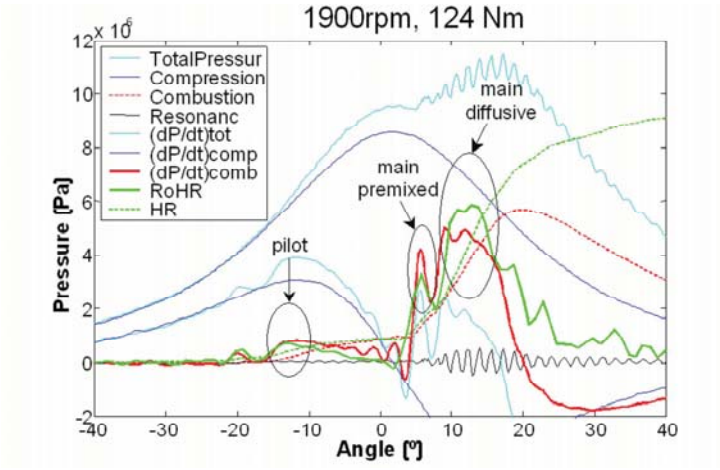

Figure 4.20: Example of in-cylinder pressure decomposition with conventional injection strategy in which the highest pressure derivative peaks are out of pilot injection

Like in the pressure derivative of the combustion curve, on the one hand, the RoHR curve shows two clear peaks relative to the combustion of the main injection, and on the other hand, the rate of burning of the fuel injected in pilot is almost negligible. Therefore, the first peak due to the main injection could be caused by a premixed combustion or by a reach diffusive combustion phase while the second peak should be associated with the diffusive combustion of the rest of fuel injected during main.

Through the in-cylinder pressure analysis of all measurements performed on the 1.6 l engine with conventional (pilot + main) injection settings, similar situations as that shown in Figure 4.20 have been detected in 33 out of the 162 evaluated tests. In all these tests, the engine was operated in medium and high load conditions, in which the fuel mass injected in main has been high enough to cause the two combustion phases discussed above.

Table 4.8 shows the statistics relative to the results obtained with the model as in Equation (4.9), using I_{3max} instead of I_3. Table 4.9 shows the same statistics obtained when I_4 component is also included in the model. Also in this case, the use of the indicator related to the resonance energy improves considerably the estimation of the noise mark. Both tables show results similar but slightly inferior to those presented in Tables 4.5 and 4.6, respectively, obtained using the preliminar model with I_3. This

Engine	c_3	ϵ_{mean}	ϵ_{max}	σ	**R(%)**
1.6 l	0.492	0.62	2.13	0.77	90

Table 4.8: Statistical parameters of estimated noise mark with one component correlation as in Equation (4.9), conventional injections strategies

Engine	c_3	c_4	ϵ_{mean}	ϵ_{max}	σ	**R(%)**
1.6 l	0.299	0.784	0.50	1.54	0.61	94

Table 4.9: Statistical parameters of estimated noise mark with two-component correlations as in Equation (4.10), conventional injections strategies

small degradation of the results with the new model is widely compensated by the practical advantage of using the same definition with both conventional and multiple injections strategies.

Furthermore, it has to be highlighted that, in the practice it is improbable to find a situation like that described in Figure 4.20. In fact, the main task of pilot injection is to reduce the ignition delay of the main injection in order to limit the quantity of fuel that burns in a premixed way. Consequently, in most of the practical situations, the maximal combustion velocity obtained with the pilot injection is comparable to that proceeding by the combustion of the main injection, and the values of I_{3max} and I_3 coincide.

Taking advantage of the fact that the I_{3max} indicator is not sensitive on the features of the combustion induced by the injection strategy, the proposed model based on Equations (4.9) and (4.10) has been calculated taking into account all the measures performed on the 1.6 l engine with both conventional and multiple injection strategies. The aim is to check the feasibility of the model to respond to any injection strategy used.

Figures 4.21 (left) and (right) show the observed-predicted plots obtained with these models, respectively. As commented before, it can be observed that a wider range of noise variation has been produced in the tests with conventional injection in comparison with those obtained with multiple injection strategy. The statistical parameters are resumed in Tables 4.10 and 4.11. With both single and two components models, high correlation coefficients have been obtained, together with limited mean and maximal absolute errors and standard deviations.

The feasibility of the model with a single component correlation to asses the combustion noise at any injection strategy has been verified. Furthermore, also in this case, the contribution of I_4 seems to improve considerably the statistics of the model. In fact, the model according to Equation (4.10) allowed a considerable increase of the percentage of points with absolute errors inferior to 0.5 and 1. With two components correlation the mark prediction with an absolute error lower than 0.5 in passed from 52.9 % (obtained with a single component model) to 60.1 % of the tests, and the percentage of error lower than 1 increased from 83.1 % to 93.2 %.

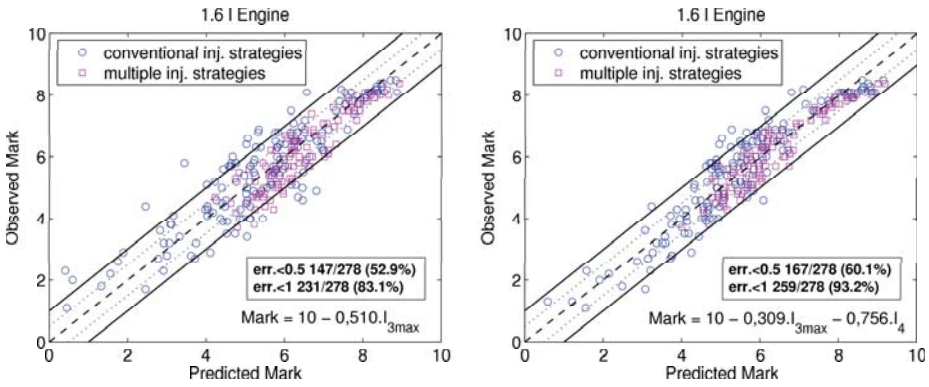

Figure 4.21: Mark noise estimation with the proposed approach 1.6 l Engine: single component (left) and two components (right) correlations.

Engine	c_3	ϵ_{mean}	ϵ_{max}	σ	**R(%)**
1.6 l	0.510	0.56	2.35	0.70	89

Table 4.10: Statistical parameters of estimated noise mark with Equation(4.9) $Mark = 10 - c_3 I_{3max}$, conventional and multiple injections strategies

Summarizing, the pressure derivative indicator (I_3) of the preliminar predicting model has been updated with the aim to respond to multiple injection strategies. The updated component I_{3max} makes use of the two highest levels of the pressure derivative of the combustion sub-signal, ignoring if these are caused by pilot/s or main injections. Even though, in the case of conventional injections settings (pilot + main), the statistical parameters obtained with the proposed indicator I_{3max} have scarcely worsen, if compared with those obtained with the former model. There is no doubt that this new diagnostic algorithm is more advantageous mainly from the point of view of its possible industrial application. Otherwise dedicated models should be required for different combustion features, the procedure becoming then too complex.

Also with the 1.6 l engine, the contribution of the indicator I_4 –relative to the combustion chamber resonance– to the model accuracy has been evidenced with both injection strategies used. These results confirm that the defined indicators contain complementary information, so that it is better to consider both components.

Engine	c_3	c_4	ϵ_{mean}	ϵ_{max}	σ	**R(%)**
1.6 l	0.309	0.756	0.46	1.63	0.57	94

Table 4.11: Statistical parameters of estimated noise mark with Equation(4.10) $Mark = 10 - c_3 I_{3max} - c_4 I_4$, conventional and multiple injections strategies

However, as commented before, the influence of the resonance indicator seems to be dependent on the engine family, but no clear tendency has been evidenced. This justifies the necessity of a further analysis focused on the sensitivity of the in-cylinder resonance and of the noise quality to the bowl geometry.

Section 4.5 is dedicated to the assessment of the contribution of the bowl geometry on the resonance generation and on the noise quality through the evaluation of the indicator I_4. The reliability of the updated model discussed in this section will also be checked on a different combustion system (bowl) using both conventional and multiple injection strategies.

4.4. Noise quality sensitivity to combustion parameters

Taking advantage of the structure of the experimental plans for multiple injection study – defined considering the variation of just one combustion parameter while the rest are kept constant – the sensitivity of combustion noise quality to injection-combustion parameters can be studied. With this purpose, plots of the marks given by the jury against the combustion parameter varied at the nine tested operation conditions were analyzed. So that, on one hand, the noise range obtained in the study is checked and on the other, some trends of noise quality evolution against combustion parameters can be evidenced and used as guidelines for future developments of combustion settings.

In agreement with engine manufacturer, the factors varied have been:

- Rail pressure
- Fuel mass injected during pilot 2 (Q_{pil2})
- Fuel mass injected during pilot 1 (Q_{pil1})
- SOI of pilot 2 and SOI of pilot 1 (the difference between both SOI has been kept constant)
- EGR rate

The variation ranges of these parameters are not unlimited but their choice comes from the best balance between two opposite requirements: on the one hand, as wider as possible noise variation is required but, on the other hand, the engine should remain stable and the torque as constant as possible. Therefore, a preliminary experimental phase was necessary in order to establish the limits of these ranges. In the previous works (with two injection strategies) the total injected mass was kept constant for a given operating condition. Therefore, the fuel mass injected at the main, obtained by subtracting the pilot quantity from the total one, could not be freely varied. Due to this fact, in every experimental plan, where engine speed and total injection quantity were kept constant, significant torque variations have been obtained and a tolerance

range of +/- 20 % from the nominal torque has been accepted. Since noise is sensitive to torque variations, risks in the study could be introduced with this procedure. To mitigate this problem in this study, the mass of the main injection has been set in order to measure similar engine torque in every experimental plan. To do this, after all parameters were set according to the experimental matrix, the variable that controls the pedal position was varied until the measured torque was similar to the base line condition.

Q pilot 2 (mg/str)	Q pilot 1 (mg/str)	Q main (mg/str)	SOI pilot 2 (° - TDC)	SOI pilot 1 (° - TDC)	SOI main (° - TDC)	Pressure Rail (bar)	EGR (%)	Torque (Nm)
1,98	1,98	17,08	30	12	2	**750**	66	124
1,98	1,98	16,52	30	12	2	**1050**	66	124,2
1,98	1,98	17,74	30	12	2	**1350**	66	124,2
3,00	1,77	16,27	30	12	2	1050	66	124,4
4,00	1,77	15,57	30	12	2	1050	66	124,3
1,77	**3,00**	15,25	30	12	2	1050	66	123,7
1,77	**4,00**	13,74	30	12	2	1050	66	123,7
1,77	**5,00**	11,87	30	12	2	1050	66	124,4
1,77	1,77	20,18	**38**	**20**	2	1050	66	123,9
1,77	1,77	20,17	**43**	**25**	2	1050	66	124,6
1,77	1,77	19,34	30	12	2	1050	**47**	123,7
1,77	1,77	16,56	30	12	2	1050	**88**	124
1,77	1,77	16,76	30	12	2	1050	66	123,9
						σ Torque		0,2976

Figure 4.22: Example of experimental plan for the study of multiple injection, 1900 rpm 124 Nm

Figure 4.22 shows an example (1900 rpm and 124 Nm) of experimental plan defined for each one the 9 engine operating conditions listed in Section 3.5. Bold letters show the variations with respect to the base line of each parameter. The standard deviation of the torque variation at each operating condition is also indicated at the last row of each table, in the example of Figure 4.22 it resulted lower than 0.3. However, even in the worst case, the torque variation was less than 2,5 %, which is advantageous for the study.

For the noise quality quotation, every experimental plan has been individually evaluated, the methodology used was the same as described in Section 3.6. Furthermore in this case, with the aim to be consistent with the quotation at the previous tests (i.e. conventional injection study described in Section 4.2.3), three additional noises (the best, the 7 and the worst) from the previous study have been included in the noise sequence to be currently evaluated at each experimental plan (defined by the engine operating condition). In this way, it is expected that all noises were

qualified as far as possible with the same metrics, so that one can be confident that a mark is always almost the same at any engine running condition or operation strategy. Every experimental plan has been composed of a maximum of 16 or 17 noises to avoid fatigue of the jury caused by long tests.

4.4.1. Rail pressure

To study the influence of the rail pressure, various levels have been considered. Normally, in the base line strategy the fuel mass injected in the pilot injections (Q_{pil}) are the minimal quantities possible to be injected at the given rail pressure level. When the rail pressure increases the minimal fuel mass should also increase in order to ensure an adequate operation of the injectors. Consequently, when the sensitivity of combustion noise to rail pressure variations is studied, Q_{pil} levels slightly higher than in base line strategy have been considered in the experimental plans. In this way, the proper operation of the injectors was ensured and the contribution of just the analyzed parameter can be quantified.

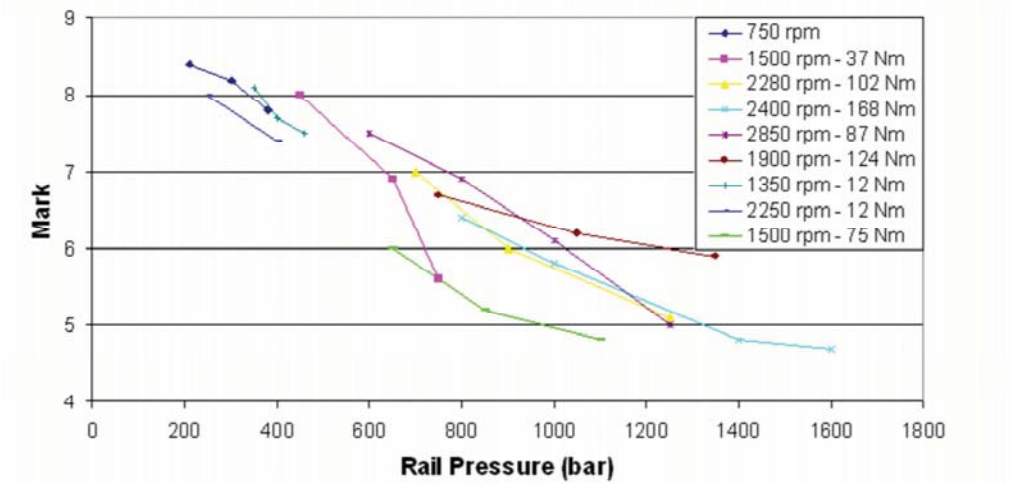

Figure 4.23: Noise sensitivity to rail pressure

Figure 4.23 shows the sensitivity of the noise to the rail pressure level. Like in the previous studies and as was expected, the rail pressure confirms to be a significant parameter on the sound quality of the combustion noise. In all running conditions, it seems clear that the higher is the rail pressure level the lower is the noise quality. This trend can be explained by the fact that a higher rail pressure improves fuel evaporation and consequently a faster combustion which provokes a higher pressure

rate of change is produced. In the opposite way, with low rail pressure levels smooth combustion is expected and so, less unpleasant combustion noise is radiated.

4.4.2. Pilot injection quantities

The noise quality sensitivity to the fuel mass quantities injected during pilots has been also analyzed. Figure 4.24 (a) presents the results obtained varying the first pilot injection (pilot 2 according to our nomenclature). The plot shows a tendency similar to that observed when the rail pressure was varied. Noise quality deteriorates in proportion to the increase of injected fuel mass. In such case, more fuel burns in a premixed combustion and therefore causes more abrupt pressure rise. The quality of the noise is then worse.

Focusing now on the influence of the fuel mass quantity injected at the second pilot (Q_{pil1}) on the combustion noise, Figure 4.24 (b) doesn't show a monotonic trend as in the preceding cases. Effectively, only at low load conditions (750 rpm, 1350 rpm 12 Nm, 1500 rpm 37 Nm and 2250 rpm 12 Nm) a decreasing monotonic trend of the noise mark with the Q_{pil1} rise is observed. In the points with medium and high loads (1500 rpm 75 Nm, 1900 rpm 124 Nm, 2280 rpm 102 Nm, 2400 rpm 168 Nm and 2850 rpm 87 Nm) an increment of the injected quantity Q_{pil1} doesn't cause an apparent degradation of the noise quality.

A deeper analysis of the sensitivity of the noise to Q_{pil} in both injections can be carried out focusing on the pressure derivative of the combustion signal obtained by means of the in-cylinder pressure decomposition algorithm. In Figures 4.25 and 4.26 the pressure derivative peak values relative to each pilot injection, $(dp_{max}/dt)^{pil2}_{comb}$ and $(dp_{max}/dt)^{pil1}_{comb}$, are plotted against the fuel mass injected in milligrams per cylinder per cycle at low and at medium and high loads respectively. In these figures, it can be clearly observed the high sensitivity of the pressure derivative peak to the injected quantity of the first pilot Q_{pil2} (blue lines), at any operating condition.

Figure 4.25 shows that, at low load operating conditions, similar conclusions can be stated for Q_{pil1} (red lines). Moreover, the proportionality coefficient (curve slope) in the case of Q_{pil1} is smaller than that observed with pilot 2. However, Figure 4.26 shows that at medium and high load conditions, the slope of the curve suffers a considerable decrease in proportion to Q_{pil1} rise. In such conditions, it seems that the pressure derivative peak is scarcely sensitive to the Q_{pil1} when it increases excessively (more than 3-4 mg/cc).

To go further in the analysis with the aim to have a physical explanation of the trends observed in the Figures 4.25 and 4.26, the attention has been focused on the pressure derivative evolution of the combustion curves through the decomposition of the in-cylinder pressure signals. Figure 4.27 shows an example of decomposition of a high load working condition (2400 rpm, 168 Nm), comparing the base line strategy (Figure 4.27 (a)) with two different strategies: high Q_{pil2} (Figure 4.27 (b)) and high Q_{pil1} (Figure 4.27 (c)).

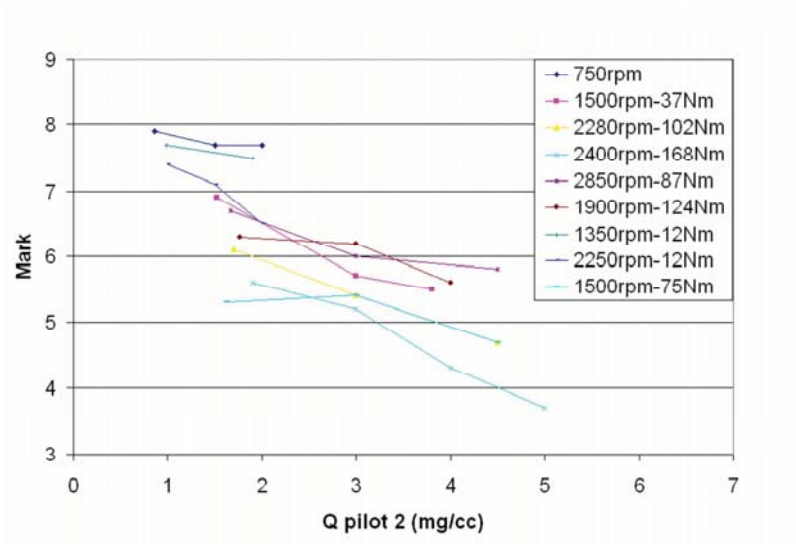

(a)

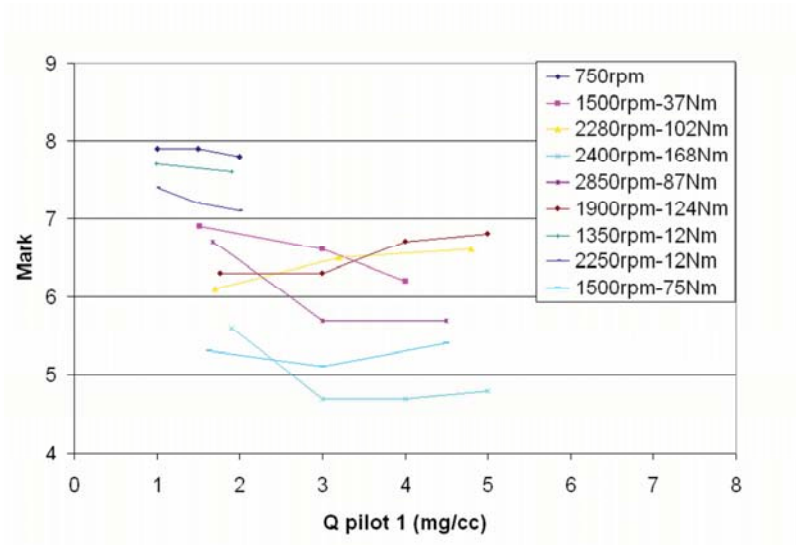

(b)

Figure 4.24: Noise quality sensitivity to fuel mass quantity: Q_{pil2} (a), Q_{pil1} (b)

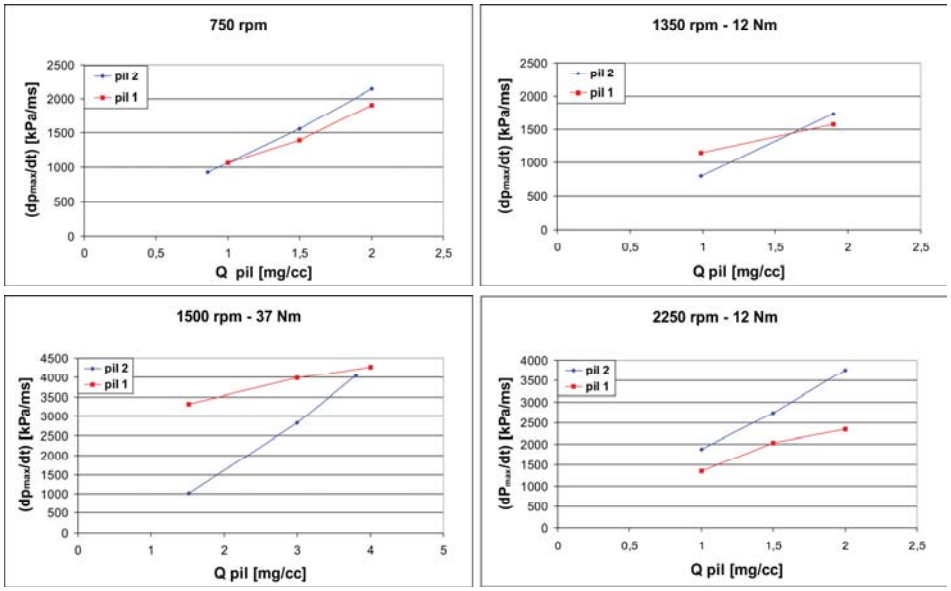

Figure 4.25: Sensitivity of the pressure derivative peak of combustion sub-signal to Q_{pil}, low load conditions

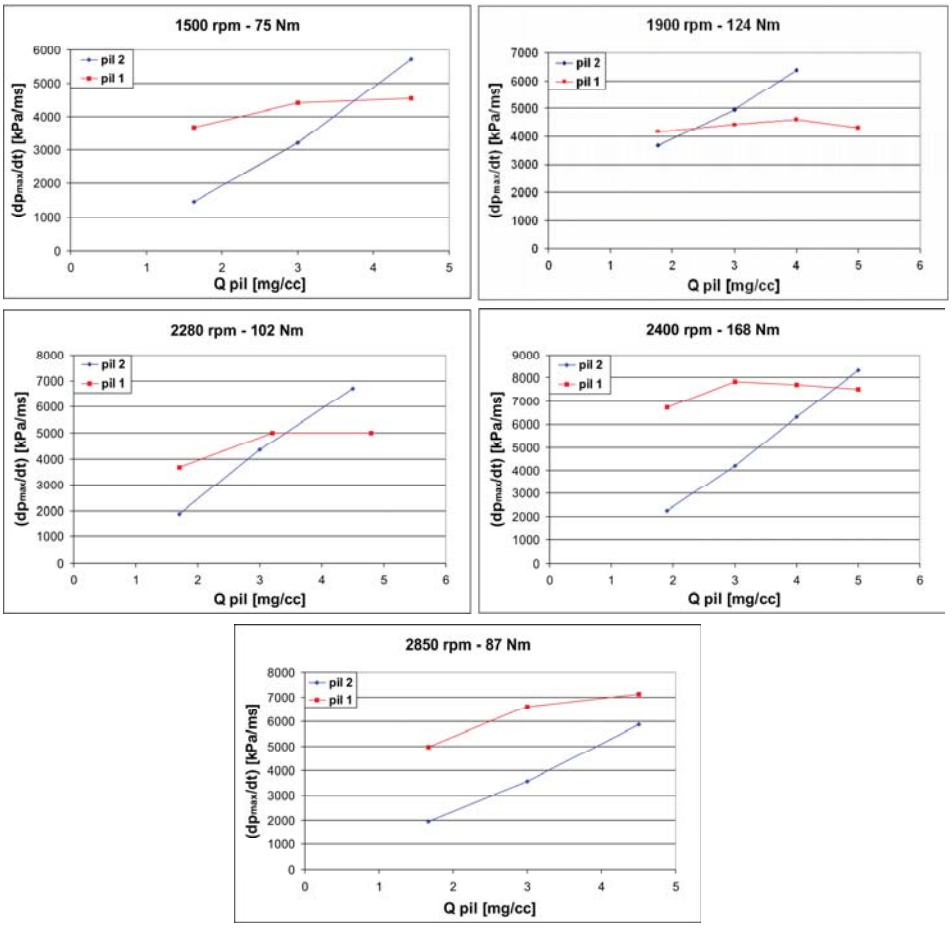

Figure 4.26: Sensitivity of the pressure derivative peak of combustion sub-signal to Q_{pil}, medium and high load conditions

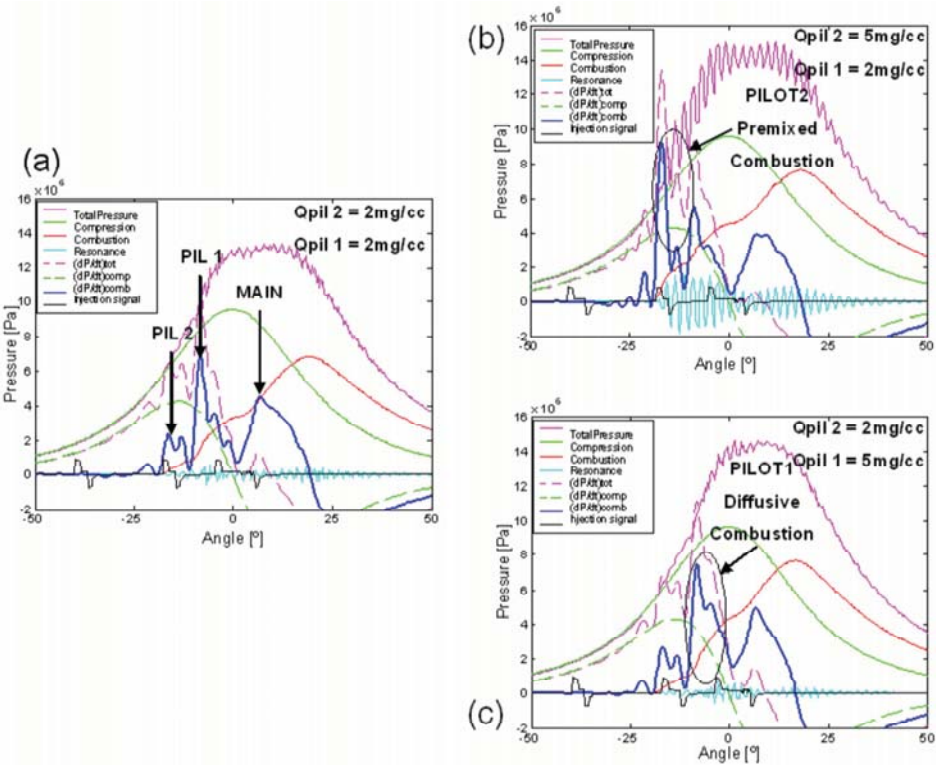

Figure 4.27: Q_{pil} analysis by means of in cylinder pressure signal decomposition

From the analysis of the base line strategy (Figure 4.27 (a)) it can be observed that the pressure derivative of the combustion curve (blue line) relative to the Q_{pil1} shows two combustion phases clearly differentiated: a first phase with quick fuel burning followed by a second slower phase. Despite the first phase seems to be a premixed combustion, it should be a reach diffusive combustion since Q_{pil1} is injected during the combustion of Q_{pil2}.

With respect to an increased Q_{pil2}, as expected a more abrupt rate of combustion pressure is observed (blue line in Figure 4.27(b)). This trend confirms that the quantity of the fuel mass burning in the first premixed combustion is controlled by the Q_{pil2}. So a direct relationship between the Q_{pil2} and the peak of the rate of combustion pressure sub-signal is given.

The comparison of the blue lines in Figures 4.27 (a) and 4.27 (c) shows that only a weak rise of the pressure derivative peak in the first combustion phase is induced when Q_{pil1} is increased. Unlike in this combustion phase, a higher Q_{pil1} seems to increase the peak of the pressure derivative of the combustion curve in the

second phase of the combustion due to this pilot (Figure 4.27 (c)). The characteristic shape of the pressure derivative curve turns wider and almost equal to that of the combustion due to the main injection.

This analysis seems to indicate that an increment of Q_{pil2} affects mainly the premixed phase of the combustion, causing an abrupt rise of the pressure and therefore the degradation of the noise should be expected. The second injection (pilot 1) takes place when the first one is already burning, so that the combustion delay is considerably shorter with respect to the pilot 2 and a small fraction of the fuel burns quickly in the first phase. For this reason, any increase of Q_{pil1} mainly contributes on the diffusive phase of the combustion that normally does not have any strong influence on the noise quality.

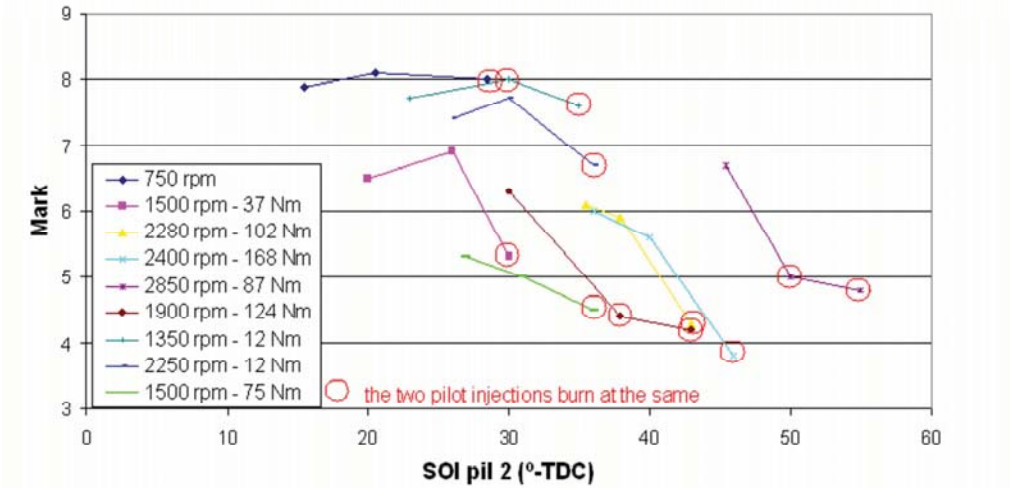

Figure 4.28: Sensitivity of noise quality to SOI_{pil2}

4.4.3. Start of injection

Concerning the effect of the start of injection (SOI), Figure 4.28 shows the noise mark variation detected when the SOI of the pilot injections was modified. Since in the experimental plans the separation between SOI_{pil2} and SOI_{pil1} was kept constant, only the results relative to SOI_{pil2} have been presented here. Thus, the analysis for SOI_{pil1} would be equivalent, resulting in a figure identical to 4.28 being the unique difference on the crank angle range.

Even though plots in Figure 4.28 do not show any clear tendency, it is interesting to note that in most of the cases with an advanced pilot injection (indicated

with a red circle) an important deterioration of the noise quality is produced. This behavior seems to be due to the fact that, at too advanced pilot injections, the combustion of both injections takes place at the same time. This fact is confirmed by the decomposition of the in-cylinder pressure signals as it has been shown in Figure 4.16. This abrupt combustion originates a high increase of the pressure rate and in consequence a sharper noise. This situation is more unlikely in engine operating conditions with very low loads, which are characterized by small fuel mass rates injected during pilots.

4.4.4. Exhaust Gas Recirculation

Since a CO_2 probe for Exhaust Gas Recirculation (EGR) mass flow measurement was not available in the test facility, an alternative procedure to estimate the EGR rate has been employed in this study in order to get a more controlled variation of the EGR. This procedure is based on the assumption that the EGR mass flow rate can be estimated by subtracting the mass flow rate of air intake with EGR (valve open) to the intake mass flow when the EGR valve is completely closed. Then, the EGR percentages shown in the figures below have been determined by the ratio between the estimated EGR mass flow and the intake mass flow without EGR.

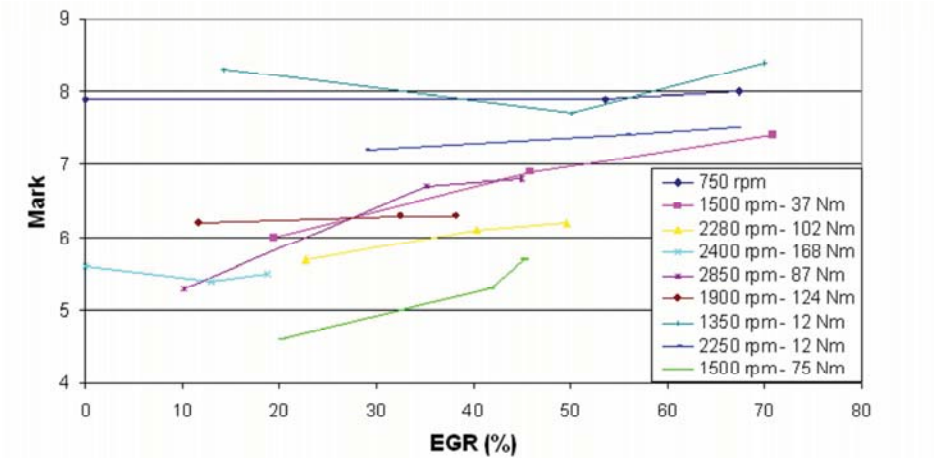

Figure 4.29: Sensitivity of noise quality to EGR

As can be observed in Figure 4.29 the sensitivity of the combustion noise to EGR rate is hard to be analyzed. In fact, the plots show that at low and high loads the mark variation is of the same order than the uncertainty of the jury evaluation, and therefore conclusions are difficult to extract. However at medium loads the quality of the noise seems to improve in proportion of the EGR rate increase, due to the softer combustion produced in such conditions.

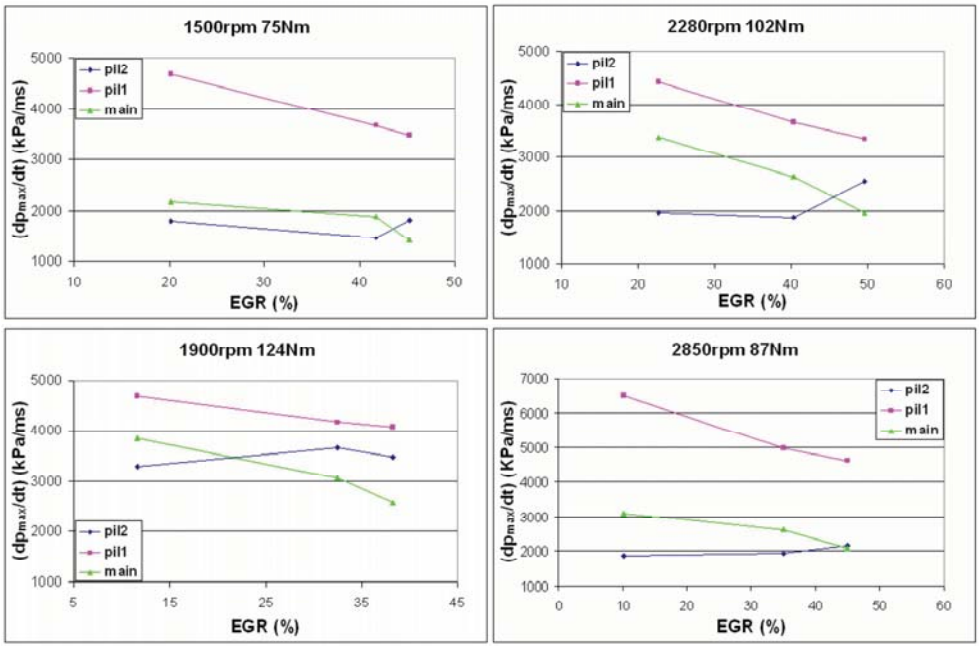

Figure 4.30: Sensitivity of the pressure derivative peak of combustion sub-signals to EGR rate at medium load

Effectively, Figure 4.30 shows plots of the variation of the pressure derivative peaks associated with the fuel burning phases of the combustion process, caused by pilots 2 and 1 and main injections at medium load conditions. The figure shows that in these cases the combustion of the fuel injected in Pilot 1 is the quickest, indeed the pressure derivative peaks relative to the Pilot 1 (plotted in magenta) are the highest.

Furthermore, in Figure 4.30 a reduction of the peak values relative to the Pilot 1 injection and to the main injection (plotted in green) in proportion to the EGR rate increase is observed, while the peak value of the Pilot 2 injection (plotted in blue) remains almost constant.

These observations confirm that at medium load conditions the EGR has a strong effect on the engine noise quality since the combustion of the Pilot 1 is the quickest and its velocity peak is strongly affected by the EGR rate.

4.5. Sensitivity of resonance energy to bowl geometry

In this section a theoretical-experimental analysis of the in-cylinder pressure resonance will be presented. The theoretical analysis is based on CFD calculations, the experiments have been conducted on the 1.6 l engine using a different shape of the piston bowls. The goal here is to investigate whether this characteristic phenomenon of the Diesel combustion had some influence on the quality of the combustion noise. Furthermore, a better understanding of the effect of the piston bowl geometry on the energy of resonance and, in turn, on the noise quality predicting model will be given.

Figure 4.31 shows the geometry of the standard and modified piston bowls, respectively Bowl A and Bowl B. The main dimensions of both geometries are indicted in millimeters in the figure. The design of this new bowl has been decided by the engine manufacturer taking care that the compression ratio was the same as for the standard engine, the intention was to get an increase of the in-cylinder resonance phenomenon without influencing the engine performance.

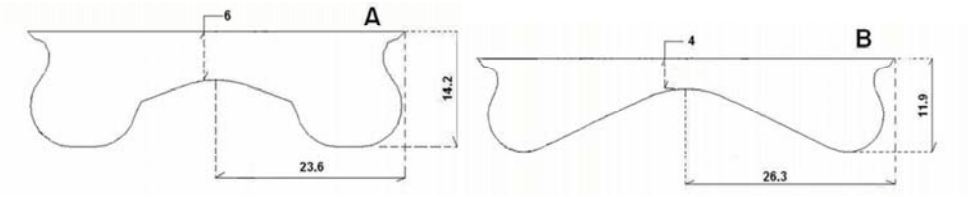

Figure 4.31: Schematic sections of the standard piston bowl A and of the modified piston bowl B

A preliminary study has been conducted using a three-dimensional CFD software, for analyzing the influence of the piston shape on the resonance generation process in order to theoretically estimate the expected increase of the energy of the resonance sub-signal and thus, the quality mark variation obtained with the predicting model.

4.5.1. Preliminary CFD calculations

Some details of the CFD approach used in this study –three-dimensional meshing, temporal discretization, simulation of the auto-ignition phenomenon– have been already described in Section 3.5.3. Here the outcomes obtained from the three-dimensional calculations will be presented. For the present study, results are presented in terms of a non-dimensional energy of resonance and the response in frequency obtained with a standard Fourier analysis. The non-dimensional energy of resonance (ER) was calculated as:

$$ER = \frac{E_{res}}{E_e} = \frac{\int \mid p_{res}(t) \mid^2 \mathrm{d}t}{E_e} \tag{4.11}$$

where E_{res} is the energy of resonance used in the definition of the resonance indicator I_4, with p_{res} the pressure of resonance, and E_e is the energy of the initial excitation pulse defined as:

$$E_e = \Delta p^2 \Delta t \frac{V_{ref}}{V_e} \tag{4.12}$$

where Δp and Δt are the amplitude and the duration of the excitation and V_{ref} and V_e refer to the volume of the reference and of the actual excitation pulse, respectively. This non-dimensionalization of the excitation energy by the volume is necessary for comparison purposes, because numerically the excitation pulse is applied in a small volume, which may vary depending on the mesh size or the excitation size. In most cases, V_{ref}/V_e is 1 or very close. The computations were stopped when there was a clear indication that the pressure waves had reached a periodic steady state.

4.5.1.1. Experimental validation of the CFD approach

Firstly, the CFD calculation has been validated by comparing its results with those of an experimental measurement. The pressure signal of a cylinder equipped with the standard piston bowl has been considered and a working condition of 1500 rpm and 37 Nm of torque characterized by a sharp resonance has been analyzed using a FFT transform.

Figure 4.32 presents a comparison between the frequency responses of the experimental measurement and the CFD calculation of Bowl A. The CFD result, obtained by a monitor located at the same position as the pressure sensor, shows three peaks of resonance in the frequency range of interest, corresponding to the first three oscillation modes. The experimental measurements only show two peaks of resonance, and it seems that the second mode is not detected. This does not represent a particular problem, since –as it was already commended in Section 2.4.3– with automotive engines, only the first circumferential mode has to be taken into account, higher modes are generally negligible and outside the audible frequency range. Furthermore as it has been evidenced in Section 2.4.3.2, the amplitude of the resonance peaks is strongly influenced by the position of the measurement point with respect to the ignition site. Consequently peak amplitude detected by the pressure transducer is expected to vary cycle-to-cycle and cylinder-to-cylinder.

Even though, in this case, the CFD calculation clearly over-predicts the amplitude of the resonance, the frequency of the first circumferential mode is approximately well captured. This can be regarded as a good result, considering the very simplistic model adopted for the excitation caused by the auto-ignition and the fact that in the calculation the movement of the piston was not taken into account.

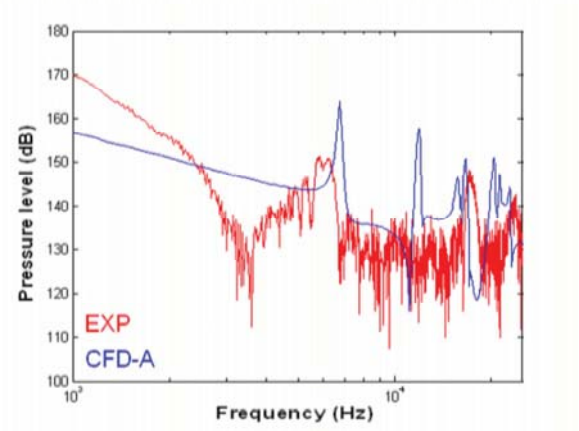

Figure 4.32: Comparison of frequency response between an experimental measurement (EXP) at 1500 rpm, 37 Nm and the CFD calculation for Bowl A (CFD-A)

Hence, from this preliminary analysis, it has been concluded that the CFD calculation may only be used qualitatively, since it is capable of adequately predict only the resonance frequencies but not the actual quantitative values of the resonance energy.

4.5.1.2. Noise quality sensitivity to bowl geometry variation through CFD calculation

Keeping in mind the conclusions from the previous section, in order to compare the results with those obtained with the standard bowl A, a calculation with the new combustion chamber (Bowl B) has been also performed. With the information given by the monitors, it is possible to appreciate the global influence of the bowl geometry on the resonance. Figure 4.33 shows the frequency response obtained at a point located close to the wall and 3 mm below the excitation plane for both combustion chambers. Consistently with the modal theory, the comparison clearly shows that the frequency of the resonance peaks decreases when the bowl characteristic dimension is larger, which corresponds to the maximum diameter in the case of the Bowl B.

A representation of the pressure level in the whole domain is given by the non-dimensional energy of resonance ER at each monitor located at position (R,θ,l). Figure 4.34 illustrates the value of ER calculated for different depths in the plane 0^o (corresponding to the symmetry plane). In both geometries, the non-dimensional energy of resonance increases with the radial distance of the monitor location due to

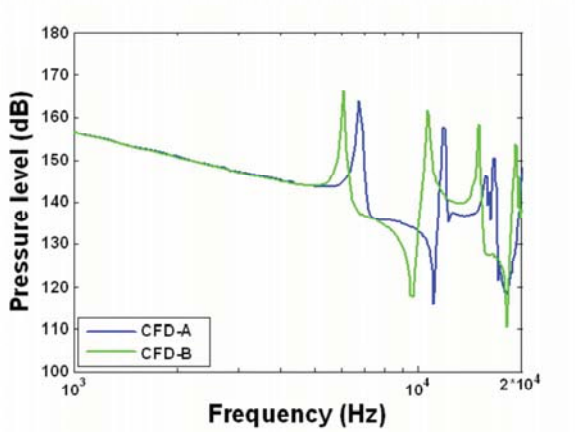

Figure 4.33: CFD results: influence of the bowl geometry on the frequency response

the pressure waves bouncing off the walls, and the minimum values correspond to the monitors located in the central part of the bowl.

The levels of ER are different in both geometries, as can be appreciated in Figure 4.35, where the maximum levels and the level at sensor position are shown for both geometries. The maximum ER of Bowl B is considerably higher than that of Bowl (A). It is also worth noting that the location of the sensor may be relevant for the estimation of the energy of resonance. Indeed, Figure 4.35 clearly shows that the monitor located in the same position as the experimental sensor does not detect the maximum value of ER. The measurement could thus underestimate the actual level of energy of resonance.

According to these calculations, at the sensor monitor:

$$\frac{(ER_B)_{sensor}}{(ER_A)_{sensor}} = 1{,}248 \tag{4.13}$$

and, at the wall monitor (condition of maximal resonance energy), will be:

$$\frac{(ER_B)_{max}}{(ER_A)_{max}} = 2{,}164 \tag{4.14}$$

Globally the Bowl B presents a higher energy of resonance with respect to Bowl A. However, it is more relevant to analyze whether this variation of the energy of resonance level is important in terms of the subjective perception of the noise. Using these results an estimation of the influence of the piston bowl change on the resonance

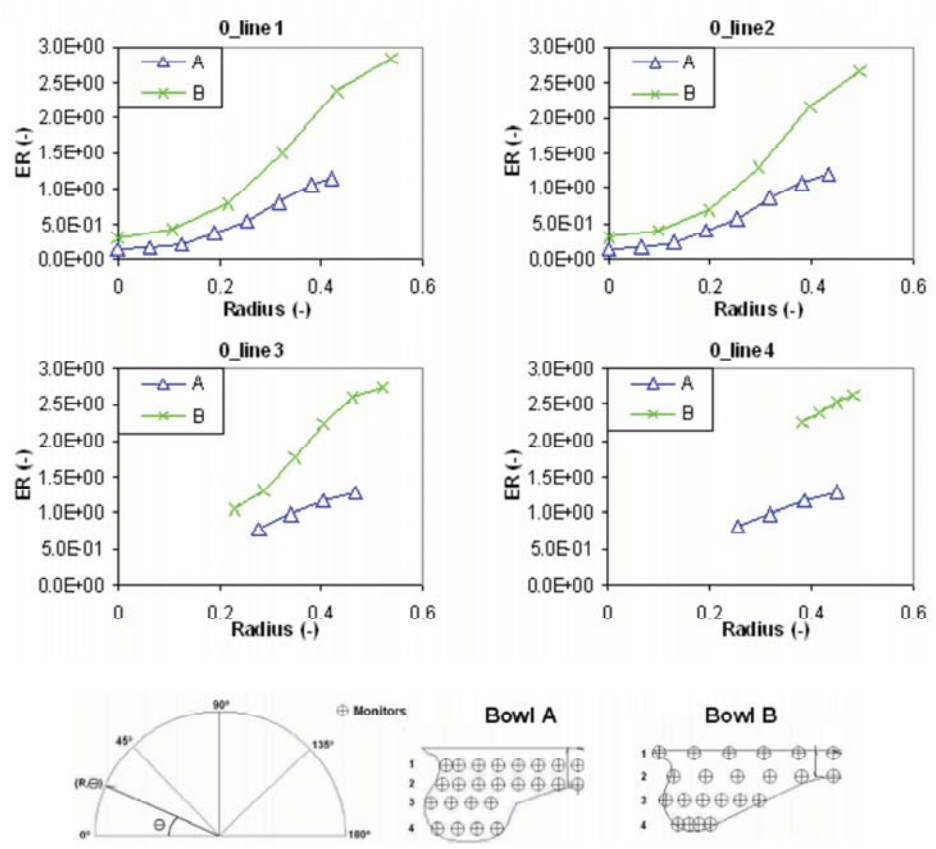

Figure 4.34: ER in plane 0^o at different depths, in bowl geometries A and B

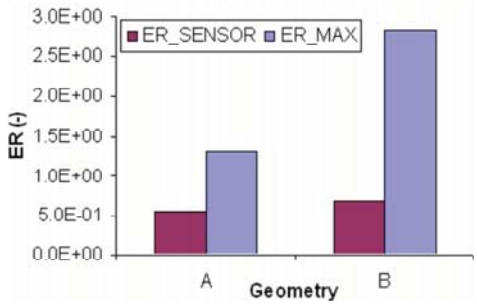

Figure 4.35: Comparison between energy of resonance at sensor location and maximum detected in the standard bowl A and modified bowl B

indicator I_4 can be obtained. Furthermore, by the definition of the prediction model with two components correlation, also the variation of the mark characteristic of the noise quality can be estimated.

Respectively, from the increments of the energy of resonance of Equations (4.13) and (4.14), the variation of the combustion indicator I_4 can be calculated, at the sensor monitor results:

$$(I_{4B})_{sensor} - (I_{4A})_{sensor} = 0{,}096 \tag{4.15}$$

and, at the wall monitor, it will be:

$$(I_{4B})_{max} - (I_{4A})_{max} = 0{,}334 \tag{4.16}$$

Using the definition of the noise quality prediction model with both combustion indicators, Equation (4.10), the influence of this variations on the mark representing the noise quality can be estimated. Using the I_4 increment calculated at the sensor monitor (4.15), it would result:

$$(\Delta Mark)_{sensor} \approx 0{,}076 \tag{4.17}$$

and, at the wall monitor (4.16), it would be:

$$(\Delta Mark)_{max} \approx 0{,}265 \tag{4.18}$$

According to these estimation, the effect of the geometry of the piston bowl on the noise quality can be considered negligible. Since the mark variation is lower than the uncertainty of the jury evaluation, it has to be expected that in the listening tests no difference will be appreciated in the noise quality estimated with different piston bowls.

4.5.2. Experimental results

In a first step, the pistons with the Bowl B shape have been assembled in the 1.6 l engine and a simplified running-in procedure (according to engine manufacturer standards) of the engine has been performed, so that the engine hardware has been checked. The aim was to evaluate if the change of the pistons affects the engine performance. In fact, even though the compression ratio was kept constant, a modified piston bowl can change the squish and swirl characteristics inside the cylinder affecting the combustion evolution. Furthermore, to replace the pistons, the injection system had to be dismounted and mounted again and it is known that this could affect also the injection rate.

With the purpose to compare the current engine performance against that of the standard engine, a full load characterization of the engine has been carried out after

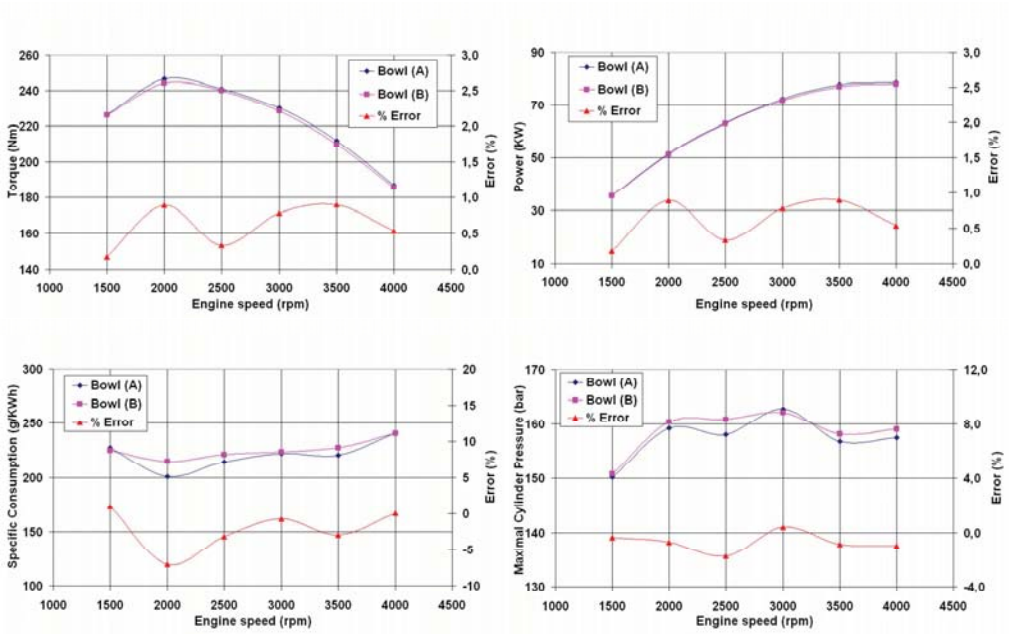

Figure 4.36: Comparison of the torque, power, specific consumption and maximal in-cylinder pressure measured at full-load with both piston bowls

engine running-in. Figure 4.36 shows the comparison of the full load torque, power, specific consumption and maximal in-cylinder pressure measured with the engine equipped with the standard pistons (Bowl A), and with the new pistons (Bowl B). The plots also indicate the percentage of error between the two engine configurations. In the case of the torque and power at full load errors lower than 1 % were observed, for the specific consumption and maximal cylinder pressure errors lower than 8 % and 2 % were measured, respectively.

The differences observed in this figure, as well as those detected in the other engine performances (intake pressure and temperature, engine efficiency, etc.) are consistent with the expected dispersion between engines of the same family. Therefore, it can be concluded that the engine performance was not affected by the substitution of the pistons with the modified bowl shape.

4.5.2.1. Definition of the experimental plans

In order to experimentally analyze the influence of the piston bowl shape on the resonance energy and on the noise quality, conventional and multiple injection strategies used in the previous studies have been considered to define the test matrix.

From the wide range of variations, just 5 settings of each injection strategy tested in the preceding studies –with the engine equipped with standard piston bowls– have been chosen for each one of the 9 operating conditions of the engine, listed in Section 3.5. The criterium employed for the settings selection has been to choice those conditions characterized by the widest variation of resonance energy and noise mark but limiting the torque dispersion.

Engine operating conditions tested in the former analysis, with both conventional and multiple injection strategies, have been reproduced with the engine equipped with the Bowl B pistons, in order to evaluate the sensitivity of the combustion noise to the combustion chamber geometry. With this purpose, the main target was to reproduce as close as possible the combustion process measured with the standard pistons. This fact, would permit to reproduce also the in-cylinder pressure evolution, namely the gas excitation, and therefore, just the effect of bowl geometry on the resonance of combustion chamber should be observed.

Engine Speed	Torque	EGR open. Valve	EGR estimated	Pression Rail	SOI pilot 2	SOI pilot 1	SOI main	Q pil 2	Q pil 1	Q main
(rpm)	(Nm)	(%)	(%)	(bar)	(° - TDC)	(° - TDC)	(° - TDC)	(mg/str)	(mg/str)	(mg/cp)
1900	124,1	45,5	31,3	**750**	30,0	12,0	2,0	2,0	2,0	16,7
1900	123,9	45,5	31,3	**1350**	30,0	12,0	2,0	2,0	2,0	16,8
1900	124	45,5	32,4	1050	30,0	12,0	2,0	**4,0**	1,8	14,3
1900	124,4	**56**	**37,1**	1050	30,0	12,0	2,0	1,8	1,8	16,4
1900	123,6	41	31,2	1050	30,0	12,0	2,0	1,8	1,8	16,3

Figure 4.37: Example of experimental plan with multiple injection strategies, 1900 rpm 124 Nm

Regarding **multiple injection strategies**, tests with five different settings have been scheduled, at each running condition (speed and torque), from that used in the experimental plans described in Section 4.4. Figure 4.37 shows an example of experimental plan at 1900 rpm and 124 Nm, performed on the engine equipped with Bowl B. In addition to the baseline settings, four different settings have been selected, taking into account the most influencing parameters on the noise quality. That is:

- Minimal and maximal rail pressure levels
- Maximal fuel mass injected during the first pilot (Q_{pil2})
- Maximal EGR rate

With the purpose to reproduce as precisely as possible the engine performance obtained with the engine equipped with standard pistons at each operating condition, a meticulous control of the engine has been carried out along this experimental task. Some refinements of the combustion settings have been done to obtain EGR rates and engine torques similar to those measured previously. As commented before, since a

CO_2 probe for the EGR mass flow measurement was not available in the test facility, the EGR rate was estimated by subtracting the mass flow rate of air intake with EGR (valve open) to the intake mass flow when the EGR valve is closed. The same procedure has been used in this case to control the EGR rate at each of the operating conditions tested.

Concerning to **conventional injection strategies**, engine operating points from those described in Section 4.2.3, have been also considered. Figure 4.38 shows an example of experimental plan at 1900 rpm and 124 Nm with pilot and main injection strategies. In this case, in addition to the base line settings, just four additional settings have been chosen from each experimental plan of the 9 running conditions introduced in Section 3.5. Unlike for multiple injection, a selection of the settings with which the lowest torque dispersion –lower than 20 %– was obtained with the standard pistons was done first.

From the previous selection, such settings that have permitted the widest range of resonance signal energies and noise variation have been finally considered. With the selected settings, a torque variation lower than 5.5 % at medium and high load conditions has been measured, while this limit has been increased up to 15 % at low load operation (1350 rpm, 12 Nm; 2250 rpm, 12 Nm). In absolute value, the torque variation at these conditions was just ± 2 Nm.

Since during the tests of the engine with standard pistons and conventional injection strategies, the EGR rate was controlled just by means of the opening percentage of the EGR valve, no estimation of the real rate was available. For the tests with the modified pistons, the EGR valve has been set to the position at which the intake air mass flow was similar to that measured in the previous phase. With this procedure, if similar torque is also produced by the engine, then similar EGR rate should be expected.

Engine Speed	Torque	EGR open. Valve	Pression Rail	SOI pilot	SOI main	Q pilot	Q main
(rpm)	(Nm)	(%)	(bar)	(º - TDC)	(º - TDC)	(mg/str)	(mg/str)
1900	120,4	15	1212	23,0	9,5	5,5	16,2
1900	128,2	47	900	33,4	9,5	1,9	21,5
1900	122,9	14	1212	33,4	0,5	1,9	20,8
1900	119,1	41	1500	33,4	9,5	5,5	16,8
1900	126,7	48	1212	33,4	4,3	1,9	20,9

Figure 4.38: Example of experimental plan with conventional injection strategies, 1900 rpm 124 Nm

Summarizing, a total of 90 tests have been performed on the 1.6 l engine equipped with the new pistons, 45 tests using conventional (pilot + main) injection strategies and an equivalent number using multiple injections.

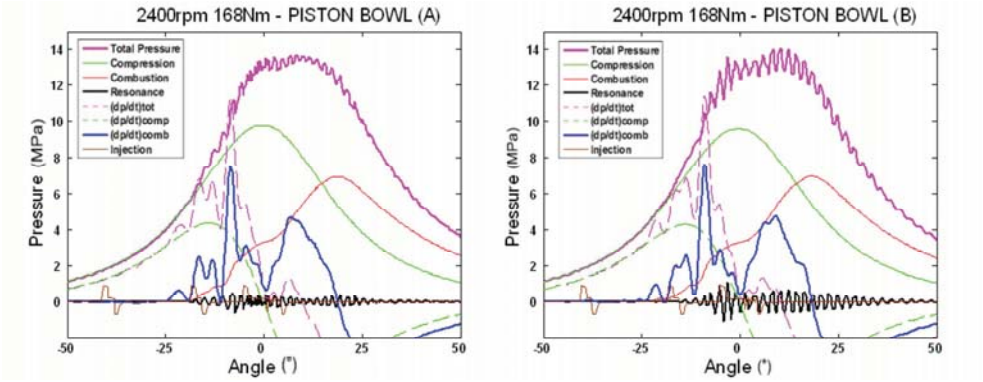

Figure 4.39: Example of comparison of in-cylinder pressure decomposition with piston bowls A (left) and B (right)

4.5.2.2. Analysis of the experiments

Like in previous studies, the in-cylinder pressure signals recorded with the engine equipped with the modified pistons were decomposed into compression, combustion and resonance sub-signals and then, the combustion indicators I_{3max} and I_4 –defined by the Equations (4.8) and (4.4)– were calculated. According to the main target of this study, the tests performed with the standard bowl geometry (Bowl A) were used as reference in the comparison with the current tests.

As was discussed above, this study would be feasible only if the same excitation of the combustion chambers is produced. In this way, any noise variation perceived by the jury should be due to changes in the bowl geometry and not to differences in the excitation itself. Moreover, it is also evident that this task is quite difficult in a complex system as an IC engine in which, apart of many parameters, the combustion process is dependent also on the bowl geometry. According to the definition of the combustion indicators, the comments given before would mean that I_{3max} –relative to the excitation provoked by the combustion– should be independent on the bowl geometry.

With the purpose to have a first evaluation of the combustion features in tests with bowls A and B, an example of their corresponding in-cylinder pressure decomposition at a representative operating condition is shown in Figure 4.39. In this figure, it can be observed that the combustion derivative curves (blue line) obtained with both bowls present a quite similar shape and that the level of the peak values used in the I_{3max} definition are of the same order. These results put in evidence that levels of excitation comparable to those produced by the combustion in the standard bowl were obtained with the modified combustion chamber. On the other hand, the black lines in the two plots of this figure, that represent the gas pressure oscillation due to the resonance of the combustion chamber, show that the amplitude of this oscillation is higher in the test with Bowl B. Then, with this amplitude increase a signal energy

level higher than that found with the standard bowl A should be expected.

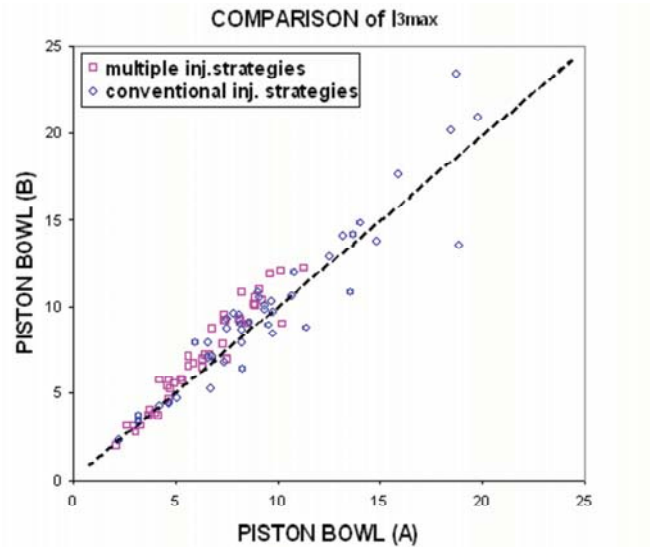

Figure 4.40: Comparison of the combustion indicator I_{3max} calculated with piston bowls A and B

Figure 4.40 shows a comparison plot between the combustion component I_{3max} obtained from tests with standard bowl (abscissa axis corresponds to Bowl A) and with modified bowl (Bowl B is in the ordinate). A quite good collapse can be observed in this plot, which indicates that quite similar excitations due to combustion have been produced with the two tested bowl geometries. Furthermore, in the same plot, more scattered results are evidenced in tests with conventional injection strategies. This trend can be justified by the fact that EGR rate was very difficult to reproduce in tests with Bowl B, because this parameter was not precisely controlled in the reference tests with Bowl A.

Considering that the Fourier transform does not give representative results with non-stationary non-periodic signals (as in the case of in-cylinder pressure resonance), a "zero-crossing" technique has been used to analyze the experimental measurements. Through the determination of the time interval that passes between the instants that the resonance sub-signal crosses zero, it is possible to estimate the variation of the resonant frequency during combustion. Figure 4.41 shows a comparison of the results obtained applying this technique to the measures obtained with the two different piston bowls. The plots refer to the same working conditions shown in Figure 4.39 and are obtained by averaging the results of approximatively 50 cycles relative to one cylinder. This figure shows that with both piston bowls the frequency of the resonance varies during combustion and decreases considerably after TDC (0°). This is due to

the fact that, after the beginning of combustion, the temperature inside the cylinder decreases together with the speed of sound, and consequently the frequency of the resonance also tends to diminish.

Another important observation is that the curves in Figure 4.41, characteristic of the two piston bowls, are frequency shifted (approximatively 500 Hz) during the resonance evolution. Assuming that the substitution of the pistons did not affect the engine performances and that, using the same injection settings, the combustion evolution has been well reproduced, it follows that this frequency difference is exclusively due to the variation of the piston geometry. This is in accordance with the modal theory (described in the Section 2.4.3): an increase of the combustion chamber diameter (as in the case of the piston bowl B) leads to a decrease of the resonance frequency. Analogous conclusions were obtained with the CFD calculation presented in Figure 4.33.

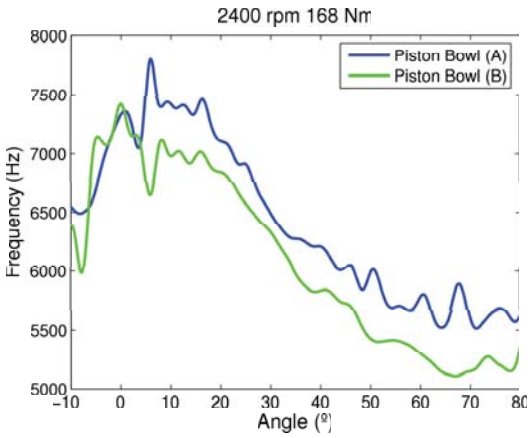

Figure 4.41: Comparison of the resonant frequencies of the two piston bowls

Focussing now on the signal energy of the resonance of the combustion chamber, the ratio of this parameter measured with Bowl B in comparison with that measured with Bowl A, calculated averaging the ratios of all the measurements performed at different working conditions (90 in total), was:

$$\frac{E_{resB}}{E_{resA}} = 2,345 \tag{4.19}$$

This value confirms that with the piston bowl B a higher resonance energy is produced. Furthermore, the energy increment is of the same order of magnitude than that calculated with CFD code.

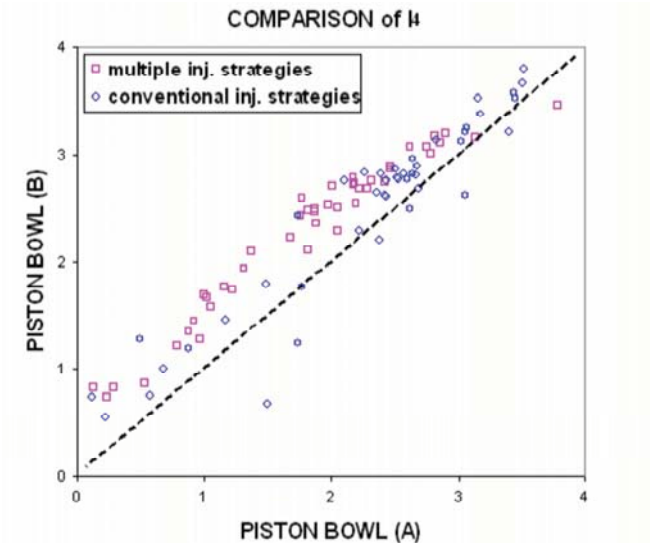

Figure 4.42: Comparison of the combustion indicator I_4 calculated with piston bowls A and B

Figure 4.42 shows now the comparison plot of the combustion indicator relative to the resonance of combustion chamber I_4 estimated for the measurements performed with the two bowl geometries. Like in Figure 4.40 relative to the combustion indicator I_{3max}, a quite good collapse is also evidenced in this plot, but the trend is now out of the "y=x line". Moreover, as it was expected, the resonance component I_4 with Bowl B results higher than that estimated with Bowl A. In average, the difference is:

$$\overline{I}_{4B} - \overline{I}_{4A} = 0{,}320 \tag{4.20}$$

According to the proposed prediction model based on Equation (4.10), this increasing of the resonance indicator would mean a diminishing of 0.25 points from the mark given by the jury to the noise with the standard engine configuration. Since the threshold of the jury perception (0.5) is higher than the estimated difference, such variations would be hardly detected by the jury. These results are consistent with the results obtained by means of CFD calculations shown in Section 4.5.1.2.

To check the sensitivity of the jury to the bowl geometry variation, the quotation of the noises recorded with the tested piston bowls have been compared. Figure 4.43 shows two graphs where the marks of the noises recorded with bowl A are plotted against to those recorded with bowl B. For clarity, results with conventional and multiple injections have been plotted separately.

As expected from the estimations in Section 4.5.1.2 obtained combining the

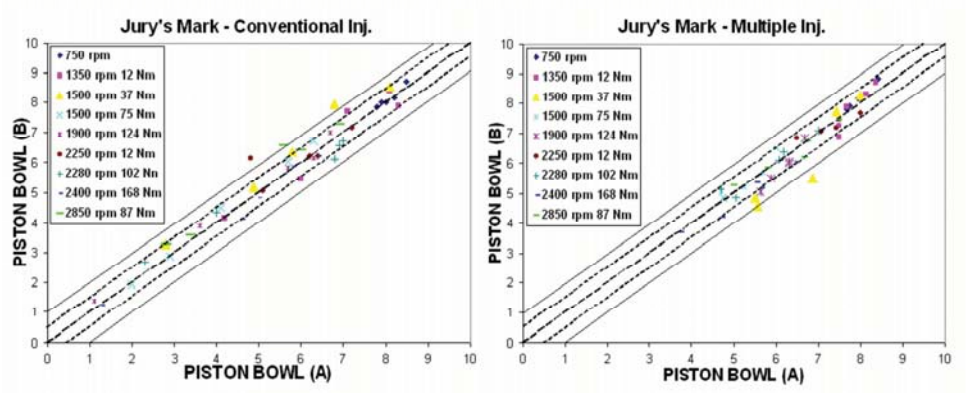

Figure 4.43: Comparison of the marks evaluated by the jury with piston bowls A and B: conventional (left) and multiple (right) injection strategies

CFD results with the quality predicting model, the plots in Figure 4.43 confirm that the noise variation produced by using these different combustion chambers was below the perception threshold of the jury. From another point of view, these results would also indicate that the geometry modification produced on the standard bowl was not significant enough so as to cause noticeable changes in the noise quality. However, an apparent modification of the geometry of the standard piston has been really performed to define a bowl (piston B) which permitted a combustion similar to that occurring with the standard configuration. Therefore, these observations seem to indicate that the combustion noise is scarcely sensitive to the geometry of the piston bowl, at least with this engine family.

4.5.3. Sensitivity of the model to bowl geometry

Taking advantage of the additional measurements performed on the 1.6 l engine equipped with the modified piston bowl B and making use of those measurements recorded at similar operating conditions with the standard piston, an analysis of the influence of the bowl geometry on the noise quality prediction model could now be done.

Considering the 90 tests performed on the engine with the modified bowl (B), the coefficients of the model for the prediction on the combustion noise quality ,with a single combustion indicator (Equation (4.9)) as well as with two components correlation (Equation (4.10)), have been calculated.

Figure 4.44 (left) shows the observed-predicted plot of the noise marks using the model based uniquely on the regression with the combustion indicator I_{3max} while in Figure 4.44 (right) the predicted noise marks by means of the complete model, based on Equation (4.10), are plotted against the marks given by the jury. Regarding

Engine	c_3	ϵ_{mean}	ϵ_{max}	σ	R(%)
1.6 l (B)	0.453	0.61	2.22	0.75	89

Table 4.12: Statistical parameters of estimated noise mark with Equation (4.9) $Mark = 10 - c_3 I_{3max}$, engine equipped with the new piston bowls B

Engine	c_3	c_4	ϵ_{mean}	ϵ_{max}	σ	R(%)
1.6 l (B)	0.322	0.489	0.52	1.85	0.67	92

Table 4.13: Statistical parameters of estimated noise mark with Equation (4.10) $Mark = 10 - c_3 I_{3max} - c_4 I_4$, engine equipped with the new piston bowls B

these results Tables 4.12 and 4.13 summarize the statistics obtained with both models, together with the c_i coefficients calculated in this case. As it was observed in previous studies, the statistics of the model is improved when the resonance component I_4 is included.

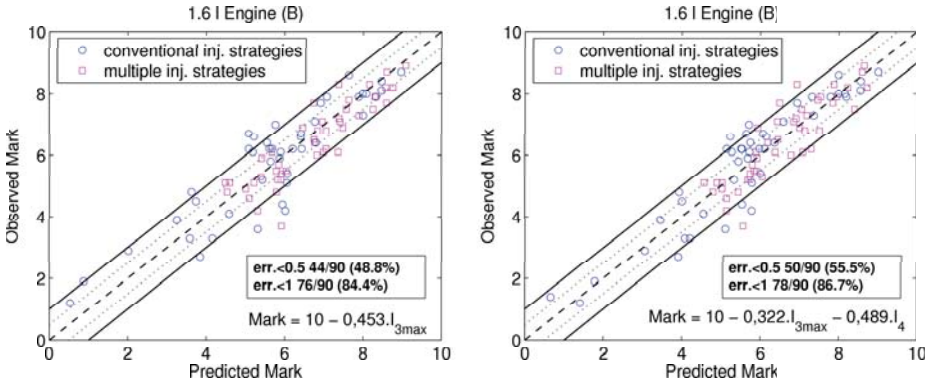

Figure 4.44: Mark noise estimation with the new piston bowl (B) 1.6 l Engine: single component (left) and two components (right) correlations.

Furthermore comparing the coefficients of the model calculated for the original engine (Tables 4.10 and 4.11) with those obtained in this study with the modified piston bowls (Tables 4.12 and 4.13), it results that c_3 is scarcely sensitive to the geometry of the combustion chamber. Just a small variation of this coefficient –for which in the worst case a maximum mark scatter lower than 0,47 could be induced– has been detected. This modification is in the expected range of variation due to the dispersion relative to the subjective evaluation of the noises by the jury. Taking into account these new results and those of the previous studies, it can be deduced that the coefficient c_3 is only dependent on the engine block structure.

Moreover, as it was expected, the c_4 coefficient seems to be highly sensitive to the geometrical features of the piston bowl. Effectively, the value of this coefficient obtained with bowl B is different than that obtained with the standard bowl. These results would induce to determine a c_4 coefficient as a function of some characteristic parameter of the bowl geometry, such as for instance, the diameter, so that a general model could be defined. However, since the bowl geometry has been varied just in two levels in the current project, an accurate function for c_4 would be hardly obtained.

Chapter 5

Combustion noise level assessment

Index

5.1. Introduction

As it was already commented in Chapter 2, nowadays, there is an increasing demand for the development of analysis tools for the study of engine acoustics. Unfortunately, only few techniques allow an estimation of the radiated noise levels and, in most of the cases, the accuracy of this estimation results inadequate. Consequently, taking into account the good results presented in the previous chapter for the assessment of the noise quality, a similar approach has been developed in order to evaluate the suitability of the in-cylinder pressure analysis to estimate the overall level of combustion noise.

In the second section, in order to have a point of reference, allowing an evaluation of the suitability of this new approach, a preliminary study is conducted using the classical methodology based on the attenuation curve, discussed in Section 2.5.1. Firstly, three standard attenuation curves found in literature and already introduced in Section 2.5.1 are used to estimate the combustion noise levels obtained with two different engine families:

- a 2.2 l engine, operating with two different injection strategies - single injection and double injection (pilot + main)
- a 1.6 l engine, operating with two different injection strategies - double injection (pilot + main) and multiple injection (2 pilots + main)

For each engine family, optimized attenuation curves are calculated by averaging the attenuation curves estimated for all the operating conditions tested and minimizing the mean errors between measured and estimated noise level. The noise level estimations obtained using these optimized attenuation curves the then compared with those obtained with standard attenuation curves. The intention is to improve the results and to test the prediction capability of this classical approach.

In the third section a new approach based on the same methodology used for the assessment of the combustion noise quality, is introduced. The procedure followed for the selection of the engine operation components and of the combustion components is highlighted. The noise levels estimated with this new approach are compared with those obtained experimentally and the results are confronted with the outcomes with the attenuation curve methodology.

In the last section of this chapter a first intent of assessing the combustion noise level in case of transient conditions is presented. Experiments are performed on the 1.6 l engine, two constant load acceleration ramps are evaluated. As for the stationary condition, also in this case two different approaches will be considered: a first based on the classical attenuation curve methodology, and a second inspired to the novel approach presented in this Thesis.

5.2. Suitability of block attenuation approach

In Section 2.5, four of the most widely used techniques for the analysis of the combustion noise have been described focusing on their suitability and limitations for the estimation of the radiated noise level. From this discussion it was concluded that the most reliable technique for the assessment of the noise level is based on the classical methodology introduced by Austen and Priede [18], also known as "block attenuation curve" or "structural attenuation" approaches.

This technique, described in Section 2.5.1, is based on the calculation of a curve representing the acoustic attenuation of the engine block, which is obtained as the difference between the in-cylinder pressure and the radiated noise 1/3-octave band spectra. In this theory, since a linear response of the engine structure is assumed, its characteristic attenuation curve can be used as a transfer function to estimate the sound pressure level spectrum of the engine noise from the in-cylinder pressure trace. Due to its simplicity and to the fact that the acquisition of the in-cylinder pressure signals is always available during engine development, this methodology is one of the most used for assessing the combustion noise level and hence, it is adopted by several commercial noise meters.

In the following sections the results of a study on the attenuation curve approach will be shown. First of all a preliminary analysis of the suitability of standard attenuation curves for combustion noise level prediction will be presented. In order to improve the results, optimized attenuation curves will be calculated for each engine family, this will also permit to evaluate the potential and limits of this classical approach for noise level assessment. This analysis will provide a term of comparison for the novel approach that will be introduced in this Thesis.

5.2.1. Standard attenuation curves evaluation

A preliminary study has been conducted in order to evaluate the suitability of the standard attenuation curves introduced in Section 2.5.1. Figure 5.1 shows three standard 1/3-octave band attenuation curves: a classical curve proposed by Anderton [8], the curve introduced by Russell [200,207] and the curve obtained from former studies at CMT Motores Térmicos [66] for a Euro III large automotive engine. Qualitatively, the three curves show similar trends. This means a high attenuation level at low frequencies that decays to a minimum in the band between 1 and 5 kHz. The attenuation level increases again for higher frequencies.

Quantitatively, in the low frequency range, a high scatter can be observed between the Anderton curve and the other two curves, and in the mid-frequency range, the attenuation levels of the three curves are different. These discrepancies could be due to the differences of the type, size and design concept of the engines tested in each case. The Anderton curve was obtained testing a wide range of classic Diesel engines for truck and automotive applications, while Russell obtained his curve for first generation high speed direct injection Diesel engines.

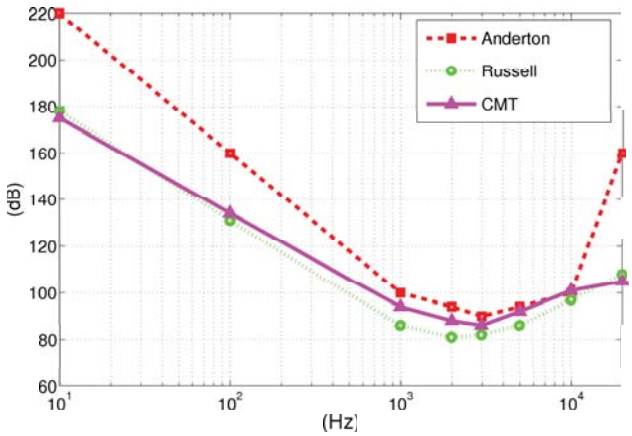

Figure 5.1: Standard attenuation curves tested in this study

Subtracting the attenuation curves from the averaged in-cylinder pressure spectrum, it is possible to estimate the sound pressure level spectrum of the radiated noise at any engine operating condition. In Figure 5.2, comparison between the overall noise levels evaluated with the standard attenuation curves discussed above and the measured noise levels is given, for the 2.2 l and the 1.6 l engines. In both cases the plots evidence that, despite the rather high dispersion, this methodology leads to a good measured-estimated correlation. The estimations obtained with the Anderton and CMT curves are closer to the measurements than those obtained with the Rusell curve. This is consistent with the fact that the highest contribution of radiated noise to the overall level is concentrated at mid-frequencies, precisely where Anderton and CMT curves are more similar.

Furthermore, it can be noticed that the standard curves are not suitable to predict the level of the noise radiated by the engine and, despite the acceptable correlation observed, an apparent disagreement between predicted and measured noise levels is noted, which indicates that the block structure response of these engine families are quite different from that of the engines characterized by the standard curves.

This observation is statistically corroborated by the absolute mean (ϵ_{mean}) and maximal (ϵ_{max}) errors, the standard deviation (σ) and the correlation coefficient (R), whose values are summarized in Table 5.1. Moreover, the disagreement is clearly more important in the case of the 1.6 l engine, which probably indicates that the block structure response of this engine is quite different to those of the engines characterized by the standard curves.

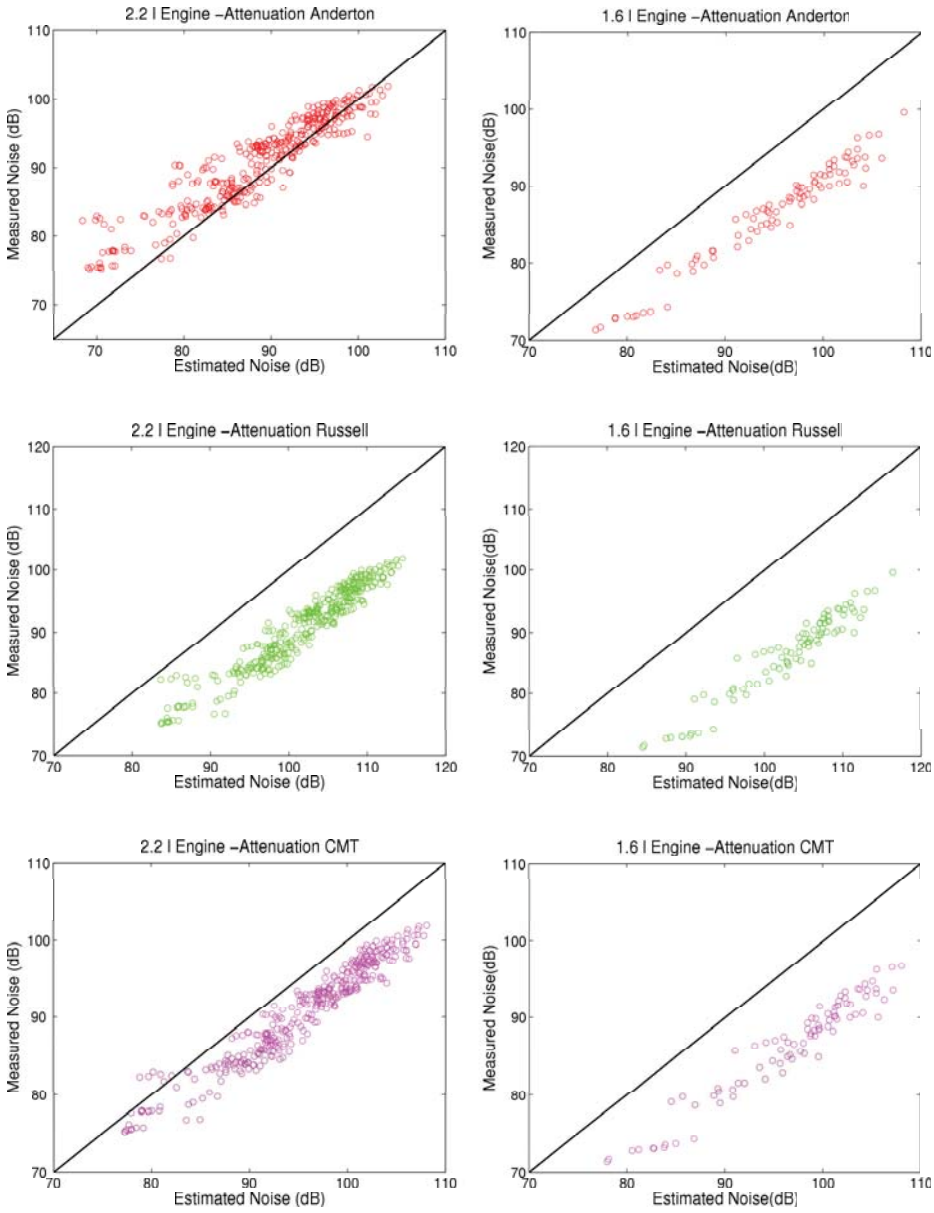

Figure 5.2: Noise level estimation with different standard attenuation curves: 2.2 l engine (left) and 1.6 l engine (right)

Attenuation Curve	2.2 l Engine				1.6 l Engine			
	ϵ_{mean} dB	ϵ_{max} dB	σ dB	**R** (%)	ϵ_{mean} dB	ϵ_{max} dB	σ dB	**R** (%)
Anderton	2,80	12,94	2,66	94	8,43	14,09	1,73	98
Russell	10,89	14,77	1,93	96	16,54	21,42	1,92	96
CMT	4,59	8,49	1,77	97	10,31	15,57	1,91	97

Table 5.1: Statistical parameters of estimated noise level with different standard attenuation curves

5.2.2. Optimized attenuation curves

In order to improve the results and to evaluate the potential of the classical approach for noise level assessment, optimized attenuation curves have been obtained for both 2.2 l and 1.6 l engines. An optimized attenuation curve has been calculated for each engine, by averaging the attenuation curves estimated for all the operating conditions tested and minimizing the mean errors between measured and estimated noise levels. The results obtained will be used as reference point for the novel approach that will be presented in this Thesis.

5.2.2.1. Curves determination

As already commented in Section 2.5.1, measurements of engine radiated noise may be used for combustion noise assessment only when the combustion contribution to the radiated noise is predominant. According to Austen [18], an advanced injection causes a combustion noise increment which is clearly higher when compared with the corresponding mechanical noise increment. Therefore, if the level of the measured engine noise remains essentially constant when advancing the injection, it can be assumed that mechanical noise is dominant and, otherwise, if the noise level increases this indicates that combustion noise is dominant. This criterion has been respected in most of the conditions analyzed, and thus it can be assumed that the noise recorded can be considered representative of combustion noise. To get better results from such an analysis, according to Russell [201] it is advisable to measure the structure attenuation at different speeds and loads, and to use at least 20 engine cycles to calculate a mean cylinder pressure spectrum. For all the operating conditions an attenuation curve was obtained from the in-cylinder pressure signals and the engine noise measurements, both calculated in 1/3-octave band.

Figures 5.3 (a) and (b) show two examples of a set of data from the 2.2 l engine working with different injection settings, running at 750 rpm and 1200 rpm, respectively. Observing the in-cylinder pressure and noise spectra, it is clear the presence of peaks in correspondence with multiple values of the firing frequency dependent on engine speed. These peaks move to higher frequency ranges as the engine speed increases. In the higher frequency range ($\sim$ 8 kHz) of the in-cylinder pressure spectrum

is also evident the presence of a peak level due to the high frequency resonant pressure oscillation in the combustion chamber.

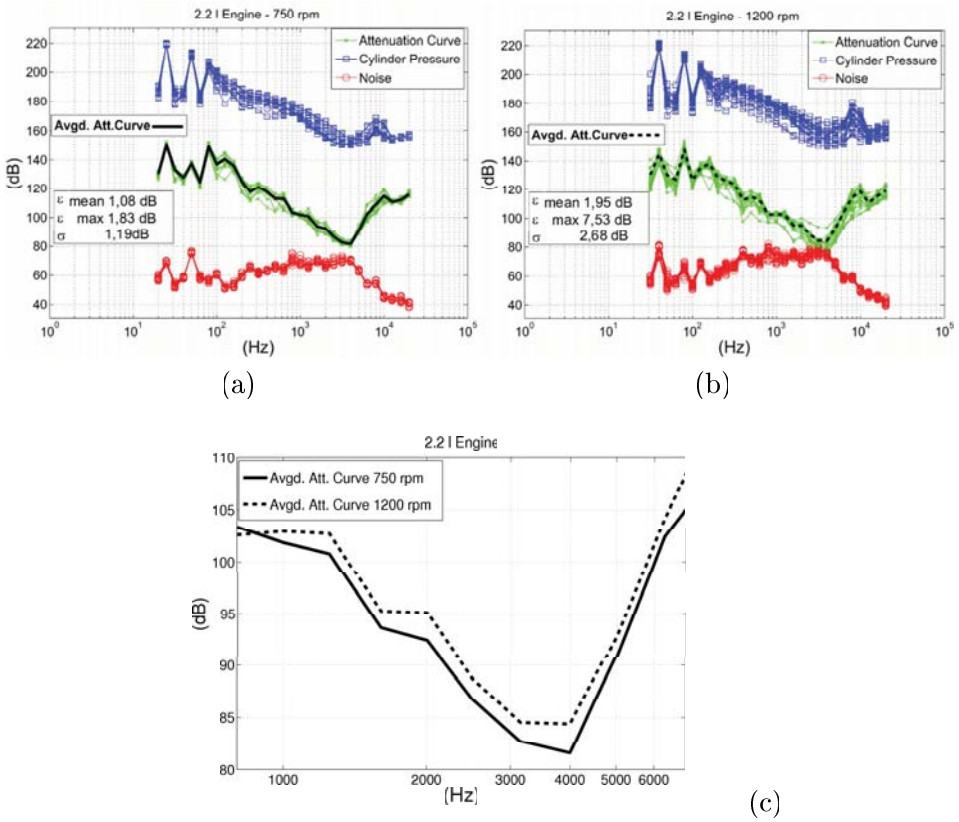

Figure 5.3: Examples of attenuation curve determination: large engine, 750 rpm (a), 1200 rpm (b). Comparison between averaged attenuation curves at different rpm (c)

In Figures 5.3 (a) and (b) are also included the averaged attenuation curves, a thick-solid line in the case of 750 rpm and a thick-dashed line for 1200 rpm. In each plot are contained the statistics relative to the comparison between the overall noise estimated with these averaged curves and the measured values. Even though in the case of the engine running at 750 rpm the use of the averaged attenuation curve for the estimation of the noise obtained with different injection settings leads to limited errors and dispersion, of the same order of the measurement uncertainties, however, in the case of 1200 rpm the idea of using a single attenuation curve seems to be a

quite rough approach since it causes unacceptable mean and maximal errors as well as a considerable dispersion.

Furthermore, notable differences can be observed also between the averaged attenuation curves calculated at different engine speeds, as shown in Figure 5.3 (c) where a comparison between the averaged curves for 750 and 1200 rpm is presented. Particularly, in correspondence of the characteristic "pass-band hole"in the range between 1 and 6 kHz, it can be observed that the averaged attenuation curves relative to these two different operating conditions present a scatter of approximately 2.5 dB.

From the previous analysis it can be concluded that different injection parameters as well as various engine working conditions should induce a considerable dispersion of the results in the assessment of the noise level with the attenuation curve methodology. In order to reduce these effects, the characteristic curve of each engine was obtained from an average of the results for all the operating conditions, minimizing the mean errors between measured and estimated noise levels.

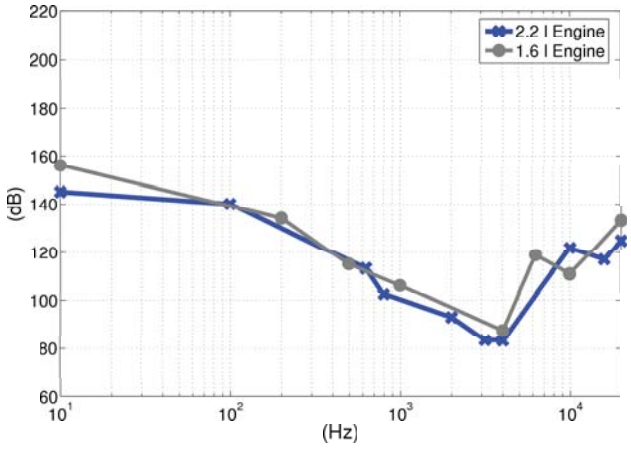

Figure 5.4: Optimized attenuation curves for the engines considered in this study

Figure 5.4 shows the optimized curves obtained for the two engine families studied here. Even though the general shapes of both curves are similar to those shown in Figure 5.1, apparent differences in the attenuation level are observed. This observation induces to remark the high sensitivity of the attenuation curve to the mechanical issues of the engine structure, which does not permit to establish any kind of "universal curve"for combustion noise assessment in any type of Diesel engine.

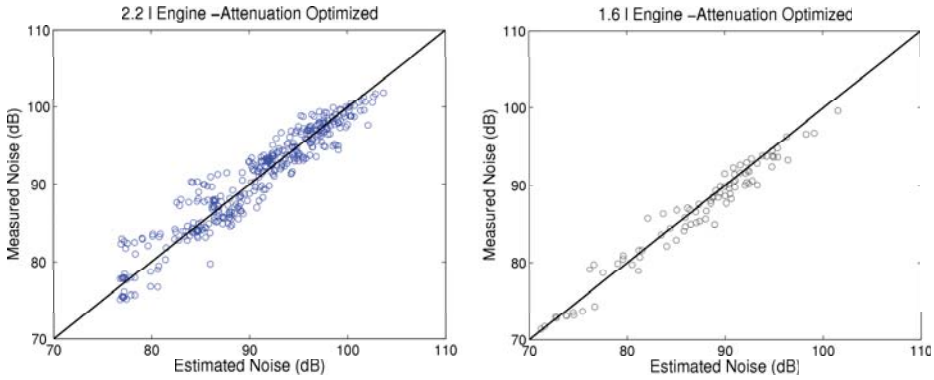

Figure 5.5: Noise level estimation with optimized attenuation curves: large engine (left), small engine (right)

Attenuation Curve	2.2 l Engine				1.6 l engine			
	ϵ_{mean} dB	ϵ_{max} dB	σ dB	**R** (%)	ϵ_{mean} dB	ϵ_{max} dB	σ dB	**R** (%)
Optimized	1,44	6,27	1,23	96	1,18	3,97	0,89	98

Table 5.2: Statistical parameters of estimated noise level with optimized attenuation curves

5.2.2.2. Noise level prediction

Figure 5.5 shows that, with the optimized attenuation curves a better collapse of the estimated noise level is obtained if compared with the results obtained with standard attenuation curves shown in Figure 5.2, whose statistics are indicated in Table 5.1. These results improve notably regarding the standard deviation σ, but mean and maximal errors are rather high, as can be verified by the statistic parameters shown in Table 5.2.

As explained before, for each engine operating condition (speed and torque) noise variations have been obtained by changing the injection schemes and parameters (injected fuel quantities, injection timing, rail pressure, etc.). Figure 5.6 shows the comparison between measured and estimated noise levels with the optimized attenuation curve in the 1.6 l engine. This plot shows different tendencies as a function of the engine operating condition, evidencing the weakness of the classical approach for combustion noise evaluation at any running point. In fact, the tendency line of any set of injection scheme variation (at constant speed and torque) is different in comparison with the main diagonal. These results indicate that the attenuation curve is highly dependant on the in-cylinder source issues, which are strongly influenced by load and speed variations and also by injection parameter changes. Furthermore, it

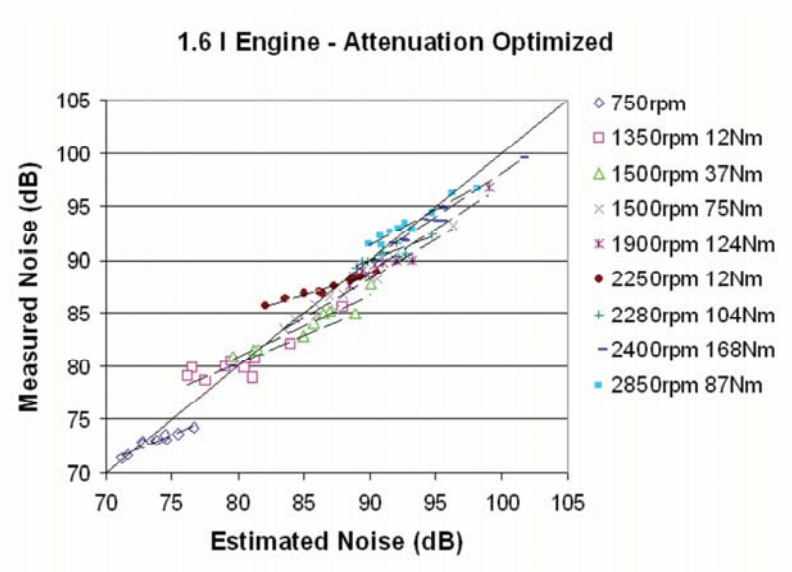

Figure 5.6: Experimental evidence of the attenuation curve sensitivity to engine operating conditions. Noise level estimation with the optimized attenuation curve

is clear that the classical approach seems to be a suitable tool only for qualitative studies, but its weakness for quantification of combustion noise level at any operating condition is also clear. This situation puts in evidence the lack of diagnostic tools that account for in-cylinder source issues, so that an accurate assessment of combustion noise in state-of-the-art Diesel engines at any operating conditions might be carried out.

5.3. Novel approach

According to the results presented in the previous section, it can be concluded that such a classical approach, based on the use of a block attenuation as a transfer function between the excitation (in-cylinder pressure) and the effect (radiated noise), do not seem to be feasible in practice for the analysis of combustion noise in state-of-the-art engines. This situation induces to attempt the combustion noise study following the same methodology that has been used for the development of the model for the assessment of the combustion noise quality.

That is, the overall level of combustion noise may be also assessed from the analysis of intuitive physical mechanisms in the noise source, directly extracted from in-

cylinder pressure measurements during engine operation. Difficulties associated with block vibration issues may thus be surpassed by establishing direct correlations between those mechanisms and the overall noise level. The sensitivity of combustion noise both to engine operating conditions and combustion strategies may be qualitatively evaluated through such correlations.

5.3.1. Indicators selection methodology

The approach proposed for the estimation of the radiated noise level in DI Diesel engines is based on the methodology presented in Chapter 3. First of all, indicators correlated with the excitation sources have been selected from the physical parameters that characterize the engine operation, i.e. engine speed, torque , fuel consumption, etc.

Then, taking advantage of the in-cylinder pressure decomposition technique described in the Section 3.5.1, indicators correlated to the combustion process. In this procedure the in-cylinder pressure trace is decomposed into three sub-signals related to pseudo-motored, combustion and combustion chamber resonance. These contributions may directly affect the level of the noise radiated by the engine. The pseudo-motored signal does not represent any tendency related to combustion and thus it is considered just as a reference signal. The combustion signal characterizes the combustion process and its associated pressure evolution is strongly influenced by the rate of heat release, which is defined by the injection strategy for any operating condition. Furthermore, this strategy controls the time variation of this signal, which therefore contains information about the Diesel knock effect. Finally, the resonance sub-signal is associated with the oscillations of the burned gas inside the bowl (combustion chamber) due to the abrupt spatial pressure gradients caused by combustion.

5.3.1.1. Selection of engine operation indicators

With the purpose of defining the indicators allowing for engine noise assessment, a first group of engine operation parameters that physically may contribute to combustion noise has been considered. The correlation of each of the indicators with the rest has been firstly evaluated in order to detect redundant parameters and to form sub-groups of those parameters. With this aim, the adopted criterion considers that two indicators are redundant and belong to the same sub-group if their correlation coefficient is higher than 90 %.

After the subgroups have been formed, the parameter having more physical sense regarding noise source issues has been selected as representative of its sub-group. Finally, a ranking of such parameters regarding their correlation with the measured engine noise has been formed. According to this procedure, the engine operation group consists of parameters that are indirectly related to the combustion process, such as engine speed, torque, intake air mass, boost pressure, fuel consumption (total and split), energizing time, timing, rail pressure, EGR rate and fluid temperatures (air, coolant, oil and fuel).

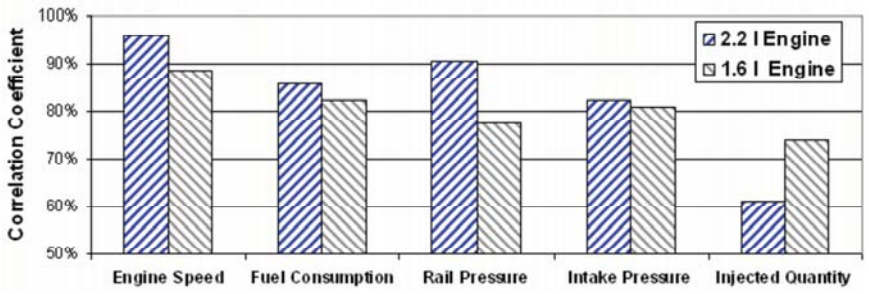

Figure 5.7: Ranking of the correlation coefficients of the engine operation parameters with the overall noise

Figure 5.7 shows the ranking of the engine operation parameters best correlated with engine noise level. This bar plot shows that in both engines, the engine speed results as the parameter with the highest correlation coefficient and that its contribution may be more important in the 2.2 l engine. These results indicate that engine speed is clearly the most relevant operation parameter that affects engine noise and therefore, it should be considered in the rest of the study.

Figure 5.8 evidences the dependence of the engine speed on the overall noise radiated by the engine. It is clear that the engine noise increases in proportion to the engine speed. As the noise level is expressed on a decibel logarithmic scale, a logarithmic fit has been evaluated to establish a relationship between engine speed and engine noise. In both engines, this alternative fit has given better correlation coefficient than the simple linear fit, as indicated in Figure 5.8.

The strong influence of engine speed on noise was already remarked in the literature. In Section 2.5.2, it has been shown that in most of the empirical formulae for the noise level prediction, the engine speed appears in a logarithmic tendency. However, Figure 5.8 shows that this parameter used singularly is not sufficient to describe the phenomenon. At a given engine speed, noise variations have been obtained by changing the combustion characteristics through injection settings, and these generated a high dispersion of the noise levels also at constant engine speed. Therefore, it seems evident that other parameters representative of the combustion process itself should be considered for an accurate prediction of the overall noise. In this sense, the main issue of the new approach is to use combustion indicators together with the most significant operation parameter in a multiple regression with the aim of estimating the level of radiated noise more accurately than with the classical approach.

Moreover, in order to achieve a more practical and useable dimension-less equation, non-dimensional parameters have been considered in the study. According to this, the selected operation indicator is associated with the engine speed non-dimensionalized by the idle speed and hence, a preliminary indicator I_n, quantified

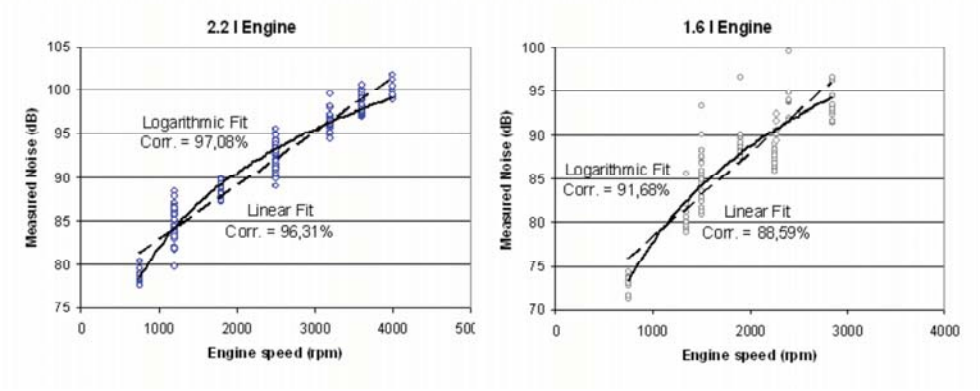

Figure 5.8: Sensitivity of engine noise to engine speed variation: 2.2 l Engine (left), 1.6 l Engine (right)

by the following equation, is defined:

$$I_n = \log_{10}\left(\frac{n}{n_{idle}}\right) \tag{5.1}$$

where n is the actual engine speed and n_{idle} is the engine speed under an idle condition, set to 750 rpm for any of the engines used in this study.

5.3.1.2. Selection of combustion indicators

According to the last comments of the previous subsection, parameters that characterize the issues of the in-cylinder source (due to combustion process) have been now defined, so that a combustion indicator group has been formed.

Several indicators determined from the decomposed signals –compression-expansion (p_{comp}), combustion (p_{comb}) and resonance (p_{res})– have been included in the list relative to the combustion indicators group. Some of the considered indicators are: the maximum pressure ($p_{\max}$) and maximum first ($\mathrm{d}p_{\max} = \mathrm{d}p_{\max}/\mathrm{d}t$) and second order pressure derivative ($\mathrm{d}^2p_{\max} = \mathrm{d}^2p_{\max}/\mathrm{d}t^2$). Other evaluated indicators have been the mean pressure (p_{mean}), signal energy (E) and sound pressure levels (L), these indicators coincide with those used in the sound quality study.

Due to the different injection strategies used in this work, some parameters have been defined considering also the contribution of the split injection through the combustion sub-signal. Consequently, considering the definition of the combustion indicator I_{3max} developed for the study of the combustion noise quality, a parameter obtained from the addition of the two maximal pressure derivative peaks of the combustion signal ($(\mathrm{d}p_{\max 1} + \mathrm{d}p_{\max 2})_{\text{comb}}$) was included as a possible component in the analysis. The characteristic value of each indicator has been quantified by the average of the values estimated for all the cycles recorded in the four cylinders.

Sub-group	Non-dimensional Indicator
i	E_{res}
ii	$(p_{\mathrm{mean}})_{\mathrm{comb}}$; $(p_{\mathrm{max}})_{\mathrm{comb}}$; E_{comb}
iii	$(\mathrm{d}p_{\mathrm{max}})_{\mathrm{comb}}$
iv	$(\mathrm{d}p_{\mathrm{max1}} + \mathrm{d}p_{\mathrm{max2}})_{\mathrm{comb}}$
v	$\left(\mathrm{d}^2 p_{\mathrm{max}}\right)_{\mathrm{comb}}$
vi	L_{comb}
vii	L_{res}

Table 5.3: Sub-groups of non-dimensional combustion indicators

Since the compression-expansion sub-signal does not contain information relative to combustion, it has been used to obtain non-dimensional indicators. To do this, each parameter relative to the combustion and resonance sub-signals has been divided by the value of the same parameter associated with the pseudo-motored signal. However, dividing the maximal first and second order pressure derivative by the same quantities relative to the pseudo-motored signal would make them lose the time information. To recover it, as in the sound quality study, the engine speed has been used in a convenient way, so that the pressure rate-of-change could be quantified by the defined indicators.

As it has been done with the operation indicators, the correlation of each one of the non-dimensional combustion indicators with the rest has been firstly evaluated in order to detect redundant parameters (correlation coefficient higher than 90 %). This procedure has led to the formation of seven sub-groups, listed in Table 5.3.

As it has been observed before during the selection of the operation indicators, the correlation of the parameters listed in Table 5.3 with the noise level is also increased when a logarithmic functional dependence is used. With this purpose, the logarithm of every "pressure element" of the combustion indicator sub-groups (the pressure level parameters were already quantified in decibels) have been calculated. In this way, the non-dimensional parameters of sub-groups (i), (ii), (iii) and (v) considerably increase their correlation with noise, while this transformation does not affect the relation with the element of sub-group (iv). In addition, this action leads to a reduction in the number of the sub-groups to be analyzed, as is shown in Table 5.4.

Concerning this ranking, a classical statistic analysis has led to conclude that the parameters in sub-groups (II) and (III) were the worst correlated with the measured noise level and therefore, have been rejected for further analysis. Furthermore, it has been verified that the parameters belonging to sub-group (V) were highly correlated with engine speed. Since the basis of the proposed procedure is to use operation and combustion indicators in a multiple regression equation for overall noise assessment, the selected parameters must be linearly independent. This condition and the fact that the operation parameter is easier to be evaluated have induced to dispense with the parameters in sub-group (V). On the other hand, the parameters in

Sub-group	Non-dimensional Indicator
I	$\log\left(E_{\mathrm{res}}\right)$, L_{res}
II	$\log\left(\left(p_{\mathrm{mean}}\right)_{\mathrm{comb}}\right)$, $\log\left(\left(p_{\mathrm{max}}\right)_{\mathrm{comb}}\right)$, $\log\left(E_{\mathrm{comb}}\right)$, L_{comb}
III	$\log\left(\left(\mathrm{d}p_{\mathrm{max}}\right)_{\mathrm{comb}}\right)$
IV	$\left(\mathrm{d}p_{\mathrm{max1}} + \mathrm{d}p_{\mathrm{max2}}\right)_{\mathrm{comb}}$
V	$\log\left(\left(\mathrm{d}^2 p_{\mathrm{max}}\right)_{\mathrm{comb}}\right)$

Table 5.4: Sub-groups of non-dimensional combustion indicators when the logarithmic dependence is assumed

sub-groups (I) and (IV) were the highest correlated with the overall noise and also linearly independent from the engine speed.

Finally, two combustion indicators have been extracted from sub-groups (IV) and (I), which have been statistically selected on the basis of their correlation degree with the noise level radiated by the engine. Respectively, the two selected combustion indicators are defined as:

$$\frac{n}{n_{\mathrm{idle}}}\left[\frac{\left(\mathrm{d}p_{\mathrm{max}}/\mathrm{d}t\right)_{\mathrm{comb}}^{\mathrm{max1}} + \left(\mathrm{d}p_{\mathrm{max}}/\mathrm{d}t\right)_{\mathrm{comb}}^{\mathrm{max2}}}{\left(\mathrm{d}p_{\mathrm{max}}/\mathrm{d}t\right)_{\mathrm{ps-mot}}}\right], \tag{5.2}$$

and

$$\log_{10}\left(\frac{E_{\mathrm{res}}}{E_{\mathrm{ps-mot}}}\right). \tag{5.3}$$

The definition of the combustion indicator extracted from the sub-groups (IV) coincide with that of the I_{3max} indicator (Equation (4.8)) selected for the assessment of the noise quality. As commented before, in a physical sense, this indicator characterizes the sudden in-cylinder pressure rise, associated with the high combustion velocity responsible for the "knock" effect characteristic of Diesel combustion. On the other hand, the combustion indicator, extracted from the sub-groups (I) and defined as Equation (5.3), is significant of the contribution of the combustion chamber resonances to block excitation. It can be transformed into the I_4 indicator (Equation (4.4)) by simply multiplying the argument of the logarithm for the constant E_0. This permits to use the same combustion indicators selected for the assessment of the combustion quality also for the analysis of the noise level.

With the aim of evaluating the correlation degree of these indicators, in Figure 5.9 the relation between these and the measured engine noise in the two engines studied is plotted. These figures show that at the same operating conditions (speed and torque) the overall noise level is linearly correlated with both indicators individually. However, it seems clear that none of them is alone suitable for engine noise assessment. This observation is supported by the statistic parameters summarized in Table 5.5, where results with the preliminary I_n indicator have been also included. These

parameters show that even though the correlation of each single indicator with the engine noise is adequately high, the errors and the dispersion level are still inadmissible for engine noise evaluation. Furthermore, these results should be also interpreted in the sense that the defined indicators contain complementary information, so that it is imperative to consider the whole set and not individual components.

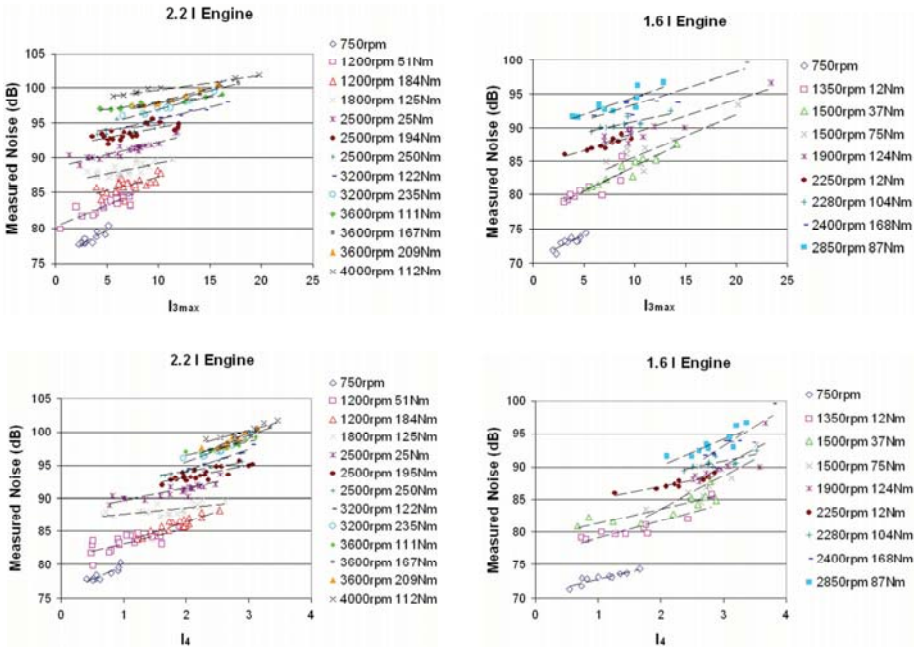

Figure 5.9: Relation between combustion indicators I_{3max} and $I_4$with the measured engine noise: 2.2 l engine (left), 1.6 l engine (right)

Single Component	**2.2 l Engine**				**1.6 l Engine**			
	ϵ_{mean} dB	ϵ_{max} dB	σ dB	**R** (%)	ϵ_{mean} dB	ϵ_{max} dB	σ dB	**R** (%)
I_n	1,18	4,44	1,53	97	1,96	9,02	2,65	92
I_{3max}	3,71	10,81	4,45	72	4,25	9,89	5,05	65
I_4	2,44	8,08	2,99	88	2,63	7,24	3,18	88

Table 5.5: Statistical parameters for single-component correlations

Two Components	2.2 l Engine				1.6 l Engine			
	ϵ_{mean} dB	ϵ_{max} dB	σ dB	**R** (%)	ϵ_{mean} dB	ϵ_{max} dB	σ dB	**R** (%)
I_n, I_{3max}	0,91	3,21	1,12	98	1,11	2,73	1,37	98
I_n, I_4	0,70	2,63	0,90	99	1,06	4,39	1,46	98
I_{3max}, I_4	2,44	7,87	2,99	88	2,61	7,27	3,18	88

Table 5.6: Statistical parameters for two-components correlations

Three Components	2.2 l Engine				1.6 l engine			
	k_0	k_n	k_3	k_4	k_0	k_n	k_3	k_4
I_n, I_{3max}, I_4	76,28	9,35	0,11	2,19	69,17	26,77	0,38	1,85

Table 5.7: Coefficient k_i calculated for three-components correlations

5.3.2. Noise level prediction

In the proposed approach the three most relevant indicators characteristic of engine operation and combustion process –selected in the previous sections– have been used to determine suitable relations with the engine noise level. The analysis exposed above evidenced that single component relations lead to results worse than those obtained with the classical approach and hence, with the aim to improve noise estimation, multiple component correlations have been also evaluated.

The results of the correlation between engine noise and two-component regressions can be evaluated through the statistical parameters given in Table 5.6. As expected, a noticeable improvement was observed in these results in comparison with those using single component regressions. Furthermore, any of the combustion indicators I_{3max} or I_4 together with the operation indicator I_n permits a noise level estimation with an accuracy higher than that expected with the classical approach. However, the pair of indicators I_{3max} and I_4 does not notably improve the statistics obtained with the single combustion component approach.

Finally, a multiple regression with the three components (I_n, I_{3max} and I_4) was considered for the overall noise ON estimation, as:

$$\mathrm{ON} = k_0 + k_n I_n + k_3 I_{3max} + k_4 I_4 \tag{5.4}$$

where coefficients k_i were found to be dependent on the engine family, as shows Table 5.7.

Results are evaluated through the statistical parameters summarized in Table 5.8, where high correlation coefficients are observed for both engines considered. Mean

Three Components	2.2 l Engine				1.6 l Engine			
	ϵ_{mean} dB	ϵ_{max} dB	σ dB	**R** (%)	ϵ_{mean} dB	ϵ_{max} dB	σ dB	**R** (%)
I_n, I_{3max}, I_4	0,69	2,46	0,88	99	0,94	2,44	1,16	98

Table 5.8: Statistical parameters for three-component correlations

and maximal errors are considerably lower compared with the results obtained with the classical block attenuation approach shown in Tables 5.1 and 5.2.

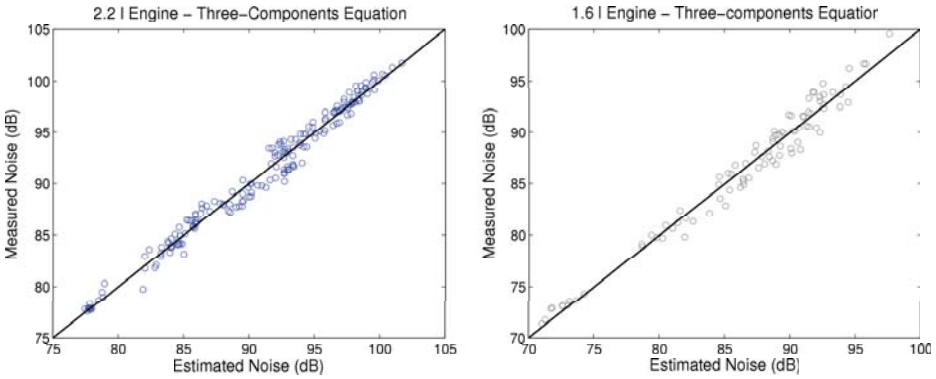

Figure 5.10: Noise estimation with the proposed approach: 2.2 l engine (left), 1.6 l engine (right)

Figure 5.10 presents the comparison between the noise levels estimated with the multiple correlation equation with three indicators and the noise levels observed experimentally. The agreement may be regarded as very good.

Figure 5.11 shows the relation between the three-components approach based on Equation (5.4) and the measured overall noise in the small engine, in which it is verified that at all operating conditions the tendency lines have a slope comparable to the diagonal, and a divergence lower than that found in the same cases evaluated with the optimized attenuation curve and shown in Figure 5.6. This observation indicates that unlike the classical methodology, the proposed approach is robust to injection parameter variations since it contains components of the combustion process that are sensitive to this changes. This feature permits not only a suitable tool for noise estimation but also the prediction of the effect of a given injection strategy on engine noise, which is useful for the optimization of injection strategies aiming at to noise reduction.

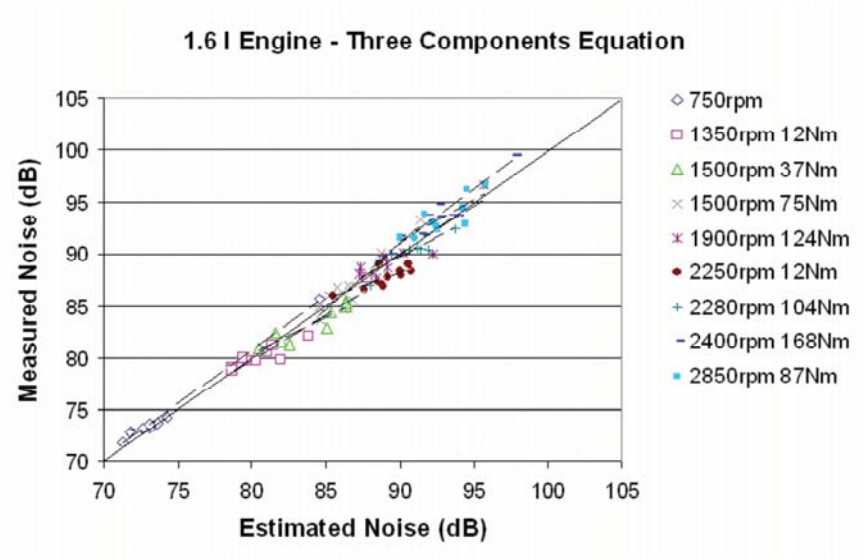

Figure 5.11: Relation between three components approach and measured engine noise in small engine

5.4. Noise level assessment in transient operation

The studies presented so far and most of the works available in the literature address combustion noise at steady operation. However, only a small portion of a vehicle's operating pattern is true steady-state, e.g. when cruising on a motorway or at idle condition. In real applications, an automotive engine is operating in transient conditions more than in steady-state. This lack of researches is mainly due to the additional difficulties that the transient operation brings to the already complex combustion noise generation phenomenon.

In transient operation, engine noise is not comparable to that radiated in steady operation, since several variables governing the combustion law and hence the noise source are changing continuously along the transient [190, 233]. Many works [68, 92, 213] evidenced that transient overall engine noise exceeds steady-state levels. This is due to the lower cylindrical wall temperature during the first phase of the transient event. On the one hand, in the first cycles, after a load or speed raise, the injected fuel quantity increases substantially cooling down the charge-air temperature. On the other hand, the temperature of the cylinder wall increases at a slower rate due to its internal inertia. This results in longer ignition delay that causes a harsher combustion and consequently higher combustion noise levels.

Modern, electronically controlled, common rail injection systems can control

this phenomenon by:

- optimizing the injection rate, for example by pilot injections, in order to reduce the premixed combustion phase
- increasing the combustion chamber temperature, by regulating the EGR valve or by increasing the turbocharger compressure boost pressure

However, also with modern engines, noise increase during transients compared with steady state operation is still apparent [4]. Accordingly it is necessity to develop experimental tools that permit the assessment of the combustion noise level also in transient operation [167, 168]. To surpass this limitation, two possible approaches –adapted from the classical and multiple regression methods– for the overall level assessment of combustion noise in transient conditions are evaluated in this section.

In the case of transient tests, experiments have been performed on the 1.6 l engine, two constant load acceleration ramps were evaluated. From a steady condition at 1300 rpm, the engine was sped up over 2700 rpm while maintaining the torque 40 Nm. The electronic control of the dynamometer permitted torque variations lower than ± 5 in all tests. In this study, two durations were considered:

- Short acceleration - acceleration time of 1 s
- Long acceleration - acceleration time of 10 s

Both in-cylinder pressure and noise records were synchronized with the crankshaft motion by means of a tachometric signal supplied by an optical encoder attached to this shaft. With this system, accurate time correlation between in-cylinder pressure and noise signals with engine speed was ensured.

Figure 5.12(a) shows the two opening laws set in the pedal actuator. In both cases, the pedal started at 11 % of full position and linearly increased up to 19 % in the acceleration times indicated above. The temporal evolutions of the engine speed measured during these accelerations are plotted in Figure 5.12(b). As expected, the duration of engine acceleration was longer than the pedal variation because of the inertia of the engine-dyno system.

5.4.1. Proposed Approach

In this study, as for the study on the engine operating in stationary condition, two different approaches will be presented. First of all the feasibility of the attenuation curve method described in Section 5.2 for noise level assessment in transient operating conditions will be explored. With this purpose, the optimized block attenuation curve (shown in Figure 5.4) has been used to predict the overall level temporal evolution of the noise radiated by the engine in transient operation.

To offer an alternative to the attenuation curve approach, a second procedure based on the definition of indicators relative to engine operation that are characteristic

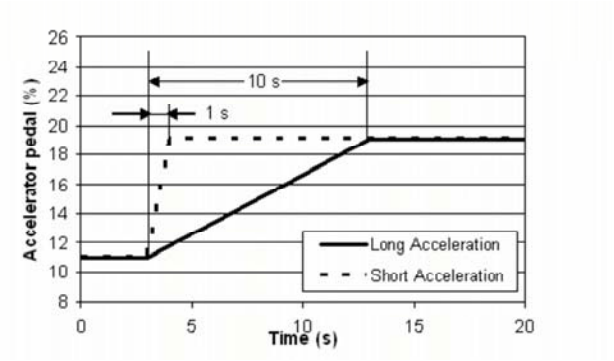

(a)

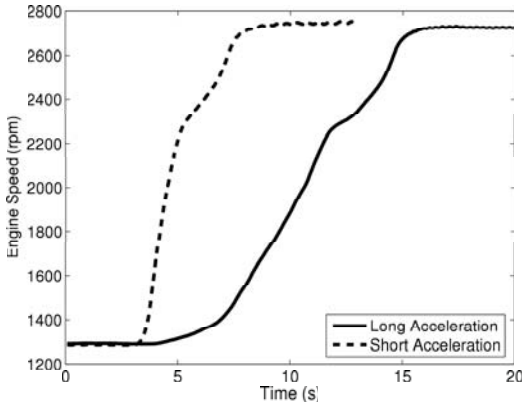

(b)

Figure 5.12: Engine control during transient tests: (a) actuation laws of the accelerator pedal; (b) temporal evolution of the engine speed

of dominant noise sources has been proposed. As a first approach, the procedure proposed in Section 5.3 was considered. In this procedure, combustion components determined from the decomposition of the in-cylinder pressure into three sub-signals –pseudo-motored, combustion and resonance– were proposed to assess the overall engine noise at steady operation conditions. Despite the high degree of accuracy of such a procedure, its application to transient running conditions was discarded, mainly due to the increased complexity that may be involved when determining the pseudo-motored sub-signal.

In the proposed approach, only the spirit of such a method has been followed, so that components representative of the noise sources were also explored. Taking advantage of the results of the study in steady condition, the engine speed in logarithmic scale has been directly selected as the most relevant operating condition parameter that affects engine noise.Combustion components that characterize the in-cylinder

Variable	Linear dependence	Logarithmic dependence
$(\mathrm{d}p/\mathrm{d}t)_{\max}$	0.83	0.89
$p_{\max}$	0.52	0.55
$\left(\mathrm{d}^2p/\mathrm{d}t^2\right)_{\max}$	0.49	0.51
p_{mean}	0.38	0.35

Table 5.9: Ranking of the correlation coefficient of combustion components with the overall noise level

source (caused by combustion), such as maximum and mean pressure, maximum first and second order pressure derivatives, and sound pressure level, were also explored. However, in this case, only the total in-cylinder pressure signal has been considered, furthermore only measures performed with multiple injection strategies have been analyzed. The value of each component was quantified by the average of the values estimated for all the cycles recorded in the four cylinders. The redundant components (variables with a correlation coefficient higher than 0.9) were grouped and the most representative one of each group was considered as a candidate.

The analysis performed with the candidates of each group led to the conclusion that –together with the engine speed– the maximum of the first order in-cylinder pressure derivative were the most significant variables that affected the measured overall noise level. The ranking of the correlation coefficient between the first four most significant combustion variables is summarized in Table 5.9. The selected combustion component characterizes the sudden in-cylinder pressure rise, which is associated with the high combustion velocity responsible for the 'knock' effect during Diesel combustion. This, in turn, induces the medium and high frequency oscillation of gas in the chamber, and hence contributes to engine noise. The effect of the engine load is included in this component.

In this approach, these two indicators that are characteristic of engine operation and the combustion process are used to determine a suitable relation with the engine noise level. As for the indicators selected for the stationary conditions, in order to achieve a more practical and useable dimensionless equation, non-dimensional parameters were considered. With this purpose, the operation and combustion components were referenced to those relative to idle operation, which is representative of the minimum running speed and the condition at which the lowest noise level due to combustion is expected. Finally the first selected indicators is I_n, the same as for the stationary condition model, defined by the Equation (5.1). The second indicator is defined as:

$$I_t = \log_{10}\left[\frac{n}{n_{idle}}\frac{(\mathrm{d}p/\mathrm{d}t)^{\max}}{(\mathrm{d}p/\mathrm{d}t)^{\max}_{idle}}\right] \tag{5.5}$$

where $(\mathrm{d}p/\mathrm{d}t)^{\max}$ is the maximum value of the in-cylinder pressure signal deriva-

Components	1.6 l Engine			
	ϵ_{mean} dB	ϵ_{max} dB	σ dB	**R** (%)
I_n, I_t	0,50	1,58	0,65	99

Table 5.10: Statistical parameters of estimated noise level with multiple regression

tive and $(\mathrm{d}p/\mathrm{d}t)_{idle}^{\max}$ is the peak value of the in-cylinder pressure derivative at idle operation.

As shown in Table 5.9, the statistical analysis carried out in the study confirmed that the use of a logarithmic functional dependence on the selected variables improves the correlation of these with the overall noise. These results are consistent with the fact that the noise level is commonly expressed on a decibel logarithmic scale. The multiple regression method for estimating the overall engine noise ON was obtained considering these two variables:

$$\mathrm{ON} = t_0 + t_n I_n + t_t I_t \tag{5.6}$$

where the coefficients t_0, t_n and t_t characterize the evaluated engine.

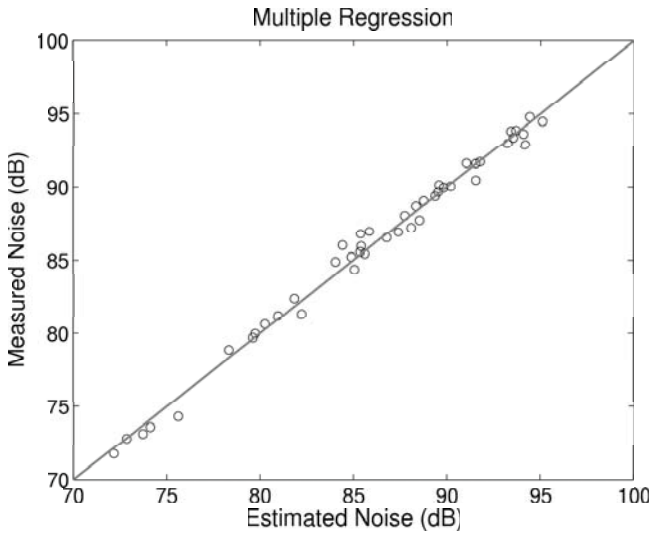

Figure 5.13: Noise level estimation with the multiple regression approach

Figure 5.13 shows the comparison between the noise levels estimated with this

multiple correlation equation with two indicators and the noise levels observed experimentally. A good collapse is observed and the agreement may also be regarded as very good. The statistical parameters, summarized in Table 5.10, evidence the high reliability of the proposed method. Mean and maximal errors, standard deviation are considerably lower compared with those obtained with the attenuation block methodology (Table 5.2).

These results are also better of the the statistical parameters obtained with three components correlations (Table 5.8). This is due to the fact that the analysis for the study in transient operation has been performed on a smaller set of measures, considering only multiple injection strategies. Generally it has been observed that the fact of replacing I_{3max} and I_4 with I_t leads to a deterioration of the results. However, as a first approach, the regression used for the transient operation provides an adequate trade-off between calculation simplicity and accuracy.

5.4.2. Noise level prediction

In both proposed approaches, the pulse signal generated by each crankshaft turn of the optical encoder was used to isolate the in-cylinder pressure traces of the four cylinders on a cycle-to-cycle basis. Then, the four traces were added in the time domain in order to obtain the pressure evolution characteristic of the noise source during each cycle.

For noise estimation through the attenuation curve approach, the 1/3 octave band spectrum of this signal was calculated using traditional Fourier analysis. Subtracting the optimized attenuation curve from the in-cylinder pressure spectrum gives an estimate of the spectrum of the radiated noise during one cycle. Finally, overall noise was calculated from the estimated spectrum. Applying the same procedure to all the measured cycles, the temporal evolution of the overall noise could be predicted.

For noise assessment by means of multiple regression, the instantaneous engine speed was determined by recording the crank angle signal supplied by the optical encoder coupled to the crankshaft. The cycle-to-cycle isolated in-cylinder pressure signals permit the calculation of four maximal pressure derivatives. Finally, the cycle-to-cycle overall noise level was calculated by using Equation (5.6) with the averaged values of those derivatives and the instantaneous engine speed.

Figure 5.14 shows the comparison between the predicted and measured engine noise level at each of the acceleration ramps considered in the study. The measurements (compare Figures 5.14 and 5.12(b)) evidence that engine noise is highly correlated with engine speed, and that the produced noise variation (around 10 dB) was high enough to permit the evaluation of the potential of both approaches for noise assessment during transients. Furthermore, the rise in noise is also due to other engine operating parameters, such as injection pressure, timings, fuel mass, and EGR rate, which are varied by the electronic control unit during the acceleration.

The comparison of the measurements with the overall noise estimated with the two procedures leads to the following remarks:

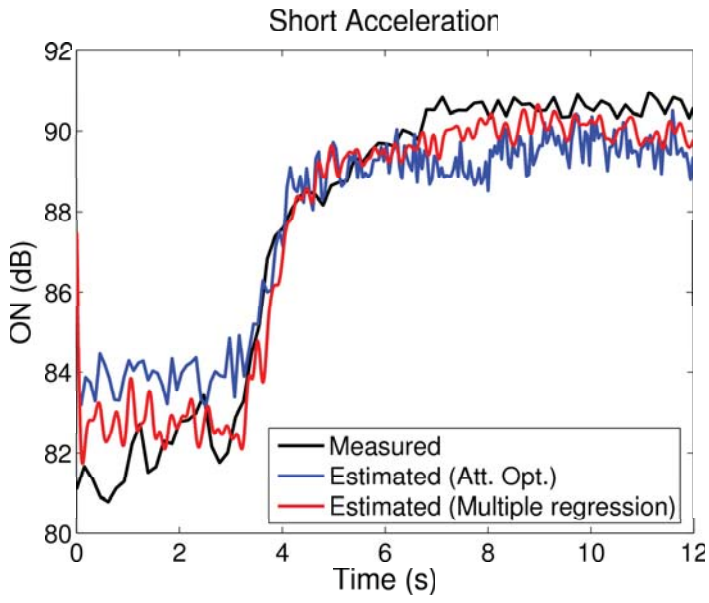

(a)

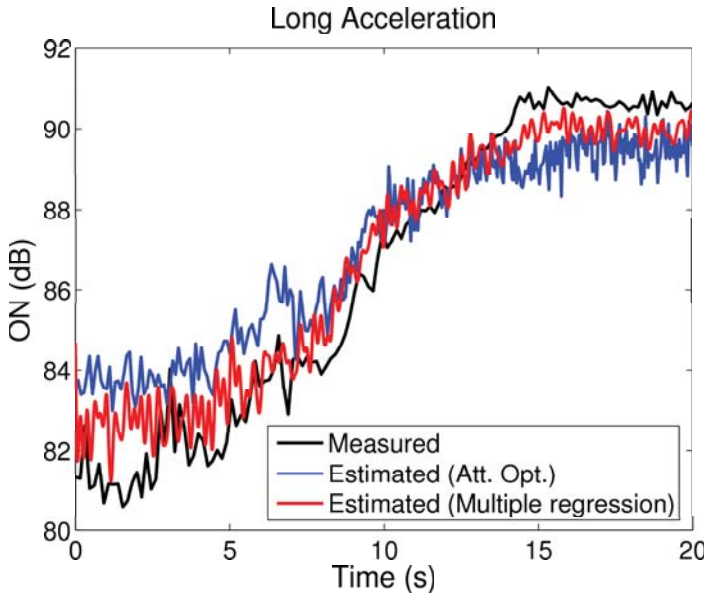

(b)

Figure 5.14: Sound pressure level at transient conditions. Comparison between measured and estimated evolution both with the classical and the multiple regression approaches: (a) short acceleration; (b) long acceleration

- Even though the predicted noise level variation during the accelerations (6-9 dB) is lower than that observed in the measurements, the temporal evolution has been acceptably reproduced with the two procedures

- The approach based on the classical attenuation curve overestimates the noise level before the acceleration, when the engine operates in the steady condition, and in the first part of the ramp. The agreement between prediction and measurement is good at the end of the ramps, but the model underestimates the sound pressure level after the acceleration, when the engine goes back to steady operation.

- As observed in the analysis in steady operation, better results were obtained with the approach based on multiple regression. A good correspondence between measure and prediction was achieved, and the maximum estimation error was below 2.5 dB for both accelerations analyzed. Despite these discrepancies, the proposed procedure can be considered to be a suitable approach for engine noise level assessment in transient conditions, since the maximum error observed is the same order of magnitude as that obtained in steady conditions and is closer to the uncertainty of the measurement.

Chapter 6

Conclusions and future works

Index

6.1. Conclusions

Summarizing the results that have been presented in this Thesis, the main conclusions can be structured in different groups, according to the various phases followed in the development of this work. The first conclusions can be deducted from the analysis of the state of the art of combustion noise, framing the problematic of the combustion noise generation and justifying the novel approach developed in this Thesis. In the second group, the conclusions deducted from the theoretical and experimental methodology will be highlighted. Finally, from the analysis of the results obtained with the proposed methodology, two categories of conclusions will be presented: the first, relative to the assessment of the combustion noise quality and the second, focused on the prediction of the overall noise level.

From the analysis of the state of the art of combustion noise a first group of conclusions can be remarked:

- The basis of the combustion noise theory has been introduced by describing the physical interpretation of the combustion noise generation phenomenon. Experimental and theoretical approaches for the analysis of simplified flame models have been described evidencing the difficulties and limitations connected to a rigorous physical methodology. The main result of this study is a general understanding of the physics of the problems related to combustion noise generation and the important influence of heat-release, fuel heating value as well as flame speed on the acoustic emission.

- The importance of the combustion as noise source has been highlighted and compared to the other sources of noise of an internal combustion engine. The main techniques for the identification of the noise sources and for the limitation of their effects have been described. From this study, it has been concluded that till now, no truly satisfactory solution in terms of costs and reliability has been found. Furthermore, the different phases of the noise transmission flow have been analyzed, from the main source –the in-cylinder combustion– to the radiation of noise due to the vibration of the engine surfaces. This has evidenced that there are several patterns of acoustic energy propagation through the engine block, whose response is highly nonlinear and time variant.

- Once the importance of the combustion has been established, a deeper analysis of the in-cylinder pressure has been done, and the main ways to control its evolution have been described. Decreasing ignition delay period, reducing fuel injected during the ignition delay period, restrict air/fuel mixing during the ignition delay period are the three basic ways to reduce the noise on fully developed engine. Moreover, the combustion chamber resonance effect has been presented and the different parameters influencing this phenomenon have been analyzed. The resonance frequencies are proporcional to the speed of sound in the gas and inversely proportional to the bore. Also the bowl geometry and the location of the start of combustion have a strong influence on this phenomenon.

- The classic techniques for the analysis of combustion noise have been presented focusing on the potential and limits of these approaches for the estimation of the radiated noise level. Due to its simplicity the block attenuation curve technique is one of the most used for the assessing of combustion noise, unfortunately this methodology leads to quite high estimation errors. This is mainly due to the inexact basic assumption that the engine structure behaves as a linear system. Also empirical formulae give only rough estimations, they can be used for the comparison of engines of different families but their use in not appropriate when an accurate assessment of the noise level is researched. The use of time-frequency methods is only limited to qualitative considerations. Numerical methods, like FEM and BEM, have the advantage that do not require hardware for their application and that a lot of modification can be analyzed through simulations. On the other hand, these methods do not give satisfactory results in a frequency range between 500 and 1500 Hz, their use is not recommended to predict absolute noise levels. This analysis of the classical approaches exhibited the necessity of developing practical and reliable techniques for the assessment of the combustion noise characteristics that could be used already in the first phases of the engine design.

- The concept of sound quality applied to the combustion noise has been described together with the basic techniques for a subjective evaluation of the noise. Furthermore, the main approaches found in literature to give an objective assessment for the concept of noise quality have been presented. This study evidenced the imperious necessity of listening tests in order to get a reliable evaluation of the combustion noise quality.

- The analysis of the state of the art of combustion noise demonstrated clearly the great difficulties to assess the combustion noise phenomenon and suggested the basic idea of the methodology developed in this Thesis: the definition of direct correlation between in-cylinder pressure evolution and the characteristics of the external sound field produced by the engine.

After evidencing the necessity of a new approach for the study of combustion noise a novel methodology has been developed. From this phase the following conclusions can be highlighted:

- As the approach described in this Thesis is basically experimental, first of all an experimental set-up has been defined, so that the simultaneous recording of in-cylinder pressure signals and radiated noise was allowed. Furthermore, due to the acoustical purpose of this work, particular characteristics of the experimental set-up have been required as the binaural recording of noise and the realization of the measurements in an anechoic room.

- Once defined the experimental devices, an adequate measurement methodology has been developed. As noise is a time-related phenomenon, all measures have been performed at time-constant sampling. Moreover, in order to record the pseudo-motored signals, an electronic device has been used to cut periodically the injection in a cylinder.

- A methodology for the decomposition of the in-cylinder pressure signals has been used, considering it as the sum of three main sub-signals: combustion, pseudo-motored and resonance. This permitted the definition of parameters related to the combustion through its in cylinder pressure evolution.

- A statistical procedure has been defined for the selection of the main engine operation indicators, as well as combustion indicators, better correlated with the characteristics of the noise radiated by the engine, taking into account subjective criteria (noise quality) and also objective criteria (overall noise level).

- A methodology in order to evaluate the noise quality through listening tests has been defined. The basic rules for the selection of the jury members have been described and a statistic analysis to assure the consistency of the jury has been performed.

The methodology introduced in this Thesis has been used for the assessment of both sound quality and overall level of combustion noise. From the results obtained in the study of the noise quality the following conclusions can be remarked:

- In case of engines operating with single and conventional injection strategies, two combustion indicators have been selected: I_3, related to the initial high fuel burning velocity, and I_4 relative to the combustion chamber resonance phenomenon. These showed to be the best correlated with the jury's mark representing the engine noise quality.

- With these selected combustion indicators, multiple linear regressions have been found that permit a good estimation of the noise quality. The indicator I_3 resulted as the most significative parameter in any possible multiple component correlation. I_4 represents a complementary variable that supply the lack of information in I_3 and its importance resulted to be dependent on the engine family considered. The coefficients of the multiple regression (c_3 and c_4) depend on the size of the engine and on the structural features of the block.

- From the preliminary study on the multiple injection it has been experimentally confirmed that the post injection does not have any influence on the noise quality, this simplified the further investigations reducing the study to three injection strategies.

- In the case of engines operating with multiple injection strategies, the combustion indicator I_{3max} has been selected (together with I_4) for the assessment of the noise quality. This new indicator, used as a single variable in a linear regression or in a multiple regression model with I_4, showed to give very good results with multiple as well as conventional injection strategies.

- In the study of the sensitivity of the noise quality to the combustion parameters the influence of the rail pressure, fuel mass injected, start of injection and EGR rate on the the jury's mark has been confirmed. The trends of noise quality evolution against combustion parameters can be used as guidelines for future developments of combustion settings offering the possibility to optimize the injection strategies from the point of view of the combustion noise quality.

- From the study on the influence of the combustion chamber geometry, it has been deducted that the combustion noise is scarcely sensitive to the geometry of the piston bowl, at least with the engine considered in the study. However, this affects the noise quality prediction model, particularly the coefficient c_4 resulted to be highly sensitive to the geometrical features of the piston bowl.

From the results obtained in the study of the noise level, the following conclusions can be drawn:

- The potential and limits of the attenuation curve methodology for the assessment of the noise level have been showed. This study demonstrated the weakness of this standard approach for quantification of combustion noise levels at any operating condition and evidenced the lack of diagnostic tools for an accurate assessment of the overall noise level.

- An engine operation indicator (I_n, logarithmically linked to the engine speed) and the same combustion indicators as before (I_{3max} and I_4) were the best correlated with the overall level (expressed in decibels) of engine noise.

- The selected indictors have been used in a multiple regression equation in order to assess the noise level radiated by the engine. The agreement between the noise estimated with this predicting model and the noise level observed experimentally may be regarded as very good. Furthermore, unlike the attenuation curve methodology, the proposed approach contains components of the combustion process that are sensitive to injection parameter variations leading to a better estimation.

- A novel approach and the classical attenuation methodology have been used to predict the instantaneous overall level of combustion noise radiated by the engine in transient operation. Both procedures reproduced with a good agreement the temporal evolution. As for the analysis in steady operation, a better agreement between measure and prediction results has been obtained with the approach based on multiple regression.

The results of this Thesis offer a direct application in the design of predicting tools suitable for the assessment of the quality of combustion noise as well as of the overall noise level. Since this approach is mainly based on the noise source diagnosis through the in-cylinder pressure trace, which is usually available during the engine development phase, it arises as an alternative to the classical approaches, suitable not only for engine noise estimation but also for the definition of optimal injection settings regarding combustion noise control.

6.2. Future works

The natural continuation of the works presented in this Thesis is the acoustical analysis based on the proposed approach of the emerging new Diesel combustion

concepts (Homogeneous Charge Compression Ignition-HCCI, Premixed Charge Compression Ignition-PCCI, etc.), which are intrinsically noisy. Since these new concepts have been developed to comply with the increasingly restrictive emission standards without efficiency penalties, for this study the experimental set-up should also permit a control of the engine emissions and performance. Analogously, acoustical analysis should be conducted considering alternative fuels such as ethanol and biodiesel.

Another possible continuation could be the development of a dedicated software for the assessment of the combustion noise characteristics. This software would be based on the predicting models developed in this work, permitting an acoustic optimization of the injection strategies from the first phases of an engine development and avoiding the necessity of long and expensive acoustic measurements and listening tests.

Furthermore, a data base of coefficients for the multiple regression equations should be created considering a wider range of engine families and sizes. Using extrapolations based on similar engines it would be possible to predict the characteristics of the noise radiated by a new engine type already in the first phases of design.

Further efforts should be dedicated to the subjective evaluation of the noise quality. Due to the high costs and complexity of the listing tests, it has also to be considered the need to develop a listening tool that may facilitate both the performance of the tests by the jury, and the evaluation a posteriori of the consistency of the jury members.

Considering the encouraging results obtained in transient operation, further investigations should be done on this topic. Other transient conditions could be considered and particular attention should be dedicated to the cold start, where much lower cylinder wall temperatures lead to even longer ignition delay periods with a consequent noise deterioration.

Appendix A

Appendix

Index

A.1. Experimental devices

In appendix the main features of the anechoic chamber will be presented, furthermore, some important characteristics of the in-cylinder pressure measurement system and of the binaural measurement system will be defined and, to conclude, a short description of the ECU control system and of the engine test bench will be given.

A.1.1. Anechoic chamber description

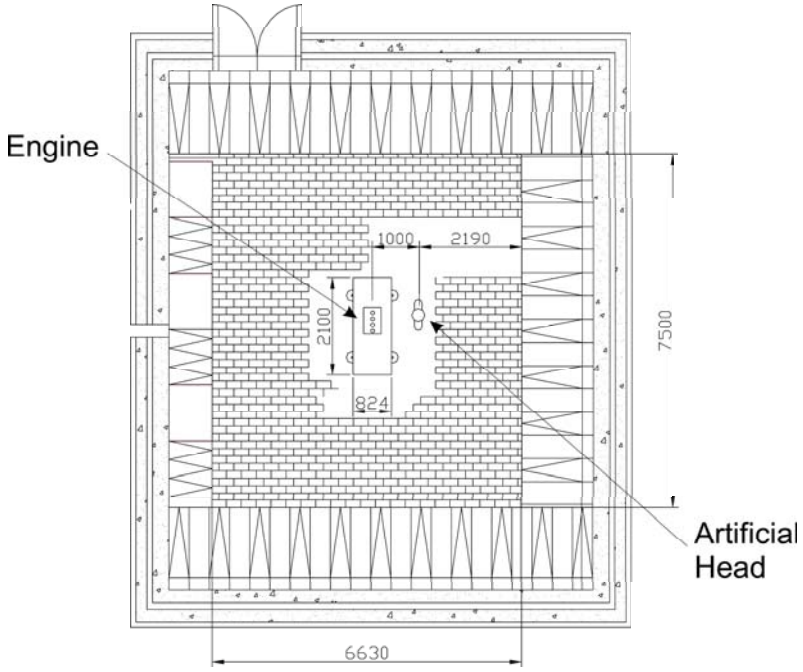

Figure A.1: Anechoic chamber plan - dimensions are expressed in mm

All combustion noise measurements have been performed in an anechoic chamber, a room in which there are no echoes. The plan is presented in Figure A.1. In order to simulate free field conditions and to easily contain an engine and an electric brake the chamber has been built with generous internal dimensions, a 9.5 x 9 m base and a height of 7.2 m. Echoes are suppressed within the chamber by the installation of wedges made of fiberglass, an acoustically absorptive material. The wedge shapes act as a waveguide to focus the incident sound waves into the absorptive material that

converts the acoustic energy to heat. The wedges are disposed in an alternating pattern in order to achieve a more uniform angular absorption. This chamber has fixed wedges on five of its six sides, the wedges of a lateral wall are removable allowing the transformation to a semi-anechoic chamber, useful for exhaust noise measurements. In anechoic chambers low frequency waves are not effectively absorbed by the wedges, the frequency at which the energy absorption drops below 99 %, or pressure reflection exceeds 10 %, is known as the low-frequency cut-off. The anechoic chamber used has a low-frequency cut-off of 100 Hz.

In order to get an effective isolation from possible noise and vibrations present in the external environment, the walls of the chamber are built of cement forming a dense shell that leans on a water-repellent coat. The bottom of the chamber is also composed of wedges and the floor is formed by iron meshes suspended above the bottom by leaning on an iron frame.

In the anechoic chamber there is an efficient ventilation system designed in order to avoid any disturbance to the acoustics measures. The speed of the air in the chamber is limited by using big section ducts, two for the introduction of the air and one for the extraction. The system is automatically controlled by the use of 4 pressure sensors, 4 temperature sensors and a carbon monoxide sensor constantly monitoring the chamber.

Every tested engine is positioned at center of the anechoic chamber and directly coupled to an electric dyno, this asynchronous electric brake is acoustically isolated from the engine by means of sound damping panels. The engine noise is binaurally recorded by a torso head located at a height of 1.65 m from the floor and 1 m away from the engine block, to avoid near field effects, and in front of cylinder 4, the farthest cylinder from the electric brake, opposite to the side where the turbo-group and the exhaust system are located. Furthermore every auxiliary element that could represent a significant noise source are covered up with isolating foam. The intention is to minimize the effects of the accessory and flow noise sources and to record a noise where the combustion contribution is predominant.

A.1.2. In-cylinder pressure measurement system

For the in-cylinder pressure measurement piezoelectric pressure transducers have been chosen, this type of sensors take advantage of the electrical properties of naturally occurring crystals that generate an electrical charge when they are strained. On the one hand, the piezoelectric sensors present some drawback: they require charge amplification circuitry, are very susceptible to shocks and vibrations and sensitive to electrical parasites. On the other hand this type of sensors present also many advantages such as a very good linearity of the response and a high dynamic range, furthermore the piezoelectric pressure transducers are rugged and, depending on the materials employed, have an extreme stability over temperature enabling sensors to have working ranges of thousands of °C. Besides, thank to their characteristic small size, these sensors can be easily assembled on a glow plug adapter and installed directly in the combustion chambers. For these reasons the piezoelectric pressure transducers

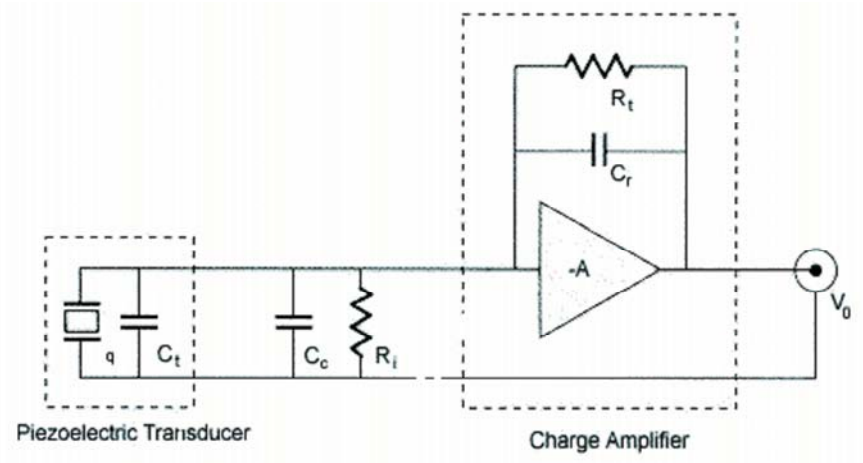

Figure A.2: Simplified transducer, cable and charge amplifier model

are commonly used for in-cylinder pressure measurements even though their use is still limited to test bench applications due to their rather high cost [46].

In our case four Kistler 6055 Bsp have been chosen, every pressure transducer has been assembled on a glow plug adapter and installed instead of the glow plugs permitting a direct access to the combustion chamber. The piezoelectric sensors are connected to charge amplifier Kistler 5011 in order to obtain an electric signal with an adequate level of voltage and impedance necessary for the further step of analogical-digital (A/D) conversion. The sensors have a natural frequency of about 130 KHz, amply over the frequency range of interest, and they present an high sensitivity, necessary to observe dynamic signals with high energy content at low frequencies, such as an in-cylinder pressure signal. Due to the high sensitivity of these sensors to electrical parasites, the election of adequate conductivity and length of the cables connecting sensors and amplifiers is essential to get a reliable measure, as well as the cleaning of the connections and an accurate calibration of the sensors.

In Figure A.2 a simplified model [115] of the set of piezoelectric transducer, cable and charge amplifier is shown, where:

- C_t and C_c are the capacities of transducer and cable

- C_r and R_t are the range capacitor and the time constant resistor of the amplifier, respectively

- R_i is the insulation resistance of input circuit (transducer and cable)

- q is the charge generated by the transducer

- V_o is the output voltage

- A is the open loop Gain

Neglecting the effects of the resistors, the resulting output voltage becomes:

$$V_o = \frac{-q}{C_r} \cdot \frac{1}{1 + \frac{1}{AC_r}(C_t + C_r + C_c)} \tag{A.1}$$

For high open loop gain, the cable and transducer capacitance can be neglected, simplifying, the output voltage results only depending on the input charge and the range capacitance:

$$V_o = \frac{-q}{C_r} \tag{A.2}$$

Summarizing, the amplifier acts as a charge integrator which compensates the weak electrical charge generated by the transducer with a charge of equal magnitude and opposite polarity and ultimately produces a voltage across the range capacitor. This permits to convert the high impedance input charge (q) into a usable output voltage. Taking into account the transducer sensitivity and the pression/volage ratio, C_r permits the setting of the amplification.

Another important characteristic of the charge amplifier is the time constant (TC), defined as the discharge time of the AC couple circuit, determined by the product of the range capacitor and the time constant resistor:

$$TC = R_t.C_r \tag{A.3}$$

In these Kistler amplifiers different time constants ("Short", "Medium" and "Long") can be selected by changing the time constant resistor (R_t). The frequency response of the system is the frequency range over which the sensor will provide a linear response, the longer the time constant, the better the low-end frequency response. Depending on the transducer sensitivity and on the measurement range, C_r and R_t are set determining the time constant and the cut-frequency that will be applied at low frequency. A deeper description of more setting details and of the calibration routine of the pressure transducer will be given in the Section A.1.2.1.

As can be observed in Figure 3.3 the in-cylinder pressure signals pass for various equipments before getting a personal computer. The signals obtained by the transducer-amplifier set reach a digital multichannel oscilloscope where are A/D converted and digitally stored in buffer memories, the range of the input signal has to be set in order to get the best resolution of the A/D conversion avoiding the saturation of the converter.

In the last step, the PC controls the transference of the data from the memory of the oscilloscope to the pc hard-disk where are stored and can be easily moved or processed. In this phase two multiplicative coefficients have to be set to convert the signals from volts to bars. The first coefficient is relative gain factor set in the charge amplifiers, the other coefficient is obtained from the calibration routine of the pressure transducers, described successively.

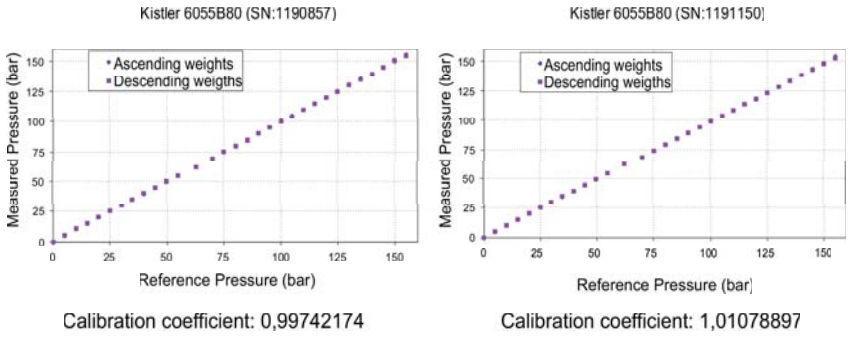

Figure A.3: Example of transducers calibration

A.1.2.1. Piezoelectric pressure sensors calibration

A careful calibration of the pressure sensors is essential to ensure that any difference between pressure records corresponding to the different transducers is due to a difference in the actual pressure signal, and not to any eventual discrepancy between the behavior of the transducers themselves.

Piezoelectric sensors generate an electrical charge when they are strained, this is a natural characteristic of the material they are made of. In the case considered, the in-cylinder pressure variation is the cause for the generation of electric charges on the sensor surface. Even though this type of sensors present a quasi-steady and approximatively linear response, the idea of performing a dynamic calibration has to be rejected. In fact, in this case, it would be necessary the development of a specific tool to simulate the changing in-cylinder pressure conditions, a task too complex and expansive. Therefore, in this study, a traditional method [261] based on a quasi-steady calibration by means of a Hotek 9000 Series hydraulic deadweight tester has been carried out.

In order to simplify the procedure and to avoid errors due to the incompatibility of the various components of the measuring system, it is convenient to calibrate at the same time the whole set of transducer, cable and amplifier. The calibration system is formed by a set of stainless steel, non magnetic weights that are positioned on a vertical free floating piston of well-known area. On the other side a screw pump generates a pressure that pushes the piston vertically upwards. When the system is balanced, the pressure in the hydraulic circuit will be determined by the weights loaded on the piston divided by effective area of the piston with corrections for value of acceleration due to gravity, air buoyancy and surface tension. Together with the deadweight tester a digital oscilloscope is used to visualize the signal given by the transducer-cable-amplifier set. The basic idea of this procedure is to compare the well-known pressure applied on the pressure transducer with the measured signal.

The first step of the calibration is to set the zero levels of the deadweight tester,

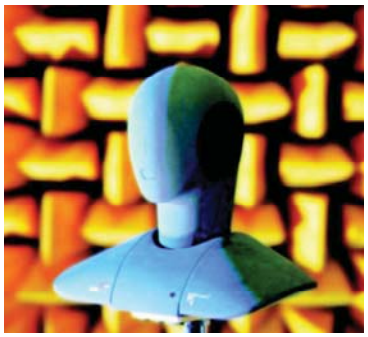

Figure A.4: Picture of the artificial head inside the anechoic chamber

the charge amplifier and the digital oscilloscope. The amplifier time constan is set on "Long", the range and other parameters of the amplifier and oscilloscope channel are adjusted. Two series of tests are performed, a first ascending the other descending the weights. The range of pressure during the calibration must include the maximal values of pressure achieved into the fired cylinders of an engine. In this study, using the various weights furnished with the tester, a pressure range between 5 and 155 bar has been covered. Through a linear interpolation, for each pressure transducer, the correlation coefficient between the reference pressure, obtained in the tester, and the pressure measured in the oscilloscope can be determined. Figure A.3 shows an example relative to two sensors calibration.

A.1.3. Binaural measurement system

Binaural recording is a method of recording audio which uses a special microphone arrangement in order to detect the noise physically in the same way the human beings do. Dummy head recording systems are used to figure in natural crossfeed or sonic shaping of the head and ear as well as sound reflections of shoulders and torso. This type of measurement is justified because in works where the recorded noise has to be not only quantified but also qualitatively analyzed through psychoacoustic parameters as well as subjectively estimated by means of listening tests [31, 82, 245].

A.1.3.1. Artificial Head

Figure A.4 shows the binaural measurement system HEAD Acoustics HMS III used in this work. This artificial head contains two microphones and simulates the torso and shoulders as well as the outer ear canals and all the acoustic relevant components of the human outer ear allowing aurally-accurate binaural recording of sound events.

24 bit technology together with the combination of analog and digital equalization enables the artificial head to achieve a high dynamic range, comparable to that encountered in the human auditory apparatus, approximately 120 dB.

The artificial head is connected to a RME DIGI98/8 Pro sound card that allows a direct transference of digital audio data to a PC. In the personal computer a set of softwares permit the control of the data acquisition, the choice of the measurement range as well as of an appropriate equalization of the acoustic signals. Five different modes of equalization are available: linear, directionally independent, free-field, diffusive field and also a user specific. The equalizers take account of the way the artificial head impacts the sound field. These settings have to be kept constant during all tests to avoid sound pressure level differences that could disturb subjective evaluation.

Another software installed in the same PC permits an automatic system check that detects any possible errors in the measurement chain, and guides the user through an accurate microphones calibration. A more detailed description of the artificial head calibration will be given in a following section.

A.1.3.2. Playback System

Binaural recording technique takes into account all characteristics of human aural perception, especially spatial hearing which represents an essential condition for a correct auditory impression during playback. The sounds indeed can be recorded and subjectively evaluated as well as objectively analyzed in a second time, this is the only way to get an easy comparison of sounds in a listening test. Furthermore, it avoids the dangerous situation that could represent the presence of people inside the anechoic chamber, listening in real time close by a running engine. Clear, spatial imaging and faithful, distortion-free reproduction of the recorded sounds at original volume are the requirements of a system for aurally-accurate playback of acoustical signals. In this way the listeners have the impression of being placed directly at the location of the sound events and are able to localize recorded sound sources.

To get a true-to-the-original reproduction of sound events the combination of the programmable equalizer PEQV and the power amplifier PVA 1V.3 of HEAD Acoustics, together with high-grade electrostatic headphones, have been used. Figure A.5 shows the set of equalizer (A), amplifier (B) and headphones (C). Playback equalization has to be matched to the Artificial Head equalization set at recording, furthermore, the playback system must be able to reproduce the high dynamic range of the recorded signal. The power amplifier has been designed specifically for the operation with electrostatic headphones (each amplifier is individually calibrated for one of the two associated headphones) and actually the electrostatic headphones are characterized by a 118 dB dynamic range, a broad frequency response and low distortion. Accordingly, this playback system ensures aurally-accurate, true-to-the-original reproduction of sound events [91].

Figure A.5: Picture of the play-back system

Figure A.6: Picture of the right artificial head microphone

Inside the ears of the artificial head are positioned two 1/2" electrostatic microphones. Figure A.6 shows a picture of the right microphone extracted from the torso head. Before every test both sensors, one by one, have to be calibrated. The calibration is performed through the control software of the binaural system, the microphone is coupled with a Brüel & Kyær 4228 pistonphone. This is a high precision sound source that emits 124 $\pm$ 0.2 dB (re. 20 μPa) at a frequency of 251.2 Hz $\pm$ 0.1 %. The pistonphone is individually calibrated by the producer with an uncertainty of less than 0.09 dB and a traceability supported by the Danish Primary Laboratory. The software that controls the binaural system during the calibration routine set the actual sound pressure level, corrected for static ambient pressure, to the nominal

A.1.3.3. Binaural system calibration

pistonphone level. Furthermore, after the calibration, the software permits an autocheck of the system indicating the gain factor to be applied to correct the measures. If the calibration has been performed correctly the gain factor equals zero.

A.1.4. ECU Control System

The Common Rail injection system is controlled and regulated electronically, this control system can be schematized in three blocks:

- Sensors and transmitters of theoretical values for the monitoring of the engine working conditions. These elements convert different physical magnitudes into

Parameter	Instrument
Atmospheric temperature (^oC)	Thermometer
Fuel temperature (^oC)	Thermistor
EGR (%)	Valve opening position
Rail pressure (bar)	Pressure transducer
Start of injection (^{o} before TDC)	ECU output
Injected quantity (mg/cc)	ECU output
Injector opening time (μs)	ECU output

Table A.1: List of parameters measured with the ECU control system

electrical signals.

- Electronic Control Unit (ECU) for the information processing, it analyzes the input data through mathematical algorithms and generates output electric signals.

- Actuators for the conversion of the ECU output signals to mechanical magnitudes.

The electronic control unit analyzes the parameters representative of the engine working condition: pressures, temperatures and mass rates, accelerator pedal position, engine speed, etc.. According to these input parameters and using maps of values stored in the ECU memory, the internal software commands the injection, regulating the pressure inside the rail and the injectors timing. Normally, the commercial ECUs are closed, that means that the parameters and maps stored in the memory can not be modified. In our study an open ECU has been used, this permitted to control with a software (INCA) installed in personal computer all the injection parameters independently. The use of this device allowed to obtain combustion noise variation keeping the engine speed and charge practically constant.

Furthermore, in every test, along with the in-cylinder pressure signals and noise, other parameters have been measured, in Table A.1 is presented the list of parameters that have been obtained taking advantage of the sensors used by the ECU control system.

The injection parameters of the list refer to a single injection, anyway, in this study different injection strategies have been considered:

- Single injection

- Conventional injection (pilot + main)

- Multiple injection (2 pilots + main and 2 pilots + main + post)

Furthermore, in order to corroborate the ECU output, an amperometric plier has been used to check the electric signal that commands the injector solenoid valve. The precision degree of the sensors used in commercial engines is not sufficiently adequate to control some parameters that have to be more accurately measured. For these

reason, in the next section, a further description of other experimental devices will be given.

A.1.5. Engine test bench

Parameter	Instrument
Engine speed (rpm)	Brake magnetic sensor
Load (Nm)	Brake charge cell
Brake cooling water temperature (^oC)	Thermocouple
Intake air mass rate (g/s)	Mass flowmeter
Intake temperature (^oC)	Thermocouple
Intake pressure (bar)	Pressure transmitter
Fuel mass rate (g/s)	Gravimetric balance
Exhaust temperature (^oC)	Thermocouple
Exhaust pressure (bar)	Pressure transmitter
Cooling circuit temperature (^oC)	Thermocouple
Lubricating circuit temperature (^oC)	Thermocouple
Accelerator pedal position (%)	Mechanical actuator
Atmospheric pressure (bar)	Manometer

Table A.2: List of parameters measured in the test bench

As commented before, the engine is coupled to an asynchronous electric brake, the main parameters relative to the brake are visualized in a personal computer using a software, Samaruc, developed at CMT-Motores Térmicos. This graphical interface indicates the main parameters that have to be monitored during the tests, giving warning alert in the case that certain limits of pressures and temperatures are exceeded. Furthermore, in the same PC are also showed other important engine parameters whose control have been considered essential for the goal of this research and that have been measured with apposite precision devices in the test bench. In Table A.2 are listed the main physical magnitudes visualized with the Samaruc together with the relative experimental instrument.

Bibliography

[1] ALBERS, P. and BRANDL, F.K. (1994)
Vehicle noise reduction strategies
Proceedings of SOBRAC Congress

[2] ALT, N.W.; WIEHAGEN, N.; STEFFENS, C. and HEUER, S.A. (2001)
Comprehensive combustion noise optimisation
SAE Paper 2001-01-1510

[3] ALT, N.W.; NEHL, J.; HEUER, S.A. and SCHLITZER, M.W. (2003)
Prediction of combustion process induced vehicle interior noise
SAE Paper 2003-01-1435

[4] ALT, N.; SONNTAG, H-D.; HEUER, S. and THIELE, R. (2005)
Diesel engine cold start noise improvement
SAE Paper 2005-01-2490

[5] ANDERTON, D. (1992)
Trends in I.C. engine noise generation and its effect on vehicle noise
ATA International Conference on Vehicle Comfort, Bologna

[6] ANDERTON, D. (1990)
Basic Origins of automotive engine noise
Course Notes, ISVR

[7] ANDERTON, D. (2003)
Noise source identification techiques
Course Notes, ISVR

[8] ANDERTON, D. (1979)
Relation between combustion system and noise
SAE Paper 790270

[9] ANDERTON, D. (1977)
Rate of heat release and Diesel engine noise
US Department of Transport Report DOT-TSC-OST-77-56

[10] ANDERTON, D. (1974)
Combustion as a source of Diesel engine noise
PhD Thesis, University of Southampton

[11] ANDERTON, D. and BAKER, J. (1973)
Influence of operating cycle on noise of Diesel engines
SAE Paper 730241

[12] ANDERTON, D. and PRIEDE, T. (1977)
The influence of automotive Diesel engine design on combustion, noise and performance
Proceedings of DOT Conference 730241

[13] ANDERTON, D., GROVER, E.C., LALOR, N. and PRIEDE, T. (1977)
The automotive Diesel engine - its combustion, noise and design
I. Mech. E. Paper C 14/77

[14] AOUICHI, A. and HERRMANN, M. (1989)
Diesel engine noise and internal excitation mechanisms
Proceedings of I. Mech. E. Conference **173**(19), London

[15] AOYAMA, T.; INAGAKI, M.; MORI, N.; IKEURA, O. and YAMAMOTO, K. (2000)
Analysis of main bearing force and cylinder block vibration related to engine air borne noise
JSAE Paper 20004145

[16] ATKINS, K.A. and CHALLEN, B.J. (1979)
A practical approach to truck noise reduction
I. Mech. E. Paper C 131/79, Appendix I

[17] AUSTEN, A.E.W. and PRIEDE, T. (1965)
Noise of automotive Diesel engines: its causes and reduction
SAE Paper 650165

[18] AUSTEN, A.E.W. and PRIEDE, T. (1958)
Origins of Diesel engine noise
Proceedings of I. Mech. E. Symposium on Engine Noise and Noise Suppression pp. 19-32, London

[19] BADAMI, M.; MALLAMO, F.; MILLO, F. and ROSSI, E.E. (2002)
Influence of multiple injection strategies on emissions, combustion noise and BSFC of a DI common rail Diesel engine
SAE Paper 2002-01-0503

[20] BALIGAND, B.; GARNIER, F.; HAUPAIS, A. and VAUCHER de la CROIX, D. (1998)
Combustiomètre : procédé pour quantifier le bruit de combustion d'un moteur Diesel
3ème Conférence Internationale CETIM sur les méthodes de surveillance et techniques de diagnostic acoustiques et vibratoires - SFM/SFA/IMEKO **1**, pp. 87-96, Senlis

[21] BALIGAND, B.; PERRIN, D.; FERNIER, D.; GUIOT B.; HAUPAIS A. and TRAVERT, M. (2001)

Quantification of the combustion noise of Diesel engine by the Combustiometre
European Automotive Congress, Bratislava 18-20 June 2001 SAITS 01182

[22] BAKER, J.M. (1990)
Engine noise harshness and its relation to bearing design
Course Notes, ISVR

[23] BAUDAOUI, M.E.; DANIÈRE J.; GUILLET F. and SERVIÈRE, C. (2005)
Separation of combustion noise and piston-slap in diesel engine-PartI: Separation of combustion noise an piston-slap in diesel engine by cyclic Wiener filtering
Mechanical System and Signal Processing 19 1209-1217

[24] BAXA, D.E. (1982)
Noise control in internal combustion engines
John Wiley & Sons, New York

[25] BEECK, M.A. and HENTSCHEL(2000)
Laser metrology - a diagnostic tool in automotive processes
Optics and Lasers in Engineering **34**, pp. 101-120

[26] BEIDL, C.V. and STÜCKLSCHWAIGER(1997)
Application of the AVL Annoyance Index for engine noise quality development
Acustica **83**, pp. 789-795

[27] BERGE, T. (1983)
Active noise cancellation of low frequency sound inside vehicle cabs
Proceedings of Inter-Noise **1**, pp. 457-460

[28] BERTOLO, R. and WORSFOLD, J.H. (1969)
Medium speed Diesel engine noise
Proceedings of I. Mech. E. Conference **183**(1), p. 129

[29] BISPING, R. (1995)
Emotional effect of car interior sounds; pleasantness and power and their relation to acoustic key features
Proceedings of SAE Conference on Noise and Vibration '95 **2**, pp. 1203-1209

[30] BISPING, R. and GIEHL, S. (1996)
Psychological analysis of the sound quality of vehicle interior noise: field and laboratory experiments
Proceedings of AVL Conference on Engine and Environment '96, pp. 65-86

[31] BLAUERT, J. and GENUIT, K. (1993)
Sound environment evaluation by binaural technology: some basic consideration
Journal of Acoustic Society of Japan **14**, pp. 139-145

[32] BLAUERT, J. and JEKOSCH, U. (1997)
Sound quality evaluation - a multi layered problem
Acustica **83**, pp. 747-753

[33] BODDEN, M. (1997)
Instrumentation for sound quality evaluation
Acustica **83**, pp. 775-783

[34] BOESCH, N.J.W. (1987)
The development of low noise DI Diesel engines
SAE Paper 870951

[35] BOLTON KNIGHT, B.L. (1971)
Engine mounts: analytical methods to reduce noise and vibration
I. Mech. E. Paper C 98/71

[36] BORRIONE, S.M. and VACCARINO, P.D. (2000)
Pressure indicating analysis on a common rail DI Diesel engine in transient operating condition
4. Internationales Symposium für Verbrennungsdiagnostik, Baden-Baden

[37] BOSSMEYER, T.M.; HANSKNECHT, D.J. and KÖNIG,D. (1992)
Time-frequency analysis of knock in spark ignition engines
Proceedings of EUSIPCO, pp. 1765-1768

[38] BOWEN, C.E.; READER, G.T. and POTTER,I.J. (1997)
The effect of exhaust gas recirculation on the combustion noise level of a indirect injection Diesel engine
Proceedings of the 32^nd *Intersociety Energy Conversion Engineering Conference* $V\ (3-4)$, *Honolulu, HI, USA, 1997*, pp. 2089-2093

[39] BRAGG, S.L. (1963)
Combustion noise
Journal of the Institute of Fuel **36**(12)

[40] BRANDL, F.K. (1992)
Low noise engine concepts to meet future legislative vehicle requirements
Proceedings of Eurosymposium on The Mitigation of Traffic Noise in Urban Areas, Nantes

[41] BRANDL, F.K.; AFFENZELLER, J. and THIEN, G.E. (1987)
Some strategies to meet future noise regulations for truck engines
SAE Paper 870950

[42] BRANDL, F.K. and BEIDL, C. (1996)
Optimization of motor vehicles acoustics at AVL with state-of-the art test ring technology
Proceedings of AVL Conference on Engine and Environment '96, pp. 147-177

[43] BRANDL, F.K. and BIERMAYER, W. (1999)
A new tool for the onboard objective assessment of vehicle interior noise quality
Proceedings of SAE Noise & Vibration Conference & Exposition, Traverse City

[44] BRANDL, F.K.; BIERMAYER, W. and STÜCKLSCHWAIGER, W. (1998)
Objective assessment of vehicle noise quality as a basic for sound engineering
JSAE Spring Convention, Yokohama

[45] BRANDL, F.K.; WÜNSCHE, P. and GSCHWEITL, E. (1991)
Design strategies for low noise engine concepts
SAE Paper 911070

[46] BRECHBÜHL, S.; SCHNEPF, M. and WOLFER, P. (2000)
New opportunities to measure pressures inside combustion engine without having separate drilling for the pressure-sensors
Internationales Symposium Für Verbrennungsdiagnostik

[47] BROATCH, A.; MARGOT, X.; GIL, A. and DONAYRE, J. (2007)
Computational study of the sensitivity to ignition characteristics of the resonance in DI diesel engine combustion chambers
International Journal for Engineering Computations **24**, pp.77-96

[48] BRYAN, M.E. (1976)
A tentative criterion for acceptable noise level in passenger vehicles
JSV **48**(4), pp. 525-535

[49] BUSCH, G.; MAURELL, R.; MEYER, J. and VORWERK, C. (1991)
Investigations on influence of engine block design features on noise and vibration
SAE Paper 911071

[50] CALLOW, G.D.C. and HEDGES, B. (1979)
The subjetive response of occupants to the noise inside vehicles and addentum: A brief subjective evaluation of noise inside cars fitted with a Diesel engine compared with a petrol engine
Motor Industry Research Association Report 1979/1 and Diesel engined vehicle addendum

[51] CARTELLIERI, W.P.; CICHOCKI, R.; THIEN, G.E. and FACHBACH, H.A. (1977)
The swirl supported Direct Injection Diesel combustion system - its potential of meeting economical and environmental requirements
I. Mech. E. Paper C 11/77

[52] CAVALCANTI, J.L.L.; FRISSE, H.P. and WEISCH, G.K. (1995)
Development and refinement of a new engine family to achieve future noise legislation and acoustic driving comfort requirements
I. Mech. E. Paper C 11/77

[53] CERDÁ, S.; ROMERO, J.; NAVASQUILLO J. and ZURITA, G. (2001)
Análisis tiempo-frequencia de las resonancias en la combustión
Revista de Acústica Vol.XXXII N. 1 y 2

[54] CHABOT, L.; YATES O.G.K. and BELL D.J. (1997)
Noise and vibration optimisation of a gasoline engine
Proceedings of the Fifth Ricardo Software International User Conference Detroit 1997 750798

[55] CHALLEN, B.J.; ATKINS, K.A. and CROCKER, D.M. (1980)
Transient and steady noise in automotive Diesel engines
Conference on Diesel Engine Noise Research '80, Loughborough University

[56] CHALLEN, B.J. and CROCKER, D.M. (1982)
A review of recent progress in Diesel engine noise reduction
SAE Paper 820517

[57] CHAMPAGNE, A.J. and SHIAU, N.-M. (1997)
Commercial van Diesel idle sound quality
SAE Paper 971980

[58] CHANG, J.; KIM, M. and MIN, K. (2002)
Detection of misfire and knock in spark ignition engines by wavelet transform of engine block vibration signals
MST Paper **13**, pp. 1108-1114

[59] CHIU, H.H. and SUMMERFIELD, M. (1974)
Theory of combustion noise
Acta Astronautica **1**(967)

[60] CHO, S.H.; Ahn S.T. and KIM, Y.H. (2002)
A simple model to estimate the impact force induced by the piston slap
Journal of Sound and Vibration **255**(2) 229-242

[61] CHRISTEN, U.; CHEVALIER A.; MORAAL P. and SCHOLL, D. (2006)
A wavelet-based combustion noise meter
Proc. of International Coherence on Control Applications Munich, October 4-6 2006 pp. 533-538

[62] CROKER, M.D. (1988)
The analysis and control of engine noise quality
I. Mech. E. Paper C 16/88

[63] CROKER, M.D. (1985)
Engine structure analysis for low noise - the options
SAE Paper 850970

[64] CROCKER, M.J. and HAMILTON J.F. (1979)
Modeling of Diesel engine noise using coherence
SAE Paper 790362

[65] DEJONG, R.G. and PARSONS, N.E. (1980)
High frequency vibration transmission through the moving parts of an engine
SAE Paper 800405

[66] DESANTES, J.M.; TORREGROSA, A.J. and BROATCH, A. (2001)
Wavelet transform applied to combustion noise analysis in High-Speed DI Diesel engines
SAE Paper 2001-01-1545

[67] DEXTER, M.; EVENSEN, H.; VAN KARSEN, C. and BLOUGH, J. (1999)
Extractio/Filtration of transient embebbed in stationary signals using wavelets; focus on extraction of frequency response functions
SAE Paper 1999-01-1824

[68] DHAENENS, M.; VAN DER LINDEN, G.; NEHL J. and THIELE, R. (2001)
Analysis of transient noise behavior of truck diesel engine
SAE Paper 2001-01-1566

[69] DHULIPUDI, M.R.; PRAKASH, J. and JAYARAMAN, S. (2007)
Engine cover radiated noise estimation using Statistical Energy Analysis approach
SAE Paper 2007-01-2301

[70] DIXON, J.D. (2003)
Gears, chains and belts
Course Notes ISVR

[71] DIXON, J.D. (2003)
Engine component nvh case histories
Course Notes ISVR

[72] DIXON, J.D. (2003)
Practical engine design for low noise
Course Notes ISVR

[73] DOAK, P.E. (1972)
Analysis of internally generated sound in continuous materials: 2. a critical review of the conceptual adequacy and physical scope of existing theories of aerodynamic noise with special reference to supersonic jet noise
JSV **25**(263)

[74] FASTL, H. (1997)
The psychoacoustics of sound quality evaluation
Acustica **93**, pp. 754-764

[75] FERRARI, G. (1992)
Motori a combustione interna
Edizioni il Capitello

[76] FISH, D.G. (1999)
Consideration of the age related hearing ability (presbycusis) in the definition of vehicle interior noise targets
I. Mech. E. Paper C 389/468

[77] FISH, D.G. (1992)
Vehicle noise quality - towards improving the correlation of objective measurements with subjective ratings
I. Mech. E. Paper C 389/468

[78] FONTANET, M.P. (1978)
Le bruit des véhicules - influence du spectre de la pression de combustion - etude de la vibration de carters moteur
Ingénieurs de l'Automobile 6-78, pp. 397-404

[79] FORD; HAYES and SMITH (1979)
Engine noise reduction by structural design using advanced experimental and finite element methods
Ingénieurs de l'Automobile 6-78, pp. 397-404

[80] GARDNER, B.K. and BERNHARD, R.J. (1987)
An experimental/numerical noise source identification technique
SAE Paper 870995

[81] GENUIT, K. (1992)
Procedure of objectivisation of subjectively perceived sound quality
Proceedings of I. Mech. E. Conference C 369, Paper 344

[82] GENUIT, K. and BURKHARD, M. (1992)
Artificial head measurement systems for subjective evaluation of sound quality
ISV Conference '92 S. 18

[83] GENUIT, K. and GIERLICH, H.W. (1989)
Investigation of the correlation between objective noise measurement and subjective classification
SAE Paper 891154

[84] GROVER, E.C. (1990)
Automotive gear box noise
Course Notes ISVR

[85] GU, F.; ; LI, W.; BALL, A.D. and LEUNG, A.Y.T. (2000)
The condition monitoring of Diesel engines using acoustic characteristics of the engine and representation of the acoustic signals
SAE Paper 2000-01-0730

[86] GUSKI, R. (1997)
Psychological methods for evaluating sound quality and assessing acoustic information
Acta Acustica

[87] HÄRLE, N. and BÖHME, J.F. (1987)
Detection ok knocking for spark ignition engines based on structural sounds
Proceedings of IEEE-ASSP, pp. 1744-1747

[88] HASHIMOTO, T.; HATANO, S. and SAITO, H. (1995)
Improvement of sound quality of exterior idling noise of small Diesel truck
SAE Paper 951289

[89] HASSAN, H.A. (1974)
Scaling of combustion generated noise
Journal of Fluid Mechanics **66**, 445

[90] HEAD ACOUSTICS GmbH (1995)
Psychoacoustic parameters and statistical analysis in the BAS
Appendix C of the Binaural Analysis System Manual

[91] HEAD ACOUSTICS GmbH (1995)
Artemis 2.0 Manual

[92] HEAD, H.F. and WAKE, J.D. (1980)
Noise of Diesel engines under transient conditions
SAE paper 800404

[93] HECKL, M. (1990)
Introduction to acoustics, aspects of vehicle acoustics
Proceedings of AVL Conference on Engine and Environment '90, pp. 29-32

[94] HERBERT, A.J. and RUSSEL, M.F. (1982)
A coherence model for piston impact generated noise
Proceedings of I. Mech. E. conference, pp. 34-39

[95] HERBERT, A.J. and RUSSEL, M.F. (1975)
Identification and modelling of rotary fuel injection pump noise processes
SAE paper 750803

[96] HICKLING, R.; FELDMAIER, D.A.; CHEN, F.H.K. and MOREL, J.S. (1983)
Cavity resonances in engine combustion chambers and some applications
JASA **73**, pp. 1170-1178

[97] HICKLING, R.; FELDMAIER, D.A. and SUNG, S.H. (1979)
Knock induced cavity resonances in open chamber Diesel engines
JASA **65**(6), pp. 1474-1479

[98] HIRANO, I et al. (1999)
Using multiple regression analysis to estimate the contributions of engine radiated noise
JSAE Review **20**(3)

[99] HÖLDRICH, R. and PFLÜGER, M. (1999)
A generalized psychoacoustical model modulation parameters (Roughness) for objective vehicle noise quality evaluation
SAE Paper 1999-01-1817

[100] HONDA, Y.; WAKABAYASHI, K.; KODAMA, T.; YAMAZAKI, H. and KIHARA, R. (2000)
A study on noise and vibration reduction of small Diesel engine cylinder block for automobile
SAE Paper 2000-01-0527

[101] HOTTA, Y.; INAYOSHI, M.; and NAKAKITA, K. (2002)
Achieving lower exhaust emissions and better performance in HSDI Disel engine with multiple injection
R & D Review of Toyota CRDL **37** (3), pp. 9-16

[102] HUSSAIN, M.; PFLÜGER, M. and BRANDL, F.K. (1998)
Intercultural differences in annoyance response to vehicle interior noise
Euronoise '98, Munich

[103] HUSSAIN, M.; GÖLLES, J.; RONACHER, A. and SCHIFFBÄNKER, H. (1991)
Statistical evaluation of an annoyance index for engine noise recordings
SAE Paper 911080

[104] IHLENBURG, F. (2003)
The medium-frequency range in computational acoustics: practical and numerical aspects
J. Comp. Acoust. **11**(2), pp. 175-193

[105] IMAI, M.; SUZUKI, S.; SUGIURA N. and SATO, H. (1986)
Radiation efficiency of engine etructures, analyzed by holographic interferometry and boundary element calculation
SAE Paper 861411

[106] INGHAM, R.; OTTO, N. and McCOLLUM, T. (1999)
Sound quality metric for Diesel engines
SAE Paper 1999-01-1819

[107] ISHIHAMA, M.; SAKAI, Y.; KATANO, I and NAKAMURA, K. (2003)
Effects of combustion process on engine sound quality
Proceedings JSAE Annual Congress 2003, **39** (03), pp.9-12

[108] IZUMI, S.; ISHIDA, M.; MAEDA, T.; TAKEMI, M. et al. (1987)
Studies on combustion, vibration and noise in High Speed Diesel engine through newly developed measuring instruments
CIMAC 1987, Warzaw

[109] KAHN, I.M. et al. (1977)
Prediction of Diesel engine noise
I. Mech. E. Paper C 15/77

[110] KAHN, M.S.; JOHANSSON, Ö.; LINDBERG, W. and SUNDBÄCK, U. (1997)
Development of an annoyance index for heavy duty Diesel engine noise using multivariate analysis
Noise Control Engineering Journal **45**(4)

[111] KAHN, M.S.; JOHANSSON, Ö.; LINDBERG, W. and SUNDBÄCK, U. (1995)
Annoyance of idling Diesel engine noise evaluated by multivariate analysis
Noise Control Engineering Journal **43**(6)

[112] KAMP, H. and SPERMANN, J. (1995)
New methods of evaluating and improving piston related noise in internal combustion engines
SAE Paper 951238

[113] KANDA, H.; OKUBO, M. and YONEZAWA, T. (1990)
Analysis of noise source and their transfer paths in Diesel engine
SAE Paper 900014

[114] KELLEY, H.H.; HOVÖAND, C.I.; SCHWARTZ, M. and ABELSON, R.P. (1955)
The influence of judges' attitudes in three methods of attitude scaling
Journal of Social Psychology **42**, pp. 179-198

[115] KISTLER (2004)
Piezoelectric Theory
20.290e-05.04

[116] KOJIMA, N. (1989)
An evaluation of combustion noise generation in Diesel engine structure
SAE Paper 890126

[117] KOJIMA, N.; ITOH, K. and FUKUDA, M. (1986)
Analysis of combustion induced noise of engine by single explosion excitation
Bulletin of JSME **29**(257), pp. 3815-3821

[118] KONDO, M.; KIMURA, S.; HIRANO, I.; URAKI, Y. and MAEDA, R. (2000)
Development of noise reduction technologies for a small direct injection Diesel engine
JSAE Paper 20004142

[119] KÖNIG, D. (1996)
Application of time-frequency analysis for optimum non-equidistant sampling of automotive signals captured at knock
Proceedings of the IEEE International Conference on Acoustics, Speech and Signal Processing 1996 **V**, pp. 2746

[120] KUBOZUKA, T.; HAYASHI, Y.; HAYAKAWA, Y. and KIKUCHI, K. (1983)
Analytical study on engine noise caused by vibration of the cylinder block and crankshaft
SAE Paper 830346

[121] LANGLEY, R.F. and BREMMER, P.(1999)
A hybrid method for the vibration analysis of complex structural-acoustic systems
JASA **105**(3), pp. 1657-1671

[122] LALOR, N. (1988)
Fundamentals of low engine noise design
Engine noise and vibration control course notes, ISVR

[123] LALOR, N. (1988)
Engine structure vibration, low noise engine design
Engine noise and vibration control course notes, ISVR

[124] LALOR, N. (1982)
Finite element optimisation techniques of Diesel engine structures
SAE Paper 820437

[125] LALOR, N. (1979)
Computer optimised design of engine structures for low noise
SAE Paper 790364

[126] LALOR, N.; GROVER, E.C. and PRIEDE, T. (1980)
Engine noise due to mechanical impacts on piston and bearings
SAE Paper 800402

[127] LALOR, N. and PETYT, M. (1975)
Modes of engine structure vibration as source of noise
SAE Paper 750833

[128] LAMOTTE, L. and BEGUET, B. (1999)
Quantification of sound quality for engine in stationnary and run-up conditions
SAE Paper 1999-01-1815

[129] LAMOTTE, L. and BEGUET, B. (1998)
QUALIdB: a software to quantify sound quality
Euronoise '98 Paper

[130] LAPUERTA, M., ARNAS, O. and HERNANDEZ, J.J. (1999)
Diagnosis of DI diesel combustion from in-cylinder pressure signal by estimation of mean thermodynamic properties of the gas
Applied Thermal Engineering, Vol. 19 No. 5, pp. 513-29.

[131] LEIPOLD, F. and BERGMANN, H. (1996)
Development stages for reducing noise emissions of the new OM 904 LA commercial vehicle engine
Proceedings of AVL Conference on Engine and Environment '96, pp. 319-322

[132] LI, Z.; AKISHITA, S. and KATO, T. (1997)
Engine failure diagnosis with sound signals using the wavelet trasnform
SAE Paper 970034, pp. 79-86

[133] LIM, T.C. and WITER, A.K. (2000)
Experimental characterization of engine crankshaft rumble noise signature
Applied Acoustics **60**, pp. 45-62

[134] LYN, W.T. (1961)
Calculations of the effect of rate of heat release on the shape of cylinder pressure ad cycle efficiency
Proceedings of I. Mech. E. Conference on Auto. Dir. **1**, pp. 34-62

[135] MAEDA, O.; MAEKAWA, Y. and NOMURA, K. (1987)
Development of an engine noise evaluation meter
SAE Paper 870965

[136] MAEKAWA, M. et al. (1994)
A study of low noise crankcase structure for light commercial vehicle
SAE Paper 942267

[137] MAETANI, Y.; NIIHURA, T.; SUZUKI, S.; ARAI, S. and OKAMURA, H. (1993)
Analysis and reduction of engine front noise induced by the vibration of the crankshaft system
SAE Paper 931336, pp. 1694-1700

[138] MALLAMO, F.; BADAMI, M. and MILLO, F. (2002)
Analysis of multiple injection strategies for the reduction of emissions, noise and BSFC of a DI small displacement non-road Diesel engine
SAE Paper 942267

[139] MARANT, V. (2005)
Contribución al análisis de la calidad sonora del ruido de combustión de los motores Diesel de inyección directa
Tesis Doctoral, Universidad Politecnica de Valencia

[140] MARTÍN DÍAZ, J. (2007)
Aportación al diagnóstico de la combustion en motores diesel de inyección directa
Tesis Doctoral, Universidad Politecnica de Valencia

[141] MIYASHITA, N. (1996)
Strategy of engine noise for trucks and buses
Proceedings of AVL Conference on Engine and Environment '96

[142] MIYASHITA, N. et al. (1994)
Automotive Diesel Engines - Fundamental technologies and applications for R & D Engineers
Sankaido Co., Ltd., Tokyo

[143] MIYAZAWA, T. (1987)
Analysis of vibration and noise for Diesel engines
Internal Combustion Engine Paper **26**(326)

[144] MOLINARO, F., CASTANIE, F. and DENJEAN, A. (1992)
Knocking recognition in engine vibration signal using wavelet transform
Proceedings of IEEE-SP International Symposium, pp. 353-356

[145] MORRISON, D.; CHALLEN, B.J. and TRELLA, T. (1980)
Passenger car noise control measures and their effects on fuel economy, weigth and cost
SAE Paper 800439

[146] MOSER, F.X.; SPESSERT, B. and HALLER, H. (1996)
Possibilities of noise reduction in commercial and industrial Diesel engines
Proceedings of AVL Conference on Engine and Environment '96, pp. 349-370

[147] MURATA, H.; TANAKA, H.; TAKADA, H and OHSASA, Y. (1993)
Sound quality evaluation of passenger vehicle interior noise
SAE Paper 931932

[148] MURAYAMA, T. and KOJIMA, N. (1974)
Studies on the combustion noise in Diesel engine*JSME Paper* **40**(336)

[149] MURAYAMA, T.; KOJIMA, N. and SATOMI, Y. (1976)
A simulation of Diesel engine combustion noise
SAE Paper 760552

[150] NAKAMURA, M. and JACOBSEN, T. (1988)
Measurement in Cars Using the RASTI Method
Application Notes AN BO 0244-11, BruelBrüel & Kjaer

[151] NAKANO, M. and MINAMI, T. (1985)
Holographic vibration analysis and a study of engine noise control
SAE Paper 850323

[152] NAKASHIMA, K. et al. (1991)
Measurement of structural attenuation of a Diesel engine and its application for reduction of noise and vibration
SAE Paper 912710

[153] NEHL, J.; WILHEM, M.; GAUCH, P. and TRAVERT, M. (1999)
Evaluation of crankshaft clearance influence on specific Roughness noise concern
SAE Paper 1999-01-1771

[154] OBERTO, L. and MANGIANTINI, R. (1996)
Noise vehicle refinement of Bravo, Brava and Marea with new turbo Diesel engine
Proceedings of AVL Conference on Engine and Environment '96, pp. 133-141

[155] OHTA, K.; IRIE, Y.; YAMAMOTO, K. and ISHIKAWA, H. (1987)
Piston slap induced noise and vibration of internal combustion engines (1st report, theoritical analysis and simulation)
SAE Paper 870990

[156] ÖNSAY, T. (1994)
The use of wavelets transform and frames in NVH applications
Michigan State University

[157] OTTO, N.C. (1997)
Listening test methods for automotive sound quality
Proceedings of the Audio Engineering Society 1997, New York

[158] OTTO, N.C.; AMMAN, S.; EATON, C. and LAKE, S. (1999)
Guidelines for jury evaluations of automoive sounds
SAE Paper 1999-01-1822

[159] OZAWA, H. and NAKADA, T. (1999)
Pseudo cylinder pressure excitation for analyzing the noise characteristics of the engine structure
JSAE Review **20**, pp. 67-72

[160] PADOAN, M.R. (1978)
Réduction des bruits des moteurs Diesel
Ingénieurs de l'Autombile 6-78

[161] PATRO, T. (1997)
Combustion induced powertrain NVH - a time-frequency analysis
SAE Paper 971874

[162] PAYRI, F.; BROATCH, A.; MARGOT, X. and MONELLETTA, L. (2009)
Sound quality assessment of Diesel combustion noise using in-cylinder pressure components
MST Paper **20**,**1**, 015107 (pp.1-12)

[163] PAYRI, F.; BROATCH, A.; TORMOS, B. and MARANT, V. (2005)
New Methodology for in-cylinder pressure analysis in DI Diesel engines - Application to combustion noise
MST Paper **16**, pp.540-547

[164] PAYRI, F.; TORREGROSA, A.; BROATCH, A. and MARANT, V. (2003)
Análisis del ruido de combustión de motores Diesel de inyección directa
Proceedings of III Congreso Bolivariano de Ingeniería Mecánica

[165] PAYRI, F.; TORREGROSA, A.; BROATCH, A.; MARANT, V. and BEAUGE, Y. (2002)
Méthodologie d'étude de la qualité du bruit de combustion d'un moteur Diesel automobile à partir de l'analyse de sa pression en cylindre
Acoustique et Techniques **30**, pp. 25-29

[166] PAYRI, F.; TORREGROSA, A.; BROATCH, A. and MONELLETTA (2006)
An innovative approach to level reduction and sound quality enhancement of combustion noise Diesel engines
International Congress of Innovative Solutions for the Advancment of Transport Industry TRANSFAC'06. San Sebastian (Spain), 4-6 October 2006

[167] PAYRI, F.; TORREGROSA, A.; BROATCH, A. and MONELLETTA (2008)
A novel approach to overall level evaluation of Diesel Combustion noise in transient operation
GPC GLOBAL POWERTRAIN CONGRESS 2008. Vaals, The Netherlands, 10-11 June 2008

[168] PAYRI, F.; TORREGROSA, A.; BROATCH, A. and MONELLETTA (2009)
Assessment of Diesel combustion noise overall level in transient operation
Article submitted and accepted for pubblication in IJAT Int. Journal of Automotive Technology from Korean Society of Automotive Engineers (KSAE)

[169] PFLÜGER, M., HÖLDRICH, R.; BRANDL, F.K. and BIERMAYER, W. (1999)
Subjective assessment of Roughness as a basis for objective vehicle interior noise quality evaluation
SAE Paper 1999-01-1850

[170] PISCHINGER, F.; SCHMILLEN, K. and LEIPOLD, F. (1979)
A new measuring method for the direct determination of Diesel combustion noise
SAE Paper 790267

[171] PISCHINGER, S.; BIERMANN, B; HAAKE, B.; WIEHAGEN, N. and BORGGRÄFE, J. (1998)
Verbrennungsgeräuschoptimierung Ottomotor, Interaktion Akustik-Thermodynamik
7. Aachener Kolloquium Fahrzeug- und Motorentechnik

[172] PRIEBSCH, H.H. et al. (1998)
Simulation of engine noise - influence of design parameters
JSAE Spring Convention Proceedings **984**, pp. 209-212

[173] PRIEBSCH, H.H.; AFFENZELLER, J. and KLUIPERS, G. (1990)
Structure borne noise prediction techniques
SAE Paper 900019

[174] PRIEBSCH, H.H.; AFFENZELLER, J. and KLUIPERS, G. (1990)
Prediction technique of vibration transfer in engines
I. Mech. E. Paper C 420/023

[175] PRIEBSCH, H.H.; HELLINGER, W.; LOIBNEGGER, B. and RAINER, G.Ph. (1992)
Application of a computer simulation for the prediction of vibration and noise in engines
Proceedings of ATA 3rd International Conference, Firenze

[176] PRIEDE, T. (1992)
Noise and vibration control of the internal combustion reciprocating engine
Chapter 19 of "Noise and vibration control Engineering", BERANEK, L.L. and VER, I.L., John Wiley & Sons, New York

[177] PRIEDE, T. (1980)
In search of origins of engine noise - an historical review
SAE Paper 800534

[178] PRIEDE, T. (1979)
Problems and developments in automotive engine noise research
SAE Paper 790205

[179] PRIEDE, T. (1966)
Some studies into origins of automotive Diesel engine noise and its control
11th Automobile Technisher FISITA Kongress Paper c12, München

[180] PRIEDE, T. (1961)
Relation between form of cylinder pressure diagram and noise in Diesel engine
Four Papers on Diesel Engine Fuel Injection, Combustion and Noise, Proceedings of I. Mech. E. Conference, London

[181] PRIEDE, T. et al. (1970)
Origins of reciprocating engine noise - its characteristics, prediction and control
ASME Paper 70-WA/DGP-3

[182] PRIEDE, T.; ANDERTON, D.; DIXON, J.; GROVER, E.C. and LAYLOR, N. (1984)
Evolution and design principles of low noise lightweight engines
I. Mech. E. Paper C 33/84

[183] PRIEDE, T.; AUSTEN, A.E.W. and GROVER, E.C. (1964)
Effects of engine structure on noise of Diesel engines
I. Mech. E. Paper **179**(4)

[184] PRIEDE, T.; BARER, J.M.; GROVER, E.C. and GHAZY, R. (1985)
Characteristics of exciting forces and structural response of turbocharged Diesel engines
SAE Paper 850972

[185] PRIEDE, T. and GROVER, E.C. (1970)
Application of acoustic diagnostics to internal combustion engines and associated machinery
Proceedings of I. Mech. E. Symposium on Acoustics as a Diagnostic Tool

[186] PRIEDE, T.; GROVER, E.C. and ANDERTON, D. (1968)
Combustion induced noise in Diesel engines
Proceedings of Diesel Engines Users Association Congress **317**, London

[187] PRIEDE, T. and GROVER, E.C. (1966)
Noise from industrial Diesel engines
Proceedings of Symposium on noise from power plant equipment, Southampton September 1966

[188] QUINN, D.C. and HOFE, VON R. (1997)
Engineering vehicle sound quality
SAE Paper 972063

[189] RANDALL, R.B.; REN, Y. and NGU, H. (1996)
Diesel engine cylinder pressure reconstruction
Proceedings of IISMA21 on Noise and Vibration Engineering

[190] RAKOPOULOS, C.D. and GIAKOUMIS, E.G. (2009)
Diesel engine transient operation
Springer

[191] READER, G.T.; BOWEN, C.E. and POTTER, I.J. (1999)
Combustion noise from a Diesel engine operating with high concentrations of intake carbon dioxide
SAE Paper 1999-01-2713

[192] REINHART, T.E. (1987)
An evaluation of the Lucas combustion noise meter on cummins B series engines
SAE Paper 870952

[193] REN, Y.; RANDALL, R.B. and MILTON, B.E. (1999)
Influence of the resonant frequency on control of knock in Diesel engines
I. Mech. E. Paper D04767, pp 127-133

[194] RICHMOND, J.W. and PARKER, D.A. (1987)
The quantification and reduction of piston slap noise
Proceedings of I. Mech. E. Conference 1987 **201**(D4)

[195] RINOLFI, R. and IMARISIO, R. (1997)
The potentials of third generation direct injection Diesel engine for passenge cars
Proceedings of AVL Conference on Engine and Environment '97

[196] RÖHRLE, M.D. (1975)
Affecting Diesel engine noise by the piston
SAE Paper 750799

[197] RUGGIERO, A. and SENATORE, A. (2003)
Computer model for the prediction of the impact force induced by piston slapin internal combustion engines *The Annals of University "Dunarea de Jos" of Galati*, fascicle**VIII**, ISSN 1221-4590, pp. 129-134

[198] RUSPA, G.; SCHELLINO, G. and TURINO, G. (1989)
Sound quality in Diesel powered passengers cars
Proceedings del 5° Congresso Nazionale del CNR-PFT-Napoli **42**(1-2), pp. 19-24

[199] RUSSEL, M.F. (1996)
Sound quality in Diesel powered passengers cars
Proceedings of AVL Conference on Engine and Environment '96, pp. 105-121

[200] RUSSEL, M.F. (1982)
Diesel engine noise: control at source
SAE Paper 820238

[201] RUSSEL, M.F. (1977)
Noise control strategy for manufacters and users
I. Mech. E. Paper C 252/77

[202] RUSSEL, M.F. (1974)
Control of noise from conventional Diesel engine
Annual Institute of Physics Conference Paper 11, University of Aston, Birmingham

[203] RUSSEL, M.F. (1973)
Automotive Diesel engine noise and its control
SAE Paper 730243

[204] RUSSEL, M.F. (1972)
Reduction of noise emissions from Diesel engine surfaces
SAE Paper 720135

[205] RUSSEL, M.F. and CAVANAGH, E.J. (1979)
Establishing a target for control of Diesel combustion noise
SAE Paper 790271

[206] RUSSEL, M.F.; GREEVES, G. and GUERRASSI, N. (2000)
More torque, less emissions and less noise
SAE Paper 2000-01-0942

[207] RUSSEL, M.F. and HAWORTH, R. (1985)
Combustion noise from High Speed Direct Injection Diesel engines
SAE Paper 850973

[208] RUSSEL, M.F., WORLEY, S.A. and YOUNG, C.D. (1987)
Towards an objective estimate of subjective reaction to Diesel engine noise
SAE Paper 870958

[209] RUSSEL, M.F. and YOUNG, C.D. (1987)
Diesel combustion noise measurement
Automotive Engineering, **12**(2), pp. 32-34

[210] RUSSEL, M.F.; YOUNG, C.D. and NICOL, S.W. (1990)
Modulation of injection rate to improve direct injection Diesel engine noise
SAE Paper 900349

[211] RUST, A. and PLUEGER, M. (2000)
Future demands for Diesel engine acoustics
Proceedings of the International SIA Congress "What challenges for the diesel engine of the year 2000 and beyond", Lyon

[212] RUST, A.; SCHIFFBÄNKER, H. and BRANDL, F.K. (1989)
Complete NVH optimisation of a passenger vehicle with a DI Diesel engine to meet subjective market demands and future legislative requirements
SAE Paper 890115

[213] RUST, A. and THIEN, G.E. (1987)
Combustion noise of direct injection Diesel engines under transient conditions
MTZ **48**

[214] SAAD, A.A.A. and EL-SEBAI, N.A. (1999)
Combustion noise prediction inside Diesel engine
SAE Paper 1999-01-1774

[215] SATO, N. and MIURA, Y. (1999)
Study of exterior idling sound quality evaluation method for Diesel engine trucks
SAE Paper 1999-01-1739

[216] SCARTH, P. and ORTIZ, D. (2004)
Idle noise reduction of light, medium and heavy duty Diesel engines
Proceedings of THIESEL 2004 Conference on Thermo- and Fluiddynamic Processes in Diesel Engines, pp. 239-249, Valencia

[217] SCHABERG, P.W.; PRIEDE, T. and DUTKIEWICZ, R.K. (1990)
Effects of a rapid pressure rise on engine vibration and noise
SAE Paper 900013

[218] SCHIFFBÄNKER, H. (1990)
Psychoacoustics - methods for the subjective assessment of noise
Proceedings of AVL Conference on Engine and Environment '90

[219] SCHIFFBÄNKER, H.; BRANDL, F.K. and THIEN, G.E. (1991)
Developpment and application of an evaluation technique to assess the subjective character of engine noise
SAE Paper 911081

[220] SCHIFFBÄNKER, H.; RUST, A. and BRANDL, F.K. (1989)
The suppression of undesirable noise phenomena in vehicles - a task to be achieved mainly for optimising the subjective noise character
I. Mech. E. Paper C 399/26

[221] SCHMILLEN, K. and SCHNEIDER, M. (1985)
Combustion chamber pressure oscillations as a source of Diesel engine noise
Proceedings of COMODIA '85

[222] SCHMILLEN, K. and WOLSCHENDORF, J. (1989)
Cycle-to-cycle variations of combustion noise in Diesel engines
SAE Paper 890129

[223] SCHMILLEN, K.; SCHWADERLAPP, M. and WOLSCHENDORF, J. (1993)
Primary noise reduction measures on IDI Diesel enines
SAE Paper 931309

[224] SCHNEIDER, M.; WILHELM, M. and ALT, N. (1995)
Development of vehicle sound quality - targets and methods
SAE Paper 951283

[225] SCHOLL, D.; BARASH, T.; RUSS, S. and STOCKHAUSEN, W. (1997)
Spectrogram analysis of accelerometer-based spark knock detection waveform
SAE Paper 972020

[226] SCHULLER, T.; SAUVAGE, O.; DIMITRIJEVIC, Z. and RYMER, G. (2005)
Acoustic analysis of unsteady Diesel engine combustion chamber pressure evolution
AIAA 2005-2910, 11th AIAA/CEAS Aeroacoustics Conference, 23 - 25 May 2005, Monterey, California

[227] SERVIÈRE, LACOUME J.L:; and BAUDAOUI, M.E. (2005)
Separation of combustion noise and piston-slap in diesel engine-PartII: Separation of combustion noise an piston-slap using blind source separation method
Mechanical System and Signal Processing 19 1218-1229

[228] SHERMAN, P.J. and WHITE L.B. (1995)
Improved periodic spetral analysis with application to Diesel vibration data
JASA **98**(6) pp. 3285-3301

[229] SHIBUYA, H.; WILGENHOF, E. and NANBU, T. (1993)
The difference in sensitivity to vehicle noise performance between European and Japanese subjects
Proceedings of Internoise '93 pp. 1513-1516, Leuven

[230] SHIGA, S.; EHARA, H.; KARASAWA T. and KURABAYASHI, Y. (1988)
Effect of exhaust gas recirculation on diesel knock intensity and its mechanism
Combustion and Flame **72** (3) pp. 53-58

[231] SHIVASHANKARA, B.N.; STRAHLE, W.C. and HANDLEY, J.C. (1975)
Combustion noise radiation by open turbulent flames
AIAA Paper 75-227

[232] SHU, G.; and LIANG, X. (2007)
Identification of complex diesel engine noise souces based on coherent power spectrum analysis
Mechanical System and Signal Processing **21** 405-416

[233] SHU, G. and WEI, H. (2007)
Study of combustion noise mechanism under accelerating operation of a naturally aspirated diesel engine
Int. J. Vehicle Des. **45, 1-2** 33-46.

[234] SPESSERT, B.; FLOTHO, A. and HALLER, H. (1990)
Acoustic aspects in the development of a new Deutz Diesel engine series
MTZ **51**

[235] STANKOVIĆ, LJ. and BÖHME, J.F. (1999)
Time-frequency analysis of multiple resonances in combustion engine signals
Signal Processing **79**, pp. 15-28

[236] STEEL, J.A. (1998)
Astudy of engine noise transmission using statistical energy analysis
*IMechE***121**(D), pp. 205-213

[237] STEIDLE, W. (1982)
Movimento del pistone e rumosità
ATA - Ingegneria automotoristica, pp. 814-818

[238] STONE, R. (1993)
Introduction to internal combustion engines, 2nd Edition
ISBN 1-56091-390-8

[239] STRAHLE, W.C. (1978)
Combustion noise
Prog. Energy Combust. Sci. **4**, pp.157-176, Pergamon Press Ltd, Great Britain

[240] STRAHLE, W.C. (1976)
Convergence of theory and experiment in direct combustion generated noise
In "Aeroacoustics: jet noise, combustion and core engine noise", SCHWARTZ (Ed) **43**(467): Progress in aeronautics, AIAA-MIT Press

[241] STRAHLE, W.C. (1975)
A review of combustion generated noise
In "Aerocoustics: jets and combustion noise; Duct Acoustics", NAGAMATSU (Ed) **37**(229): Progress in aeronautics and astronautics, AIAA-MIT Press

[242] STRAHLE, W.C. (1971)
On combustion generated noise
J. Fluid. Mech. **49**, 339

[243] STRAHLE, W.C. and HANDLEY, J.C. (1977)
Stochastic combustion and Diesel engine noise
SAE Paper No 770408

[244] STRAHLE, W.C. and SHIVASHANKARA, B.N. (1974)
A rationnal correlation of combustion noise results from open turbulent premixed flames
Fifteenth Symposium (International) on combustion, pp. 1379, The Combustion Institute, Pittsburgh

[245] STUECKLSCHWAIGER, H. and BRANDL, F.K. (1990)
Experience and potential for noise evaluation using an artificial head recording system
Isata Paper 90625

[246] STUECKLSCHWAIGER, H.; SCHIFFBÄNKER, H. and BRANDL, F.K. (1993)
Improving the noise quality of combustion engines
Lyon Congress SIA N. 93075

[247] STUMP, G. and RICCO, M. (1996)
Common rail - an attractive fuel injection system for passenger car DI Diesel engines
SAE Paper 960870

[248] SUH, I.-S. and LYON, R.H. (1999)
An investigation of valve train noise for the sound quality of I.C. engines
SAE Paper 1999-01-1711

[249] SULLIVAN J.L.; BAKER R.E.; BOYER B.A.; HAMMERLE R.H.; KENNEY T.E.; MUNIZ L. and WALLINGTON T.J. (2004)
CO2 Emission Benefit of Diesel (versus Gasoline) Powered Vehicles
Environ. Sci. Technol. 2004, **38** (12), pp. 3217-3223

[250] SUNG, S.H.; NEFSKE, D.J.; CHEN, H.K. and FANNIN, M.P. (1997)
Development of an engine system model for predicting structural vibration and radiated noise of the running engine
SAE Paper 972039

[251] TABUCHI, T.; FUJITANI, N. and MAKINO, N. (1995)
Recent technology to improve engine combustion noise and exhaust emission by optimizing fuel injection system
SAE Paper 951791

[252] TAKAO, H.; HASHIMOTO, T. and HATANO, S. (1993)
Quantification of subjective unpleasantness using Roughness level
SAE Paper 931332

[253] TANAKA, H.; KAWATA, K.; MIKAMI, M. and KOJIMA, N. (1999)
Noise extraction analysis in small Diesel engine - Application of time-frequency analysis to noise extraction
SAE Paper 1999-80-0415

[254] THIEN, G.E. (1979)
A review of basic design principles for low-noise Diesel engines
SAE Paper 790506

[255] THIEN, G.E. (1973)
The use of specially designed covers and shields to reduce Diesel engine noise
SAE Paper 730244

[256] THIEN, G.E. and FACHBACH, H.A. (1976)
Quiet automobiles - a realistic objective
FISITA Paper 3-1

[257] THIEN, G.E. and FACHBACH, H.A. (1975)
Design concepts of Diesel engines with low noise emission
SAE Paper 750838

[258] THOMAS, R.S.; STANECKI, P.J. and CREUTZ, H.P. (1991)
A development process to improve vehicle sound quality
SAE Paper 911079

[259] THOMPSON, L.L. (2006)
A review of finite-element methods for time-harmonic acoustics
JASA **119**(3), pp. 1325-1330

[260] THOMSON, J.K.; KUNG, L.E. and TREE, D.R. (1983)
Noise source identification for three small engines
Noise Control Engineering Journal **21**(2), pp. 74-80

[261] TICHÝ, J. and GAUTSCHI, G. (1980)
Piezo-elektrische Meßtechnik
Berlin: Springer-Verlag

[262] TORREGROSA, A.J.; BROATCH, A.; MARANT, V. and BEAUGE, Y. (2002)
Analysis of combustion chamber resonance in DI automotive Diesel engines
Proceedings of THIESEL 2002 Conference on Thermo- and Fluiddynamic Processes in Diesel Engines, pp. 239-249, Valencia

[263] TORREGROSA, A.J.; BROATCH, A.; MARGOT, X. and MARANT, V. (2003)
Combustion chamber resonances in DI automotive Diesel engines: a numerical approach
IJER Paper 02103

[264] TORREGROSA, A.J.; BROATCH, A.; MARTÍN, J. and MONELLETTA, L. (2007)
Combustion noise level assessment in direct injection Diesel engines by means of in-cylinder pressure components
MST Paper **18**,**7**, pp. 2131-2142

[265] TUNG, V.T.C. and CROCKER, M.J. (1982)
Diesel engine noise and relationship to cylinder pressure
SAE Paper 820237

[266] USAMI, T.; WADA, S. and SONODA, S. (1975)
Piston slap noise of indirect combustion Diesel engines
SAE Paper 750801

[267] USUDA, S.; OTSUKA, M. and NAGATA, M. (2002)
Noise and vibration reduction of newly developed 3.0l direct injection diesel engine
JSAE Paper **23**, pp. 285-289

[268] VAN DER AUVERAER, H.; WYCKAERT, K. and HENDRICX, W. (1997)
From sound quality to engineering of solution for NHV problems: case studies
Acustica **83**, pp. 796-804

[269] VORA, K.C. and GHOSH, B. (1991)
Vibration due to piston slap and combustion in gasoline and Diesel engines
SAE Paper 911060

[270] WEISCH, G.; STÜCKLSCHWAIGER, W.; DE MENDONCA, A.A.; MONTEIRO, N.T.S. and DOS SANTOS, L.A. (1997)
The creation of a car interior noise quality index for the evaluation of rattle phenomena
SAE Paper 972018

[271] WERNER, L.E. (1987)
Control of Piston Stick Slip Noise in a 4-cylinder Gasoline Engine
SAE Paper 870991

[272] WILHELM, M.; ALT, N. and WIEHAGEN, N. (1998)
Optimization of SI combustion noise - development process and basic analysis
I. Mech. E. Paper C 521/034

[273] WINKLHOFER, E. and THIEN, G.E. (1985)
A review of parameters affecting the noise and vibration in Diesel powered passenger cars
SAE Paper 850966

[274] WOLSCHENDORF, J.; DÜRNHOLZ, M. and SCHMILLEN, K. (1991)
The IDI Diesel engine and its combustion noise variations
SAE Paper 910228

[275] WOOD, J.J. and LEATHERWOOD, J. (1985)
A new Ride Quality Meter
SAE Paper 850981

[276] WOSCHNI, G. (1967)
A universally applicable equation for the instantaneous heat tranfer coefficient in the internal combustion engine
SAE Paper 670931

[277] YAJIMA, Y. and NAKASHIMA, K. (1998)
New measuring technique of cylinder pressure and its application to combustion noise reduction. Time-frequency analysis of combustion excitation using wavelet transform analysis
JSAE Review 19, pp 277-282

[278] YAWATA, Y. and CROCKER, M.J. (1983)
Identification of internal noise sources in Diesel engines
SAE Paper 831330

[279] YOHIKAWA, K. (1986)
Vibration of crankshafts at high engine speeds
SAE Paper 865026

[280] ZHANG, L. (1999)
A study of pilot injection in a DI Diesel engine
SAE Paper 1999-01-3493

[281] ZHANG, L.; HUANG, Y.; CHENG, Y.; WU, B. and QIAO, X. (1991)
On combustion noise and working stability of 6130Q Diesel engine
SAE Paper 911072

[282] ZHANG, Z. and TOMOTA, E. (2000)
A new diagnostic method of knocking in a spark-ignition engine using the wavelet transform
SAE Paper 2000-01-1801

[283] ZHAO, H. and REINHART, T.E. (1999)
The influence of Diesel engine architecture on noise levels
SAE Paper 1999-01-1747

[284] ZHENG, G.T. and LEUNG, A.Y.T. (2002)
Internal combustion engine noise analysis with time-frequency distribution
ASME Journal of Engineering for Gas Turbines and Power **124**, pp. 645-649

[285] ZOU, J.; CHEN J. and GENG, Z.M. (2001)
Application of wavelet packets algorithm to Diesel engines' vibroacoustics signature extraction
IMech **215**(D), pp. 987-993

[286] ZOUBIR, M. and BOSSMEYER, M. (1990)
Optimization of sensor positions for dectecting knock in spark ignition engines
Traitement du signal **8**(5)

[287] ZURITA VILLARROEL, G. and ÄGREN, A. (1997)
Wavelet transform analysis of measurements of engine combustion noise
SAE Paper 972003

[288] ZURITA VILLAROEL, G.; ÄGREN, A. and PETTERSSON, E. (1999)
Reconstruction of the cylinder pressure from vibration measurements for prediction of exhaust and noise emissions in ethanol engines
SAE Paper 1999-01-1658

[289] ZURITA VILLAROEL, G.; HAUPT D. and ÄGREN, A. (2004)
Reconstruction of the cylinder pressure through multivariate data analysis: for prediction of noise and exhaust emissions
Noise Control Eng. J. **52**(4), pp. 154-163

[290] ZWICKER, E. and FASTL, H. (1999)
Psychoacoustics - Facts and models. Second updated edition
Springer